

ANGEL 2018 - FINAL PROGRAM

Monday, June 4		Tuesday, June 5		Wednesday, June 6		Thursday, June 7	
7:30 – 8:15	REGISTRATION			8:00 – 9:00	PC & IAB meeting : Hearing of applicants for ANGEL 2020 venue	8:00 – 9:00	PC & IAB meeting
8:15 – 8:30	OPENING (Chairs)	8:30 – 10:15	V. Amendola (Tutorial) D. Guay (Keynote) G. Marzun (Invited) Chairman : D. Amans	9:00 – 10:30	E. Barmina (Invited) K. Tibbetts T. Okamoto * J. Bárta	9:00 – 10:50	D. Mukherjee (Invited) A. Popov * B. Gökce L. D’Urso C. Rehbock
8:30 – 8:45	A. Gheisi (Sponsor)						
8:45 – 10:30	A. Vogel (Keynote) A. Nath Chairman : S. Barcikowski H.J. Jung * T. Hupfeld *						
10:30 – 10:50	COFFEE BREAK	10:15 – 10:35	COFFEE BREAK	10:30 – 10:50	COFFEE BREAK	10:50 – 11:10	COFFEE BREAK
10:50 – 12:10	A. Kanitz * S. Reich * Chairman : L. Zhigilei A. Plech S. Barcikowski	10:35 – 12:25	G. Baffou (Invited) S. Mérabia Y. Cai R. Kihara * G. Shafeev Chairman : A. Vogel	10:50 – 12:20	Z. Swiatkowska-Warkocka (Invited) N. Koshizaki A.R. Ziefuß * M. Lau Chairman : G. Shafeev	11:10 – 12:00	CLOSING REMARKS & STUDENT AWARDS
12:10 – 14:00	LUNCH BREAK	12:25 – 14:15	LUNCH BREAK	12:20 – 14:00	LUNCH BREAK		LUNCH BOXES
14:00 – 15:40	T. Sakka (Invited) L. Zhigilei (Invited) Chairman : T. Itina N. Inogamov V. Zhakhovsky	14:15 – 18:30	GUIDED TOUR OF OLD CITY	14:00 – 15:40	A. Fojtik A. Kabashin C. Bravin C. Doñate Buendía * R. Intartaglia Chairman : S. Kudryashov		* STUDENT
15:40 – 16:00	COFFEE BREAK			15:40 – 16:00	COFFEE BREAK		
16:00 – 17:20	Q. Yuan * V. Shur Chairman : G. Compagnini S. Shaji M. Dell’Aglío			16:00 – 17:30	S. Kudryashov (Invited) C. Liang T. Chen * N. Tarasenko Chairman : A. Kabashin		
17:20 – 18:00	GROUP PHOTO			17:30 – 19:00	POSTER SESSION II		
18:00 – 19:00	FLASH TALKS FOR POSTERS & SPONSORS			19:00 – 21:00	Wine & Cheese COCKTAIL		
19:00 – 21:00	POSTER SESSION I & DINNER COCKTAIL	19:30 – 23:30	GALA DINNER : The Abbaye, Paul Bocuse				

DETAILED PROGRAM

SUNDAY, June 3

17:00 – 19:00	Programme Committee Meeting	
17:00 – 20:00	REGISTRATION	Hall of Domaine Saint-Joseph
19:00 – 21:00	Welcome Cocktail	Garden of Domaine Saint-Joseph

MONDAY, June 4

7:30 – 8:15	REGISTRATION	Hall of Domaine Saint-Joseph
8:15 – 8:30	OPENING TALK	
8:30 – 8:45	SPONSOR : Nano website	

	A. Gheisi	How nature indexing helps you find nanotechnology Literature and data efficiently
--	-----------	---

8:45 – 10:30	SESSION 1 : Dynamics of laser-induced cavitation	
	Chairman : S. Barcikowski	
S1-1	A. Vogel	Ablation and cavitation dynamics in laser-based nanoparticle generation and excitation
S1-2	A. Nath	Implications of Focusing Effect on Cavitation Bubble Dynamics and Nanoparticles formed via Laser Ablation in Liquids
S1-3	H.J. Jung *	Synthesis of Nickel Nanoparticles using Pulsed Laser Ablation in Various Solvents: Cavitation Bubble Dynamics and Characterization Studies
S1-4	T. Hupfeld *	Influence of wettability and high viscosity on the cavitation bubble dynamics during pulsed laser ablation in liquid

10:30 – 10:50	COFFEE BREAK	
---------------	---------------------	--

10:50 – 12:10	SESSION 2 : Overview on process from in-situ measurements	
	Chairman : L. Zhigilei	
S2-1	A. Kanitz *	Investigation of femtosecond laser ablation of iron in

		different liquids at ultrashort timescales
S2-2	S. Reich *	Fast multi-contrast imaging of the ablation process in liquids adding X-ray bright-field and dark-field methods
S2-3	A. Plech	Disentangling competitive hierarchical processes in pulsed laser ablation in liquids
S2-4	S. Barcikowski	Size quenching during laser synthesis of colloids happens already in the vapor phase of the cavitation bubble

12:10 – 14:00 **LUNCH BREAK**

14:00 – 15:40 **SESSION 3 : Modelling**

Chairman : T. Itina

S3-1	T. Sakka	Dynamics of laser-induced plasma in water and mechanism of cluster formation
S3-2	L. Zhigilei	Atomistic modelling of the generation of nanoparticles and surface nanostructuring by short pulse laser ablation in liquids
S3-3	N. Inogamov	Laser ablation of gold inside water I
S3-4	V. Zhakhovsky	Laser ablation of gold into water II: Comparative atomistic and hydrodynamics modeling

15:40 – 16:00 **COFFEE BREAK**

16:00 – 17:20 **SESSION 4 : Nanomaterials I**

Chairman : G. Compagnini

S4-1	Q. Yuan *	Facet-Dependent Selective Adsorption of Mn-Doped α -Fe ₂ O ₃ Nanocrystals Prepared by Laser Ablation in Liquids
S4-2	V. Shur	Shape control of PbO nanoparticles produced by laser ablation in liquid
S4-3	S. Shaji	Copper Antimony Sulfide (CuSbS ₂) nanoparticles by pulsed laser ablation in liquid
S4-4	M. Dell'Aglio	Characterization of Au and Ag nanoparticle produced by PLAL for considerations on their stability

17:20 – 18:00 **GROUP PHOTO**

18:00 – 19:00 **FLASH TALKS FOR POSTERS**

Chairman : D. Amans

19:00 – 21:00

POSTER SESSION I & DINNER COCKTAIL

TUESDAY, JUNE 5

8:30 – 10:15

SESSION 5 : The Basics of Catalysis

Chairman : D. Amans

S5-1	V. Amendola	Laser fabrication of nanoalloys for catalysis: generalities and opportunities
S5-2	D. Guay	Catalysis and electrocatalysis on well-defined model systems generated by laser ablation
S5-3	G. Marzun	Prospects and challenges of laser-generated nanoparticles for industrial applications in catalysis

10:15 – 10:35

COFFEE BREAK

10:35 – 12:25

SESSION 6 : Photothermal effect

Chairman : A. Vogel

S6-1	G. Baffou	Photothermal effects of gold nanoparticles. Applications in chemistry and cell biology
S6-2	S. Mérabia	Nanobubbles generated by laser heated nanoparticles
S6-3	Y. Cai	Laser irradiation guided anchoring of Au colloidal nanoparticles on α -Fe ₂ O ₃ nanoparticles for photothermal effect
S6-4	R. Kihara *	Transient Absorption Spectroscopic Study on Phase Transition Dynamics of Phthalocyanine Nanocrystals Induced by ns-laser Irradiation in Liquid
S6-5	G. Shafeev	Spatial distribution of breakdown plasma under laser exposure of colloidal solutions of nanoparticles

12:25 – 14:15

LUNCH BREAK

14:15 – 18:30

GUIDED TOUR OF LYON

19:30 – 23:30

GALA DINNER : The Abbaye, Paul Bocuse

WEDNESDAY, JUNE 6

8:00 – 9:00

PC & IAB meeting : hearing of the applicants for ANGEL2020 venue

9:00 – 10:30

SESSION 7 : Photochemistry

Chairman : Z. Swiatkowska-Warkocka

S7-1	E. Barmina	Generation of H ₂ , O ₂ and Hydrogen peroxide by laser-induced breakdown aqueous solutions of nanoparticles
S7-2	K. Tibbetts	Controlling the photochemical reduction of metal ions in optical breakdown plasma
S7-3	T. Okamoto *	Synthesis of single-nano-sized Au nanoparticles from liquid/liquid dispersion system by femtosecond laser irradiation
S7-4	J. Bárta	Photochemical synthesis of nanoparticles in aqueous solutions

10:30 – 10:50

COFFEE BREAK

10:50 – 12:20

SESSION 8 : Laser-induced modifications

Chairman : G. Shafeev

S8-1	Z. Swiatkowska-Warkocka	Laser-Induced Composite Particle Formation in Liquid: Insight in Physico-Chemical Processes
S8-2	N. Koshizaki	Fracture Strength of Submicrometer Spherical Particles Fabricated by Pulsed Laser Melting in Liquid
S8-3	A.R. Ziefuß *	Nanosecond laser fragmentation of colloidal gold nanoparticles with high intensity nanosecond pulses is driven by a single step fragmentation mechanism
S8-4	M. Lau	Sequential and energy dose defined irradiation of particles in a free liquid jet: modification of ITOs optical and cobalt ferrites catalytic properties

12:20 – 14:00

LUNCH BREAK

14:00 – 15:40

SESSION 9 : Theranostics

Chairman : S. Kudryashov

S9-1	A. Fojtik	Smart nanostructures for biomedical applications.
S9-2	A. Kabashin	Novel advanced laser-synthesized nanomaterials for biomedical applications
S9-3	C. Bravin	Laser-generated Metal Nanoparticles as Multifunctional Agents for Sensing and Nanomedicine Applications
S9-4	C. Doñate Buendia *	Carbon Quantum Dots Fluorescent Labels Generated in a Continuous Flow Jet Configuration
S9-5	R. Intartaglia	Germanium and Silicon: Laser-synthesized nanoparticles for bio-imaging applications

15:40 – 16:00 **COFFEE BREAK**

16:00 – 17:30 **SESSION 10 : Nanomaterials II**

Chairman : A. Kabashin

S10-1	S. Kudryashov	Laser fabrication of colloidal hybrid nanoparticles: formation scenario and potential applications
S10-2	C. Liang	Ubiquitous Metal Carbonization, Carbon Encapsulation, Metal-Catalyzed Graphitization during Laser Ablation of Metal in Organic Solvents
S10-3	T. Chen *	Fullerene-Like MoS ₂ Nanoparticles as Cascade Catalyst Improving Lubricant and Antioxidant Abilities of Artificial Synovial Fluid
S10-4	N. Tarasenko	Liquid Assisted Laser Fabrication of Binary Nanocrystalline Structures Based on Germanium and Silicon

17:30 – 19:00 **POSTER SESSION II**

19:00 – 21:00 **Wine & cheese cocktail with an oenologist**

THURSDAY, JUNE 7

8:00 – 9:00 **PC & IAB meeting**

9:00 – 10:50 **SESSION 11 : Nanomaterials III**

Chairman : V. Amendola

S11-1	D. Mukherjee	Nanocomposites and nanoalloys with engineered interfacial structures and functionalities made via Laser Ablation Synthesis in Solution (LASIS)-based routes
S11-2	A. Popov *	Fabrication of organic solvent and surfactant free fluorescent organic nanoparticles by laser ablation of aggregation-induced enhanced emission dyes
S11-3	B. Gökce	Laser Synthesis of Nanocomposites for Additive Manufacturing
S11-4	L. D'Urso	Hybrid nanostructures of metal/one-dimensional carbon allotropes prepared by laser ablation in liquid
S11-5	C. Rehbock	The internal phase structure of LAL-fabricated FeAu alloy nanoparticles is determined by solvent properties and target composition

10:50 – 11:10

COFFEE BREAK

11:10 – 12:00

CLOSING REMARKS & STUDENT AWARDS CEREMONY

LUNCH BOXES

POSTER SESSION I, Monday, June 4

* STUDENT

Flash talks for posters : #

P-I- 1	H. Liu	Temporal and spatial diagnosis for laser ablation on silicon carbide in water	1
P-I- 2	A. Nastulyavichus *	Antibacterial Se and Si nanoparticles	2
P-I- 3	A. Schielke *	Laser-generated gold nanoparticle nano-bio-conjugates featuring cationic ligands for biomedical diagnostics and therapy	3
P-I- 4	I. Trenque	Synthesis routes of CeO ₂ nanoparticles dedicated to organophosphorus degradation: a benchmark	4
P-I- 5	F. Waag *	Continuous laser fragmentation of colloidal particles: improving the process control and efficiency	5
P-I- 6	M. Chen	Wavelength dependent electron temperature distribution in plasma produced by laser ablation in the water	6
P-I- 7	R. Streubel *	Exploring the origin of bimodal size distribution during picosecond laser ablation in liquids	7
P-I- 8	A. Singh *	Pulsed laser ablation in supercritical CO ₂ to synthesize Ti _x O _y nanoparticles	8
P-I- 9	T. Nakamura	Effect of Irradiation Time on Crystalline Structure of Silver Submicron Spherical Particles by Pulsed Laser Melting in Liquid	9
P-I- 10	I. Saraeva *	Milligram per second femtosecond laser generation of functional Se nanoparticles	10
P-I- 11	R. Kuroda *	Surface Modification of Metal and Alloy Nanoparticles Fabricated by Laser-Induced Nucleation in Liquid	11
P-I- 12	M. Labusch *	Automated focus adjustment for a high particle productivity rate by PLAL	12
P-I- 13	S. Kohsakowski *	A continuous and contamination-free process chain produces monodisperse, laser-synthesized heterogeneous co-catalysts	13
P-I- 14	M.R.Kalus *	Influence of persistent microbubbles on nanoparticle productivity in laser synthesis of colloids	14
P-I- 15	R. Torres-Mendieta	Single-stage formation of Ag nanoparticles on α -Ag ₂ WO ₄ network by femtosecond laser irradiation	15
P-I- 16	M. Zhilnikova *	Laser-assisted generation of elongated Au nanoparticles and subsequent dynamics of their morphology under pulsed irradiation in water	16
P-I- 17	J. Tang *	MoS ₂ quantum dots synthesized by pulsed laser ablation in a binary liquid	17
P-I- 18	J. Johnny *	Effects of ablation energy and time on SnS ₂ nanoparticles by pulsed laser ablation in liquid	18
P-I- 19	G. Laurens *	Surface Chemistry Of Colloidal Ligand-Free Gold Nanoparticles Generated By Laser Ablation	19
P-I- 20	A. Chemin *	Doping inclusion in nanoparticles using pulsed laser ablation in liquid	20
P-I- 21	B. Chandu *	Graphene Quantum Dots, Microstructures Fabricated using	21

Femtosecond Laser Ablation in liquids

P-I- 22	I.	Baymler *	Hydrogen generation by laser irradiation of organic liquids
P-I- 23	S.	Aksoy	Fabrication of metal nanoparticles and nanoalloys by laser ablation in liquids

POSTER SESSION II, Wednesday, June 5

* STUDENT

P-II- 1	S.	Kulinich	Gas Sensing by Laser-Ablated Nanomaterials
P-II- 2	M.	Dell'Aglio	Interaction of AgNPs produced by PLAL with human proteins and protein corona assessment
P-II- 3	L.	Escobar-Alarcon	Hydrogen production by ultrasound assisted liquid laser ablation of an Al-Mg alloy in water
P-II- 4	Y. K.	Kim	Stable colloidal suspension of TiO ₂ nanoparticles in aqueous solution prepared by nanosecond laser pulses and their photocatalytic performances
P-II- 5	S. H.	Lee *	Improved photocatalytic activity of Au-doped Au@ZnO core-shell flower shaped nanocomposites
P-II- 6	V. A.	Zuñiga-Ibarra *	Synthesis and characterization of black TiO ₂ nanoparticles by pulsed laser ablation in liquid for photocatalysis
P-II- 7	J.	Liu	Laser Ablation in Liquids Induced Ni/rGO Catalysts with Ultrahigh Electrocatalytic Activity and Stability in Methanol Oxidation
P-II- 8	M.	Condorelli *	Plasmon sensing properties of laser prepared noble metal colloids
P-II- 9	D.	Chen	Laser fabrication and temperature dependent upconversion properties of Gd ₂ O ₃ :Yb ³⁺ , Ho ³⁺ nanoparticles
P-II- 10	C.	Zhang	Laser-induced Au Nanoparticles Encapsulated in Ultrathin Carbon Shells as Excellent Bifunctional Electrocatalysts
P-II- 11	T.	Itina	Possible mechanisms of bimetallic nanoparticle formation by laser co-ablation of liquid colloids
P-II- 12	S.J.	Lee *	Solvent as a Carbon and Nitrogen Source for Graphitic Carbon and Nitrogen-doped Graphitic Carbon Shells on Nickel Nanoparticles
P-II- 13	S.	Kudryashov	Laser-ablative fabrication of hybrid Se@Au, Si@Au/Ag nanoparticles via heterogeneous condensation
P-II- 14	T.	Asahi	Laser Fabrication of Organic Nanoparticle Colloids Having Strong Near-Infrared Absorption
P-II- 15	M.	John *	Optimizing the catalytic activity of Pulsed Laser Ablation Surface-Mediated Excitation and Reduction (PLASMER) synthesized metal-silica nanocomposites
P-II- 16	S.	Siebeneicher *	A Study on the Origin of Oxygen in Particles Synthesized by Laser Ablation in Liquids
P-II- 17	Y.	Ishikawa	An Approach for High-Yield Submicrometer Spherical Particles by Pulsed Laser Melting in Liquid
P-II- 18	S.	Sakaki *	Influence of Picosecond Laser Irradiation on Synthesis of Spherical Particles by Pulsed Laser Melting in Liquid
P-II- 19	G.	Shafeev	Influence of external magnetic field on the morphology of Au nanoparticles obtained by laser ablation in water
P-II- 20	N.	Tarasenka	Laser Assisted Formation of Immiscible Alloy Nanoparticles in Liquids
P-II- 21	V.	Svetlichnyi	Comparison of Magnetite Nanoparticles Obtained by Pulsed Laser

Ablation in Water and Air

P-II- 22	D.	Goncharova *	Structure of nanoparticles from colloids obtained by pulsed laser ablation of copper in a liquid
P-II- 23	A.	Nastulyavichus *	Scaling relationships for film-to-nanoparticles conversion during nanosecond laser ablation of silver films of variable thickness
P-II- 24	L.	D'Urso	Photo-catalytic activity of ZnO nanostructures obtained by micromachining a high purity Zn target with a picosecond pulsed laser
P-II- 25	I.	Saraeva *	Femto/picosecond pulsewidth-dependent yield of metal and Si nanoparticles
P-II- 26	R.	Soni	Plasmonic and Magnetic Nanocomposites
P-II- 27	D.	Popovic	The Luminescence of Silicon-based Nanoparticles Produced by Laser Ablation in Liquid

Ablation and cavitation dynamics in laser-based nanoparticle generation and excitation

A. Vogel, S. Freidank, X.-X. Liang, N. Linz

Institute of Biomedical Optics, University of Lübeck, Peter-Monnik-Weg 4, 23562 Lübeck, Germany

vogel@bmo.uni-luebeck.de

The lecture addresses a number of questions that are discussed in the context of laser-based nanoparticle (NP) generation and excitation, such as: Which phase transitions occur upon ablation, and are they altered by liquid confinement? Do ablation products push the liquid, or are some injected? How can we look into the laser-generated bubble to assess whether NPs are formed already upon ablation or later, during the bubble oscillation? Which laws govern the bubble dynamics at the target surface upon particle generation? Does the bubble collapse influence NP generation? Can we avoid target shielding by the bubble to increase NP production efficiency? Do cavitation bubbles produced upon nanoparticle excitation exhibit a similar dynamics as laser-produced bubbles in free liquid?

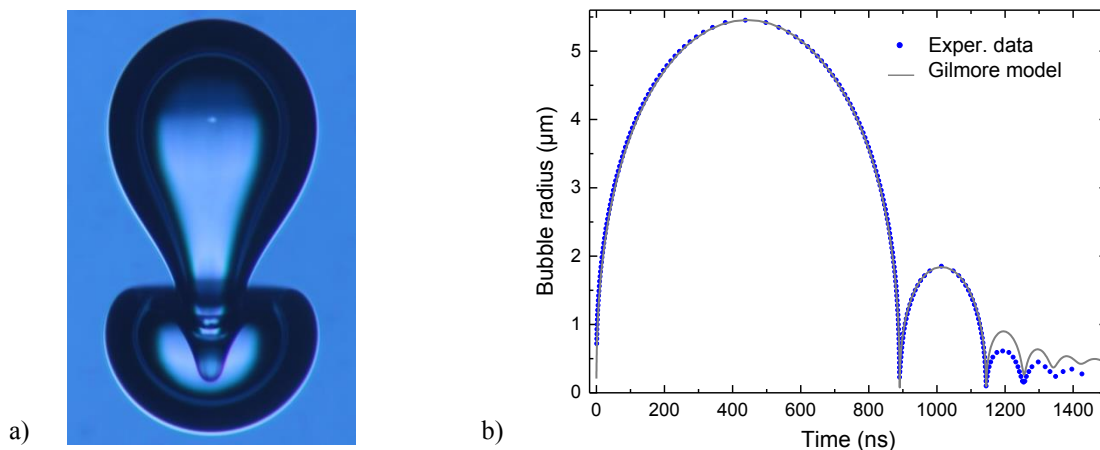


Figure 1 (a) view into two interacting laser-produced bubbles achieved by incoherent Köhler illumination using a spark-gap flash-lamp. (b) Radius-time curve of a spherical laser-produced bubble with 5.4 μm maximum radius obtained by single-shot backscattering interferometry. The fitted curve was calculated using the Gilmore model of cavitation dynamics, which considers surface tension, viscosity, and compressibility. Liquid compressibility is modeled using the Tait EOS. An excellent fit of the first oscillations is achieved with room temperature values for surface and viscosity of water. Damping in collapse is mainly due to shock wave emission – 96% of the bubble energy is radiated away as acoustic transient. The fit is not as good for later oscillations – likely because the Gilmore model considers neither heat diffusion nor temperature-dependent changes of water properties.

Answers to these questions will be derived based on our own work on pulsed laser ablation [1-3] and bubble dynamics [4,5], and by reviewing the literature in the field [6-8]. Two examples are given in Fig. 1: Using illumination techniques originally developed for light microscopy, one can explore the dynamics inside of laser-produced bubbles [Fig. 1 (a)]. Laser-induced bubble dynamics can be explored experimentally with nanometer resolution and precisely fitted using a model that considers liquid compressibility [6] [Fig. 1 (b)]. The same model provides good fits also when applied to bubble dynamics around laser-irradiated nanoparticles [8].

- [1] I. Apitz and A. Vogel, Material ejection in ns Er:YAG laser ablation of water, liver and skin, *Appl. Phys. A* 81, 329–338 (2005).
- [2] A. Vogel and V. Venugopalan, Mechanisms of pulsed laser ablation of biological tissues, *Chem. Rev.* 103, 577-644 (2003).
- [3] A. Vogel, I. Apitz, S. Freidank and R. Dijkink, Sensitive high-resolution white-light Schlieren technique with a large dynamic range for the investigation of ablation dynamics, *Opt. Lett.* 31, 1812-1814 (2006).
- [4] A. Vogel, N. Linz, S. Freidank, and G. Paltauf, Femtosecond-laser-induced nanocavitation in water: implications for optical breakdown threshold and cell Surgery, *Phys. Rev. Lett.* 100, 038102 (2008)
- [5] A. Vogel, N. Linz, S. Freidank, IR and UV vortex beams for ultraprecise plasma-mediated eye surgery, *SPIE Newsroom*, DOI: 10.1117/2.1201511.006157 (2016).
- [6] W. Lauterborn and T. Kurz, Physics of bubble oscillations, *Rep. Prog. Phys.* 73, 106501, 1-88 (2010).
- [7] D. Kröniger, K. Köhler, T. Kurz and W. Lauterborn, Particle tracking velocimetry of the flow field around a collapsing cavitation bubble, *Exper. Fluids* 48, 395-408 (2010).
- [8] C. Boutopoulos, A. Hatef, M. Fortin-Deschênes, and M. Meunier, Dynamic imaging of a single gold nanoparticle in liquid irradiated by off-resonance femtosecond laser, *Nanoscale* 7, 11758-11765 (2015).

Implications of Focusing Effect on Cavitation Bubble Dynamics and Nanoparticles formed via Laser Ablation in Liquids.

P. K. Baruah¹, A. Khare¹, P. Sharma², A. Nath^{2,*}

1-Department of Physics, Indian Institute of Technology Guwahati, Guwahati -781039, India
 2- Department of Physics, National Institute of Technology Meghalaya, Shillong-793003, India

*email address: n.arpita@nitm.ac.in; n.arpita@gmail.com

The irradiation of pulsed high power laser onto a titanium target immersed in water, leads to transient plasma formation with emission of high speed shockwaves. The extreme conditions of transient plasma ensues interaction of titanium plasma with surrounding water plasma which accredits cluster formation through plasma condensation. These clusters under suitable condition nucleate and if it achieves the critical size grow into Titanium Oxide nanoparticles. Figure 1(a) and 2(a) depicts the effect of focusing condition in flicking the phases of TiO₂ nanoparticles [1]. Comprehensive work has been done to synthesize these metal oxide nanoparticles but the investigation on phase transition mechanism & nucleation dynamics of these nanoparticles via laser-target-liquid interaction remain unexplored. Thus, the role of nucleation time and growth velocity onto phase transition phenomena with an additional attempt of comparing the analytically estimated particle statistics with that of experimentally documented results is carried out as illustrated in figure 1(c) and 2 (c) [2, 3]. Keeping a note on the conjecture associated to the role of cavitation bubbles in nucleation of nanoparticles in liquids, the implication of cavitation bubbles for different focusing condition as depicted in figure 1(d) and 2(d) respectively is investigated.

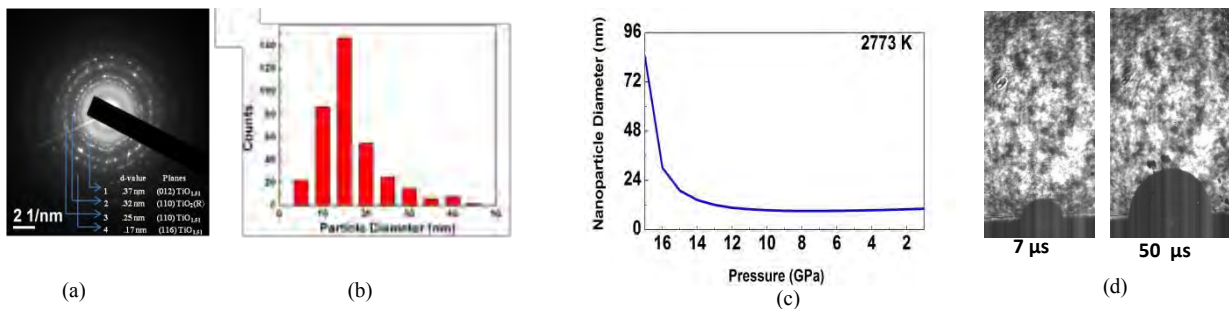


Figure 2. For laser ablation of titanium target immersed in water under tightly focussed condition. (a) SAED pattern affirms formation of Rutile phase of TiO₂ (b) The corresponding particle statistics from TEM (c) The nanoparticle diameter extracted from nucleation theory (d) The cavitation bubble dynamics at 7 μs and 50 μs after elapse of laser pulse.

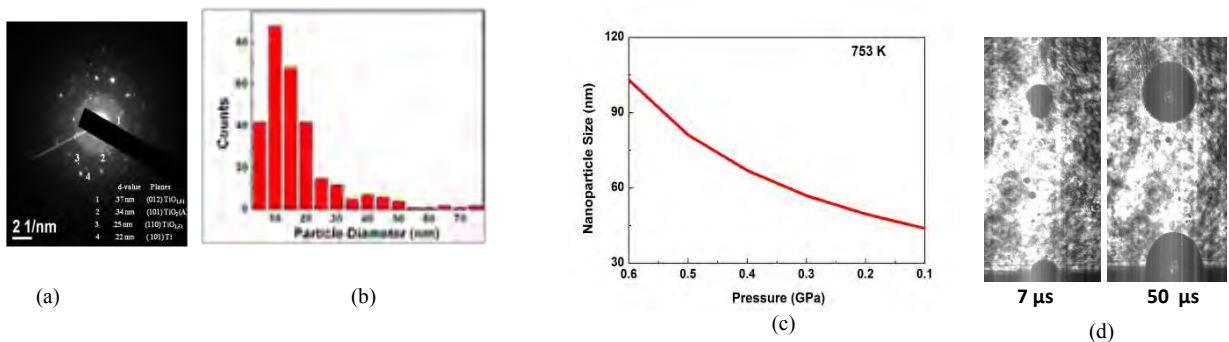


Figure 2. For laser ablation of titanium target immersed in water under de-focussed condition. (a) SAED pattern affirms formation of Anatase phase of TiO₂ (b) The corresponding particle statistics from TEM (c) The nanoparticle diameter extracted from nucleation theory (d) The cavitation bubble dynamics at 7 μs and 50 μs after elapse of laser pulse.

[1] A. Nath, S. S. Laha, A. Khare, Applied Surface Science, **257**, 3118, (2011).
 [2] C. X. Wang, P. Liu, H. Cui, G. W. Yang, Applied Physics Letters, **87**, 201913 (2005)
 [3] A. Nath, P. Sharma, A. Khare, Laser Physics Letters, **15**, 026001, (2018)

Synthesis of Nickel Nanoparticles using Pulsed Laser Ablation in Various Solvents: Cavitation Bubble Dynamics and Characterization Studies

Hyeon Jin Jung, Myong Yong Choi*

*Department of Chemistry (BK21+) and Research Institute of Natural Science,
Gyeongsang National University, Jinju 52828, Republic of Korea*

*laser02hj@gmail.com, mychoi@gnu.ac.kr**

Pulsed laser ablation in liquid (PLAL) is an environment-friendly, facile, and clean method for the synthesis of nanoparticles (NPs). Using PLAL, we have synthesized numerous metal NPs in various solvents, investigated the dynamics of cavitation bubble formation, and characterized the chemical/physical properties of the NPs.

I present a simple and controllable preparation of face-centered cubic (fcc) and hexagonal close-packed (hcp) structure of nickel (Ni) NPs by a PLA method in the following four solvents: deionized water, methanol, hexane, and acetonitrile. Remarkably, the phases of Ni NPs prepared via PLAL show a strong dependence on the solvents used in the PLA processes. We suggested that the solvent dependence on the phase of nanocrystals is related to the specific heat of the solvents which may have played an important role kinetically and thermodynamically in the cooling process of the plasma plume where the NPs nucleate and coalesce to a specific phase.

We performed a dynamic study of cavitation bubble formation during PLAL. We have found a strong relation of specific phase formation of Ni NPs with the lifetimes of the induced cavitation bubbles (LICBs). In this work, we have found that relatively short and long lifetime of the cavitation bubble as compared to that of deionized water generates the hcp and fcc phase Ni NPs, respectively. From this study, we were able to suggest for the first time that the crystal phase formed in PLAL is strongly dependent on the lifetime of the cavitation bubbles. The dynamics study of PLAL was conducted by measuring the time-resolved cavitation bubble size through an intensified charge coupled device (ICCD) camera.

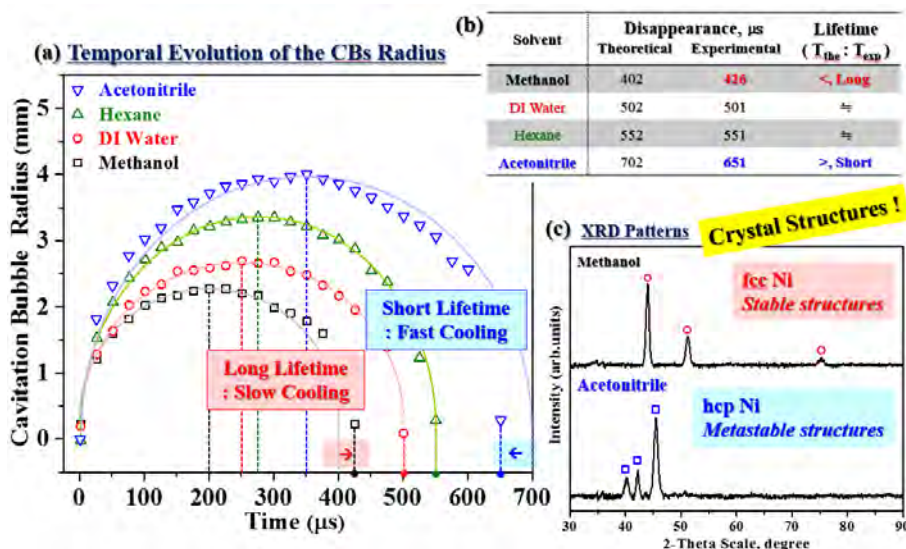


Figure 3. Time-evolution dynamics of induced cavitation bubbles (LICBs) radius obtained after laser ablation in various solvents.

- [1] H. J. Jung, M. Y. Choi, Specific Solvent Produces Specific Phase Ni Nanoparticles: A Pulsed Laser Ablation in Solvents, *J. Phys. Chem. C*, 118, 14647-14654, (2014)
- [2] Kim, K. K.; Roy, M.; Kwon, H.; Song, J. K.; Park, S. M., Laser ablation dynamics in liquid phase: The effects of magnetic field and electrolyte, *J. Appl. Phys.*, 117, 074302-7, (2015)
- [3] J. Lam, J. Lombard, C. Dujardin, G. Ledoux, S. Merabia, and D. Amans, Dynamical study of bubble expansion following laser ablation in liquids, *Appl. Phys. Lett.*, 108, 074104-5, (2016)

Influence of wettability and high viscosity on the cavitation bubble dynamics during pulsed laser ablation in liquid

T. Hupfeld¹, G. Laurens², D. Amans², S. Barcikowski¹, B. Gökce¹

¹ Technical Chemistry I and Center for Nanointegration Duisburg-Essen (CENIDE), University of Duisburg-Essen, Universitaetsstrasse 7, 45141 Essen, Germany

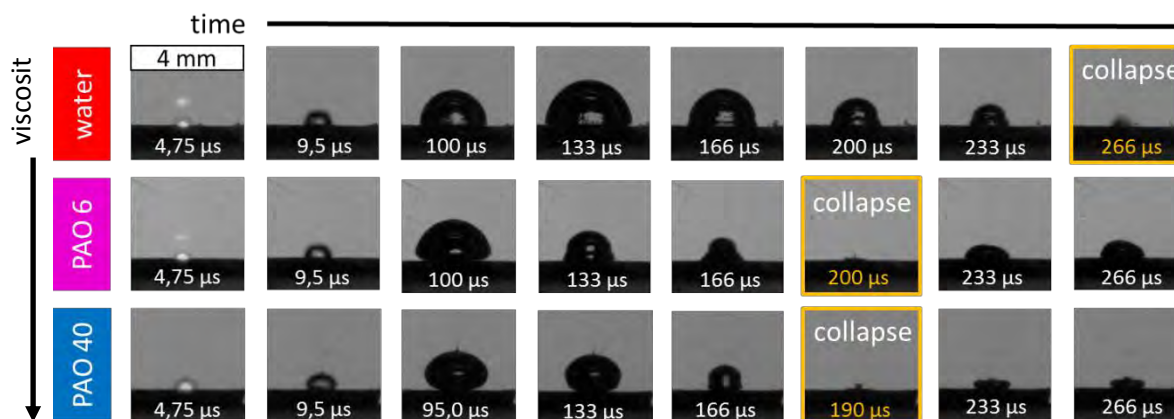
2

-69622 Lyon, France

tim.hupfeld@uni-due.de

Producing colloids through pulsed laser ablation in liquid (PLAL) has become a popular technique because of its versatility towards a wide variety of liquids and nanoparticle materials. To fully benefit from this versatility, it is necessary to deepen the understanding of how liquid parameters such as the viscosity and target wetting angle influence PLAL. The dynamics of the laser-induced cavitation bubble (bubble lifetime and maximum size) is known to influence the particle generation^[1-2]. However, for bubbles generated on a solid-water interface, it is mostly unknown how the viscosity influences its shape and dynamics. There are only a few reports, suggesting that an asymmetric shrinking^[3] and an inward jet might be linked to the wetting angle of the initial bubble^[4].

Figure 4 : Dynamics of the cavitation bubble in three liquids for PLAL of a gold target is shown.



In this contribution, the dynamics of laser-induced bubbles is investigated as a function of the liquid viscosity, using an ultrafast shadowgraphy imaging setup. Pulsed laser ablation of a gold foil and a yttrium-iron-garnet wafer are performed in water and highly viscous synthetic poly-alpha-olefins (PAO), often used as model fluids for engine oil. The dynamics of laser-induced bubbles is driven by inertial forces in water, leading to a half sphere shape^[5]. When increasing the liquid viscosity, and by this, the capillary Number Ca we observed the appearance of a contact angle hysteresis for the contact lines. The hysteresis between advancing and receding angles is similar to the hysteresis observed for a moving liquid droplet or a dynamic sessile drop. It is found that an increase of the viscous forces has a significant impact on the cavitation bubble shape and dynamics resulting in higher damping of the cavitation bubble, and fewer oscillations after the first collapse. Further, we show clear evidence that friction determines the thickness of the interface layer. Thus, the interface layer thickness depends on the velocity of the boundary and the viscosity of the liquid.

[1] C.L. Sajti, R. Sattari, B. N. Chichkov, S. Barcikowski, J. Phys. Chem. C **114**, 2421–2427 (2010).

[2] R. Streubel, S. Barcikowski, B. Gökce, Opt. Lett. **41**, 1486–1489 (2016).

[3] J. Tomko, J. J. Naddeo, R. Jimenez, Y. Tan, M. Steiner, J. M. Fitz-Gerald, D. M. Bubb, S. M. O'Malley, Phys. Chem. Chem. Phys. **17**, 16327–16333 (2015).

[4] S. Ibrahimkuty, P. Wagener, T. D. S. Rolo, D. Karpov, A. Menzel, T. Baumbach, S. Barcikowski, A. Plech, Sci. Rep. **5**, 1–11 (2015).

[5] J. Lam, J. Lombard, C. Dujardin, G. Ledoux, S. Merabia, D. Amans, Appl. Phys. Lett. **108**, 1–6 (2016).

Investigation of femtosecond laser ablation of iron in different liquids at ultrashort timescales

A. Kanitz¹, D.J.Förster², J.S.Hoppius¹, R.Weber², A.Ostendorf¹, E.L.Gurevich¹

1- Ruhr-Universität Bochum, Applied Laser Technologies, Universitätsstr. 150, 44801 Bochum, Germany

2- Universität Stuttgart, Institut für Strahlwerkzeuge, Pfaffenwaldring 43, 70569 Stuttgart, Germany

kanitz@lat.rub.de

Due to its versatility, pulsed laser ablation in liquids yields the opportunity to generate a variety of nanoparticles by simply changing the target, liquid or laser parameters [1,2]. Nevertheless, the complex interaction between laser-excited material and liquid environment lead to ongoing research regarding the understanding of nanoparticle formation. Especially, processes beginning with the laser beam impact until plasma formation are still a barely investigated topic due to the use of challenging diagnostic methods.

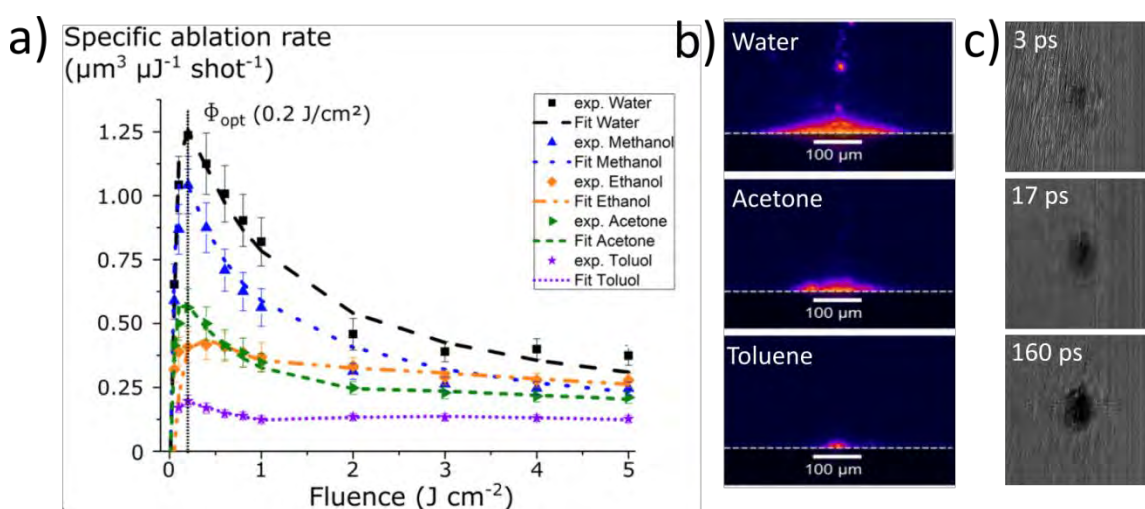


Figure 5: a) Specific ablation rate of femtosecond laser ablation of iron in different liquids. Dotted lines represent fitted lines according to the ablation law, b) Plasma images with a gating time of 3 ns for ablation in water, acetone and toluene at 1 J/cm^2 [2]. c) pump-probe Microscopy images of ablation in acetone at delay times of 3 ps, 17 ps, and 160 ps after the laser beam impact.

In this study, we present our investigation of femtosecond (fs) laser ablation of iron in different liquids (water, methanol, ethanol, acetone, toluene) from the fs to nanosecond (ns) timescale by several diagnostic methods, namely, plasma imaging, reflectivity measurements and pump-probe microscopy. Additionally, these measurements are embedded into a framework using the two-temperature model, valid on ultrashort timescales, as a description for the ablation process and the ablation rate.

Thereby, we could show that the two-temperature model is legitimate for ablation in liquids. However, the ablation depth was strongly altered by the liquid environment. Reflectivity measurements showed that effects responsible for a decreased ablation depth occur at the stage after the energy deposition. This was additionally shown by plasma emission images with a temporal resolution of three ns [3].

We present results of a pump-probe microscopy study, showing the development of reflectivity change during the ablation process from the laser beam impact up to one ns with fs resolution. In pump-probe microscopy, the ablation process is observed by a microscope using a second femtosecond laser beam in combination with a delay stage as illumination source. The study shows the difference between ablation in air and different liquids and the strong interaction of the ablation process with the liquid environment. Possible theories on the laser-triggered processes at the metal-liquid interface are discussed.

[1] V. Amendola, P. Riello, M. Meneghetti, Magnetic Nanoparticles of Iron Carbide, Iron Oxide, Iron@Iron Oxide, and Metal Iron Synthesized by Laser Ablation in Organic Solvents, *J. Phys. Chem. C* 115, 5140 (2011)

[2] A. Kanitz, J.S. Hoppius, M.M. Sanz, M. Maicas, A. Ostendorf, E.L. Gurevich, Synthesis of magnetic nanoparticles by ultrashort pulsed laser ablation of iron in different liquids, *ChemPhysChem* 18 (9), 1155-1164, (2017)

[3] A. Kanitz, J.S. Hoppius, M. Fiebrandt, P. Awakowicz, C. Esen, A. Ostendorf, E.L. Gurevich, Impact of liquid environment on femtosecond laser ablation, *Applied Physics A* 123 (11), 674 (2017)

Fast multi-contrast imaging of the ablation process in liquids adding X-ray bright-field and dark-field methods

S. Reich¹, A. Letzel², T. dos Santos Rolo¹, B. Gökce², S. Barcikowski², T. Baumbach^{1,3}, M. Olbinado⁴, A. Plech¹

¹ Karlsruhe Institute of Technology, IPS, Eggenstein-Leopoldshafen, Germany

² Universität Duisburg-Essen, Technical Chemistry I and Center for Nanointegration Duisburg-Essen (CENIDE), Essen, Germany

³ Karlsruhe Institute of Technology, Laboratory for Applications of Synchrotron Radiation, Karlsruhe, Germany

⁴ European Synchrotron Radiation Facility, 71, avenue de Martyrs, Grenoble, France

stefan.reich@kit.edu

Imaging the ablation bubble and the nanoparticle (NP) distribution during pulsed laser ablation in liquids requires multiscale and fast imaging tools. In situ quantitative detection of the NPs is reserved to X-ray techniques and has been investigated earlier by scanning small-angle X-ray scattering (SAXS) [1,2], while the macroscale has been resolved by optical and X-ray radiography [3]. These techniques in combination revealed several aspects of the ablation process as e.g. that (i) NPs are confined mainly within the vapor bubbles [2,4] and (ii) quenching processes through electrolytes happen already inside the bubble [5].

We present a new approach of merging X-ray scattering detection and imaging in a single fast time-resolved measurement in full field by X-ray multi-contrast imaging. Here, the primary X-ray beam is splitted in many beamlets across the field of view. The change in intensity, position and width are recorded and decoded into absorption, phase and dark-field contrast, respectively. The latter is particularly sensitive on particles in the nanometer to micrometer range [6].

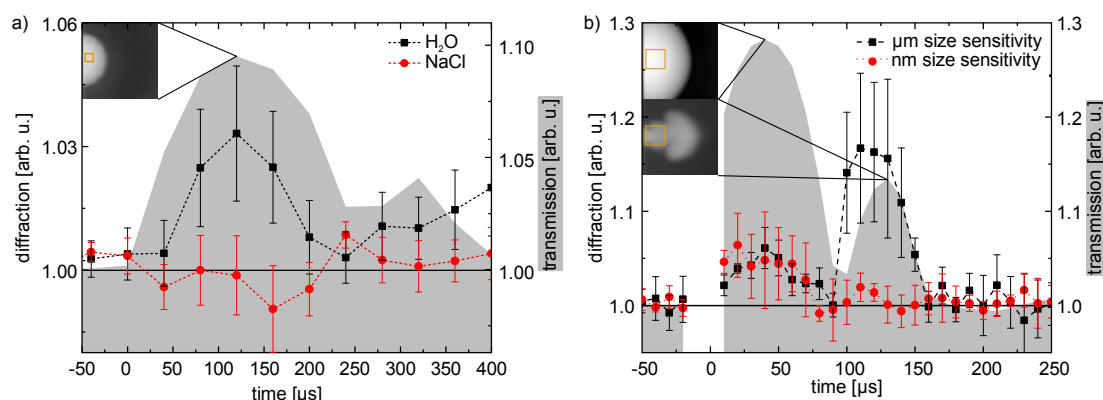


Fig. 1: X-ray dark-field imaging of the ablation process. (a) Diffraction intensity in the center of the first ablation bubble showing a higher amount of big nanoparticles in H₂O compared to NaCl. (b) Nanoparticles are mostly present in the first bubble while vapor micro bubbles dominate in the bubble stem during the first rebound [6].

The validity of the approach is demonstrated on the question of (a) size quenching on the microsecond scale and (b) discrimination of NPs versus microbubbles. As shown in Fig. 1 (a), the scattering intensity of NPs (sizes from 30-200 nm) ablated from a gold target in 0.5 mM NaCl (aq.) is strongly reduced compared to pure H₂O. This confirms our previous results of NP size quenching within the vapor bubble by NaCl [5]. As shown in Fig. 1 (b), by changing the size sensitivity we were further able to distinguish between generated NPs and microbubbles during bubble dynamics on zinc ablation [6].

[1] S. Reich, P. Schönfeld, P. Wagener, A. Letzel, S. Ibrahimkutty, B. Gökce, S. Barcikowski, A. Menzel, T. dos Santos Rolo, A. Plech, Pulsed laser ablation in liquids: Impact of the bubble dynamics on particle formation, *J. Coll. Interf. Sci.*, 489, 106-113, (2017).

[2] S. Ibrahimkutty, P. Wagener, T. dos Santos Rolo, D. Karpov, A. Menzel, T. Baumbach, S. Barcikowski, A. Plech, A hierarchical view on material formation during pulsed-laser synthesis of nanoparticles in liquid, *Sci. Rep.*, 5, 16313, (2015).

[3] S. Reich, J. Göttlicher, A. Letzel, B. Gökce, S. Barcikowski, T. dos Santos Rolo, T. Baumbach, A. Plech, X-ray spectroscopic and stroboscopic analysis of pulsed-laser ablation of Zn and its oxidation, *Appl. Phys. A*, 124, 71 (2018).

[4] S. Ibrahimkutty, P. Wagener, A. Menzel, A. Plech, S. Barcikowski, Nanoparticle formation in a cavitation bubble after pulsed laser ablation in liquid studied with high time resolution small angle x-ray scattering, *Appl. Phys. Lett.*, 101, 103104, (2012).

[5] A. Letzel, B. Gökce, P. Wagener, S. Ibrahimkutty, A. Menzel, A. Plech, S. Barcikowski, Size Quenching during Laser Synthesis of Colloids Happens Already in the Vapor Phase of the Cavitation Bubble, *J. Phys. Chem. C*, 121, 5356-5365, (2017).

[6] S. Reich, T. dos Santos Rolo, A. Letzel, T. Baumbach, A. Plech, Scalable, large area compound array refractive lens for hard X-rays, *Appl. Phys. Lett.*, submitted (2018).

Disentangling competitive hierarchical processes in pulsed laser ablation in liquids

S. Reich¹, A. Letzel², J. Göttlicher¹, T. dos Santos Rolo¹, P. Schönfeld¹, B. Gökce², A. Menzel³, S. Ibrahimkutty^{1,4}, S. Barcikowski², T. Baumbach^{1,5}, A. Plech¹

¹ Karlsruhe Institute of Technology, Institute for Photon Science and Synchrotron Radiation, Eggenstein-Leopoldshafen, Germany

² Universität Duisburg-Essen, Technical Chemistry I and Center for Nanointegration Duisburg-Essen (CENIDE), Essen, Germany

³ Swiss Light Source, Paul-Scherrer Institute, Villigen, Switzerland

⁴ Max-Planck Institute for Solid State Science, Stuttgart, Germany

⁵ Karlsruhe Institute of Technology, Laboratory for Applications of Synchrotron Radiation, Karlsruhe, Germany

anton.plech@kit.edu

Nanoparticle synthesis by pulsed laser ablation in liquids is a process of high complexity. Structure formation occurs on a multiple of time scales from the femtosecond up to second scale and involving atomic scale process to millimetre scale dynamics. In order to bridge fundamental investigations [1] on the atomic scale to post-mortem particle yield [2] we seek to disentangle fundamental steps and interactions by applying a comprehensive set of experimental tools. While fast imaging methods (both with visible light and X-rays) reveal macroscale behaviour such as cavitation bubble dynamics and overall nanoparticle distribution [3,4] we also use microscopical tools, such as small angle X-ray scattering [5] or X-ray spectroscopy [6] for a microscopic view on the nanoscale distribution of matter. Generally, the very early occurrence of nanoparticles is confirmed as well as a rich interaction of particle growth and ejection with the sub-millisecond bubble dynamics and the influence of the laser source [7], in particular differences between nanosecond and picosecond irradiation.

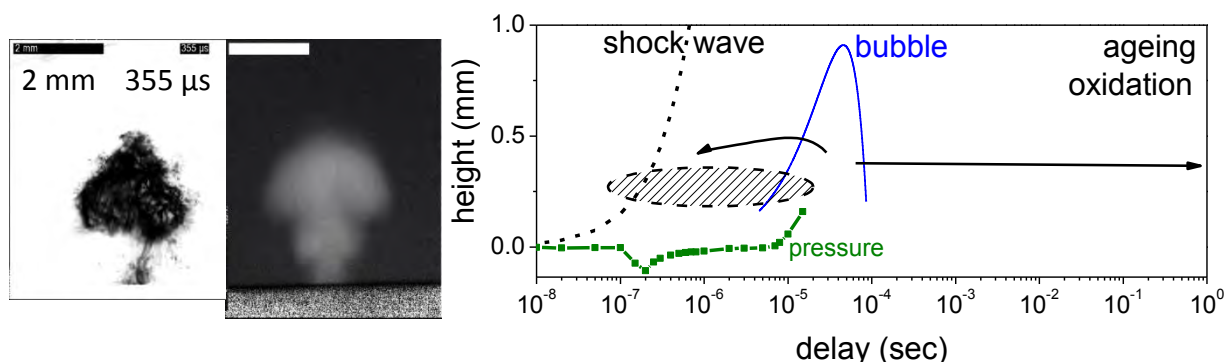


Fig. 1: Left: Visible snapshot of bubble rebound from a Zn wire target together with an X-ray radiograph [6]. Right: Targeted timescales from a sub-microsecond delay to seconds needed for a comprehensive recording of structure formation. Earlier results during bubble cavitation [3-5] are put in context of new data of expanded timescales (as indicated by arrows).

[1] C.-Y. Shih, M. V. Shugaev, C. Wu, and L. V. Zhigilei: *Generation of Subsurface Voids, Incubation Effect, and Formation of Nanoparticles in Short Pulse Laser Interactions with Bulk Metal Targets in Liquid: Molecular Dynamics Study*, J. Phys. Chem. C, **121**, 16549 (2017).

[2] V. Amendola and M. Meneghetti: *What controls the composition and the structure of nanomaterials generated by laser ablation in liquid solution?*, Phys. Chem. Chem. Phys., **15**, 3027 (2013).

[3] S. Ibrahimkutty, P. Wagener, T. dos Santos Rolo, D. Karpov, A. Menzel, T. Baumbach, S. Barcikowski, A. Plech, *A hierarchical view on material formation during pulsed-laser synthesis of nanoparticles in liquid*, Sci. Rep., **5**, 16313, (2015).

[4] S. Reich, P. Schönfeld, P. Wagener, A. Letzel, B. Gökce, A. Menzel, T. dos Santos Rolo, S. Barcikowski, A. Plech: *Pulsed laser ablation in liquids: Interaction of the bubble with particle formation*, J. Coll. Interf. Sci., **489**, 106, (2017).

[5] S. Ibrahimkutty, P. Wagener, A. Menzel, A. Plech, S. Barcikowski: *Nanoparticle formation in a cavitation bubble after pulsed laser ablation in liquid studied with high time resolution small angle x-ray scattering*, Appl. Phys. Lett., **101**, 103104, (2012).

[6] S. Reich, J. Göttlicher, A. Letzel, B. Gökce, S. Barcikowski, T. dos Santos Rolo, T. Baumbach, A. Plech, *X-ray spectroscopic and stroboscopic analysis of pulsed-laser ablation of Zn and its oxidation*, Appl. Phys. A, **124**, 71 (2018).

[7] S. Reich, P. Schönfeld, A. Letzel, S. Kohsakovski, B. Gökce, S. Barcikowski, M. Olbinado, A. Plech: *Fluence threshold behavior on ablation and bubble formation in pulsed laser ablation in liquids*, ChemPhysChem, **9**, 1084 (2017).

Size quenching during laser synthesis of colloids happens already in the vapor phase of the cavitation bubble

A. Letzel¹, B. Gökce¹, S. Ibrahimkuty², A. Menzel³, A. Plech⁴, S. Barcikowski¹

1- Universität Duisburg-Essen, Technical Chemistry I and Center for Nanointegration Duisburg-Essen (CENIDE), Essen, Germany

2- Max-Planck-Institute for Solid State Research, 70569 Stuttgart, Germany

3- c. Paul-Scherrer Institute, 5232 Villigen PSI, Switzerland

4- Karlsruhe Institute of Technology, IPS, Eggenstein-Leopoldshafen, Germany

stephan.barcikowski@uni-due.de

Although nanoparticle synthesis by pulsed laser ablation in liquids (PLAL) is gaining wide applicability, the mechanisms of particle formation, in particular, size-quenching effects by dissolved anions are not fully understood yet. It is known that the size of primary particles ($d \leq 10$ nm), secondary particles (spherical particles $d > 20$ nm) and agglomerates observed ex situ is effectively reduced by the addition of small amounts of monovalent electrolyte to the liquid prior to laser ablation.¹ Furthermore the amount of secondary particles and agglomerates is significantly reduced. As the size distributions of additive-free colloids synthesized by PLAL are polydisperse already inside cavitation confinement, we focus on the particle formation and evolution inside the vapor filled cavitation bubble.^{2,3} This polydispersity may compromise applications of the as synthesized nanoparticles. The cavitation bubbles vapor phase is enriched with ions from the afore added electrolyte.⁴ By probing the cavitation bubbles interior by means of small-angle X-ray scattering (SAXS), the reaction between nanoparticles and ions is observed. We find that particle size quenching occurs already within the first bubble oscillation (approximately 100 μ s after laser impact), still inside the vapor phase.² This shows that nanoparticle-ion-interactions during PLAL are in fact a gas phase phenomenon.

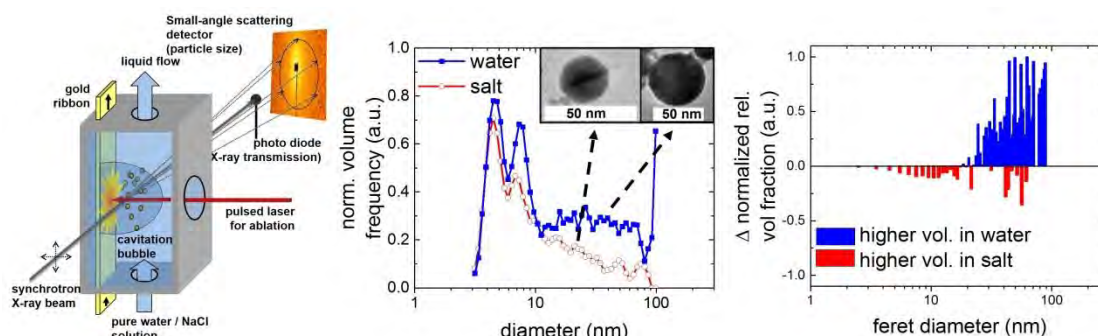


Figure 1. (Left) Scheme of experimental setup. The interior of the cavitation bubble is probed by SAXS. (Middle) In situ size distributions of gold nanoparticles ablated 100 μ s after laser impact in pure water and saline solution obtained from SAXS. (Right) Subtraction of the resulting ex situ TEM-histograms.²

These interactions include size reduction of both primary and secondary particles and a decreased abundance of the latter as shown by in situ SAXS and confirmed by ex situ particle analysis (e.g. SAXS, TEM).⁵

[1] V. Merk, C. Rehbock, F. Becker, U. Hagemann, H. Nienhaus and S. Barcikowski, In Situ Non-DLVO Stabilization of Surfactant-Free, Plasmonic Gold Nanoparticles: Effect of Hofmeister's Anions, *Langmuir* 2014, 30, 4213.

[2] A. Letzel, B. Gökce, P. Wagener, S. Ibrahimkuty, A. Menzel, A. Plech, Size Quenching during Laser Synthesis of Colloids Happens Already in the Vapor Phase of the Cavitation Bubble, *J. Phys. Chem. C* 2017, 121, 5356.

[3] C.-Y. Shih, C. Wu, M. V. Shugaev and L. V. Zhigilei, Atomistic modeling of nanoparticle generation in short pulse laser ablation of thin metal films in water, *J. Coll. Interf. Sci.* 2017, 489, 3.

[4] A. Matsumoto, A. Tamura, T. Honda, T. Hirota, K. Kobayashi, S. Katakura, N. Nishi, K. Amani and T. Sakka, Transfer of the Species Dissolved in a Liquid into Laser Ablation Plasma: An Approach Using Emission Spectroscopy, *J. Phys. Chem. C* 2015, 119, 26506.

[5] A. Letzel, B. Gökce, A. Menzel, A. Plech, S. Barcikowski, Primary particle diameter differentiation and bimodality identification by five analytical methods using gold nanoparticle size distributions synthesized by pulsed laser ablation in liquids, *Appl. Surf. Sci.* 2018, 435, 743.

Dynamics of laser-induced plasma in water and mechanism of cluster formation

T. Sakka

Department of Energy and Hydrocarbon Chemistry, Graduate School of Engineering, Kyoto University

sakka.tetsuo.2a@kyoto-u.ac.jp

Emission spectroscopy of laser ablation plasma in water can be applied to in-situ elemental analysis of a solid target immersed in water [1,2]. This method is called underwater laser-induced breakdown spectroscopy (LIBS), and attracting increasing attention. For instance, Thornton et al. have developed an underwater LIBS instrument for the deep-sea application, and carried out an on-site trial for in-situ analysis of underwater rock samples at the depth of 1000 m [3]. Laser-induced breakdown spectroscopy usually uses intensities of atomic lines for quantitative analysis. It is the free atoms in the plasma that is actually measured by LIBS, and hence, the reactions related to the free atoms in the plasma directly affect the results of the analysis. Especially, cluster formation from the free atoms in the plasma, including oxide formation, changes the density of atomic species, and hence, affects seriously the quantitative relation between the spectral intensity of atomic lines and the amount of the target element.

Since atomic density of laser plasma in water is very high [4], it is very likely that kinetic energy and excitation energy are in local thermal equilibrium [5]. By assuming chemical equilibrium among free atoms and diatomic molecules at each delay time, we estimated the amount of remaining atomic species as a function of temperature. This temperature was then replaced with time by using the experimentally obtained relation between temperature and time [6]. The results agree with the experimental data obtained by transmission spectroscopy. This method, however, cannot be applied to larger clusters, since at low temperatures the thermodynamically stable state must be a single crystal, while we know that numerous nanoparticles are generated in this process. Therefore, kinetic effect of the growth of the clusters or particles should be considered to account for the production of the particles. We have applied a collision-based kinetic model to the cluster formation in the plasma with its temperature decreasing steeply. The results show that a fast temperature decrease or a fast quenching results in the formation of nanoparticles with a finite size distribution (see Figure 1). Such a simulation will help designing a laser-based particle generation process in water.

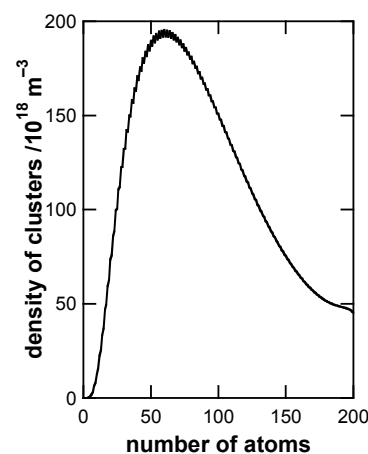


Figure 6. Example of the cluster size distribution obtained by the collision-based kinetic simulation. Atoms and clusters are assumed to coalesce upon collision. Carbon atoms with the density of $2.0 \times 10^{24} \text{ m}^{-3}$ at 8000 K were assumed for the initial conditions, and the temperature was assumed to decay exponentially with the time constant of 5 μs . Cluster size in the abscissa is represented by the number of atoms in a cluster. Here, the activation energy is assumed to depend on the size of the cluster.

- [1] A. E. Pichahchy, D. A. Cremers, M. J. Ferris, *Spectrochim. Acta B*, 52, 25-39 (1997).
- [2] T. Sakka, S. Iwanaga, Y. H. Ogata, A. Matsunawa, T. Takemoto, *J. Chem. Phys.*, 112, 8645-86553 (2000).
- [3] B. Thornton, T. Takahashi, T. Sato, T. Sakka, A. Tamura, A. Matsumoto, T. Nozaki, T. Ohki, K. Ohki, *Deep-Sea Research I*, 95, 20-36 (2015).
- [4] K. Saito, K. Takatani, T. Sakka, Y. H. Ogata, *Appl. Surf. Sci.*, 197-198, 56-60 (2002).
- [5] H. R. Griem, *Phys. Rev.* 131, 1170-1176 (1963).
- [6] K. Saito, T. Sakka, Y. H. Ogata, *J. Appl. Phys.*, 94, 5530-5536 (2003).

Atomistic modelling of the generation of nanoparticles and surface nanostructuring by short pulse laser ablation in liquids

Cheng-Yu Shih, Maxim V. Shugaev, Chengping Wu, and Leonid V. Zhigilei

University of Virginia, Department of Materials Science & Engineering, 395 McCormick Road, Charlottesville, VA 22904-4745, USA

E-mail address: lz2n@virginia.edu

The ability of short pulse laser ablation in liquids to produce clean colloidal nanoparticles and unusual surface morphology and microstructure has been employed in a broad range of practical applications. In this presentation, we report the results of large-scale molecular dynamics simulations aimed at revealing the key processes that control the structure of laser-modified surfaces and nanoparticle size distributions generated by pulsed laser ablation in liquids [1-4]. The simulations of Ag and Cr targets irradiated in water are performed with an advanced computational model combining a coarse-grained representation of liquid environment and an atomistic description of laser interaction with metal targets. The simulations reveal that at relatively low laser fluences, in the regime of melting and resolidification, the presence of a liquid environment suppresses nucleation of sub-surface voids, provides an additional pathway for cooling of the metal surface, and facilitates the formation of nanocrystalline structure of the resolidified region of the metal target (Fig. 1) [1]. One of the most interesting predictions of simulations performed at sufficiently high laser fluences, in the regime of phase explosion, is the emergence of Rayleigh–Taylor and Richtmyer–Meshkov hydrodynamic instabilities at the interface between ablation plume and superheated water (Fig. 1b), leading to the formation of nanojets and emission of large droplets into the water environment (Fig. 1c) [2-4]. The droplets are rapidly quenched and solidified into nanoparticles featuring complex microstructure and metastable phases. Rapid nucleation and growth of small nanoparticles in the expanding metal–water mixing region and the breakup of the hot metal layer into larger droplets due to the hydrodynamic instabilities represent two distinct mechanisms of the nanoparticle formation that yield nanoparticles of two different size ranges as early as several nanoseconds after the laser irradiation. This computational prediction provides a plausible explanation for experimental observations of bimodal nanoparticle size distributions in short pulse laser ablation experiments [4].

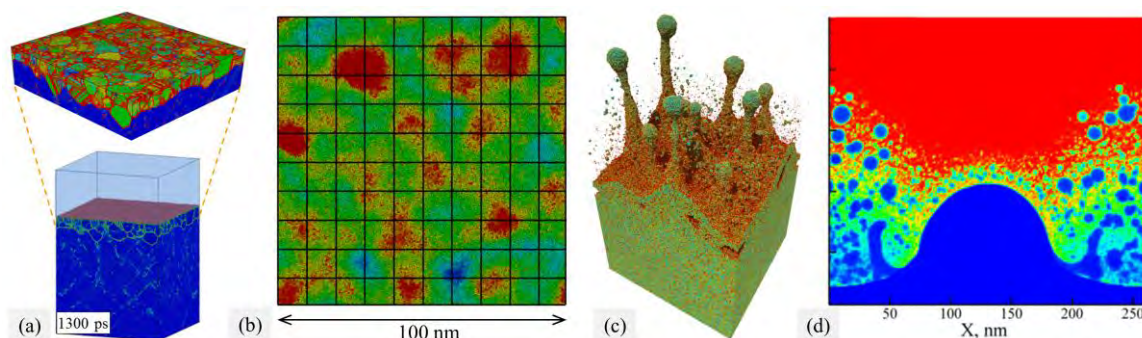


Figure 7. Results of large-scale atomistic simulations of laser interactions with metals in water environment: (a) the nanocrystalline surface layer generated by irradiation of Ag target in water [1]; (b,c) the roughness of ablation plume – superheated water interface generated by the Rayleigh-Taylor instability of the rapidly decelerated interface and leading to nano-jetting and generation of large nanoparticles [2-4]; and (d) mixing of Cr (blue) and water (red) in spatially-modulated laser ablation of a bulk Cr target irradiated in water environment. The molecules representing water environment are blanked in (a) and (c) to expose the surface of the metal targets.

- [1] M. V. Shugaev, C.-Y. Shih, E. T. Karim, C. Wu, L. V. Zhigilei, Generation of nanocrystalline surface layer in short pulse laser processing of metal targets under conditions of spatial confinement by solid or liquid overlayer, *Appl. Surf. Sci.* **417**, 54-63 (2017).
- [2] C.-Y. Shih, C. Wu, M.V. Shugaev, and L.V. Zhigilei, Atomistic modeling of nanoparticle generation in short pulse laser ablation of thin metal films in water, *J. Colloid Interface Sci.* **489**, 3-17 (2017).
- [3] C.-Y. Shih, M. V. Shugaev, C. Wu, and L. V. Zhigilei, Generation of subsurface voids, incubation effect, and formation of nanoparticles in short pulse laser interactions with bulk metal targets in liquid: Molecular dynamics study, *J. Phys. Chem. C* **121**, 16549-16567 (2017).
- [4] C.-Y. Shih, R. Streubel, J. Heberle, A. Letzel, M. V. Shugaev, C. Wu, M. Schmidt, B. Gökce, S. Barcikowski, and L. V. Zhigilei, Two mechanisms of nanoparticle generation in picosecond laser ablation in liquids: The origin of the bimodal size distribution, *Nanoscale*, submitted (2018).

Laser ablation of gold inside water I

N. Inogamov^{1,2}, V. Zhakhovsky^{2,1}, V. Khokhlov¹,

1- Landau Institute for Theoretical Physics of Russian Academy of Sciences, prospekt Akademika Semenova 1A, Chernogolovka 142432, Moscow Region, Russia

2- Dukhov Research Institute of Automatics (VNIIA), Rosatom, Sushchevskaya street, 22, Moscow 127055, Russia

nailinogamov@gmail.com

Studies of formation of metal colloids and surface structures by laser ablation in liquid are very important for technologies and have rather long history [1-7]. In two reports for the ANGEL2018 conference we present physical model and simulation results, shortly described in [7]. We consider ablation of gold bulk target into water by ultrashort pulse (duration less than 1 ps). Absorbed energy belongs to the range 3-9 times higher than ablation threshold 100-150 mJ/cm² for gold (Au) irradiated by ultrashort pulse in vacuum. Laser action causes multistep hierarchy of processes. In case of ablation in liquid this hierarchy lasts much longer than in the case of ablation in vacuum [3,4] or in the case of ablation of absorbing metal into solid transparent matter initially in contact with metal, e.g. a contact between Al and silica [8,9], Figs. 5-7 in [9]. Final stages with overexpansion of vapor bubble and its successive oscillations are well described by Rayleigh-Plesset equation and are confirmed experimentally in many works, see reviews [5,6]. Recently the initial stages lasting from ~ 1 ps to ~ 1 ns were also studied [3,4,7]. The main problem remains in covering the intermediate stages. Our reports for the conference are devoted to this problem. We develop combined approach. The approach is based on using of two-temperature hydrodynamics code (2T-HD), molecular dynamics plus Monte-Carlo (MD-MC) code, and smoothed particles hydrodynamics (SPH) code. Instant 2T-HD profiles are shown in Figure. Comparison of SPH and MD-MC codes is given in the separate report.

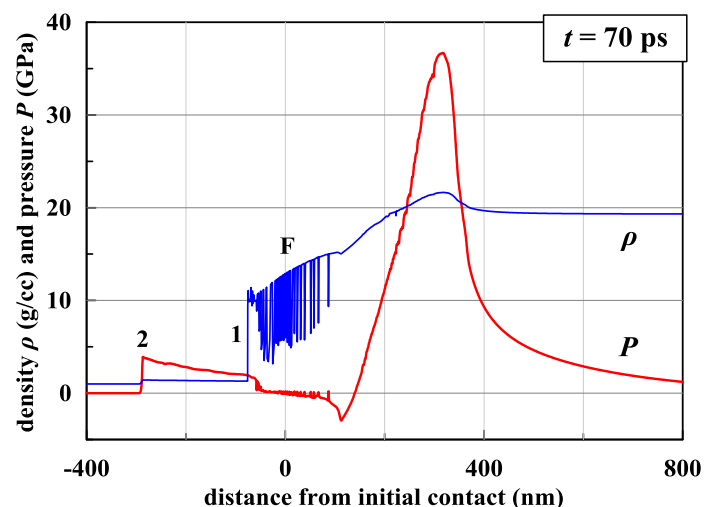


Figure. Formation of very deep nucleation zone F (Foam) later transferring to a wide expanding foamy layer. Pulse duration is 100 fs, absorbed energy is 400 mJ/cm². The density jump 1 corresponds to the Au-water contact. Before laser action the contact was in the point "0". Au is hot, its states near the contact locates above a critical point at the instant shown; pressure in critical state is 0.53 GPa according to equation of state used in 2T-HD. The interval 2-1 is shocked water. The Au layer near the contact approximately 25 nm thick is formed thanks to deceleration of Au by water. Au located to the right relative to this layer doesn't "know" about water. Thus propagation of compression wave and nucleation proceed as in the case of expansion to vacuum. Decrease of pressure behind the shock 2 means that the shock and the contact decelerate. The deceleration begins after a few picoseconds of acceleration of the contact.

- [1] E. Zavedeev et al., Form. of Nanostruct. Upon Laser Ablation of Silver in Liquids, *Quantum Electron.*, vol. 36, pp. 978-980 (2006).
- [2] T.E. Itina, On Nanoparticle Formation by Laser Ablation in Liquids, *J. Phys. Chem. C*, vol. 115, pp. 5044-5048, (2011).
- [3] M.E. Povarnitsyn, T.E. Itina, *Hydrod. Modeling of Fs Laser Ablation... in Liquid*, *Appl. Phys.A*, vol. 117, pp. 175-178, (2014).
- [4] Cheng-Yu Shih et al., Generation of Subsurface Voids, ...: ...MD Study, *J. Phys. Chem. C*, vol. 121, pp. 16549-16567, (2017).
- [5] J. Xiao et al., External field-assisted laser ablation in liquid: ..., *Progress in Materials Science*, vol. 87, pp. 140-220, (2017).
- [6] D. Zhang et al., Laser Synthesis and Processing of Colloids: Fundam. and Appl., *Chem. Rev.*, vol. 117 (5), pp. 3990-4103, (2017).
- [7] N. Inogamov, V. Zhakhovsky, V. Khokhlov, *Laser Ablation of Metal into Liquid: Near Critical ...*, *AIP Conf. Proc.* (accepted).
- [8] M.B. Agranat et al., Strength properties of an aluminum melt at extremely high tension..., *JETP Lett.*, vol. 91, pp. 471-477 (2010).
- [9] N.A. Inogamov et al., Laser acoustic probing of two-temperature zone..., *Contrib. Plasma Phys.*, vol. 51, pp. 367-374 (2011).

Laser ablation of gold into water II: Comparative atomistic and hydrodynamics modeling

V. Zhakhovsky^{1,2}, S. Dyachkov^{1,2}, N. Inogamov^{2,1}

1- Dukhov Research Institute of Automatics (VNIIA), ROSATOM, st. Sushchevskaya, 22, Moscow 127055, Russia
2- Landau Institute for Theoretical Physics of RAS, pr. Akademika Semenova 1A, Chernogolovka 142432, Moscow Region, Russia

6asi1z@gmail.com

Laser-induced fragmentation of gold in water is simulated by molecular dynamics (MD) and smoothed particles hydrodynamics (SPH) methods [1]. MD utilizes the EAM interatomic potential for gold [2] and a newly developed potential for water. The last has EAM form and reproduces the mechanical characteristics of water in liquid state, including its density, bulk modulus and shock Hugoniot. To produce comparative results the equations of states of water and gold for SPH modeling are derived from MD. The tensile strength of gold determined in MD is also utilized in SPH. In our MD and SPH modeling the 2T-HD code [3] is used to obtain the deposited energy distribution in gold during the femtosecond laser pulse. Figure 1 shows good agreement between MD and SPH. Both MD and SPH modeling shows that the velocity of contact between high-dense gold and low-dense water decreases rapidly which leads to development of Rayleigh-Taylor (RT) instability. For the same size of samples the SPH modeling provides results similar to those from MD, but RTI development is slower than in MD due to high numerical viscosity in SPH, see Fig. 2. For a few nanoseconds the RTI produces the gold spikes long enough to be fragmented into nano-droplets via the Plateau-Rayleigh instability, if the contact was accelerated initially above 1 km/s.

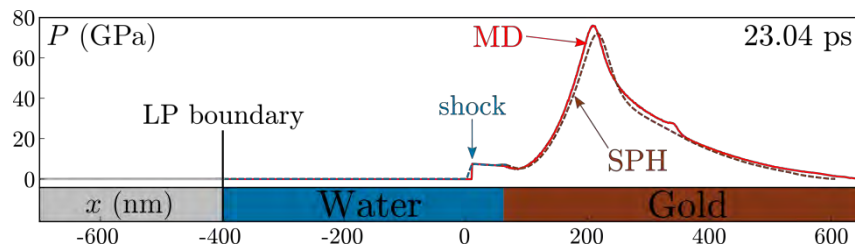


Figure 8 Pressure profiles after 23 ps from the laser pulse simulated consistently by both SPH and MD methods. The shock in water will propagate through the predetermined Lagrangian particle (LP) without reflection. LP position is used as an origin in Fig. 2.

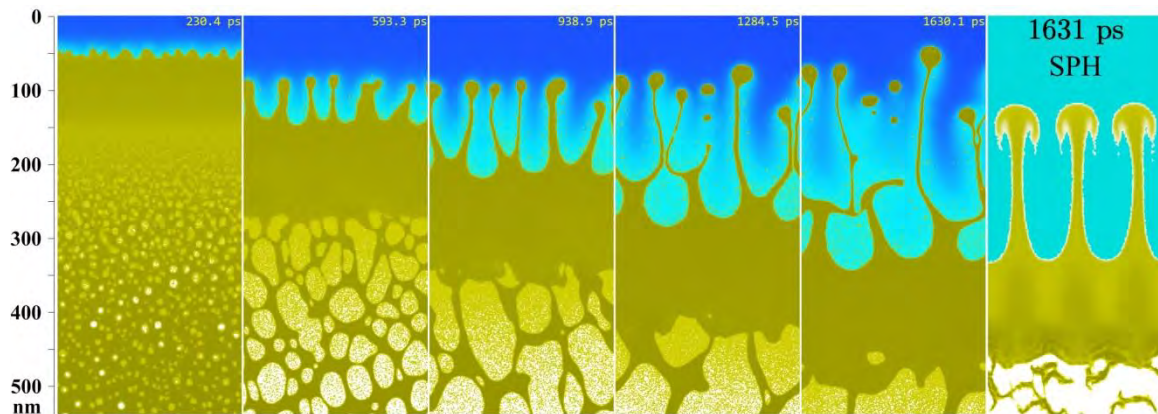


Figure 2 The left five snapshots show density of water (blue) and gold (yellow) in the moving LP coordinate system from MD. Cavitation in molten gold produces a top layer, which velocity toward the water decreases with time. It leads to RT instability producing the gold spikes in water. Similar RTI developed in SPH with initial perturbation mode 3 is shown in the rightmost snapshot.

- [1] S. Dyachkov, A. Parshikov, V. Zhakhovsky, Ejecta from shocked metals: Comparative simulations using molecular dynamics and smoothed particle hydrodynamics, *AIP Conference Proceedings*, vol. 1793, UNSP 100024 (2017)
[2] V.V. Zhakhovskii, N.A. Inogamov, Yu.P. Petrov, S.I. Ashitkov, and K. Nishihara, Molecular dynamics simulation of femtosecond ablation and spallation with different interatomic potentials, *Applied Surface Science*, vol. 255, pp. 9592-9596 (2009)
[3] N.A. Inogamov, V.V. Zhakhovskii, S.I. Ashitkov, et al, Two-temperature relaxation and melting after absorption of femtosecond laser pulse, *Applied Surface Science*, vol. 255, pp. 9712-9716 (2009)

Facet-Dependent Selective Adsorption of Mn-Doped α -Fe₂O₃ Nanocrystals Prepared by Laser Ablation in Liquids

Qinglin Yuan^{1,2}, Pengfei Li¹, Jun Liu¹, Yue Lin², Yunyu Cai¹, Yixing Ye¹, and Changhao Liang^{1,2}

1-Key Laboratory of Materials Physics and Anhui Key Laboratory of Nanomaterials and Nanotechnology, Institute of Solid State Physics, Hefei Institutes of Physical Science, Chinese Academy of Sciences, Shushanhu Road 350, Hefei 230031, China.

2-Hefei National Laboratory for Physical Sciences at the Microscale, University of Science and Technology of China, Jinzhai Road 96, Hefei 230026, China.

Qinglin Yuan: yuanql@mail.ustc.edu.cn

Exploring facet-dependent properties of metal oxides is always attracted topics in nanocrystalline. The doping impurities can significantly affect the crystalline growth and engineer exposed active facets [1-4]. Three kinds of hematite nanocrystallines with preferably exposed facets are prepared through tuning the amount of MnO_x colloidal solution generated by laser ablation in liquids technique. With the increase of addition of MnO_x colloidal solution, Mn doping level goes up, and the hematite crystals evolve sequentially from isotropic polyhedral nanoparticles (NPs) to {116}-faceted saucer-shaped nanosheets (NSs), and then to {001}-faceted hexagonal NSs. These faceted Mn-doped α -Fe₂O₃ NCs also show a facet-dependent adsorption ability toward Pb(II), Cd(II), and Hg(II) heavy-metal ions. Density functional theory (DFT) calculations demonstrated the difference of adsorption energy on the mainly exposed facets and consistency with the experiment. The experimental and computational results not only provide new insights into the facet-related properties, but also guide the design of crystals with exposed active facets for specific applications by using the technique of laser ablation in liquids.

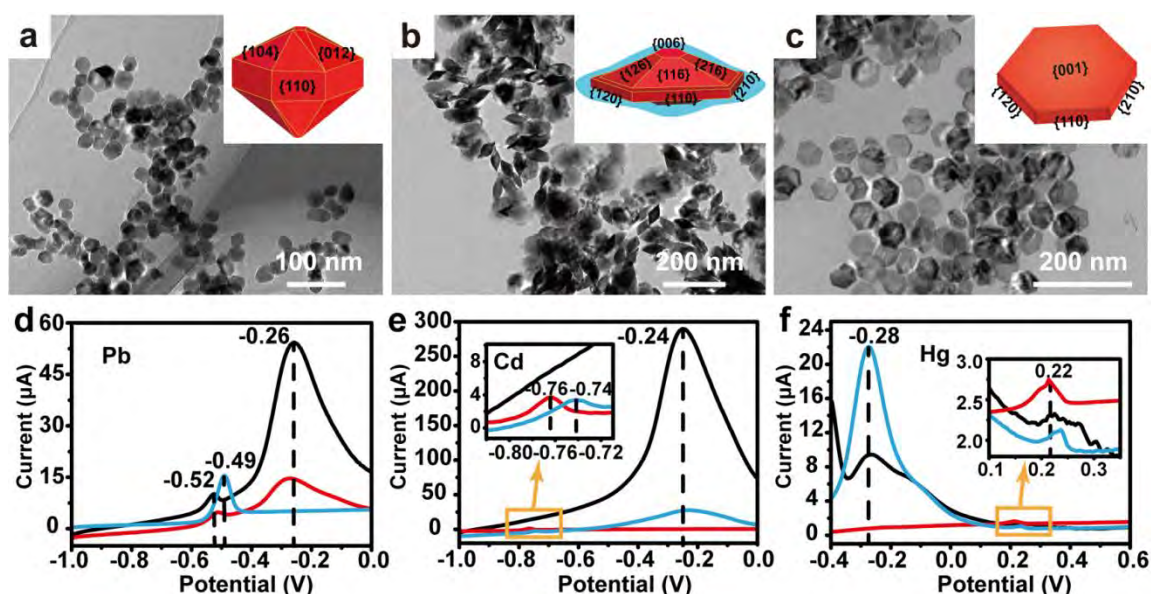


Figure 1 (a-c) Typical low-magnification TEM images of the Mn-doped α -Fe₂O₃ NCs with shapes of polyhedral nanoparticles (NPs), saucer-shaped nanosheets (NSs), and hexagonal nanosheets (NSs). Insets in panels a-c are simulated crystal morphology of the Mn-doped α -Fe₂O₃ NCs. Typical SWASV responses of three Mn-doped α -Fe₂O₃ NCs: polyhedral NPs (black lines), saucer-shaped NSs (red lines), and hexagonal NSs (blue lines), with a modified GCE for analysis of (d) 1.6 μ M Pb(II), (e) 2.0 μ M Cd(II), and (f) 2.0 μ M Hg(II). Insets in panel e and f are magnified views of the respective plots outlined by the gold boxes.

- [1] J. Liu, C. H. Liang, H. M. Zhang, S. Y. Zhang, Z. F. Tian, Silicon-Doped Hematite Nanosheets with Superlattice Structure, *Chemical Communications*, 47., 8040–8042. (2011)
- [2] J. Liu, C. H. Liang, H. M. Zhang, Z. F. Tian, S. Y. Zhang, General Strategy for Doping Impurities (Ge, Si, Mn, Sn, Ti) in Hematite Nanocrystals, *the Journal of Physical Chemistry C*, 116., 4986–4992. (2012)
- [3] J. Liu, C. H. Liang, G. P. Xu, Z. F. Tian, G. S. Shao, L. D. Zhang, Ge-Doped Hematite Nanosheets with Tunable Doping Level, Structure and Improved Photoelectrochemical Performance, *Nano Energy*, 2., 328–336. (2013)
- [4] J. Liu, Y. Y. Cai, Z. F. Tian, G. S. Ruan, Y. X. Ye, C. H. Liang, G. S. Shao, Highly oriented Ge-doped hematite nanosheet arrays for photoelectrochemical water oxidation, *Nano Energy*, 9., 282-290. (2014)

Shape control of PbO nanoparticles produced by laser ablation in liquid

**V.Ya. Shur, E.V. Gunina, D.K. Kuznetsov, E.V. Shishkina, V.E. Kisurin,
E.A. Linker, E.D. Greshnyakov, A.A. Esin**

School of Natural Science and Mathematics, Ural Federal University, 620000 Ekaterinburg, Russia

vladimir.shur@urfu.ru

The water suspensions of PbO nanoparticles (NPs) have been synthesized by laser ablation of lead target in deionized water using IR nanosecond pulse laser. The spherical NPs, circular and hexagonal nanosheets, and nanooctahedron shapes have been produced by variation of the ablation parameters and subsequent suspension heating. Various pretreatments of the target surface have been used.

The Yb fiber laser with 1062 nm wavelength and 100 ns pulse duration has been used. The laser beam has been focused on the target surface (fluence 80 J/cm², spot diameter 40 μm). The NPs synthesis was performed in several stages: target surface pretreatment, laser ablation in deionized water, separated additional fragmentation and heating of the suspension for nanoparticle self-organization and formation of proper shapes [1,2].

The target pretreatment have been realized by plasma or water oxidation. The target surface composition was analyzed by X-ray photoelectron spectrometer K-ALPHA, Thermo Fisher Scientific and by Raman confocal microscope Alpha 300 AR, WiTec. Scanning electron microscope CrossBeam Workstation Auriga, Carl Zeiss, scanning probe microscope MFP 3D SA, Asylum Research, and particle size analyzer Zetasizer Nano ZS, Malvern were used for NPs characterization (ζ - potential, sizes and shapes) after each step of the synthesis.

The dependence of the NPs shape on the energy density, composition and absorption coefficient of the modified surface layer has been revealed. The separated additional fragmentation has been applied to create the nanooctahedron NPs. The process of the formation of nanosheets with hexagonal and during heating of the suspension has been studied in details.

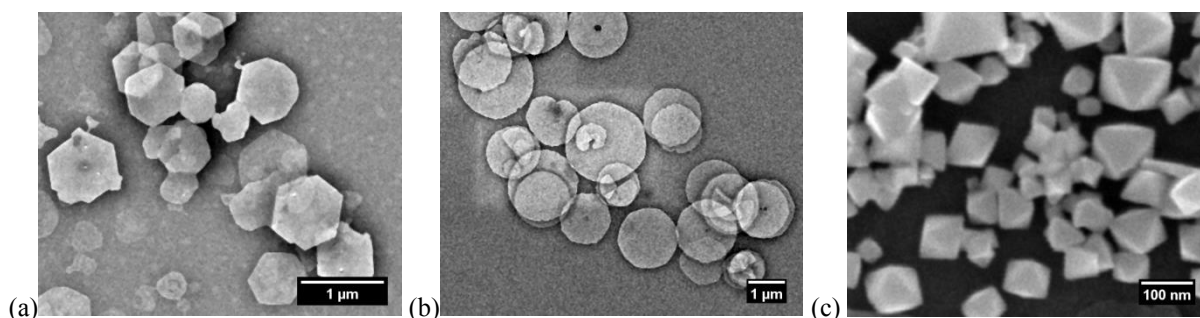


Figure 1. SEM images of PbO nanoparticles produced by laser ablation in deionized water: (a) hexagonal nanosheets, (b) circular nanosheets, (c) nanooctahedrons.

The obtained PbO NPs of various controlled shapes will be used for creation of antibacterial coatings [3] and nanotoxicological research [4].

The equipment of the Ural Center for Shared Use “Modern nanotechnology” School of Natural Science and Mathematics, Ural Federal University was used. The work was supported by Government of the Russian Federation (Act 211, Agreement 02.A03.21.0006).

[1] S. Barcikowski and G. Compagnini, Advanced nanoparticle generation and excitation by lasers in liquids, *Phys. Chem. Chem. Phys.*, vol.15, pp. 3022-3026, (2013).

[2] A.E. Tyurnina, V.Ya. Shur, R.V. Kozin, D.K. Kuznetsov, E.A. Mingaliev, Synthesis of stable silver colloids by laser ablation in water, *Proc. SPIE 9065, Fundamentals of Laser-Assisted Micro- and Nanotechnologies*, 90650D (2013).

[3] P.K. Stoimenov, R.L. Klinger, G.L. Marchin, K.J. Klabunde, Metal oxide nanoparticles as bactericidal agents, *Langmuir*, vol.18 (17), pp. 6679-6686, (2002).

[4] I.A. Minigaliyeva, B.A. Katsnelson, V.G. Panov, L.I. Privalova, A.N. Varaksin, V.B. Gurvich, M.P. Sutunkova, V.Ya. Shur, E.V. Shishkina, I.E. Valamina, I.V. Zubarev, O.H. Makeyev, E.Y. Meshtcheryakova, S.V. Klinova, In vivo toxicity of copper oxide, lead oxide and zinc oxide nanoparticles acting in different combinations and its attenuation with a complex of innocuous bio-protectors, *Toxicology*, vol.380, pp. 72-93, (2017).

Copper Antimony Sulfide (CuSbS₂) nanoparticles by pulsed laser ablation in liquid

V.Vinayakumar¹, B. Krishnan^{1,2}, S. Sepulveda Guzman^{1,2}, D. Avellaneda¹, J.A.A. Martinez^{1,3}, S. Shaji^{1,2,*}

1. Facultad de Ingeniería Mecánica y Eléctrica, Universidad Autónoma de Nuevo León, San Nicolás de los Garza, Nuevo León 66455 México.
 2. Centro de Innovación, Investigación y Desarrollo de Ingeniería y Tecnología (CIIDIT)- Universidad Autónoma de Nuevo León, Apodaca, 66600, Nuevo León, México.
 3. Centro de Investigación e Innovación en Ingeniería Aeronáutica (CIIIA); Facultad de Ingeniería Mecánica y Eléctrica, Carretera a Salinas Victoria, km. 2.3, C.P. 66600 Apodaca, Nuevo León, México.
- E-mail: sshajis@yahoo.com, sadasivan.shaji@uanl.edu.mx

Copper antimony sulphide (CuSbS₂) is a promising candidate in photovoltaic and photodetector applications due to its excellent optoelectronic properties[1-3]. Pulsed laser ablation in liquid (PLAL) is an environment friendly technique for producing nanoparticles of metals, semiconductors, ceramics etc.[4, 5]. In this work, we report the synthesis and characterization of CuSbS₂ nanoparticles (NPs) by pulsed laser ablation in liquid medium. The nanoparticles were synthesized in different liquid media such as acetone, isopropyl alcohol, dimethyl formamide, methanol and ethanol using 2 distinct output wavelengths (532 and 1064 nm) of an Nd:YAG laser (10 ns, 10Hz). Various techniques such as X-Ray Diffraction (XRD), X-Ray Photoelectron Spectroscopy (XPS), Raman Spectroscopy, Transmission Electron Microscopy (TEM), Scanning Electron Spectroscopy (SEM), UV-Vis NIR Spectroscopy and photoluminescence spectroscopy were employed for the characterization of the as prepared nanoparticles. Morphology of the NPs are determined using TEM and SEM. The Crystalline structure of the particles are analyzed by XRD, selected area electron diffraction (SAED) and Raman analysis. XPS analysis is done for the elemental composition and chemical states of the NPs. These nanocolloids showed variation in their absorption edges and optical bandgaps in different solvents as effects of their size and morphologies.

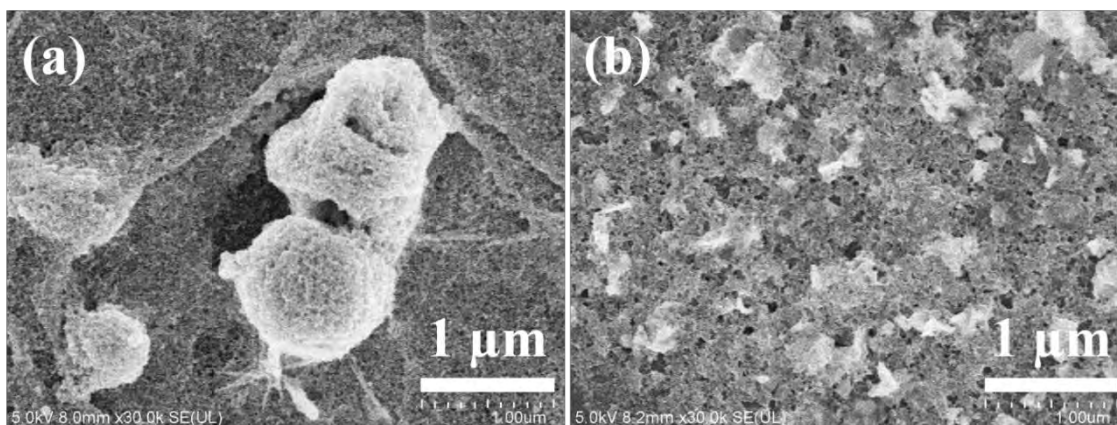


Fig 1. SEM images of CuSbS₂ NPs prepared by 532 nm laser ablation for 30 sec in different liquid media (a) isopropyl alcohol (b) Dimethyl formamide

1. Pal, M., et al., *Phase controlled synthesis of CuSbS₂ nanostructures: Effect of reaction conditions on phase purity and morphology*. Materials & Design, 2017. **136**: p. 165-173.
2. Hao, M., et al., *CuSbS₂ Nanocrystals Applying in Organic-Inorganic Hybrid Photodetectors*. ECS Solid State Letters, 2014. **3**(9): p. Q41-Q43.
3. Welch, A.W., et al., *Accelerated development of CuSbS₂ thin film photovoltaic device prototypes*. Progress in Photovoltaics: Research and Applications, 2016. **24**(7): p. 929-939.
4. Zhang, D., B. Gökce, and S. Barcikowski, *Laser Synthesis and Processing of Colloids: Fundamentals and Applications*. Chemical Reviews, 2017. **117**(5): p. 3990-4103.
5. Mendivil, M.I., et al., *CuInGaSe₂ nanoparticles by pulsed laser ablation in liquid medium*. Materials Research Bulletin, 2015. **72**: p. 106-115.

Characterization of Au and Ag nanoparticle produced by PLAL for considerations on their stability

M. Dell'Aglio^{1,2}, G. Valenza^{1,2}, G. Palazzo², N. Cioffi², R. Picca², A. De Giacomo^{2,1}

1. Institute of Nanotechnology, CNR-NANOTEC, c/o Department of Chemistry, University of Bari, Via Orabona 4, 70126 Bari-Italy
2. Department of Chemistry, University of Bari, Via Orabona 4, 70126 Bari-Italy

marcella.dellaglio@cnr.it

Au and Ag nanoparticles are produced in ultrapure water (milliQ), in absence and in presence of different salts, by pulsed laser ablation in liquid (PLAL) with particular attention on the target cleaning procedure to avoid any organic contaminant in the final colloidal solution. The NPs were characterized by UV-Vis absorption spectroscopy, Dynamic Light Scattering (DLS), ζ -potential, Transmission Electron Microscopy (TEM) and X-ray Photoelectron Spectroscopy (XPS) in order to understand the intrinsic NPs stability that is still a controversial issue in the literature. The stability of the metal NPs produced by PLAL in water is usually attributed to a partially surface oxidation [1] or to other kind of mechanisms of colloidal stabilization, as for example the anions adsorption on the NP surface, as reported in the most of literature, or it can be mainly ascribed to the physical processes occurring during the ablation in water [2] e.g. the laser induced plasma and cavitation bubble processing [3]. In this work, some critical considerations have been reported on the NPs stability, starting from the NPs characterization and linking these results to the PLAL processes. A special emphasis has been done on AuNPs with their production at different pH in order to clarify if the amphifunctional groups, eventually due to the surface oxidation, can play a role in the stabilization or not. A set of experiment were also performed to test the reduction capacity of the gold surface with different cations (Ag^+ and K^+) having different affinity to reduction. The attention was finally focus on the possibility that the excess of electrons formed within the plasma phase during the PLAL processes could charge the metallic particles giving them stability.

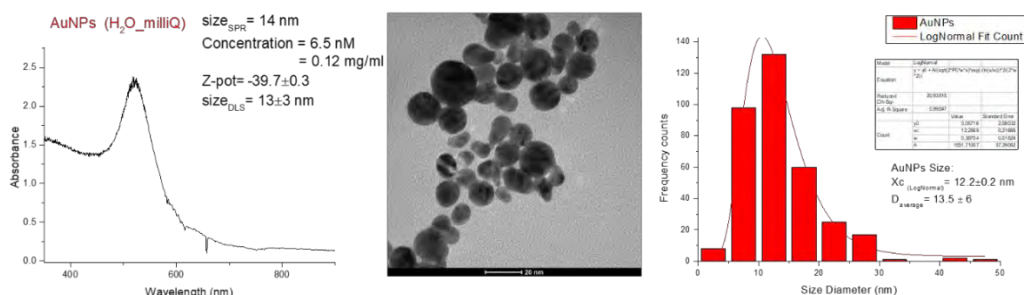


Fig. 1 SPR spectrum, DLS and Z-pot measurements, TEM images and statistics of AuNPs produced by PLAL in Milli-Q water.

[1] J.P. Sylvestre, S. Poulin, A.V. Kabashin, E. Sacher, M. Meunier, J.H.T. Luong, Surface chemistry of gold nanoparticles produced by laser ablation in aqueous media, *J. Phys. Chem. B* 108 (2004) 16864.

[2] Palazzo, G., Valenza, G., Dell'Aglio, M., De Giacomo, A. On the stability of gold nanoparticles synthesized by laser ablation in liquids (2017) *Journal of Colloid and Interface Science*, 489, pp. 47-56.

[3] M. Dell'Aglio, R. Gaudiuso, O. De Pascale, A. De Giacomo, Mechanisms and processes of pulsed laser ablation in liquids during nanoparticle production, *Appl. Surf. Sci.* 348 (2015) 4–9.

Laser fabrication of nanoalloys for catalysis: generalities and opportunities

V. Amendola

Department of Chemical Sciences, University of Padova, Via Marzolo 1, 35131 Padova

vincenzo.amendola@unipd.it

Nanoalloys, being different from bulk-alloys and single-metal nanoparticles, are endowed with peculiar electronic structures, physical properties and chemical reactivity. Traditionally, these features opened great prospects in heterogeneous catalysis, a field which also requires tuneable alloy composition, high purity, easy processing of nanoparticles.

Laser synthesis of colloids is intrinsically suited for the realization of nanoalloys having many of the required features for an heterogeneous catalyst. In fact, the reports about catalytic applications of laser generated multimetallic nanoparticles have flourished in the last few years. In addition, alloys with composition not easily achievable because of thermodynamic constraints, are often accessible by laser synthesis thanks to the fast mechanism of nanoparticles nucleation and growth.[1]

This talk will provide an overview of the topic, with a tutorial approach aimed at neophytes in the field. Some of the challenges emerged so far in the exploitation of laser generated nanoalloys for heterogeneous catalysis will be also highlighted.

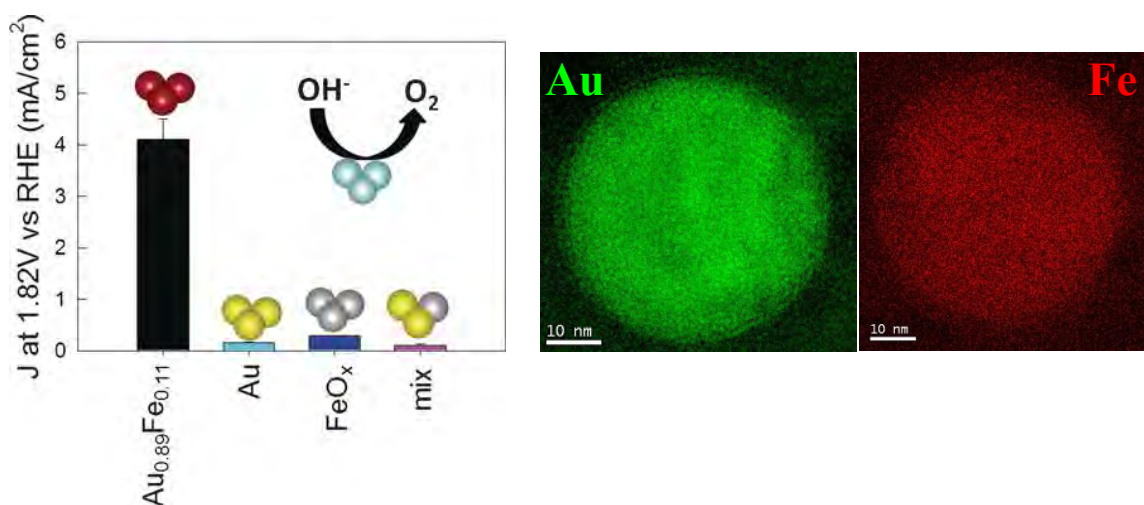


Figure 9. Left: Laser generated Au-Fe nanoalloys provide superior electrocatalytic oxygen evolution performances compared to single element equivalents. From ref.[2] Right: Although Au-Fe alloys are not thermodynamically stable, the production of homogeneous alloys by laser ablation of an Au-Fe target was possible, as demonstrated by the bidimensional element distribution map obtained with transmission electron microscopy analysis. From ref.[3]

[1] J. Lam, J. Lombard, C. Dujardin, G. Ledoux, S. Merabia, D. Amans, Dynamical study of bubble expansion following laser ablation in liquids, *Appl. Phys. Lett.* 108, 074104, (2016).

[2] I. Vassalini, L. Borgese, M. Mariz, S. Polizzi, G. Aquilanti, P. Ghigna, A. Sartorel, V. Amendola, I. Alessandri, Enhanced Electrocatalytic Oxygen Evolution in Au-Fe Nanoalloys, *Angew. Chem. Int. Ed.* 56, 6589 (2017).

[3] V. Amendola, M. Meneghetti, O. M. Bakr, P. Riello, S. Polizzi, D. H. Anjum, S. Fiameni, P. Arosio, T. Orlando, C. de Julian Fernandez, F. Pineider, C. Sangregorio, A. Lascialfari, Coexistence of plasmonic and magnetic properties in Au 89 Fe 11 nanoalloys, *Nanoscale* 5, 5611-5619 (2013).

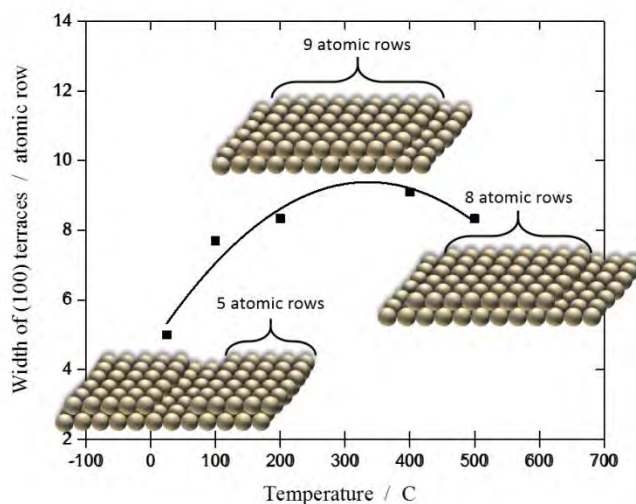
Catalysis and electrocatalysis on well-defined model systems generated by laser ablation

D. Guay

*INRS Énergie Matériaux Télécommunication, 1650 boul. Lionel Boulet,
CP 1020, Varennes, QC Canada J3X 1S2
E-mail: guay@emt.inrs.ca*

The intrinsic catalytic and electrocatalytic activity of materials is critically dependent on their composition and surface orientations. It is well known that the addition of a second element (bimetallic catalysts) to a metal has a profound effect on the activity and stability of the resulting materials through ensemble, ligand, and strain effects. Likewise, it has been known for a long time that an element's electrocatalytic activity is critically dependent upon surface orientation and atomic surface arrangement. For example, the following electrocatalytic reactions occur more easily at metals that exhibit perfect two-dimensional (100) terraces: (i) reduction of CO on copper; and (ii) ammonia oxidation on platinum. Other examples abound in the literature. Accordingly, it is of the utmost importance to control both the composition and surface orientation of electrodes to determine as precisely as possible the intrinsic electrocatalytic activity of materials.

Pulsed laser deposition (PLD) was used to prepare epitaxial thin films with well-defined composition and surface orientation. PLD is a particularly attractive deposition method for the formation of epitaxial layers, since it has an unmatched ability to vary the kinetic energies of the species impinging on the substrate, along with the nature and the pressure of the gas in the deposition chamber. Most importantly, almost all elements can be deposited by PLD. Moreover, PLD is considered a non-equilibrium deposition technique and several metastable alloys have been prepared so far, allowing the investigation of bimetallic compounds that are kinetically stable but would be difficult to obtain by following a heat-treatment step, as the elements are not miscible, or only partially so.



In this presentation, we will focus on Pt alloys thin films with (100) orientation and investigate the effect of the alloying element (Ir, Ru, Rh and Pd) on the electrocatalytic activity for the oxidation of ammonia (NH_3). We first undertook a detailed investigation of the growth and the surface arrangement of Pt thin films deposited on (001)-oriented MgO substrates as a function of the deposition conditions. It will be shown that the width of the (100) terraces vary with the deposition temperature and shows a maximum value corresponding to 9 atoms at 325°C . Then, we will look at the effect of the alloying element on both the growth mode and the electrocatalytic activity. We will show that all Pt alloys thin films investigated here exhibit only one diffraction peak (the (001) peak) and a 4-fold in-plane symmetry, indicating epitaxial growth is achieved independently of the deposition temperature. The pole figure indicates that all films exhibit a Pt(001)[010]//[010](001)MgO cube-on-cube epitaxial relationship, consistent with the AFM images. The effect of the alloying element (Ir, Ru, Rh and Pd) on the electrocatalytic activity for the oxidation of NH_3 will be discussed.

Prospects and challenges of laser-generated nanoparticles for industrial applications in catalysis

G. Marzun¹, S. Kohsakowski¹, T. Vinnay², S. Siebeneicher¹, S. Barcikowski¹

1- Technical Chemistry I and Center for Nanointegration Duisburg-Essen (CENIDE), University of Duisburg-Essen, Universitätsstr. 7, 45142 Essen, Germany

2- Carl-Padberg Zentrifugenbau GmbH, Geroldsecker Vorstadt 60, 77933

galina.marzun@uni-due.de

Pulsed laser ablation in liquids (PLAL) has already reached the interest of many researchers, especially because of the nanoparticles' unique features. So far academic investigations show a significant progress and a lot of activity in this field. However, up to now less industrial directions are addressed or reported. The time has come, that also the interest from several industries was awoken.

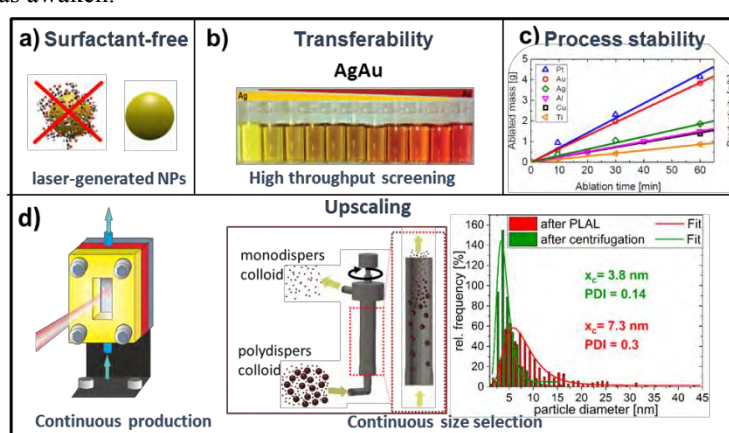


Figure 10 Benefits of PLAL: surfactant-free nanoparticles (a), transferability [2] (b), process stability [3] (c) and upscaling using a continuous ablation chamber and a bowl centrifuge

The benefits of laser-generated nanoparticles are clear: a) a surfactant-free particle surface, which allows a high accessibility of reactants or a selective functionalisation by molecules, b) the transferability of the synthesis route to a variety of materials and liquids that enables a high-throughput screening of materials and c) a good reproducibility as well as the possibility for a continuous linear nanoparticle production that allows an upscaling. Especially the last two points are paramount, since upscaling of wet chemical methods is often not trivial and synthesis parameters are often difficult to transfer to other materials. Thus a continuous NP synthesis by PLAL and transferability to different kind of materials open new possibilities. Upscaling to a pilot scale is conceivable which enables feasibility studies with screening approaches. However, therefore not only a high quantity of NPs are needed, but also a top quality. A big issue of laser-generated NPs is the broad size distribution and the limited efficiency to size control. Even though several approaches for size control of laser-synthesized NPs are established (adding a salt, re-irradiation or centrifugation [4]), the main challenge is to upscale the synthesis by ensuring the purity of the catalyst. Thus, a method is in investigation how to optimize the NP size in a continuous process for a large scale using tubular bowl centrifugation. After the continuous centrifugation, the small NPs can be directly transferred in a static mixer for a continuous particle adsorption. But also the *in situ* particle adsorption appears to be another attractive approach for a one-step laser synthesis of small NPs adsorbed on a support as a co-catalyst.

[1] D. Zhang, B. Gökce, A. Barcikowski, Laser synthesis and processing of colloids: fundamentals and applications, *Chemical Reviews*, 117 (5), 3990-4103 (2017)

[2] A. Neumeister, J. Jakobi, C. Rehbock, J. Moysig, S. Barcikowski, Monophasic ligand-free alloy nanoparticle synthesis determinants during pulsed laser ablation of bulk alloy and consolidated microparticles in water, *Physical Chemistry Chemical Physics*, 16 (43), 23671-23678 (2014).

[3] R. Streubel, S. Barcikowski, B. Gökce, Continuous multigram nanoparticle synthesis by high-power, high-repetition-rate ultrafast laser ablation in liquids, *Optics letters* 41 (7), 1486-1489 (2016).

Photothermal effects of gold nanoparticles. Applications in chemistry and cell biology

Guillaume Baffou

Institut Fresnel, CNRS, Aix Marseille Univ, Centrale Marseille, Marseille (France)

guillaume.baffou@fresnel.fr

Under illumination at their plasmonic resonance, gold nanoparticles can behave as efficient nanosources of light remotely controllable by light. This scheme is at the basis of a field of research named *thermoplasmonics* [1,2]. Many applications of thermoplasmonics have been developed these last two decades, e. g. in nanochemistry, biosensing, microscopy, biomedicine, magnetic recording, etc.

This presentation will focus on thermoplasmonics. The importance and impact of this field of research will be presented through an short overview of the applications. Then, research work carried out at the Institut Fresnel in Marseille will be presented, namely in microbubble formation [3], microscale hydrothermal chemistry [4] and cell biology.

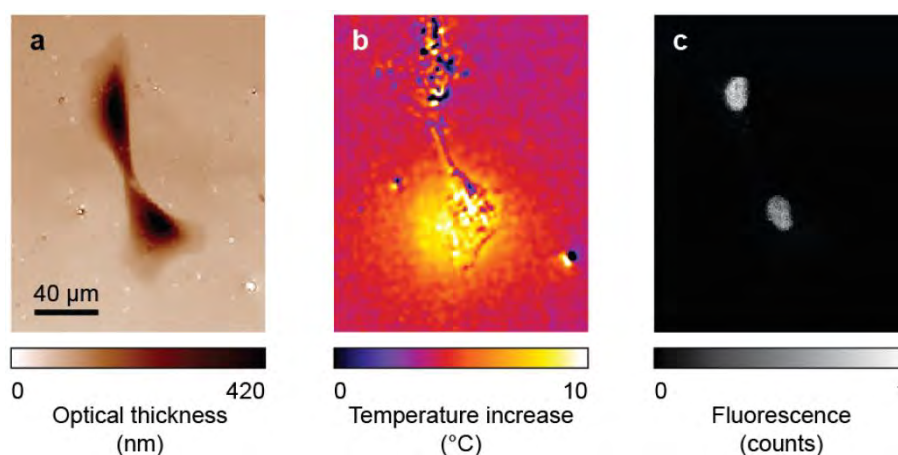


Figure 1. (a) RPE cells on gold nanoparticles imaged using QLSI. (b) Map of the temperature increase when shining a cell with a laser using quantitative phase imaging [5]. (c) Parallel acquisition of the fluorescence to monitor the expression of heat-shock proteins.

- [1] G. Baffou and R. Quidant, Thermo-plasmonics: using metallic nanostructures as nano-sources of heat, *Lasers & Photonics Reviews*, 7, 171-187, (2013).
- [2] G. Baffou, *Thermoplasmonics* (Cambridge University Press) (2017).
- [3] G. Baffou, J. Polleux, H. Rigneault, S. Monneret, Super-Heating and Micro-Bubble Generation around Plasmonic Nanoparticles under cw Illumination, *Chemical Society Reviews*, 43, 3898-3907 (2014)
- [4] H. Robert, F. Kundrat, E. Bermudez-Urena, H. Rigneault, S. Monneret, R. Quidant, J. Polleux, G. Baffou, Light-Assisted Solvothermal Chemistry Using Plasmonic Nanoparticles, *ACS Omega*, 1, 2-8 (2016)
- [5] G. Baffou*, P. Bon, J. Savatier, J. Polleux, M. Zhu, M. Merlin, H. Rigneault and S. Monneret, Thermal Imaging of Nanostructures by Quantitative Optical Phase Analysis, *ACS Nano*, 6, 2452–2458 (2012)

Nanobubbles generated by laser heated nanoparticles

J. Lombard¹, T. Biben¹, S. Merabia¹

1- Institut Lumière Matière, CNRS – Université Lyon 1,

samy.merabia@univ-lyon1.fr

Metallic nanoparticles may be heated up by a laser pulse, generating locally very large temperature gradients in a liquid environment. If the energy supplied by the laser is high enough, transient vapor nanobubbles may be produced around the heated nanoparticles, growing and expanding in the liquid on nanosecond timescale. Plasmonic vapor nanobubbles have been shown to be efficient in cancer cell therapy, as they concentrate large amounts of thermomechanical stresses that may be employed to destruct diseased genetic material [1, 2]. Despite their promising use, the fundamental description of the mechanisms at the origin of nanobubble generation is still missing. Theoretical modeling of the process at the origin of ultrafast cavitation around optically heated nanoparticles is thus highly desired to understand both the nanobubble threshold and their dynamics.

In this contribution, we model nanobubble generation driven by thermal transport from optically heated gold nanoparticles in water [3], using a hydrodynamic phase field model. We show that nanobubble generation corresponds to the crossing of the spinodal line in water at a distance 1-2 nm from the hot nanoparticle. We compare our simulation results with available experimental data, and conclude that nanobubbles are generated around molten nanoparticles [4]. We will also discuss the physics of nanobubble dynamics. We unveil the major role played by ballistic thermal transport inside the nanobubble [5]. On the basis of a simple kinetic model, we can predict the maximal nanobubble size as a function of the laser fluence, in good agreement with experimental observations [5].

Finally, if time permits we will present preliminary results concerning the acoustic wave generated by fast water expansion preceding vaporization.

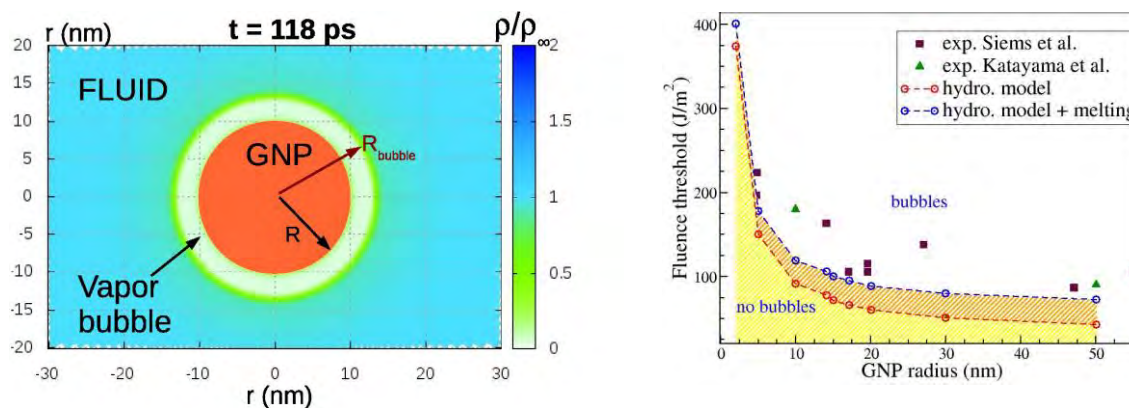


Figure 11 Left: simulation of the formation of a vapor nanobubble generated by a heated nanoparticle. From [3]. Right: comparison between the nanobubble threshold obtained in the simulations and experimental results. From [4].

- [1] Z. Qin and J.C Bischoff, *Chem. Soc. Rev.*, 2012, 41, 1191–1217
- [2] A. Siems, S.A.L. Weber, J. Boneberg and A. Plech, *New J. Phys.* 13 043018 (2011)
- [3] J. Lombard, T. Biben, S. Merabia, *Phys. Rev. Lett.* 112 106701 (2014)
- [4] J. Lombard, T. Biben and S. Merabia, *J. Phys. Chem. C* 121, 15402-15415 (2017)
- [5] J. Lombard, T. Biben and S. Merabia, *Nanoscale* 8, 14870-14876 (2016)

Laser irradiation guided anchoring of Au colloidal nanoparticles on α -Fe₂O₃ nanoparticles for photothermal effect

Y. Y. Cai¹, H. Zhang¹, J. Liu¹, Y. X. Ye¹, C. H. Liang¹

1- Key Laboratory of Materials Physics, Institute of Solid State Physics, Hefei Institutes of Physical Science, Chinese Academy of Sciences, Shushanhu Road 350, Hefei 230031, China

Main author email address: yycail@issp.ac.cn; chliang@issp.ac.cn

Tailoring the separation and position of noble metal nanoparticles in clusters could induce peculiar near-infrared (NIR) extinctions [1,2]. Herein, a mixture of Au and α -Fe₂O₃ nanoparticles dispersed in deionized water were irradiated by a pulse laser with wavelength of 355 nm and pulse width of 7 ns. With laser irradiation for several minutes, Au/ α -Fe₂O₃ nanocomposites form and present strong absorption band in NIR region. It's believed that small separation of Au nanoparticles gives rise to the enhanced NIR extinction in absorption spectrum [3]. Such products are proved to be with excellent performance in photothermal treatment for human lung carcinoma cells. Compared with traditional chemical methods, our approach could avoid complicated procedures and toxic chemical reagents, which provide an available strategy for convenient preparing green therapy agents for cancer.

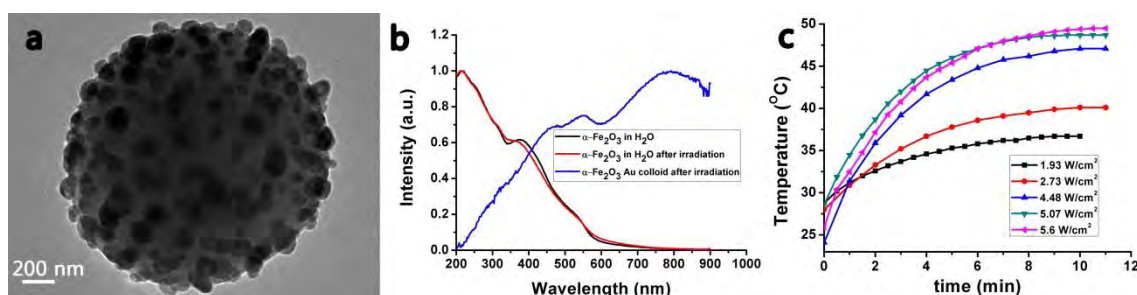


Figure 12 Characterization of Au anchored α -Fe₂O₃ nanoparticle : (a) TEM image; (b) Extinction spectra of Au anchored α -Fe₂O₃ nanoparticle, pure α -Fe₂O₃ nanoparticle in water before and after irradiation by 355 nm laser; (c) Temperature change with time under the irradiation of 808 nm laser.

- [1] J. A. Fan, C. H. Wu, K. Bao, J. M. Bao, R. Bardhan, N. J. Halas, V. N. Manoharan, P. Nordlander, G. Shvets, F. Capasso, Self-Assembled Plasmonic Nanoparticle Clusters, *Science*, 28, 1135-1138, (2010).
 [2] R. J. Stover, E. Moaseri, S. P. Gourisankar, M. Iqbal, N. K. Rahbar, B. Changalvaie, T. M. Truskett, K. P. Johnston, Formation of Small Gold Nanoparticle Chains with High NIR Extinction through Bridging with Calcium Ions, *Langmuir*, 32, 1127-1138, (2016).
 [3] A. Klinkova, R. M. Choueiri, E. Kumacheva, *Chem. Soc. Rev.*, 43, 3976-3991, (2014)

Transient Absorption Spectroscopic Study on Phase Transition Dynamics of Phthalocyanine Nanocrystals Induced by ns-laser Irradiation in Liquid

R. Kihara, Y. Ishibashi, T. Asahi

Graduate School of Science and Engineering, Ehime University, 3 Bunkyo, Matsuyama, Ehime, Japan

Main author email address: e862001u@mails.cc.ehime-u.ac.jp

Intense pulse laser irradiation to organic microcrystals dispersed in a poor solvent leads to not only formation of nanoparticle colloids but also phase transition in crystal structure. The mechanism has been discussed in terms of ultrafast transient heating of micro- and nanocrystals excited densely with a laser pulse. [1] Here, we induced the crystalline phase transition of copper phthalocyanine (CuPc) nanocrystals in ethanol by ns-laser irradiation, and investigated the dynamics and mechanism by measuring the transient absorption spectra during and after irradiation of single-shot of pulse laser.

Figure 1 shows the steady state absorption spectra of β -phase CuPc nanocrystals colloid which excited for 1 min using second harmonic ns Nd³⁺YAG laser (532-nm of wavelength, 8 ns in fwhm and 200 mJ/cm² of laser fluence). After laser irradiation, the 780 nm absorption peak decreased and the 600 nm peak increased. The spectral shape change was described well as to a change in molecular packing from thermally stable β -phase to metastable α -phase in nanocrystals. [2] Figure 2 shows the transient absorption spectra of CuPc nanocolloid during and after single ns-pulse irradiation at 200 mJ/cm². At -6 to 0 ns, the transient absorption spectra having a positive peak at 750 nm and negative peaks at 580 nm and 790 nm wavelength were observed. The spectral shape could be assigned to the “hot band” of the electrically ground state formed through rapid nonradioactive relaxation of the excited state. Temperature of excited nanoparticles at 0 ns was estimated more than approximately 300°C by comparing with the temperature difference absorption spectra. A broad background increased in the spectra after 2 ns and disappeared in 100 ns. The broad signal will indicate that the formation and disappearance of nanoscale vapor bubbles (nanobubbles) around the CuPc nanocrystal’s surface. A similar nanobubble formation was reported for gold nanoparticles colloid excited with intense picosecond laser. [3] At 10 ns, on the other hand, a new positive peak at 620 nm characteristic of the absorption of α -phase CuPc was observed, so that the phase change was considered to finish in a 10-ns time scale. From the observed results, the ns-laser induced phase transition dynamics could be summarized in Figure 3.

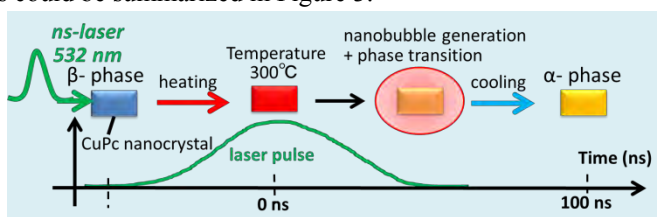


Figure 3 Schematic illustration of ns-laser induced phase transition of CuPc nanocrystal.

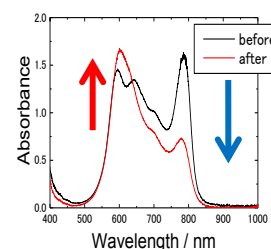


Figure 1 Absorption spectra of CuPc colloid before and after laser irradiation at 200 mJ/cm² for 1 min

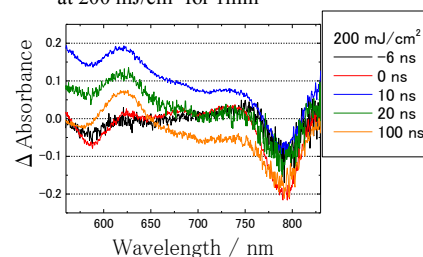


Figure 2 Transient absorption spectra of CuPc colloid excited by single ns-pulse irradiation at 200 mJ/cm²

[1] T. Asahi, T. Sugiyama, and H. Masuhara, Laser Fabrication and Spectroscopy of Organic Nanoparticles, *Acc. Chem. Res.*, 41, 1790-1798, (2008).

[2] S. Karan, B. Mallik, Templating Effects and Optical Characterization of Copper (II) Phthalocyanine Nanocrystallites Thin Film: Nanoparticles, Nanoflowers, Nanocabbages, and Nanoribbons, *J. Phys. Chem. C*, 111, 7352-7365, (2007).

[3] T. Katayama, K. Setoura, D. Werner, H. Miyasaka and S. Hashimoto. Picosecond-to-Nanosecond Dynamics of Plasmonic Nanobubbles from Pump-Probe Spectral Measurements of Aqueous Colloidal Gold Nanoparticles, *Langmuir*, 30, 9504-9513, (2014).

Spatial distribution of breakdown plasma under laser exposure of colloidal solutions of nanoparticles

E.V. Barmina¹, A.V. Simakin¹, and G. A. Shafeev^{1,2}

¹Wave Research Center of A.M. Prokhorov General Physics Institute of the Russian Academy of Sciences, 38, Vavilov street, 119991 Moscow Russian Federation

²National Research Nuclear University MEPhI (Moscow Engineering Physics Institute), 31, Kashirskoye highway, 115409, Moscow, Russian Federation

shafeev@kapella.gpi.ru

The spatial structure of the plasma of laser breakdown of colloidal solutions is experimentally studied. It is found that the breakdown occurs in isolated points of the liquid (Fig. 1) under irradiation of the colloidal solution of Co nanoparticles in water with scanning beam of a Nd:YAG laser with pulse duration of 10 ns and energy per pulse of 2 mJ. These points are associated with the fluctuations of nanoparticles density that leads to appearance of dimers and aggregates. The fluctuations of their density is modelled within the formalism of stochastic geometry. The critical concentration of fluctuations is related to the average density of nanoparticles. The laser breakdown of the colloidal solutions at the peak intensity of 10^{10} W/cm² takes place in the regions where the both the size and density of fluctuations exceed certain values. Aggregates of nanoparticles may be responsible for the enhancement of the laser field. In turn, these fluctuations explain the influence of laser irradiation on the activity of several radionuclides [1,2], since the enhancement factor may be as high as $10^3 - 10^4$ [3]. The influence of laser radiation on the nuclides is interpreted via the influence of enhanced laser intensity on their electronic structure. The modelling predicts different behavior of nanoparticles density in cases of spherical and elongated nanoparticles.



Fig. 1. Microscopic view of plasma entities (negative image). Each vertical line corresponds to single laser pulse. Scale bar denotes 250 μm . The laser breakdown of liquid occurs around fluctuations of nanoparticles density. As one can see, plasma entities are isolated from each other. Similar features are observed at energy per pulse up to 700 mJ.

1. S. N. Andreev, E. V. Barmina, V. G. Kalinnikov, A. V. Simakin, A. A. Smirnov, V. I. Stegailov, S. I. Tyutyunnikov, G. A. Shafeev, and I. A. Scherbakov, Observation of Laser-Light Effect on ¹³⁷Cs Radioactivity in Colloidal Gold: First Results, *Physics of Particles and Nuclei Letters*, Vol. 14, No. 6, pp. 894–897 (2017).
2. E. V. Barmina, A. V. Simakin, V. I. Stegailov, S. I. Tyutyunnikov, G. A. Shafeev, I. A. Shcherbakov, Effect of laser radiation on aqueous solutions of beta-active nuclides, *Quantum Electronics* V.47(7) pp. 627-630 (2017).
3. E. Hao, G.C. Schatz, Electromagnetic fields around silver nanoparticles and dimers, *J. Chem. Phys.*, 120 (1), 357 (2004).

Generation of H₂, O₂ and Hydrogen peroxide by laser-induced breakdown aqueous solutions of nanoparticles

E. V. Barmina¹

1-Wave Research Center of A.M. Prokhorov General Physics Institute of the Russian Academy of Sciences, 38, Vavilov street, 119991 Moscow, Russian Federation

barminaev@gmail.com

Since pulsed laser ablation in liquids is become technique for the synthesis of colloidal metal nanomaterials, most researches focus on the nanoparticle formation mechanism, productivity and the specific functionalization of nanoparticles in liquid. Besides the process of interaction of laser beam with colloidal solutions is not investigated very carefully. It was shown that generation of molecular hydrogen is possible by pulsed laser irradiation of NPs in water [1-3].

In this report the principal results are summarized on laser induced generation of different gases and Hydrogen peroxide from colloidal solutions and organic liquids. Interaction of Nd:YAG laser pulsed beam (energy from 1 to 700 mJ) with ferromagnetic and lanthanide series of NPs metals leads to H₂, O₂, H₂O₂ synthesis. In the present work emphasis is done to investigation of dependence of gases production rate on NPs concentration and redox potential of metals. The choice of NPs material affects the NPs absorption cross section and as consequence the efficiency of plasma interaction with liquid molecules. Besides, it was shown that maxima of H₂, O₂, H₂O₂ production strongly correlate with maxima of luminosity of breakdown plasma (fig. 1). Generation of Hydrogen and Oxygen is interpreted as dissociation of water molecules by direct electron impact from breakdown plasma [4]. However formation of H₂O₂ is caused either by association of H₂ and O₂ molecules or hydroxyl ions as well as by interaction of photons of breakdown plasma with liquid [5-6].

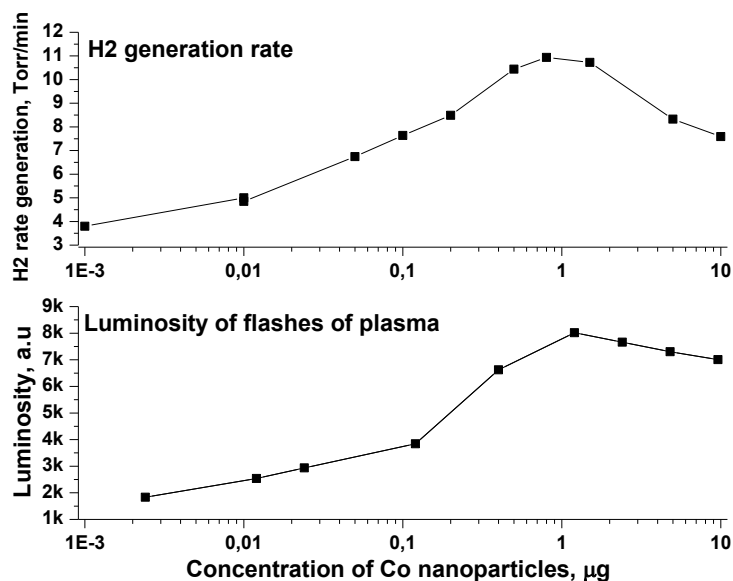


Fig. 1. Dependence of H₂ generation on NPs Tb concentration in water. Interaction of Nd:YAG pulsed laser radiation with Tb colloidal solution in water.

- [1]. D Zhang, B G kce, S Barcikowski, Chemical Reviews, vol. 117, p. 3990, (2017).
- [2]. E.V. Barmina, A.V. Simakin, G.A. Shafeev, Hydrogen emission under laser exposure of colloidal solutions of nanoparticles, Chemical Physics Letters, vol. 655–656, pp. 35–38, (2016).
- [3]. I.A. Sukhov, G.A. Shafeev, E.V. Barmina, A.V. Simakin, O.V. Uvarov, V.V. Voronov, Hydrogen generation by laser irradiation of colloids of iron and beryllium in water, Quantum Electronic, vol. 47, p. 533, (2017).
- [4]. G. Mallard, P.J. Linstrom, NIST Standard Reference Database, vol. 69, (2000).
- [5]. D. N. Nikogosyan, A. A. Oraevsky, V. I. Rupasov, Two-photon ionization and dissociation of liquid water by powerful laser UV radiation, Chemical Physics, vol. 77, pp. 131-143, (1983).
- [6]. O. Legrini, E. Oliveros, A. M Braun, Photochemical processes for water treatment, Chemical reviews, vol. 93, pp. 671-698, (1993).

Controlling the photochemical reduction of metal ions in optical breakdown plasma

Victoria Kathryn Meader, Mallory G. John, Eric Broadhead, Katharine Moore Tibbetts

Department of Chemistry, Virginia Commonwealth University, Richmond, VA 23284, USA

Main author email address: kmtibbetts@vcu.edu

Focusing femtosecond laser pulses into aqueous solution results in the ionization of the water molecules and generation of a spatially localized plasma through optical breakdown (OB) of the medium. This plasma contains a high density of free electrons [1], as well as hydrogen and hydroxyl radicals that result in the production of H_2 , O_2 , and H_2O_2 [2]. These reactive species in the OB plasma can drive the photochemical reduction of a number of metal salts to form colloidal metal and alloy nanoparticles [3-6]. This talk will present our recent work on the characterization and manipulation of the chemical reactions in OB plasmas to form surfactant-free colloidal metal nanoparticles and metal-decorated laser-induced periodic surface structures (LIPSS) [7] on Si (Figure 1). Aqueous $KAuCl_4$ is easily reduced in OB plasma because the hydrated electrons efficiently reduce $[AuCl_4]^-$ to form Au^0 and the H_2O_2 drives autocatalytic growth of the Au nuclei to form Au nanoparticles (AuNPs). AuNPs as small as 3.5 nm (Figure 1(a)) are formed in the absence of any surfactant by optimizing the solution pH and laser pulse energy [4,5]. In contrast to the facile synthesis of AuNPs, aqueous $AgNO_3$ does not form any Ag nanoparticles (AgNPs) under the same laser irradiation conditions because the hydroxyl radicals and H_2O_2 back-oxidize any reduced Ag^0 to Ag^+ [6]. AgNPs are formed when a small amount of NH_3 is added to the aqueous solution under basic conditions (Figure 1(b)). The AgNP size and morphology are highly sensitive to the concentration of NH_3 , which is attributed to distinct reactions in the OB plasma involving NH_3 , OH^- , and H_2O_2 at different concentrations [6]. Finally, we will present recent results demonstrating the deposition of Au on Si LIPSS through ablation of a Si wafer in aqueous $H[AuCl_4]$ solution (Figure 1(c)). The reactions in the plasma generated on the Si surface both reduce $[AuCl_4]^-$ and deposit the Au^0 species onto the ablated Si surface during the formation of the LIPSS.

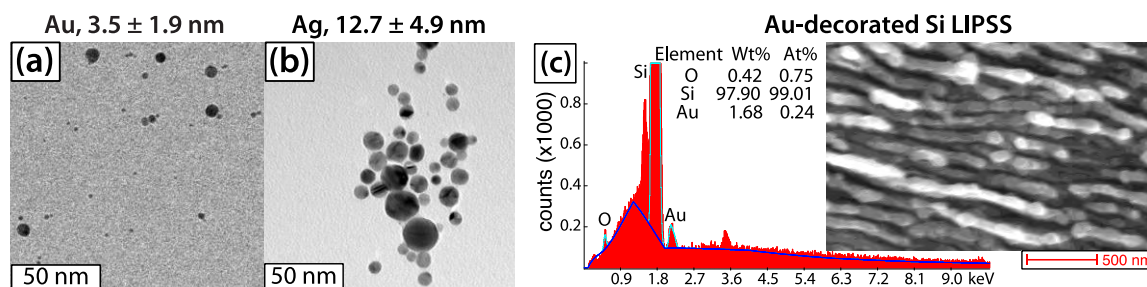


Figure 13: (a) AuNPs synthesized by photochemical reduction of aqueous $KAuCl_4$. (b) AgNPs synthesized by photochemical reduction of $AgNO_3$ in aqueous NH_3 . (c) Au-decorated LIPSS on Si synthesized by Si wafer ablation in aqueous $KAuCl_4$.

- [1] J. Noack and A. Vogel, "Laser-Induced Plasma Formation in Water at Nanosecond to Femtosecond Timescales: Calculation of Thresholds, Absorption Coefficients, and Energy Density" *IEEE J. Quant. Electron.* **35** 1156-1167 (1999)
- [2] S. L. Chin and S. Lagacé, "Formation of H_2 , O_2 , and H_2O_2 from Water by the Use of Intense Femtosecond Laser Pulses and the Possibility of Laser Sterilization" *Appl. Opt.* **35** 907-911 (1996)
- [3] Y. Herbani, T. Nakamura, and S. Sato, "Synthesis of Platinum-Based Binary and Ternary Alloy Nanoparticles in an Intense Laser Field" *J. Colloid Interface Sci.* **375** 78-87 (2012)
- [4] K. M. Tibbetts, B. Tangeysh, J. H. Odhner, and R. J. Levis, "Elucidating Strong Field Photochemical Reduction Mechanisms of Aqueous $[AuCl_4]^-$: Kinetics of Multiphoton Photolysis and Radical-Mediated Reduction" *J. Phys. Chem. A* **120**(20) 3562-3569 (2016)
- [5] V. K. Meader, M. G. John, C. J. Rodrigues, and K. M. Tibbetts, "Roles of Free Electrons and H_2O_2 in the Optical Breakdown-Induced Photochemical Reduction of Aqueous $[AuCl_4]^-$ " *J. Phys. Chem. A* **121**(36) 6742-6754 (2017)
- [6] V. K. Meader, M. G. John, L. M. Frias Batista, S. Ahsan, and K. M. Tibbetts, "Radical Chemistry in a Femtosecond Laser Plasma: Photochemical Reduction of Ag^+ in Liquid Ammonia Solution" submitted to *Molecules* (2018)
- [7] T. J.-Y. Derrien, R. Koter, J. Krüger, S. H. hm, A. Rosenfeld, and J. Bonse, "Plasmonic formation mechanism of periodic 100-nm-structures upon femtosecond laser irradiation of silicon in water" *J. Appl. Phys.* **116** 074902 (2014)

Synthesis of single-nano-sized Au nanoparticles from liquid/liquid dispersion system by femtosecond laser irradiation

T. Okamoto¹, T. Nakamura², T. Yatsuhashi¹

¹- Graduate School of Science, Osaka City University, 3-3-138 Sugimoto, Sumiyoshi, Osaka 558–8585 (Japan)

²- Institute of Multidisciplinary Research for Advanced Materials Department of Materials Science and Biotechnology, Tohoku University, Katahira 2-1-1, Aoba-ku, Sendai 980-857 (Japan)

Main author email address: okamoto@sci.osaka-cu.ac.jp

Recently, gold nanoparticles (AuNPs), which are widely used in a variety of fields such as catalysis and medicine, have been synthesized from Au³⁺ aqueous solution by femtosecond laser (fs-laser) irradiation [1, 2]. Active species formed by the multiphoton ionization of water reduce Au³⁺ to form AuNPs [1]. This bottom up synthesis process of AuNPs requires surfactants [1] or long term (>1 h) laser irradiation [2] to control the size of AuNPs. On the other hand, it has been reported that the size of AuNPs are controlled by the size of the droplets of the Au³⁺ aqueous solution in the case of chemical reduction methods [3].

The water droplet of HAuCl₄ can be formed by stirring the aqueous HAuCl₄ and organic solvent mixtures without any additives. However, there is a concern that carbon nanoparticles are formed from aromatic solvent by fs-laser irradiation [4]. Therefore, we used aqueous HAuCl₄ and hexane (Au³⁺_{aq}/Hex) mixtures in order to exclude the possibility of carbon aggregates formation.

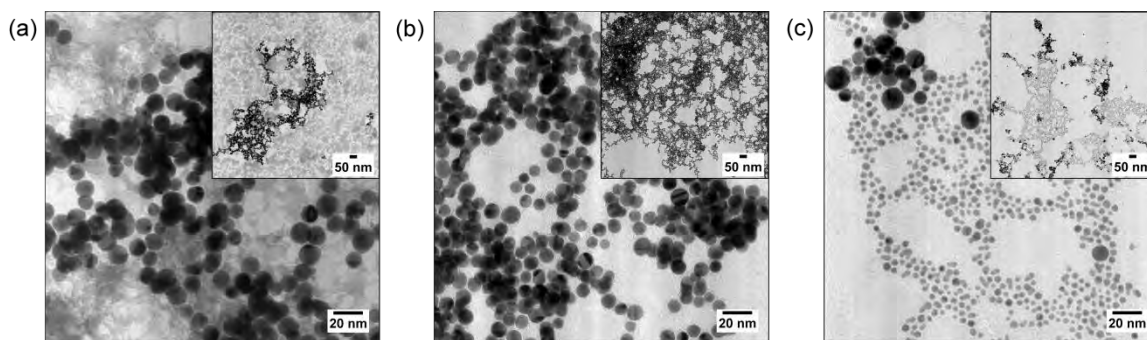


Fig. 1 TEM images of AuNPs synthesized by fs-laser irradiation (scale bar: 20 nm; inset, 50 nm). AuNPs collected from aqueous HAuCl₄ after the 10 min fs-laser irradiation (a) without and (b) with stirring. (c) Single-nano-sized AuNPs collected from the water layer of Au³⁺_{aq}/Hex mixtures after the 10 min fs-laser irradiation with stirring.

In this study, we synthesized single-nano-sized AuNPs from Au³⁺_{aq}/Hex mixtures by fs-laser irradiation (0.8 μm, 40 fs, 0.4 mJ, 1 kHz). Aqueous HAuCl₄ was also exposed to the focused fs-laser pulses for comparison purpose. The size and morphology of AuNPs were analyzed by transmission electron microscope (TEM). The aggregates of spherical particles of 10 nm in diameter were produced from aqueous HAuCl₄ by the 10 min fs-laser irradiation. It is noted that low-contrast components observed in Fig. 1a were not found when aqueous HAuCl₄ was stirred during laser irradiation (Fig. 1b). The mean size of AuNPs observed in Fig. 1b was 9.3±1.3 nm. In contrast, dispersed AuNPs (mean size was 4.7±1.9 nm) were dominantly formed in the water layer of Au³⁺_{aq}/Hex mixtures by the 10 min fs-laser irradiation with stirring (Fig. 1c). We conclude that the reaction environments prepared by stirring as well as by using a liquid/liquid dispersion system is important to control the growth process of nanoparticles. The effect of concentration and stirring speed as well as time evolution of size distribution will be discussed.

- [1] B. Tangeysh, K. M. Tibbetts, J. H. Odhner, B. B. Wayland, R. J. Levis, Gold Nanoparticle Synthesis Using Spatially and Temporally Shaped Femtosecond Laser Pulses: Post-Irradiation Auto-Reduction of Aqueous [AuCl₄]⁻, *J. Phys. Chem. C*, vol. 117, pp. 18719–18727, (2013).
- [2] T. Nakamura, Y. Herbani, D. Ursescu, R. Banici, R. V. Dabu, S. Sato, Spectroscopic study of gold nanoparticle formation through high intensity laser irradiation of solution, *AIP Advances*, vol. 3(8), 082101, (2013).
- [3] S. Sachdev, R. Maugi, J. Woolley, C. Kirk, Z. Zhou, S. D. R. Christie, M. Platt, Synthesis of Gold Nanoparticles Using the Interface of an Emulsion Droplet, *Langmuir*, vol. 33 (22), pp. 5464–5472, (2017).
- [4] T. Hamaguchi, T. Okamoto, K. Mitamura, K. Matsukawa, T. Yatsuhashi, Synthesis of Hydrophilic and Hydrophobic Carbon Nanoparticles from Benzene/Water Bilayer Solution with Femtosecond Laser Generated Plasma Filaments in Water, *Bull. Chem. Soc. Jpn.*, vol. 88(2), pp. 251–261, (2015).

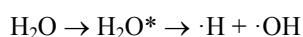
Photochemical synthesis of nanoparticles in aqueous solutions

J. Bárta^{1,2}, K. Tomanová^{1,2}, L. Procházková^{1,2}, V. Vaněček¹, M. Kuzár¹, M. Nikl², V. Čuba¹

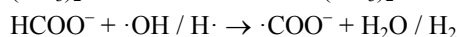
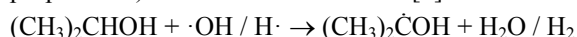
1- Czech Technical University in Prague, Faculty of Nuclear Sciences and Physical Engineering, ř h á t P g z ch p b c
2- Academy of Sciences of the Czech Republic, Institute of Physics, Cukrovarnická 10, Prague 6, Czech Republic

jan.barta@fffi.cvut.cz

Irradiation of diluted aqueous solutions with 254 nm UV-C light may initiate various photochemical reactions, which can be utilized for production of inorganic nanoparticles via several different processes. The core principle is the photolysis of water. Even after the absorption of UV-C (254-nm) light, water molecules undergo a photolysis [1]. The suggested mechanism involves the excitation to a triplet state, which is unstable and readily decomposes to H and OH radicals:



The quantum yield of OH radicals was determined as ~0.08, i.e. roughly one in twelve efficiently absorbed photons results in creation of one OH radical, which can react with other species present in the irradiated solution. The ·OH radicals formed during photolysis of either water or other dissolved compounds efficiently react with specific additives (radicals scavengers). These reactions limit the influence of oxidative processes; the products of interaction with scavengers can, in turn, induce the desired chemical reactions. Typical ·OH scavengers are e.g. alcohols (such as propan-2-ol) or formate ions HCOO^- [2]:



Both intermediate radicals $(\text{CH}_3)_2\dot{\text{C}}\text{OH}$ and $\cdot\text{COO}^-$ may reduce many metal ions to lower oxidation states. In noble metals (silver, gold and platinum group), the reduction and coalescence of reduced ions occur simultaneously, forming metallic nanoparticles [2,3]. Photolysis of formate ions also produces CO_2 , which can precipitate many metal ions in the form of carbonates or hydroxides-carbonates [4].

To amend a generally low efficiency of photolysis of water or diluted aqueous solutions, specific sensitizers can be added to the solutions, i.e. compounds that efficiently absorb UV or visible light and form reactive species. Compounds such as hydrogen peroxide or ketones can be used for this purpose, each utilizing different mechanism of interaction with UV light.

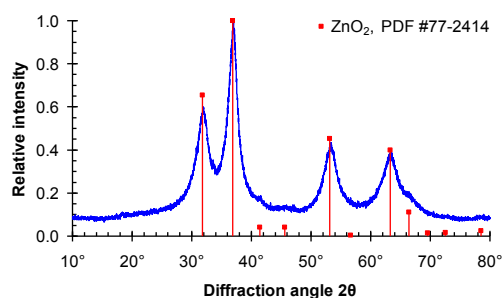


Figure 14 – X-ray diffraction pattern of nanocrystalline zinc peroxide formed during UV irradiation of aqueous solution containing zinc nitrate, ammonium formate and hydrogen peroxide.

The mechanisms discussed are shown for specific cases, i.e. photoinduced syntheses of copper, gold, silver, rhodium, zinc peroxide, magnesium hydroxide and yttrium/lutetium carbonate nanoparticles.

- [1] K. Tomanová, M. Přeček, V. Můčka, L. Vyšín, L. Juha, V. Čuba, At the crossroad of photochemistry and radiation chemistry: formation of hydroxyl radicals in diluted aqueous solutions exposed to ultraviolet radiation, *Phys. Chem. Chem. Phys.* 19, 29402-29408 (2017)
[2] G.V. Buxton, C.L. Greenstock, W.P. Helman, A.B. Ross, Critical review of rate constants for reactions of hydrated electrons, hydrogen atoms and hydroxyl radicals ($\cdot\text{OH}$, $\cdot\text{O}$) in aqueous solution, *J. Phys. Chem. Ref. Data*, 17, 513-886, (1988).
[3] J. Bárta, M. Pospíšil, V. Čuba, Photo- and radiation-induced preparation of nanocrystalline copper and cuprous oxide catalysts, *J. Radioanal. Nucl. Chem.*, 286, 611-618 (2010).
[4] V. Čuba, L. Procházková, J. Bárta, A. Vondrášková, T. Pavelková, E. Mihoková, V. Jarý, M. Nikl, UV radiation: a promising tool in the synthesis of multicomponent nano-oxides, *J. Nanopart. Res.* 16, 2686, (2014)

Laser-Induced Composite Particle Formation in Liquid: Insight in Physico-Chemical Processes

Zaneta Swiatkowska-Warkocka¹, Tatiana Itina², Alexander Pyatenko³, Naoto Koshizaki⁴, Marta Wolny-Marszalek¹

1- Institute of Nuclear Physics Polish Academy of Sciences, PL-31342Krakow, ul. Radzikowskiego 152, Poland

2- Lab. H. Curien, CNRS, UJM, IOGS, membre Univ. de Lyon, 18 rue B. Laurus, F-42000 Saint-Etienne, France

3- National Institute of Advanced Industrial Science and Technology, Tsukuba, 305-8565, Japan

4- Hokkaido University, Sapporo, 060-8628, Japan

Zaneta.Swiatkowska@ifj.edu.pl

Pulsed laser irradiation in liquids is a versatile and promising method for synthesis of colloidal submicrometer spheres are particularly attractive for bio-sensing, medical application, lithium-ion batteries (LIBs), catalysis, and photonics. Composite particles based on metals exhibiting strong absorption in the visible region of the spectrum (Au, Ag) and/or transition metal (Fe, Co, Ni) are successfully produced and tailoring by using laser method with various experimental parameters; wavelengths, laser fluence, irradiation time, raw material or solvent [1,2]. The mechanisms involved in the formation of these particles are, however, still under consideration [3].

Here, we focus our attention at the better understanding of the physical and chemical processes occupied in particles formation by pulsed laser irradiation in liquids. For this, a series of both experimental and numerical studies were performed. In particular, by using various experimental parameters composite particles with different size and composition were obtained. The structure, phase composition, size, morphology and magnetic properties were confirmed by XRD, TEM, EDS, SEM and SQUID.

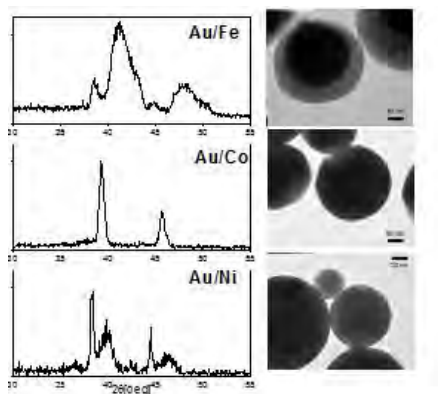


Figure 1 Typical XRD patterns and TEM images of Au/transition metals nanocomposite particles obtained by pulsed laser irradiation in ethanol (532 nm, 100 mJ/pulse cm², 1h)

Figure 1 illustrated XRD and TEM results of obtained two-component particles among Au with Fe, Co and Ni. Submicrometer spherical particles with various inner structures are generated. XRD patterns clearly show that laser irradiation of (Fe, Co, Ni)-oxides nanoparticles dispersed in ethanol leads to reduction of oxides and formation of alloys (AuFe, AuCo, AuNi) [1, 2, 4].

Furthermore, the role of the solution, liquid properties, interaction not only between particles but also between particles and solvent molecules was demonstrated. The detailed discussion will be reported at the conference. We believe, that exploring the formation mechanism, roles of physico-chemical effects in the particle formation will help in creation of materials with specific size, structures and unique properties.

[1] Z. Swiatkowska-Warkocka, A. Pyatenko, F. Krok, B. R. Jany, M. Marszalek, Synthesis of new metastable nanoalloys of immiscible metals with a pulse laser technique, *Scientific Reports* 5:09849 (2015)

[2] Z. Swiatkowska-Warkocka, A. Pyatenko, K. Koga, K. Kawaguchi, H. Wang, N. Koshizaki, Synthesis and Control of Various Morphologies/Phases of Au-based Nanocomposite Particles by Pulsed Laser Irradiation in Liquid Media, *J. Phys. Chem. C* 121, 8177–8187 (2017)

[3] P. Wagener, J. Jakobi, C. Rehbock, V.S.K. Chakravadhanula, C. Thede, U. Wiedwald, M. Bartsch, L. Kienle, and S. Barcikowski, Solvent-surface interactions control the phase structure in laser-generated iron-gold core-shell nanoparticles, *Scientific Reports*, 6: 23352 (2016)

[4] Z. Swiatkowska-Warkocka, K. Koga, K. Kawaguchi, H. Wang, A. Pyatenko N. Koshizaki, Pulsed laser irradiation of colloidal nanoparticles: a new synthesis route for the production of non-equilibrium bimetallic alloy submicrometer spheres, *RSC Advances* 3, 79-83 (2013)

Fracture Strength of Submicrometer Spherical Particles Fabricated by Pulsed Laser Melting in Liquid

N. Koshizaki¹, M. Kondo¹, N. Shishido², S. Kamiya³, Y. Ishikawa⁴

1- Graduate School of Engineering, Hokkaido University, Sapporo, Hokkaido 060-8628, Japan

2- Green Electronics Research Institute, Kitakyushu, Kitakyushu, Fukuoka 808-0135, Japan

3- Nagoya Institute of Technology, Nagoya, Aichi 466-8555, Japan

4- Nanomaterials Research Institute, National Institute of Advanced Industrial Science and Technology (AIST), Tsukuba, Ibaraki 305-8565, Japan

koshizaki.naoto@eng.hokudai.ac.jp

The strength of materials is substantially governed by unavoidable defects that are distributed within the materials. Recently nanoscience research has revealed that the high strength of various nanomaterials, such as carbon nanotubes, silicon nanowires, etc. is due to their defect-free 1D nanostructures [1]. However, studies on mechanical properties of 0D nanoparticles have been quite limited so far.

Submicrometer spherical particles can be synthesized by pulsed laser melting in liquid (PLML) as a new type of 0-D nanoparticles. In PLML, raw nanoparticles generally aggregated in liquid are selectively heated over the melting point to form large submicrometer-sized droplets and quenched by the surrounding liquid to become submicrometer spherical particles. Using PLML, highly crystalline non-porous submicrometer spherical particles can be fabricated for various materials, such as metals, oxides, semiconductors, and even carbides. As commercially available submicrometer spherical particles are limited to amorphous particles made of glass or polymer, the material versatility of PLML is an important advantage over other particle fabrication process. Further, the particles obtained by PLML are unique in that they are spherical and crystalline [2]. These two features are generally incompatible because crystalline particles should be faceted and, therefore, should form a polyhedral shape with stable low-indexed crystalline faces. In addition, the non-porous nature of these particles, which is not observed in spherical particles obtained by chemical methods, also leads to improved mechanical properties.

Recently, the lubrication property of oil has been reported to be greatly improved by the addition of ceramic submicrometer spherical particles fabricated by PLML [3]. This finding is quite an interesting example of the utilization of the good mechanical properties and the sphericity of these particles. While single-crystalline submicrometer spherical particles with few structural defects are predicted to have good mechanical properties, their fracture strength has not been reported.

Here we perform the compression test on various submicrometer spherical particles fabricated by PLML to demonstrate their advantages for mechanical applications. To investigate the hardness and brittleness of submicrometer spherical particles, the fracture strengths of B_4C and TiO_2 submicrometer spherical particles are measured (Fig. 1) and compared with fracture strengths of bulk ceramics.

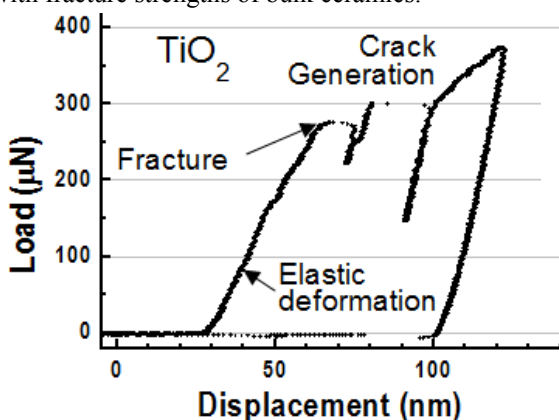


Figure 15 Typical load-displacement curves of submicrometer spherical particles of TiO_2 fabricated by PLML.

[1] S. Wang, Z. Shan, H. Huang, The mechanical properties of nanowires, *Advanced Science* 4, 1600332, (2017).

[2] Y. Ishikawa, N. Koshizaki, A. Pyatenko, N. Saitoh, N. Yoshizawa, and Y. Shimizu, Nano- and submicrometer-sized spherical particle fabrication using a submicroscopic droplet formed using selective laser heating, *Journal of Physical Chemistry C*, 120, 2439-2446, (2016).

[3] X. Hu, H. Gong, Y. Wang, Q. Chen, J. Zhang, S. Zheng, S. Yang, B. Cao, Laser-induced reshaping of particles aiming at energy-saving applications, *Journal of Materials Chemistry* 22, 15947-15952, (2012).

Nanosecond laser fragmentation of colloidal gold nanoparticles with high intensity nanosecond pulses is driven by a single step fragmentation mechanism

A. R. Ziefuß¹, S. Reichenberger¹, C. Rehbock¹, I. Chakraborty², W. J. Parak², H. Huang³, L. V. Zhigilei³, S. Barcikowski¹

1- Technical Chemistry I and Center for Nanointegration, Duisburg-Essen (CENIDE), University of Duisburg-Essen, Universitaetsstrasse 7, 45141 Essen, Germany

2- Fachbereich Physik und Chemie, CHyN, Universität Hamburg, Luruper Chaussee 149, 22607 Hamburg, Germany

3- Department of Materials Science and Engineering, University of Virginia, 395 McCormick Road, Charlottesville, Virginia, USA
anna.ziefuss@uni-due.de

Pulsed laser fragmentation in liquid is a useful tool to control the particle size of laser-fabricated nanoparticles [1], but adequate process control requires a proper understanding of the underlying mechanisms. Typically, the pulse duration is discussed as a decisive criterion ruling the fragmentation process. Commonly, distinctions are made between electronically induced Coulomb explosion for high laser peak powers (ultrashort pulses) and thermally induced evaporation for low laser peak powers [2]. For the fragmentation with high intensity ns pulses, however, the mechanism is poorly understood. While photothermal mechanisms are often assumed as the electrons and the lattice are in a thermal equilibrium, ejection of electrons was also reported [3].

In this work, we systematically examine the pulsed laser fragmentation of gold nanoparticles in liquid with high intensity nanosecond pulses and correlate them with the educt particle size, the number of pulses and the laser intensity. These experiments were carried out in a liquid flow passage reactor, which allows a precise control of the energy input per volume (Figure 1a). We could conclusively prove that the fragmentation process of gold nanoparticles is a one pulse and one step event, yielding monomodal ultra small nanoparticles in case a pulse peak power of 1.62×10^{12} W/m² is exceeded and all educt particles are larger than 13.4 ± 2.1 (Figure 1b, regime 2). For lower peak powers, we found a bimodal size distribution, which can be explained by theoretical calculations and molecular dynamics simulations (Figure 1c). Furthermore, we found strong evidence that the number of irradiation cycles can be used to tune the surface charge density of the resulting ultra small nanoparticles in aqueous medium, which was verified by titration curves and zeta potential measurements. These particles are highly interesting for both, biomedicine and catalysis.

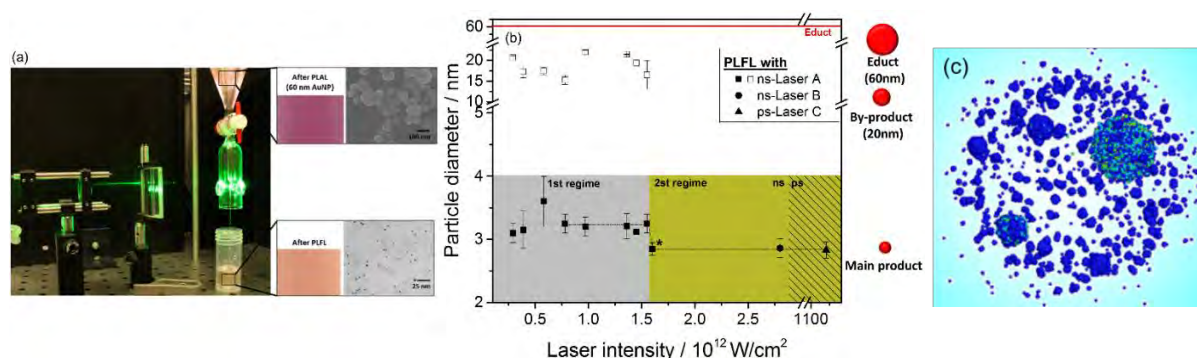


Figure 16: a) Illustration of the fragmentation process. b) Plot of the resulting particle sizes after fragmentation with different laser intensities. Squares show the results after fragmentation with a 9 ns laser with 0.1 kHz (ns-Laser A), circles show the result after fragmentation with a 2 kHz, 7 ns laser (ns-Laser B) and triangles the results after PLFL with a 10 ps laser with 80 kHz (ps-Laser C) c) snapshot from a molecular dynamics simulation of laser-induced fragmentation of a gold nanoparticle in water.

[1] V. Amendola, M. Meneghetti, Controlled size manipulation of free gold nanoparticles by laser irradiation and their facile bioconjugation, *J. Mater. Chem.* 17, 4705, 2007

[2] S. Hashimoto, D. Werner, T. Uwada, Studies on the interaction of pulsed lasers with plasmonic gold nanoparticles toward light manipulation, heat management, and nanofabrication, *Journal of Photochemistry and Photobiology C*, 13, 2012

[3] K. Ymada, Y. Tokumoto, T. Nagata, F. Mafune, Mechanism of Laser-induced Size-reduction of Gold Nanoparticles as Studied by Nanosecond Transient Absorption Spectroscopy, *J. Phys. Chem. B.* 24, 110, 2006

Sequential and energy dose defined irradiation of particles in a free liquid jet: modification of ITOs optical and cobalt ferrites catalytic properties

M. Lau¹, F. Waag², T. Straube³, H. Lutz⁴, T. Textor⁵, S. Barcikowski²

1- TRUMPF Laser- und Systemtechnik GmbH, Johann-Maus-Strasse 2, 71254 Ditzingen, Germany

2- University of Duisburg-Essen, Universitaetsstrasse 2, 45141 Essen, Germany

3- Deutsches Textilforschungszentrum Nord-West gGmbH (DTNW), Adlerstrasse 1, 47798 Krefeld, Germany

4- CHT Germany GmbH, Bismarckstrasse 102, 72072 Tübingen, Germany

5- Zentrum für Interaktive Materialien, Reutlingen University, Alteburgstrasse 150, 72762 Reutlingen, Germany

marcus.lau@de.trumpf.com

Since the first reports on laser-generated nanoparticles it is known that fragmentation of particles captured in liquid environment is likely when the particles are irradiated with sufficient laser fluences and intensities [1]. But feeding micro- and sub-microparticles in a controlled manner into the laser light at sufficient and defined intensities is challenging. Using a free liquid jet [2] for step-wise irradiation has proven as sufficient approach to investigate and study laser fragmentation of microparticles in liquids [3]. Based on this set-up the gradual modification of ITO particles is investigated here [4].

The set-up allows scaling the colloid volume independent from the irradiation parameters. Up to 500 ml with 500 mg ITO particles were processed and particle coatings investigated upon their optical properties covering the infrared regime. It turned out that energy density and liquid environment are crucial for the modification of ITO particles optical properties. Recent investigations additionally simulated the energy density distribution within the liquid jets cross section and demonstrate a correlation with catalytic properties at the example of cobalt ferrite nanoparticles [5]. This demonstrates that energy dose-controlled particle irradiation in a free liquid jet allows adjusting optical and catalytic particle properties.

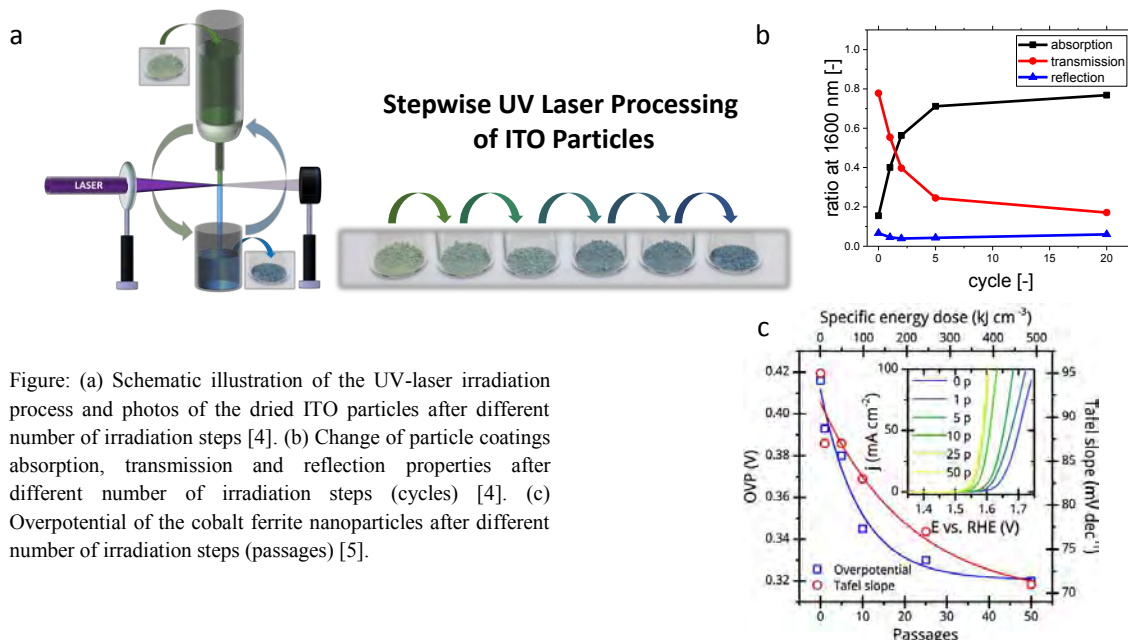


Figure: (a) Schematic illustration of the UV-laser irradiation process and photos of the dried ITO particles after different number of irradiation steps [4]. (b) Change of particle coatings absorption, transmission and reflection properties after different number of irradiation steps (cycles) [4]. (c) Overpotential of the cobalt ferrite nanoparticles after different number of irradiation steps (passages) [5].

[1] A. Fojtik and A. Henglein, Laser ablation of films and suspended particles in a solvent: formation of cluster and colloid solutions, *Ber. Bunsenges. Phys. Chem.*, 97, pp. 252-254, (1993).

[2] P. Wagener and S. Barcikowski, Laser fragmentation of organic microparticles into colloidal nanoparticles in a free liquid jet, *Appl. Phys. A*, 101, pp. 435-439, (2010).

[3] M. Lau and S. Barcikowski, Quantification of mass-specific laser energy input converted into particle properties during picosecond pulsed laser fragmentation of zinc oxide and boron carbide in liquids, *Appl. Surf. Sci.*, 348, pp. 22-29, (2015).

[4] M. Lau, T. Straube, V. Aggarwal, U. Hagemann, B. de Oliveira Viestel, N. Hartmann, T. Textor, H. Lutz, J. Gutmann, S. Barcikowski, Gradual modification of ITO particle's crystal structure and optical properties by pulsed UV laser irradiation in a free liquid jet, *Dalton Trans.*, 46, pp. 6039-6048, (2017).

[5] F. Waag, B. Gökce, C. Kalapu, G. Bendt, S. Salamon, J. Landers, U. Hagemann, M. Heidelmann, S. Schulz, H. Wende, N. Hartmann, M. Behrens, S. Barcikowski, Adjusting the catalytic properties of cobalt ferrite nanoparticles by pulsed laser fragmentation in water with defined energy dose, *Sci. Rep.*, 7, 13161, (2017).

Smart nanostructures for biomedical applications

Anton FOJTÍK^{1,2,3}

¹Faculty of Biomedical Engineering, Czech Technical University, Prague, Czech Republic

²Institute for Nanomaterials, Advanced Technologies and Innovation, Technical University of Liberec, CR

³Institute of Engineering Physics for Biomedicine, National Research Nuclear University (NRNU, MEPHI), Russia

email: fojtiant@fbmi.cvut.cz

Today's technology already reached the levels that makes possible to peep into very tiny pieces of matter to observe natural processes taking place inside and copy the process of formation tiny structures. Allows us to imitate these structures in „nanosize" scale, or to find the ways how to prepare them. As these structures exhibit unique characteristics, unknown in the macro-world, it can be said that from the point of view of utilization of these structures for practical applications, doors are becoming wide open to undreamt-of development of science and technology. .

This field is getting more attention and is becoming emerging topic of recent days [1]. Its biological and medical approaches and applications are opening novel, unpredicted and efficient ways of solving health issues. Laser synthesis of colloids, pulsed laser ablation in liquids (PLAL) [2], is one of promising approached to synthesize nanomaterials for health sciences, and this extraordinary field of nanobiotechnology is shaping into one of the leading sciences of the 21st century...

Goal of the new projects is to functionalize Fe₃O₄ /Ag magnetic nanoparticles, which according to chemical groups attached at the surface, are able to bond to special pathogens (bacteria or virus) and being easily manipulated by magnetic field, they can be removed from the system taking the pathogens with them as well.

Nanoparticles are produced by 'wet' way using pulse laser ablations, under special conditions; (Angel-Advanced Nanoparticle Generation and Excitation by Lasers in Liquids). Final product is several tens of nanometers in diameter, (*chemically very clean*) and possesses special superparamagnetic or ferromagnetic properties, which give it ability to be manipulated while working in complex biological systems such as human body. Shape and size of nanoparticles are evaluated using AFM, magnetic properties measured by Mössbauer Spectroscopy and Superconducting Quantum Interference Device (SQUID). Surface of the particles is stabilized and treated, so that they maintain their unique properties and remain stable and separated. Certain chemical groups, proteins or residues are attached onto the surface to functionalize it. Particles are then ready to play a key role in recognition of the pathogens bonding to the surface of nanoparticles and following applied magnetic field to get out of the system. Cancer tumours can be necrotized by heating them through magnetic nanoparticles

Si nanoparticles prepared by thermal decomposition of silan SiH₄ due to size restriction possess “creep effect” (climb up at inner surface of glass wall of vessel), use for biomedical applications to control diffusion through cell membrane [3].

Charge transfer processes (biological systems and catalyse) can be controlled by size of nanoparticles [4].

[1] Fojtik A and coll. , book: NANO – Today's Fascinating Phenomenon, COMTES, Dobřany, 2016. 300 pp. ISBN 978-80-270-0477-5

[2] Fojtik A., Henglein A.: Laser Ablation of Films and Suspended particles in a Solvent: Formation of Cluster and Colloid Solutions; Ber. Buns.Phys.Chem.Vol.97, No.9, 1993, p.252

[3] Fojtik A., Henglein A.:Surface Chemistry of Luminescent Colloidal Silicon Nanoparticles; J. Phys. Chem. B, Vol. 110, No.5, 2006, p.1994-1998.

[4] Henglein A., Guttierrez M., Weller H., Fojtik A., Jirkovsky: Photochemistry of Colloidal Semiconductors. Reactions and Fluorescence of AgI and AgI-Ag₂S Colloids. Ber.Buns.Phys.Chem. 93, 1989, p.593.

Novel advanced laser-synthesized nanomaterials for biomedical applications

A. V. Kabashin^{1,2}

1- Aix Marseille Univ, CNRS, LP3, Marseille, France

2- “E Ph” f E g g Ph c f c (Ph) 5409 c w

email: kabashin@lp3.univ-mrs.fr

The presentation will overview our on-going activities on laser ablative synthesis of some biocompatible colloidal nanomaterials (Au, Si etc) and their testing in biomedical tasks with particular emphasis on cancer therapy and diagnostics (theranostics). Our approach is based on ultra-short (fs) laser ablation from a solid target [1] or already formed water-suspended colloids [2,3] to fabricate “bare” (ligand-free) nanoparticles (NPs) with well-controlled size characteristics, as well as the ablation in the presence of functional molecules (dextran, PEG, proteins, etc.) to properly coat NPs surface in order to minimize immune response and enable tumor-vectoring functionality. Our experiments in vitro demonstrate an excellent cell uptake of both bare and functional nanomaterials, while the composition of protein corona covering NPs complexes in biological environment promises a good transport of nanomaterials in vivo [4-6]. In addition, the intravenous administration of Si NPs using small animal model did not reveal any toxicity effects, which was confirmed by behavior of mice, stability of blood content and other biochemical parameters, as well as by histology analyses of all organs and biodistribution of NPs in tissues [5,6]. Furthermore, the NPs rapidly biodegraded in the organism and were completely cleared 2-3 days after their injection [5]. In general, our tests evidenced a negligible toxicity and much faster clearance of laser-synthesized Si NPs compared to all chemically-synthesized Si NPs counterparts [5-7]. We are now actively testing laser-synthesized nanomaterials in cancer theranostics and other tasks [7]. In particular, our experiments showed that laser-synthesized NPs can provide a much better efficiency compared to chemically synthesized counterparts in a newly introduced method of mild cancer therapy using Si nanoparticles as sensitizers of radiofrequency radiation-based hyperthermia [8], as well as be efficient markers for bioimaging [9]. We then showed that bare laser-synthesized Au NPs can provide an order of magnitude better response in glucose oxidation tasks, which promises their use as electrocatalysts in bioimplantable therapeutic devices [10], as well as serve as additive functional elements for the development of promising tissue engineering platforms [11]. We finally reported successful use of laser-synthesized Au NPs as SERS probes in tasks of yeast [12] and bacteria [13] identification with better efficiency compared to all chemically-synthesized counterparts.

- [1] A. V. Kabashin, M. Meunier, Synthesis of colloidal nanoparticles during fs laser ablation of gold in water, *J. Appl. Phys.*, 94, 7941 (2003)
- [2] P. Blandin, K. A. Maximova, M. B. Gongalsky, J. F. Sanchez-Royo, V. S. Chirvony, M. Sentis, V. Yu. Timoshenko, A. V. Kabashin, Femtosecond laser fragmentation from water-dispersed microcolloids: toward fast controllable growth of ultrapure Si-based nanomaterials for biological applications, *J. Mater. Chem. B*, 1, 2489-2495 (2013)
- [3] K. Maximova, A. I. Aristov, M. Sentis, A. V. Kabashin, Size-controllable synthesis of bare gold nanoparticles by femtosecond laser fragmentation in water, *Nanotechnology*, 26, 065601 (2015)
- [4] F. Correard, K. Maximova, M.-A. Estève, C. Villard, A. Al-Kattan, M. Sentis, M. Roy, M. Gingras, A. V. Kabashin, D. Braguer, Gold nanoparticles prepared by laser ablation in aqueous biocompatible solutions: assessment of safety and biological identity for nanomedicine applications, *Int. J. Nanomedicine*, 9, 5415 (2014)
- [5] T. Baati, A. Al-Kattan, M. Esteve, L. Njim, Y. Ryabchikov, F. Chaspoul, M. Hammami, M. Sentis, A. Kabashin, D. Braguer, Ultrapure laser-synthesized Si nanomaterials for biomedical applications: in vivo assessment of safety and biodistribution, *Sci. Rep.*, 6, 25400 (2016)
- [6] A. Al-Kattan, Y. Ryabchikov, T. Baati, V. Chirvony, J. F. Sanchez-Royo, M. Estève, M. Sentis, V. Timoshenko, D. Braguer, A. Kabashin, Ultrapure laser-synthesized Si NPs with variable oxidation state for biomedical applications, *J. Mater. Chem. B*, 4, 7852 (2016)
- [7] A. Kabashin, V. Timoshenko, What theranostic appl. could ultrapure laser-synth. Si NPs have in cancer?, *Nanomedicine*, 11, 2247 (2016)
- [8] K. Tamarov, L. Osminkina, S. Zinovyev, K. Maximova, J. Kargina, A. Sviridov, M. Sentis, A. Ivanov, V. Nikiforov, A. Kabashin, V. Timoshenko, RF radiation-induced hyperthermia using biodegradable Si-based nanosensitizers for biomedical appl., *Sci. Rep.*, 4, 7034 (2014)
- [9] M. Gongalsky, L. Osminkina, A. Perreira, A. Manankov, A. A. Fedorenko, A. N. Vasiliev, V. V. Soloviev, A. A. Kudryavtsev, M. Sentis, A. V. Kabashin, V. Yu. Timoshenko, Laser-synthesized oxide-passivated bright Si quantum dots for bioimaging, *Sci. Rep.*, 6, 24732 (2016)
- [10] S. Hebié, Y. Holade, K. A. Maximova, M. Sentis, P. Delaporte, K. B. Kokoh, T. W. Napporn, A. V. Kabashin, Advanced Electrocatalysts on basis of bare Au nanomaterials for Biofuel Cell Applications, *ACS Catalysis*, 5, 6489 (2015)

Laser-generated Metal Nanoparticles as Multifunctional Agents for Sensing and Nanomedicine Applications

C. Bravin¹, A. Fabris¹, V. Amendola¹

1- Department of Chemical Sciences, University of Padova, Via Marzolo 1, 35131, Padova.

carlo.bravin@studenti.unipd.it

Detection of chemical agents plays a fundamental role in biomedical, forensic and environmental sciences. In these fields, one of the main objective is to implement multiple functionalities in a single scaffold with nanometric size to develop efficient tools for sensing and nanomedicine applications. For these purposes, metal nanoparticles (MeNPs) possess distinct physical and chemical properties that make them excellent scaffolds for the assembly of novel chemical sensors or for the formation of hybrid nanostructure used as biological devices.[1] To this purpose, the ability of laser ablation in liquid to generate MeNPs free of chemicals or other contaminants adsorbed on the surface, as well as to easily access nanomaterials that are difficult to obtain by other synthetic routes are two important advantages.[2]

In this context, we firstly report a novel system for the detection of Hg^{2+} ions. The scaffold is based on opportunely functionalized “unconventional” plasmonic nanoparticles, which allow the development of a new and practical assay that exploit the characteristic surface plasmon resonance of these nanosystems.

On the other hand, the use of plasmonic nanoparticles for biomedical applications has led to significant advancements in the construction of ultrasensitive bioassays and effective therapeutic agents.[3] For this reason, we present gold nanoparticles (AuNPs) functionalized with a biocompatible thiolated polymer endowed with the chemical functionality required for cancer therapy by a nuclear medicine approach.

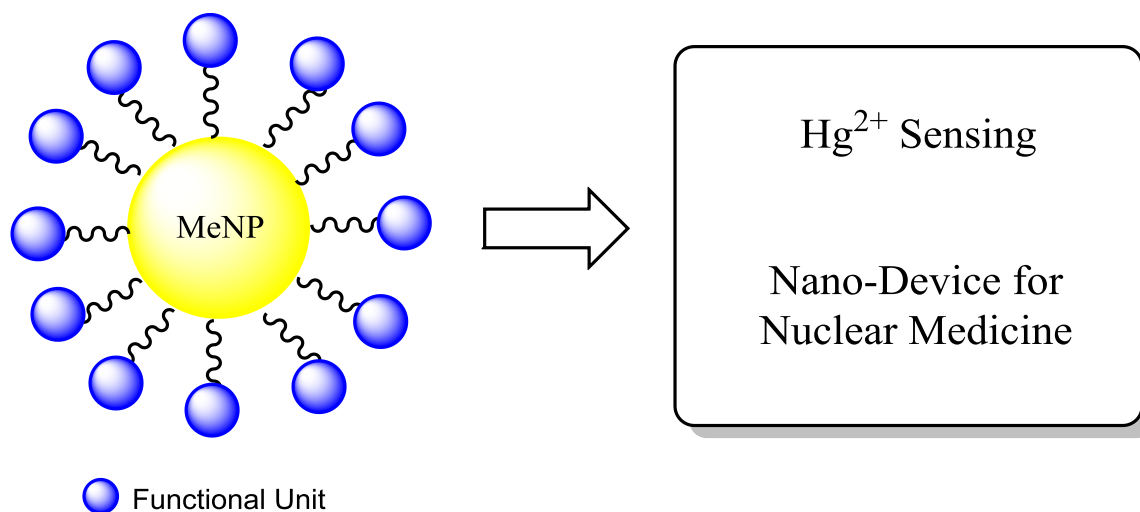


Figure 17 Metal Nanoparticles (MeNPs) are used as sensor for Hg^{2+} detection or as nano-device in nuclear medicine cancer therapy.

[1] K. Saha, S. S. Agasti, C. Kim, X. Li and V. M. Rotello, Gold Nanoparticles in Chemical and Biological Sensing, *Chem. Rev.*, 112, 2739–2779, (2012).

[2] V. Amendola, M. Meneghetti, Laser ablation synthesis in solution and size manipulation of noble metal nanoparticles, *Phys. Chem. Chem. Phys.*, 11, 3805-3821, (2009).

[3] G. Chen, I. Roy, C. Yang and P. N. Prasad, Nanochemistry and Nanomedicine for Nanoparticle-based Diagnostics and Therapy, *Chem. Rev.*, 116, 2826-2885, (2016).

Carbon Quantum Dots Fluorescent Labels Generated in a Continuous Flow Jet Configuration

**C. Doñate-Buendía¹, R. Torres-Mendieta², A. Pyatenko³, E. Falomir⁴,
M. Fernández-Alonso¹ and G. Mínguez-Vega¹**

1- GROC·UJI, Institute of New Imaging Technologies, Universitat Jaume I, Avda. Sos Baynat sn, 12071 Castellón, Spain

2- Institute for Nanomaterials, Advanced Technologies and Innovation, Technical University of Liberec, Studentská 1402/2, 461 17 Liberec, Czech Republic

3- Nanomaterials Research Institute, National Institute of Advanced Industrial Science and Technology (AIST), Tsukuba Central 5, 1-1-1 Higashi, Tsukuba, Ibaraki 305-8565, Japan

4- Department of Inorganic and Organic Chemistry, University Jaume I, Avda. Sos Baynat sn, 12071 Castellón, Spain

gminguez@uji.es

Carbon quantum dots (CQDs) have been proved as an outstanding material in applications such as bioimaging, cancer therapy or sensing [1]. High purity samples are needed to avoid cell damage for in vivo and in vitro applications, and laser generation techniques ensure the required high purity as no by-products are needed in the process. In this work, improvement in the synthesis efficiency of CQDs with a pulsed laser is proved by applying for first time with this material a cost effective flow jet configuration [2], Fig. 1 (a). The most used laser technique for this purpose is irradiation of the colloid in a bucket, but the proposed flow jet set up achieves an increase of 15 % in production. The generated CQDs exhibit an increment in quantum yield of one order of magnitude and its photoluminescence keeps constant for a long period of time, even after cell internalization. A study of the surface functional groups by XPS and FTIR demonstrates the presence of C=O, C-OH, C-O-C and C-O-OH groups, which have a great potential for biological applications in conjugating drug or targeting moieties.

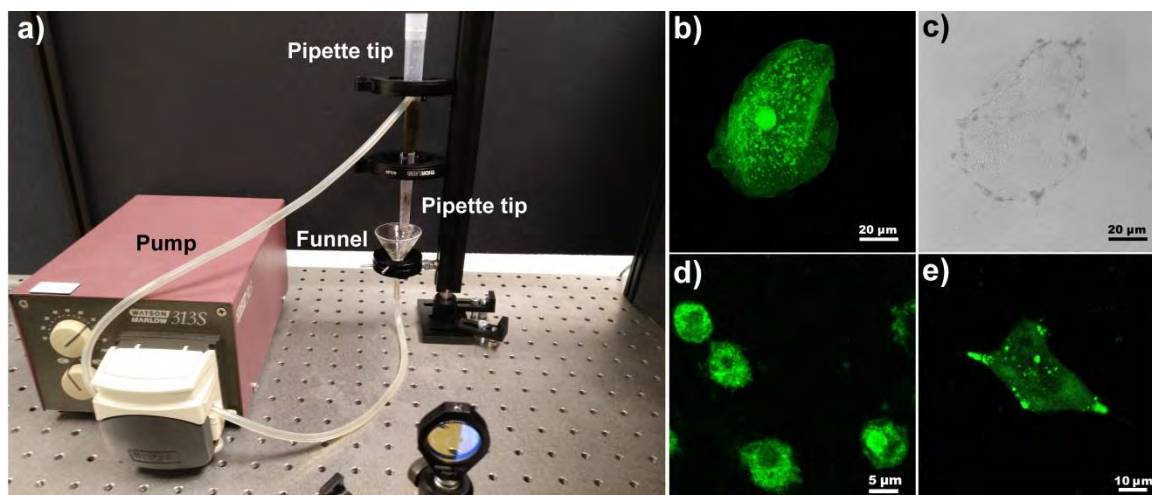


Figure 18. (a) Flow Jet experimental setup based on two pipette tips to circulate the liquid flow. A funnel to collect the falling liquid. A silicon tube to take the liquid from the funnel to the pipette tip and a pump to generate the liquid flow in closed loop. Fluorescence confocal microscope image (b) and transmission image (c) of healthy oral epithelial cell. (d) Fluorescence confocal microscope image of colon cancer cells line HT29. (e) Fluorescence confocal microscope image of lung cancer cells line A549.

Fast internalization of less than 10 min is proved, without any need of extra processing, inside healthy oral epithelial cells, Fig. 1 (b, c), HT-29 colon cancer cells, Fig. 1 (d), and A-549 lung cancer cells, Fig. 1. (e). A real time measurement of the integrated photostability in the cells is performed to demonstrate that the CQDs have a reduced photobleaching compared to standard fluorescence markers [3]. These features prove them as an excellent fluorescent label for in-vivo and in-vitro fluorescence applications.

[1] F. Yuan, S. Li, Z. Fan, X. Meng, L. Fan and S. Yang, Shining Carbon Dots: Synthesis and Biomedical and Optoelectronic Applications, *Nano Today*, 11, pp. 565–586, (2016).

[2] P. Wagener, S. Barcikowski, Laser Fragmentation of Organic Microparticles into Colloidal Nanoparticles in a Free Liquid Jet, *Appl. Phys. A Mater. Sci. Process.*, 101, pp. 435–439, (2010).

[3] Y. Hayashi-Takanaka, T.J. Stasevich, H. Kurumizaka, N. Nozaki, H. Kimura, Evaluation of Chemical Fluorescent Dyes as a Protein Conjugation Partner for Live Cell Imaging, *PLoS One*, 9, e106271, (2014).

Germanium and Silicon: Laser-synthesized nanoparticles for bio-imaging applications

M. Rodio^{1, 2, 3}, R. Intartaglia¹

1- Nanophysics, Istituto Italiano di Tecnologia, Via Morego 30, Genoa, 16163, Italy

2- The Hamburg Centre for Ultrafast Imaging, CUI, Luruper Chaussee 149, Hamburg, 22761, Germany

3- Institute for Physical Chemistry, University of Hamburg, Martin-Luther-King Platz 6, Hamburg, 20146, Germany

romuald.intartaglia@iit.it

Nanoparticles (NPs) of group IV semiconductors such as germanium (Ge) and silicon (Si) have wide applications in optics and electronic devices, as well as in biological fluorescence imaging, because of their size-dependent optical properties and relatively low toxicity. [1] Ge is particularly attractive due to its narrow bulk bandgap (0.67 eV) as infrared bio-labels at tissue-transparent wavelengths (700-1100nm). However, NPs of group IV have been proven to be much more difficult to synthesize colloiddally, which has been attributed to the high crystallization temperatures of these materials due to strong covalent bonding.[1]

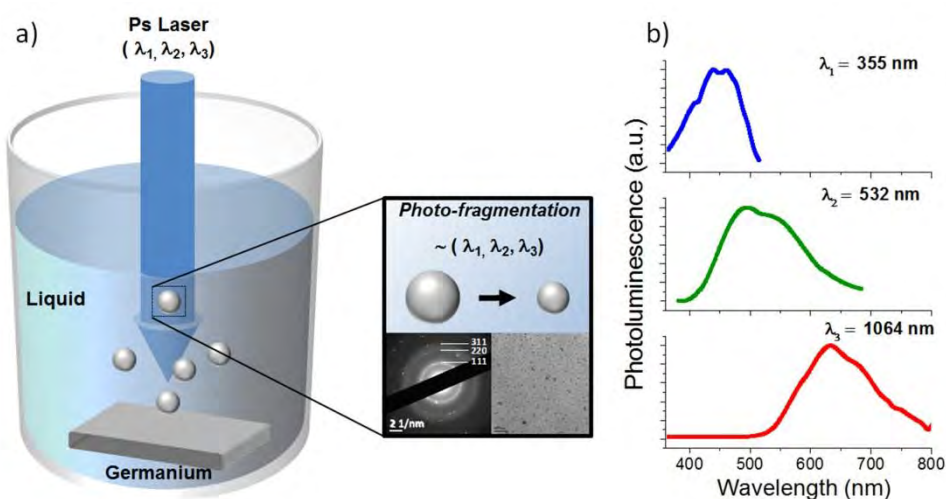


Figure 19: (a) Schematic of *in-situ* ablation/photo-fragmentation process during pulsed laser ablation in liquid (b) Photoluminescence spectra of Ge-NPs freshly prepared by picosecond laser ablation of the Ge target in aqueous solution, at different irradiation wavelengths ($\lambda = 355$ nm, $\lambda = 532$ nm and $\lambda = 1064$ nm).

We will report on the synthesis and surface modification [2] of Si nanoparticles prepared by ultra-fast (fs, ps) laser ablation of silicon target in liquid, resulting in functional Si-NPs bio-conjugates useful for bio-labelling and drug delivery applications. Furthermore, we will present an example of their *in-vivo* use by imaging of Zebrafish model animal. Additionally to Si based nanomaterials, we have developed a laser based-approach for the size control of Ge nanoparticles. Ge-NPs suspensions with different emission colors, blue (≈ 450 nm), green (≈ 510 nm) and red (≈ 650 nm), were prepared at room temperature via 60 ps pulsed laser ablation of the Ge target in liquid. (Figure 20) The emission color of the obtained Ge-NPs is tuned by adjusting the laser wavelengths ($\lambda = 355$ nm, $\lambda = 532$ nm and $\lambda = 1064$ nm), and is explained in terms of an *in-situ* ablation/photo-fragmentation process [3]. Results on the crystalline structure, optical properties and stability of the colloidal solutions assessed by the means of transmission electron microscopy, photoluminescence, X-ray photoelectron spectroscopy, UV-visible and infrared spectroscopy will be discussed.

[1] Fan, Jiyang, Paul K. Chu, Group IV nanoparticles: synthesis, properties, and biological applications, *Small* 6, 2080-2098, (2010).

[2] Rodio, M., Brescia, R., Diaspro, A., Intartaglia, R., Direct surface modification of ligand-free silicon quantum dots prepared by femtosecond laser ablation in deionized water, *Journal of colloid and interface science*, 465, 242-248, (2016).

[3] Intartaglia, R., Bagga, K., Brandi, F., Study on the productivity of silicon nanoparticles by picosecond laser ablation in water: towards gram per hour yield, *Optics express*, 22, 3117-3127, (2014).

Laser fabrication of colloidal hybrid nanoparticles: formation scenario and potential applications

S. Kudryashov¹, I. Saraeva², A. Ivanova², A. Levchenko², A. Ionin², A. Kudryavtseva²,
N. Tcherniega², A. Samokhvalov¹, V. Veiko¹

1- ITMO University, Kronverksky prospect 49, 197101 St. Petersburg, Russia
2- Lebedev Physical Institute, Leninsky prospect 53, 119991 Moscow, Russia

Main author email address: sikudryashov@corp.ifmo.ru, sikudr@lebedev.ru

Nanosecond laser ablation in liquids (ns-LAL) was comparatively studied regarding “dry” ns-LA and fs-LAL to figure out relationships between LA mechanisms and fabrication mechanisms for colloidal nanoparticles (NPs) [1-2]. Broadband ultrasonic diagnostics indicates the same ns-LA focusing and thresholds for copper and stainless steel in air and water ambients, with one order of magnitude higher compressive ultrasonic signals for their ns-LAL in sub-GW/cm² to a few GW/cm² laser intensity range. Likewise, sub-critical plasma-mediated yield of colloidal nanoparticles was observed in water in this intensity range, resulting in the non-linear – third-power – intensity-dependent NP yield via complete dissociation of ablation products in the hot plasma core and the following recondensation, with the NP yield limited at higher intensities by intense micro-droplet expulsion of the molten material. In contrast, at the absence of ablative plasma fs-LAL provides direct expulsion of nanoparticles via post-spallative nanojetting or “phase explosion” [1]. This enables in the ns-LAL case laser fabrication of codeposited or merged hybrid nanoparticles (diamond or silicon core – plasmonic metal shell, etc. – see Figure 1) in plasma via plasma-induced or chemical reduction, however, the first collapse of the near-surface vapor/plume bubble brings the most part of the ablated/modified products back on the surface, as revealed by using chemical markers.

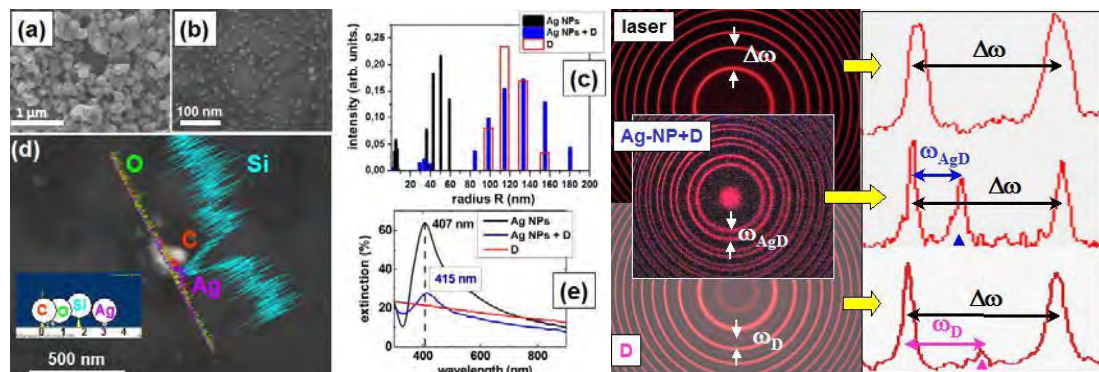


Figure 21. (left) top-view SEM images of bare nanodiamonds (a) and silver nanoparticles (b), and their size distributions (c); EDX analysis – linear scan and its spectrum (d), extinction (absorbance + scattering) spectra of bare and silver-coated diamonds, as well as silver nanoparticles (e). (right)

Fabry-Perot diffractograms for low-frequency stimulated Raman scattering in colloidal solutions of bare (D) and silver-coated (Ag-NP+D) nanodiamonds (laser scattering in clean water is given for the reference (“laser”)) and their high non-linear conversion of the pump laser radiation shown by the corresponding spectral shifts.

Finally, NP size-engineered chemosensing [1] and non-linear conversion [3] (Figure 1) by bare dielectric Mie-resonant or hybrid plasmonic/Mie-resonant NPs was demonstrated in various spectral ranges.

[1] A. Ionin, A. Ivanova, R. Khmel'nitskii, Yu. Klevkov, S. Kudryashov, N. Mel'nik, A. Nastulyavichus, A. Rudenko, I. Saraeva, N. Smirnov, D. Zayarny, A. Baranov, Milligram-per-second femtosecond laser production of Se nanoparticle inks and ink-jet printing of nanophotonic 2D-patterns, Applied Surface Science, vol. 436, pp. 662-669, (2018).

[2] A. Ionin, A. Ivanova, R. Khmel'nitskii, S. Kudryashov, A. Rudenko, I. Saraeva, D. Zayarny, Plasma-mediated nanosecond-laser generation of Si nanoparticles in water, Applied Surface Science (2017, submitted).

[3] A. Baranov, A. Butsen, A. Ionin, A. Ivanova, A. Kuchmizhak, S. Kudryashov, A. Kudryavtseva, A. Levchenko, A. Rudenko, I. Saraeva, M. Stokov, N. Tcherniega, D. Zayarny, The double-resonance enhancement of stimulated low-frequency Raman scattering in silver-capped nanodiamonds, AIP Conference Proceedings, vol. 1874, 030031, (2017).

Ubiquitous Metal Carbonization, Carbon Encapsulation, Metal-Catalyzed Graphitization during Laser Ablation of Metal in Organic Solvents

Dongshi Zhang,^{1,3} Chao Zhang^{1,2} Jun Liu,¹ Changhao Liang*^{1,2}

1-Key Laboratory of Materials Physics and Anhui Key Laboratory of Nanomaterials and Nanotechnology, Institute of Solid State Physics, Hefei Institutes of Physical Science, Chinese Academy of Sciences, Shushanhu Road 350, Hefei 230031, China.

2-Department of Materials Science and Engineering, University of Science and Technology of China, Jinzhai Road 96, Hefei, 230026, China

3- RIKEN-SIOM Joint Research Unit, RIKEN Center for Advanced Photonics, Wako, Saitama 351-0198, Japan

Changhao Liang: chliang@issp.ac.cn

Laser ablation of metal targets in organic solvents (LAMO) is considered as one of the most efficient strategy to generate carbon encapsulation of metal or metal carbide (M@C, MC_x@C) core-shell nanostructures. Herein, we aim for clarifying the panorama of chemical reactions occurred in (LAMO) by comparative experiments using sixteen transition metallic targets (Cu, Ag, Au, Pt, Pd, Ti, V, Nb, Cr, Mo, W, Ni, Zr, Zn, Mn and Fe), involving laser-induced target material atomization and organic solvent decomposition, carbon/metal and metal-oxide/reductive-gas (CO, CH₄, etc.) reactions for carbide formation, carbon generation/precipitation/segregation and metal-catalyzed graphitization for the onion-like carbon shell evolution. The reactivity of target materials and the carbon solubility in metals are the main factors governing the compositions of core particles and the type of carbon shell. After LAMO, the insert metals (Cu, Ag, Au, Pt, Pd) evolve into pure metal nanoparticles covered by onion-like carbon shell, but the reactive metals (Ti, V, Nb, Cr, Mo, W, Ni, Zr) transform into metal carbides encapsulated in amorphous or onion-like carbon shell. Differently, for Zn, Mn, Fe, the products are mixture of metal/metal oxides encapsulated in carbon shell, which is ascribed to the poor carbon solubility and strong affinity to oxygen atoms.

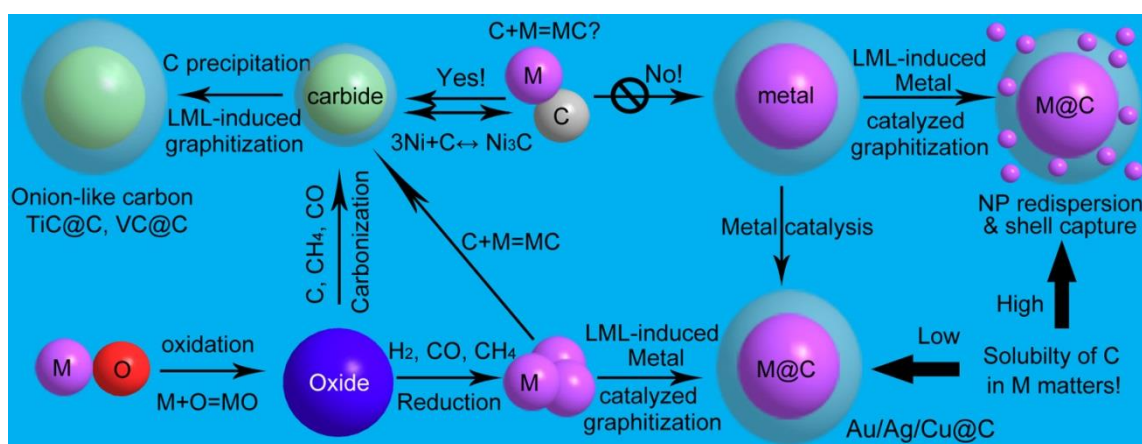


Figure 1 Formation routes for the TMC@C and M@C nanoparticles.

- [1] H. M. Zhang, C. H. Liang, J. Liu, Z. F. Tian, G. S. Shao, The formation of onion-like carbon-encapsulated cobalt carbide core/shell nanoparticles by the laser ablation of metallic cobalt in acetone, *Carbon*, 55, 108-115, (2013).
- [2] H. M. Zhang, J. Liu, Z. F. Tian, Y. X. Ye, Y. Y. Cai, C. H. Liang, K. Terabe, A general strategy toward transition metal carbide/carbon core/shell nanospheres and their application for supercapacitor electrode, *Carbon*, 100, 590-599, (2016).
- [3] S. K. Yang, W. P. Cai, H. W. Zhang, H. B. Zeng, Y. Lei, A General Strategy for Fabricating Unique Carbide Nanostructures with Excitation Wavelength-Dependent Light Emissions, *J. Phys. Chem. C* 2011, 115, 7279–7284
- [4] Y. J. Kim, R. Ma, D. A. Reddy, T. K. Kim, Liquid-phase pulsed laser ablation synthesis of graphitized carbon-encapsulated palladium core-shell nanospheres for catalytic reduction of nitrobenzene to aniline, 357, 2112-2120, (2015).
- [5] V. Amendola, P. Riello, M. Meneghetti, Magnetic Nanoparticles of Iron Carbide, Iron Oxide, Iron@Iron Oxide, and Metal Iron Synthesized by Laser Ablation in Organic Solvents, *J. Phys. Chem. C* 115, 5140-5146, (2011).

Fullerene-Like MoS₂ Nanoparticles as Cascade Catalyst Improving Lubricant and Antioxidant Abilities of Artificial Synovial Fluid

Tongming Chen, Guowei Yang

State Key Laboratory of Optoelectronic Materials and Technologies, Nanotechnology Research Center, School of Physics, School of Materials Science & Engineering, Sun Yat-sen University, Guangzhou 510275, Guangdong, P. R. China
Main author email address: chentm3@mail2.sysu.edu.cn

Osteoarthritis (OA) is a disease of the synovial joint, causing pain and loss of movement. Attempts to slow the progression of OA have been made using nutritional and pharmaceutical supplements, physical therapy, and other approaches. Since the joint fails can be traced to a lubrication deficiency, intraarticular injections of hyaluronic acid (HA) for viscosity supplementation is a non-surgical treatment for OA [1]. However, the HA will be depolymerized by the overproduction of reactive oxygen species (ROS) in OA state, which results in the decrease of its viscosity.

Molybdenum disulfide (MoS₂), one of the typical layered transition metal dichalcogenide materials, exhibit the unique mechanical, optical, electrical and chemical properties. Recently, MoS₂ nanostructures have a wide range of potential in biomedical application, such as blood glucose detection, DNA biosensors, antibacterial, near-infrared photothermal agent, and drug delivery, which shows their low toxicity and excellent biocompatibility in living organisms.

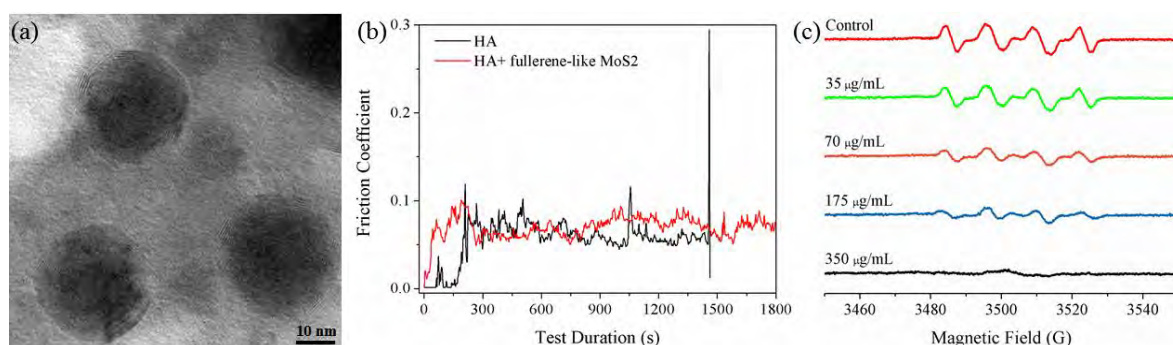


Figure 22 (a) TEM image of fullerene-like MoS₂ nanoparticles. (b) Friction coefficient of HA contained fullerene-like MoS₂ nanoparticles with test durations. (c) ESR spectrum of BMPO•OOH adducts incubated with different concentration of fullerene-like MoS₂ nanoparticles.

Here, we for the first time reported that fullerene-like MoS₂ nanoparticles are efficient additive for artificial synovial fluid protection. The fullerene-like MoS₂ nanoparticles were synthesized via laser ablation of MoS₂ target in pure water. Figure 1a illustrates the TEM image of produced fullerene-like MoS₂ nanoparticles [2]. The tribological tests show that they markedly improve the anti-wear and friction-reducing abilities of the artificial synovial fluid contained HA (Figure 1b). Surprisingly, ESR experiments reveal they possess intrinsic dualenzyme-like activity, mimicking superoxide dismutases and catalases under physiological conditions (Figure 1c) [3]. Coupling these properties, a self-organized cascade catalytic system was constructed, which includes the dismutation of superoxide radicals (O₂^{•-}) to produce oxygen (O₂) and hydrogen peroxide (H₂O₂) and subsequently the H₂O₂ degradation to form O₂. Based on this system, the fullerene-like MoS₂ nanoparticles were used to regulate the ROS level in artificial synovial fluid. The relative viscosity measurement showed the superior protective effect of fullerene-like MoS₂ nanoparticles against O₂^{•-}-induced HA oxidative damage. These results proposed that fullerene-like MoS₂ nanoparticles are promising candidate for treatment of OA and other disease caused by oxidative stress.

- [1] M. J. Furey and B. M. Burkhardt. Biotribology: friction, wear, and lubrication of natural synovial joints. *Lubrication Science*, 9(3), 255-271 (1997).
[2] J. Xiao, P. Liu, C. X. Wang, G. W. Yang. External field-assisted laser ablation in liquid: An efficient strategy for nanocrystal synthesis and nanostructure assembly. *Progress in Materials Science*, 87, 140-220 (2017).
[3] T. M. Chen, X. M. Tian, L. Huang, J. Xiao, G. W. Yang. Nanodiamonds as pH-switchable oxidation and reduction catalysts with enzyme-like activities for immunoassay and antioxidant applications. *Nanoscale*, 9(40), 15673-15684 (2017).

Liquid Assisted Laser Fabrication of Binary Nanocrystalline Structures Based on Germanium and Silicon

N. Tarasenka, A. Butsen, M. Nedelko, N. Tarasenko,

B. I. Stepanov Institute of Physics, National Academy of Sciences of Belarus, Nezalezhnasti Ave. 68, 220072 Minsk, Belarus

n.tarasenko@ifanbel.bas-net.by

Recently, synthesis of nanocrystalline structures based on germanium and silicon has received great interest. In particular, silicon carbide nanocrystals are characterized by the enlarged band gap in comparison with silicon, high thermal and chemical stability and exhibit luminescent properties. Nanostructures based on the alloys $\text{Ge}_x\text{Si}_{1-x}$ and GeSn are interesting due to the possibility of adjusting the lattice parameters and the width of the band gap, changing the mobility of charge carriers. Despite some progress in preparation of these structures, the development of new approaches for the controlled synthesis of nanocrystals based on silicon and germanium remains an urgent task. In the last decade, laser ablation in liquids has become effective route for synthesis of nanoparticles (NPs), due to its simplicity of implementation and universality [1, 2]. NPs are obtained as colloidal solutions, and they can be incorporated into polymer and glass matrices, and can also be applied as thin films. It should be noted that laser ablation method has been well developed for monoelement NPs, whereas the generation of stoichiometric compound NPs involves a careful selection of experimental conditions [2]. In this paper, we demonstrate the capabilities of the liquid assisted laser ablation technique in combination with laser-induced modification for synthesis of binary SiC, SiGe and GeSn NPs. To find the optimal conditions for the formation of binary compound NPs, the analysis of the inner structure and phase composition of NPs prepared under different experimental conditions was carried out using HRTEM, SAED, XPS, Raman and FTIR methods. The main physical factors determining the formation of nanostructures with the required parameters are discussed. As an example, Figure 1 illustrates the schematic diagram of the experimental procedure and some results of characterization of binary SiC nanocrystals prepared by 532 nm laser irradiation of the mixture of Si and C colloids produced by pulsed laser ablation in ethanol. In addition, a way for assembling of colloidal NPs into nanostructured layers based on laser induced deposition of colloidal NPs on the pre-prepared template is analyzed.

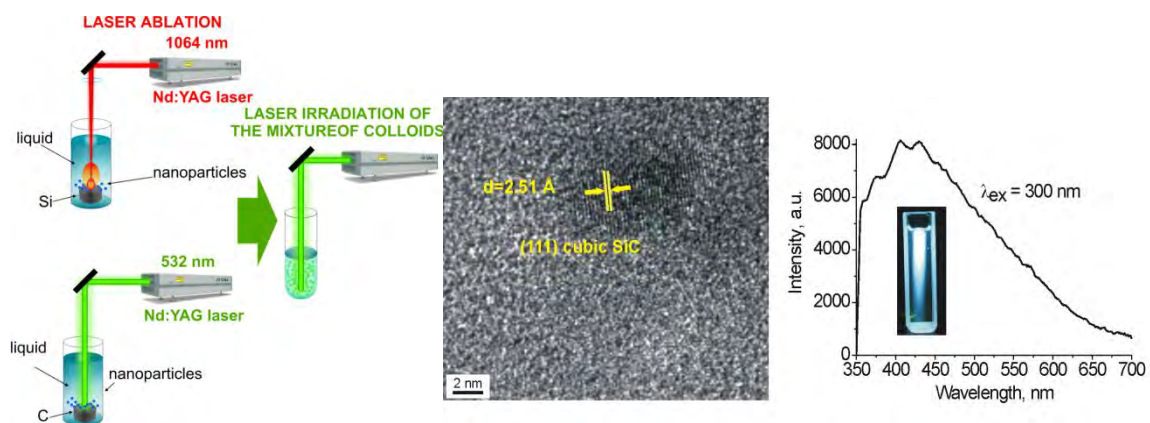


Figure 23 Schematic diagram of the experimental set-up and results of characterization of the synthesized SiC particles.

[1] D. Zhang, B. Gökce, and S. Barcikowski Laser Synthesis and Processing of Colloids: Fundamentals and Applications. Chem. Rev., vol. 117, pp. 3990 - 4103 (2017).

[2] N.V. Tarasenko, A.V. Butsen Laser synthesis and modification of composite nanoparticles in liquids, Quantum Electronics, vol. 40, pp. 986 –1003 (2010).

Nanocomposites and nanoalloys with engineered interfacial structures and functionalities made via Laser Ablation Synthesis in Solution (LASiS)-based routes

Dibyendu Mukherjee

Department of Mechanical, Aerospace, & Biomedical Engineering; Nano-BioMaterials Laboratory for Energy, Energetics & Environment (nbml-E³); University of Tennessee, Knoxville, Tennessee, 37996.

Email address: dmukherj@utk.edu

Rational synthesis and design of intermetallic nanoalloys (NAs) and nanocomposites (NCs) as efficient, low-cost electrocatalysts require robust understanding of processing-structure-property relations to enable systematic tailoring of their architectures, confinements and compositions. This talk shall showcase our research efforts in addressing these challenges with our recently developed and highly versatile Laser Ablation Synthesis in Solution-Galvanic Replacement Reaction (tandem LASiS-GRR) [1-3] technique (see Fig. 1) as a facile, green yet, efficient route for colloidal synthesis of: 1) binary (PtCo)/ternary (PtCuCo) NAs, [4,5] and 2) Co₃O₄/nitrogen-doped graphene oxide (NGO) hybrid NCs (HNC) [6] as efficient ORR electrocatalysts. Here, the transformative concept is that LASiS-GRR exploits the high-energy physico-chemical pathways emerging from liquid-confined, laser-induced plasma, and GRR mechanisms to produce NAs/NCs with varied sizes, compositions and alloying without using any detrimental chemicals/surfactants. Firstly, detailed structural and chemical analyses reveal uniform alloyed cores with Pt-rich shells for PtCo NAs and PtCu-rich shells with minor Cu contents for PtCuCo NAs. Our previous studies have established outstanding ORR activities for PtCo NAs in acid electrolytes while enabling Pt content reductions [5]. Recent results for Pt₇₀Cu₂₁Co₉ NAs with 25-30% (at.) reduction in Pt indicate a c.a. 4 and 6-fold increase in mass and specific activities respectively as compared to commercial Pt/C catalysts.[4] On the other hand, spectroscopic studies on HNC samples reveal both chemical and charge-driven embedment of Co₃O₄ nanoparticles (NPs) onto NGO films. ORR activities for the Co₃O₄/NGO HNCs are comparable to commercial Pt catalysts.[6] Such enhanced activities are attributed to: 1) surfactant-free syntheses that prevent catalytic site degradations; 2) systematic alloying of transition metals (Cu) that allow optimal positioning of Pt d-band centers to tune their binding affinities for oxygen/oxygenated species; and 3) N-doping in 2D HNCs that promote electron conductivity while hindering Co₃O₄ NP aggregations. The talk will conclude with our recent use of LASiS-GRR to synthesize catalytic Pt NPs confined within porous Metal Organic Frameworks (MOFs) that hinder NP aggregations with post-calcination treatments to achieve well-dispersed and spatially confined NPs on suitable substrates. Preliminary results for post-calcined Pt/MOF NCs show promising ORR activities. Our results indicate the yet-to-be-unleashed potential of LASiS-GRR in the manufacturing of diverse NPs with interfacial structures and functionalities.

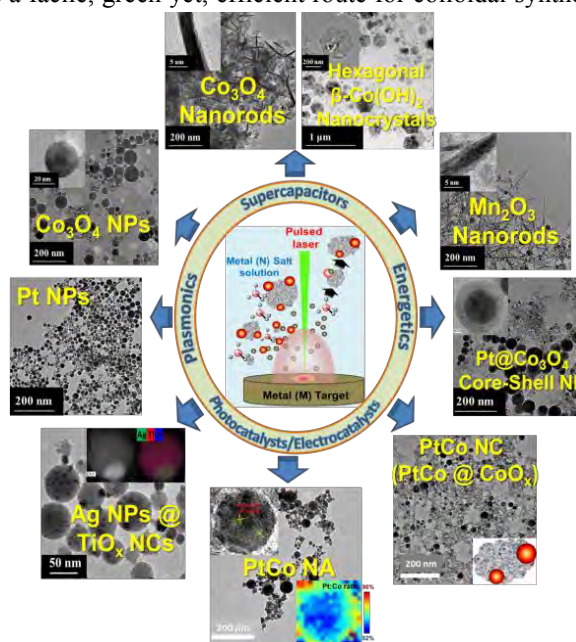


Figure 1 LASiS-GRR makes diverse functional nanomaterials.

- [1] Mukherjee, D. and S. Hu, *Compositions, Systems and Methods for Producing Nanoalloys, and/or Nanocomposites using tandem Laser Ablation Synthesis in Solution-Galvanic Replacement Reaction*. USA Patent No: 20170296997A1 (2016).
- [2] Hu, S., et al., *PtCo/CoOx nanocomposites: Bifunctional electrocatalysts for oxygen reduction and evolution reactions synthesized via tandem laser ablation synthesis in solution-galvanic replacement reactions*. Applied Catalysis B: Environmental, 182: p. 286-296, (2016).
- [3] Hu, S., C. Melton, and D. Mukherjee, *A facile route for the synthesis of nanostructured oxides and hydroxides of cobalt using laser ablation synthesis in solution (LASiS)*. Physical Chemistry Chemical Physics, 16(43): p. 24034-24044, (2014).
- [4] Hu, S., et al., *A facile and surfactant-free route for nanomanufacturing of tailored ternary nanoalloys as superior oxygen reduction reaction electrocatalysts*. Catalysis Science & Technology, 7(10): p. 2074-2086, (2017).
- [5] Hu, S., et al., *Tandem laser ablation synthesis in solution-galvanic replacement reaction (LASiS-GRR) for the production of PtCo nanoalloys as oxygen reduction electrocatalysts*. Journal of Power Sources, 306: p. 413-423, (2016).
- [6] Hu, S., et al., *Hybrid nanocomposites of nanostructured Co₃O₄ interfaced with reduced/nitrogen-doped graphene oxides for selective improvements in electrocatalytic and/or supercapacitive properties*. RSC Advances, 7(53): p. 33166-33176, (2017).

Fabrication of organic solvent and surfactant free fluorescent organic nanoparticles by laser ablation of aggregation-induced enhanced emission dyes

A. A. Popov¹, C.-K. Lim^{2,3}, G. Tselikov¹, J. Heo, A. Pliss, S. Kim, A. V. Kabashin, P. N. Prasad¹

1- Aix Marseille Univ, CNRS, LP3, Marseille, France

2- Department of Chemistry and Institute for Lasers, Photonics, and Biophotonics, University at Buffalo, The State University of New York, Buffalo, New York 14260, United States

3- Center for Theragnosis, Korea Institute of Science and Technology, 39-1 Hawolgok-dong, Seongbuk-gu, Seoul 136-791, Republic of Korea

4- ch c "E Ph" fE g gPh c f c (Ph) 5409 c w ia

email: anton.popov@lp3.univ-mrs.fr

We used methods of femtosecond laser ablation in liquids to fabricate small (< 2 nm) nanoparticles of organic aggregation induced (enhanced) emission (AIE) luminophore dyes, which are free of any organic solvent and surfactant. As these dyes exhibit aggregation enhanced emission and provide no concentration quenching, the increased number of photoluminescent molecules in nanoparticles produce bright fluorescence even with their small size, making them highly suitable for intracellular uptake and imaging for a variety of biomedical applications. We report here the design and synthesis of a new aggregation induced enhanced emission luminophore, DCEtDCS, and demonstrate its photoluminescent quantum yield enhancement up to 58% in the aggregated state. We fabricated extremely stable nanoparticles of this luminophore with narrow size distribution by laser ablation in water and verified the superior optical properties comparable to quantum dots. The highly negative surface charge of these nanoparticles impeded their cellular uptake, but when the surface was coated with chitosan, a cationic polymer, intracellular uptake in microglia was demonstrated [1]. Our strategy provides a novel tool to produce in water, ultrasmall and surfactant free highly fluorescent organic nanoparticles suitable for biomedical applications.

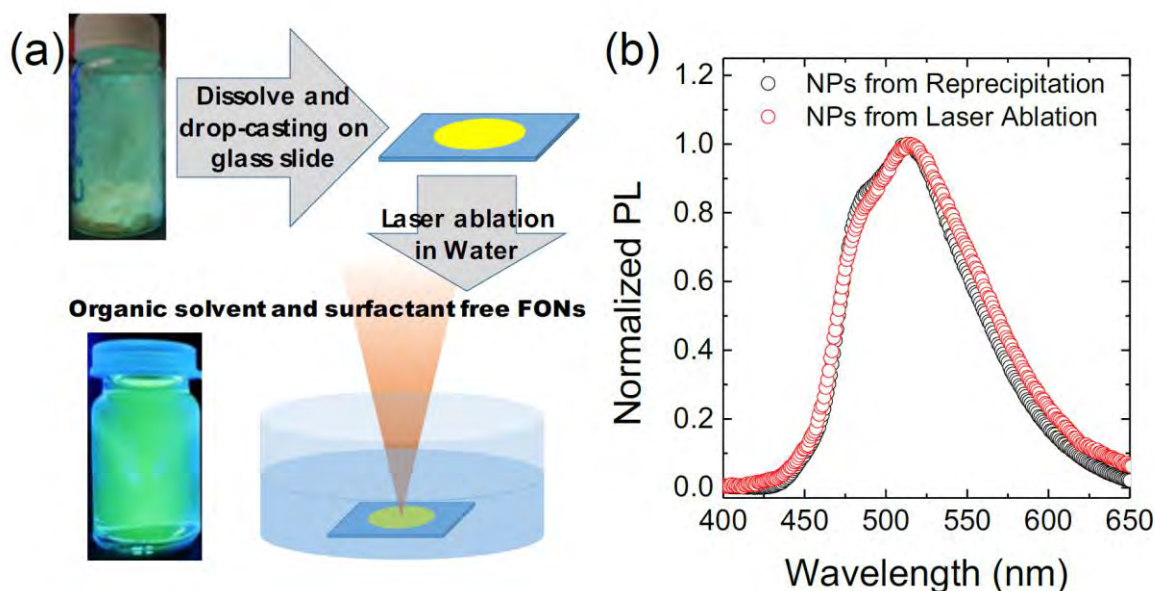


Figure 24 Fabrication of AIE FON by laser ablation. (a) Schematic representation of laser ablation process of DCEtDCS in water. (b) Normalized PL spectra of DCEtDCS NPs fabricated by reprecipitation and laser ablation..

[1] C.-K. Lim, A. A. Popov, G. Tselikov, J. Heo, A. Pliss, S. Kim, A. V. Kabashin, P. N. Prasad, Organic solvent and surfactant free fluorescent organic nanoparticles by laser ablation of aggregation-induced enhanced emission dyes, *Adv. Opt. Mater.*, in press (2018).

Laser Synthesis of Nanocomposites for Additive Manufacturing

**B. Gökce,¹ T. Hupfeld,¹ R. Streubel,¹ C. Doñate-Buendía,² G Mínguez-Vega,²
M. Schmidt,³ J.H. Schleifenbaum,⁴ S. Barcikowski¹**

¹Technical Chemistry I, University of Duisburg-Essen and Center for NanoIntegration Duisburg-Essen CENIDE, Germany

²GROC-UJI, Institute of New Imaging Technologies, Universitat Jaume I, Spain

³Digital Additive Production, RWTH Aachen University and Fraunhofer Institute of Laser Technology, Germany

⁴Department of Photonic Technologies, University of Erlangen-Nuremberg and Bayerisches Laserzentrum, Germany

bilal.goekce@uni-due.de

During the past few years laser synthesis and processing of colloids (LSPC) has been established as an economically feasible [1] synthesis method that addresses real-world problems [2]. The recent significant progress [3] in nanoparticle productivity opened up new areas of application where nanomaterials in the gram-scale are required. In this contribution, we present our results in such a new area of application, i.e. additive manufacturing. By pH-controlled, colloidal adsorption of laser-generated nanoparticles on metal or polymer powders we are able to produce new compound materials that are highly relevant for powder-based 3D-printing methods such as selective laser melting (SLM) or selective laser sintering (SLS) (Fig. 1). Due to the barrier-free surface of the small, highly dispersed colloidal nanoparticles, a high surface coverage can be achieved even with mass loadings of 0.1 wt%, as shown in Fig. 1 for silver nanoparticles supported on polyamide (PA12) or yttrium oxide nanoparticles supported on steel powder (PM2000).

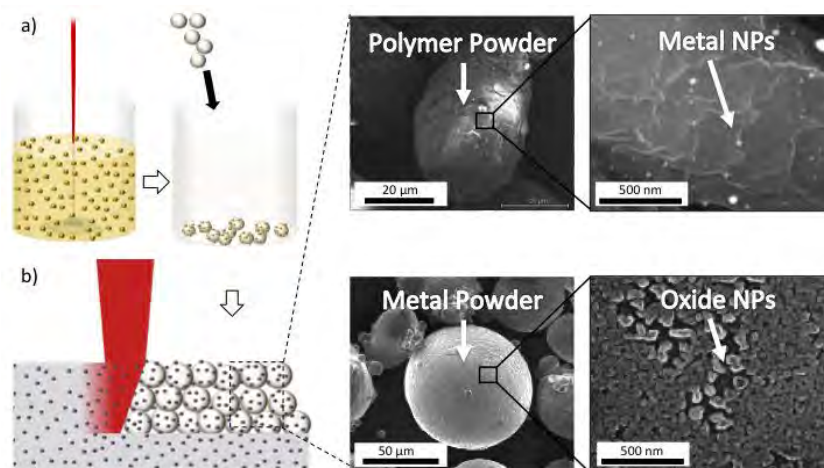


Figure 25 (a) Schematic illustration of the process steps involved in the adsorption process of laser-generated nanoparticles on polymer or metal powders: Laser generation of nanoparticles, mixing of polymer particles with the colloid and sedimentation of the powder compound. (b) Selective Laser Melting/Sintering of powder compounds from (a). Magnification shows SEM images of a polyamide 12 powder decorated with silver nanoparticles (top) and iron-chromium powder decorated with Y_2O_3 nanoparticles (bottom).

Studies on SLS and SLM-built parts show that the homogeneity of the surface coverage can be transferred to the final part. While silver nanoparticles are used for plasmonic enhancement of the polymer composite, Y_2O_3 nanoparticles are used for oxide dispersion strengthening of the steel. Within the additively manufactured metal component, we further show that the particle spacing of the oxide inclusion can be adjusted by the initial mass fraction of the adsorbed Y_2O_3 particles on the micropowder [4].

- [1] S. Jendrzej, B. Gökce, M. Epple and S. Barcikowski, How Size Determines the Value of Gold - Economic Aspects of Wet Chemical and Laser-Based Metal Colloid Synthesis, *Chemical Physics and Physical Chemistry*, 18, pp. 1012-1019, (2017).
- [2] D. Zhang, B. Gökce and S. Barcikowski, Laser Synthesis and Processing of Colloids – Fundamentals and Applications, *Chemical Reviews*, 117, pp. 3990-4103, (2017).
- [3] R. Streubel, S. Barcikowski and B. Gökce, Continuous Multigram Nanoparticle Synthesis by High-Power, High-Repetition-Rate Ultrafast Laser Ablation in Liquid, *Optics Letters*, 41, pp. 1486-1489, (2016).
- [4] R. Streubel, M. B. Wilms, C. Doñate-Buendía, A. Weisheit, S. Barcikowski, J. H. Schleifenbaum, and B. Gökce, Depositing laser-generated nanoparticles on powders for additive manufacturing of parts of oxide dispersed strengthened alloys via laser metal deposition, submitted

Hybrid nanostructures of metal/one-dimensional carbon allotropes prepared by laser ablation in liquid

D.W. Boukhvalov^{1,2}, I.S. Zhidkov³, E.Z. Kurmaev^{3,4}, E. Fazio⁵, S.O. Cholakh³, F. Neri⁵, M. Condorelli⁶, G. Compagnini⁶, L. D'Urso⁶

1- Department of Chemistry, Hanyang University, 17 Haengdang-dong, Seongdong-gu, Seoul 04763, South Korea

2- Theoretical Physics and Applied Mathematics Department, Ural Federal University, Mira Street 19, 620002 Yekaterinburg, Russia

3- Institute of Physics and Technology, Ural Federal University, Mira Street 19, 620002 Yekaterinburg, Russia

4- M.N. Mikheev Institute of Metal Physics, Russian Academy of Sciences, Ural Branch, S. Kovalevskaya Street 18, 620990 Yekaterinburg, Russia

5- Dipartimento di Scienze Matematiche e Informatiche, Scienze Fisiche e Scienze Della Terra (MIFT), Università di Messina, 98166 Messina, Italy

6- Dipartimento di Scienze Chimiche, Università di Catania, Viale Andrea Doria 6, 95125 Catania, Italy

ldurso@unict.it

Synthesis of hybrid carbon-based nanostructures is an actual task of current nanotechnology because of technological breakthroughs offered by carbon allotropes, such as graphene, fullerenes, nanodiamond, carbon nanotubes. Between them, linear carbon chains (LCCs) have attracted a persistent interest of scientists due to their potential application as one-dimensional conducting materials [1] or as materials for optoelectronics [2]. Compared to other carbon structures, LCCs remain the most challenging and difficult to obtain at high concentration because they tend to react and cross-link toward sp^2 hybridizations [3]. To overcome these problems, metal colloidal nanoparticles (Me Nps=Ag, Au, Pt) were employed as end-capping link to stabilize LCCs. Hybrid nanostructures Me@LCCs were prepared by a pulsed laser ablation procedure in water and characterized both in liquid (SERS) and solid state (XPS, STEM). The possibility to establish a LCC–metal bond was also investigated by carrying out XPS analysis on Me@LCCs hybrid nanostructures. It was found that covalent carbon-metal bonds are mainly formed after Me Nps-LCC interaction and that several detected oxidation phenomena on nanoparticles surface lead to negligible carbon-oxygen bonds. Theoretical modeling also supports the formation of carbon metal bonds between linear carbon chains and pure and partially oxidized metal surfaces. The chemical stability was also evaluated by a study of the energetics of physical adsorption of oxidative species (water and oxygen).

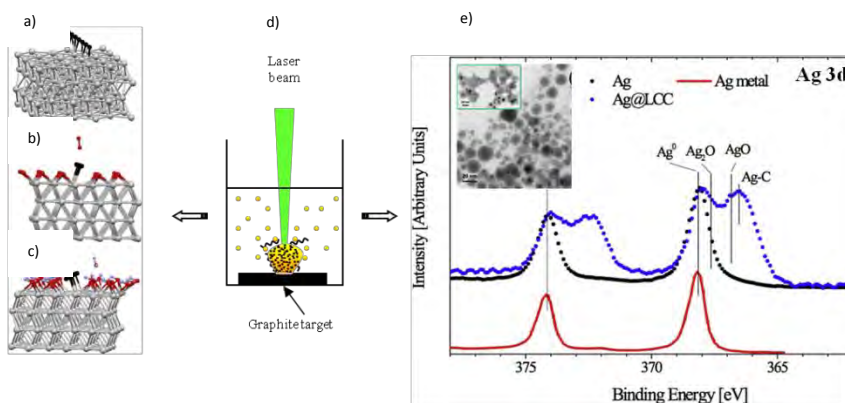


Figure 1- Optimized atomic structure of a linear carbon chain over pristine (a), oxidized (b) and passivated by hydroxyl groups (c) silver; (d) schematic representation of the experimental setup; (e) XPS Ag-3d spectra and STEM micrograph of Ag@LCC nanoparticles.

[1] Z. Crljen, G. Baranovic', Unusual conductance of polyene-based molecular wires. Phys Rev Lett 98:116801/1–4 (2007);

[2] E. Fazio a, F. Neri, S. Patane, L. D'Urso, G. Compagnini, Optical limiting effects in linear carbon chains Carbon 49, 306-310 (2011);

[3] L. D'Urso, G. Compagnini, O. Puglisi, sp/sp^2 bonding ratio in sp rich amorphous carbon thin films, Carbon 44, 2093-2096 (2006).

The internal phase structure of LAL-fabricated FeAu alloy nanoparticles is determined by solvent properties and target composition

A. Tymoczko, C. Rehbock¹, M. Kamp², J. Jakobi¹, U. Schürmann², L. Kienle², O. Prymak³, S. Barcikowski¹

1- Technical Chemistry I and Center for Nanointegration Duisburg-Essen (CENIDE), University of Duisburg-Essen, Universitätsstrasse 7, 45141 Essen, Germany; 2- University of Kiel, Technical Department, Synthesis and Real structure, TEM- Centrum, Kaiserstr. 2, 24143 Kiel, Germany; 3- Inorganic Chemistry and Center for Nanointegration Duisburg-Essen (CENIDE), University of Duisburg-Essen, Universitätsstrasse 7, 45141 Essen, Germany

Christoph.rehbock@uni-due.de

Alloy nanoparticles (NP) composed of gold and iron, particularly when arranged in a core-shell structure with an iron core and a gold shell, are highly interesting as they combine magnetic and plasmonic properties, which would make them highly useful e.g. during MRI/optical dual imaging. [1] The generation of FeAu NP by Laser Ablation in Liquids (LAL) from gold-rich bulk targets has already been studied by the Amendola group and alloy particles without phase segregation were reported, while the solubility of iron in gold was significantly higher than in the bulk. [2] In this work, the impact of the solvent and the target composition during LAL from FeAu bulk targets was systematically studied. We found that NP derived from a 50:50 alloy target in water and acetone exhibited a clear phase segregation and the formation of a core-shell morphology (Figure 1a). While in aqueous media a gold core and an iron oxide shell was found, in acetone a metallic iron core and a gold shell emerged (Figure 1b). This phenomenon probably originates from specific solvent-surface-interactions. [3] In consecutive experiments we further studied to what extent the composition of the target may influence the internal phase structure in acetone. High resolution TEM and high angle annular dark field scanning TEM (HAADF-STEM) studies revealed that alloy NP (solid solution) and core-shell NP formed in parallel. Interestingly, core-shell formation was only observed for iron molar fractions of > 50% in the target as well as for NP >10 nm (Figure 1c). In further experiments the crystal structure of the resulting NP was probed with X-ray diffraction (XRD). We exclusively found the formation of substituted FCC-gold and -iron crystal structures in NP from gold rich targets, while the presence of a BCC iron structure could be clearly correlated with the formation of core-shell NP in iron rich targets.

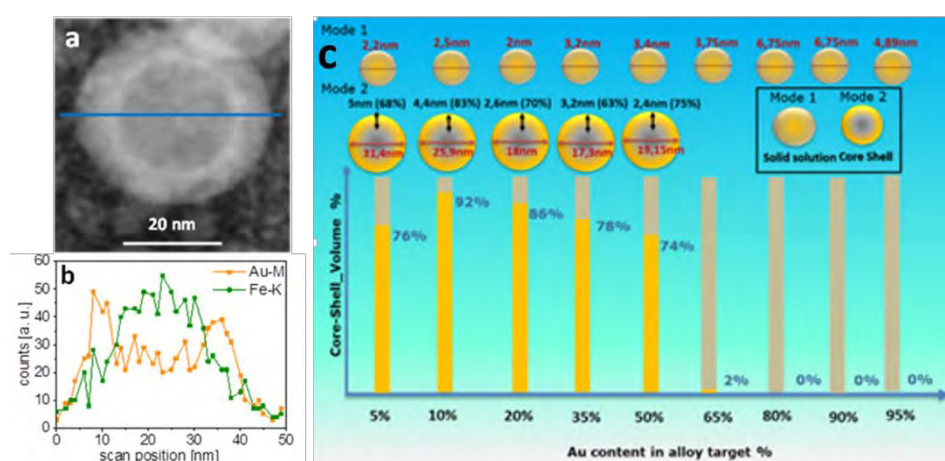


Figure 26 (a) HAADF-STEM image of a core-shell FeAu NP. (b) EDX-line scan verifying a core-shell structure. (c) Portion of core/shell NP (by volume) as well as average particle sizes in correlation with the Au content in the target.

[1] T. A. Larson, J. Bankson, J. Aaron, K. Sokolov, *Nanotechnol.* **18** (2007), 325101.

[2] S. Scaramuzza, S. Agnoli and V. Amendola, *Physical Chemistry Chemical Physics*, **17**, (2015), 28076.

[3] P. Wagener, J. Jakobi, C. Rehbock, V. S. K. Chakravadhanula, C. Thede, U. Wiedwald, M. Bartsch, L. Kienle and S. Barcikowski, *Scientific Reports*, **6** (2016), 23352.

Temporal and spatial diagnosis for laser ablation on silicon carbide in water

Hao Liu¹, Minsun Chen¹, Xin Peng¹, Guomin Zhao¹

1- College of Advanced Interdisciplinary Studies, National University of Defence Technology, Changsha 410073, P. R. China

Main author email address: haoliu1989@hotmail.com

We present a versatile method to diagnose laser induced plasma in liquid with good temporal (here 10 ns) and spatial (here sub-millimeter) resolution. The spatially resolved emission image from plasmas formed by 532 nm picosecond laser ablation of a silicon carbide target in water were recorded at different time delays using a time-gated iCCD camera attached to a spectrograph and imaging optics. The spectroscopic emission lines associated with different charged species are assigned in the NIST Atomic Spectra Database. The figure 1 shows that the spatial distribution of different emitters with a given charge state are displayed as high uniformity, the higher charged ions (e.g. Si^{3+}), however, always spread further away from the target surface, illustrating a larger expansion velocity as high as ~ 4 km/s in the water. These emission features indicate the dominance of acceleration dynamics due to the internal electric gradient between the fastest electrons at the leading edge of the plasma plume and the net positively charged bulk of the plume, which is also supported by previous works [1,2].

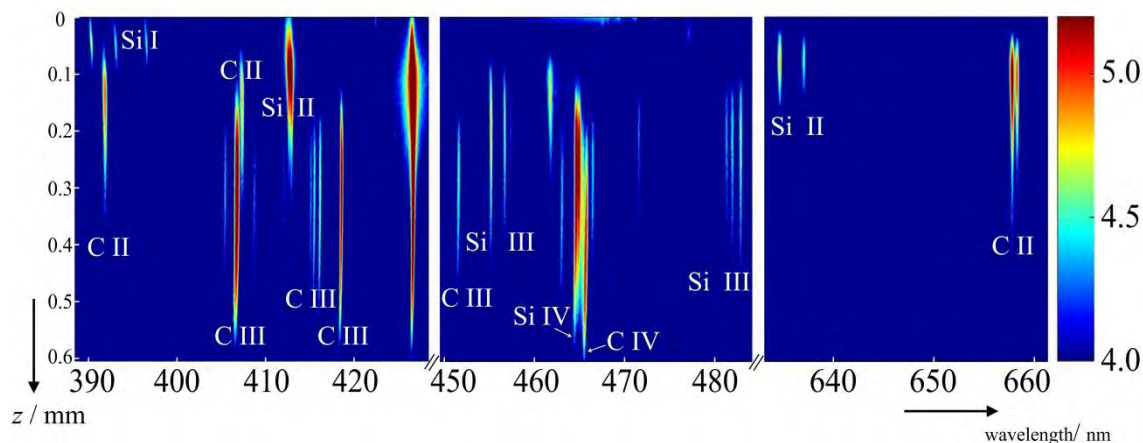


Figure 27

Spatially resolved optical emission spectra measured at $\Delta t = 100$ ns over the wavelength range $388 < \lambda < 660$ nm following 532 nm laser ablation of a SiC target (the surface of which is located at $z = 0$) in the water. The logarithmic false colour intensity scale is shown at the right of the image.

The further analysis of Stark broadened line shapes of those emission images allows tracking the plume dynamics and provides insight into the mechanism of laser-target interaction and the subsequent laser-plasma coupling. The electron density (N_e) and temperature (T_e) values and their variations with space and time are obtained from best-fitting model to the observed line shapes. The value of N_e and T_e respectively declined from 10^{23} to 10^{21} m^{-3} and 10 to 0.1 eV since the plasma expansion. Some other diagnosis methods[3] also show the same of magnitude. The time-gated emission images and the spatial and temporal variation of the N_e and T_e values both highlight the inhomogeneity of the plasma in liquid, and support the claim that the species with different charge states expand in different velocity sub-groups, each propagating with attendant quasi-independent electron clouds. It provides the further theoretical analysis of the nanoparticles excited by pulsed laser and better design of functional nanoparticles production.

[1] Wagener P, Ibrahimkuty S, Menzel A, Plech A, Barcikowski S. Dynamics of silver nanoparticle formation and agglomeration inside the cavitation bubble after pulsed laser ablation in liquid. *Phys Chem Chem Phys* 15, 68–74, (2013).

[2] Povarnitsyn ME, Itina TE, Levashov PR, Khishchenko KV. Mechanisms of nanoparticle formation by ultra-short laser ablation of metals in liquid environment. *Phys Chem Chem Phys* 15, 3108–3114, (2013).

[3] Xiao, J., Liu, P., Wang, C. X. & Yang, G. W. External field-assisted laser ablation in liquid: An efficient strategy for nanocrystal synthesis and nanostructure assembly. *Prog Mater Sci* 87, 140-220, (2017).

Antibacterial Se and Si nanoparticles

**A. Nastulyavichus¹, N. Smirnov¹, I. Saraeva¹, A. Rudenko¹, S. Kudryashov^{1,2},
E. Tolordava³, S. Gonchukov⁴, A. Ionin¹, D. Zayarny¹**

1- Lebedev Physical Institute, Leninskiy prospect 53, 119991 Moscow, Russia

2- ITMO University, Kronverkskiy prospect 49, 197101 St. Petersburg, Russia

3- N.F. Gamaleya Federal Research Centre of Epidemiology and Microbiology, Gamalei street 18, 123098 Moscow, Russia

4- National research nuclear university MEPH, Kashirskoe shosse 31, 115409 Moscow, Russia

email: ganuary_moon@mail.ru

At present, one of the problems of a global scale is the fight against pathogenic microorganisms. Especially resistant are pathogens capable of forming biofilms. Biofilms are resistant to the action of various stresses, including the action of antibiotics, disinfecting chemicals. Therefore, the search for alternative ways of dealing with pathogenic microorganisms is on the agenda of modern medical microbiology. Recently, nanotechnology has played a large role in applications for medicine and microbiology [1-2]. Antibacterial properties of a wide range of nanoparticles have long been known, but the most promising results have been obtained with silver, selenium and silicon nanoparticles. In this work, selenium and silicon were used for the experiment. Selenium and silicon nanoparticles were produced by a method of laser ablation with the use of an Yb³⁺-doped fiber laser HTFMark, Bulat (central wavelength $\lambda = 1064$ nm, pulsewidth FWHM $\tau = 120$ ns), equipped with a galvanometric scanner and an f-theta objective (focal length $F = 160$ mm). The resulting ablation products in form of colloidal solutions were deposited on these silver films and on bare silica glass.

The antibacterial action of selenium and silver nanoparticles was tested on Gram-positive bacteria of *Staphylococcus aureus* and Gram-negative *Pseudomonas aeruginosa* (Fig.1).

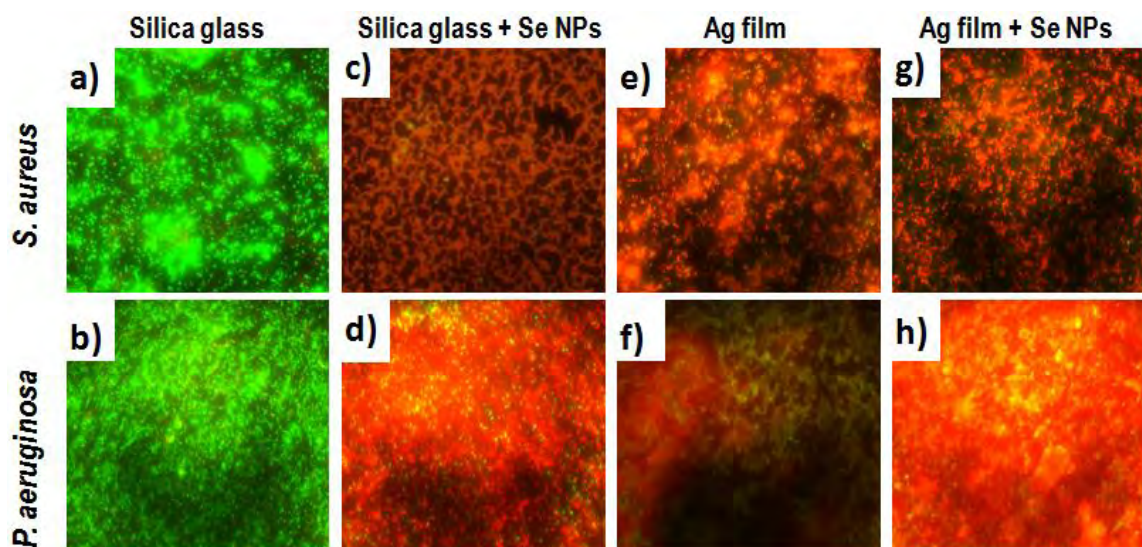


Figure 28 Optical images of assays of live (green) and dead (red) cells in bacteria biofilms: (a, b) bare silica-glass slide; (c, d) silver film on the glass slide; (e, f) Se-coated silver film on the glass slide; (g, h) Se-coated glass slide (the instrumental magnification – 600x). Top and bottom lines correspond to *S. aureus* and *P. aeruginosa* biofilms, respectively [3].

The predominating red color of the *S. aureus* biofilms in our experiments with the Se NP solid coating demonstrates the strong inhibitory effect on biofilm formation (Fig. 1c, d), which is comparable to the cytotoxic effect of the nanocrystalline silver film (Fig. 1e,f). The same inhibitory effects for the Se NP coating and the thin as-deposited nanocrystalline silver film were found against the Gram-negative *P. aeruginosa* bacteria [3].

[1] W. Lim, Z. Gao, Plasmonic nanoparticles in biomedicine, *Nano Today*, vol. 11, pp. 168–188, (2016).

[2] A. Gobin, M. Lee, N. Halas, W. James, R. Drezek, J. West, Near-infrared resonant nanoshells for combined optical imaging and photothermal cancer therapy, *Nano letters*, vol. 7, pp. 1929-1934, (2007).

[3] A. Ionin, A. Ivanova, R. Khmel'nitskii, Yu. Klevkov, S. Kudryashov, A. Levchenko, A. Nastulyavichus, A. Rudenko, I. Saraeva, N. Smirnov, D. Zayarny, S. Gonchukov, E. Tolordava, Antibacterial effect of the laser-generated Se nanocoatings on *S. aureus* and *P. aeruginosa* biofilms, *Laser Physics Letters*, vol. 15, 015604, (2018).

Laser-generated gold nanoparticle nano-bio-conjugates featuring cationic ligands for biomedical diagnostics and therapy

L. Gamrad, C. Streich, C. Rehbock, A. Schielke, S. Barcikowski

Technical Chemistry I and Center for Nanointegration
Duisburg-Essen (CENIDE), University of Duisburg-Essen,
Universitaetsstrasse 7, 45141 Essen, Germany

andreas.schielke@uni-due.de

Gold nanoparticles are interesting for biomedicine as they are considered highly biocompatible, are suitable for imaging due to their surface plasmon resonance and furthermore can be easily functionalized with biomolecules via thiol chemistry, forming hybrid materials termed nano-bio-conjugates. Laser ablation in liquids has proven to be particularly suitable for nano-bio-conjugates synthesis as it enables an additive free route, an exceptionally high surface coverage [1] as well as precise control of ligand/nanoparticle ratios [2]. In previous experiments we could conclusively verify that these conjugates can be fabricated with a multitude of different ligands, while particularly nucleotide [1] and peptide based conjugates [2] proved relevant. In this work, applications of laser fabricated nano-bio-conjugates with a focus on cationic ligands and biomolecule-specific binding are presented.

In one approach, monodisperse gold nanoparticles (< 10 nm) were utilized as a platform for functional peptide ligands, aiming at the dissociation of protein aggregates, believed to be involved in the pathology of neurodegenerative diseases using the model protein A β . With a set of complementary biophysical methods, we could conclusively show that the conjugates performed similar, in some cases even better than the free ligands in dissolving A β fibrils and oligomers (Figure 1a) [3], some data even indicated that the multivalent decoration of two different functional ligands could render further improvement. A second approach entailed the use of deliberately agglomerated nanoparticle-peptide-conjugates as platforms for photo-induced intracellular release. The agglomerates were internalized by model cell lines and pulsed laser irradiation induced a controlled endosomal rupture and desagglomeration of the particles. This went along with the release of cargo molecules (dyes) into the cytoplasm (Figure 1b), while overall cell viability was unaffected. [4] These works could offer novel strategies towards laser-induced drug delivery. In a final experimental approach, we examined the conjugation of gold nanoparticles with aptamer sequences, at different core particle sizes and surface coverage.

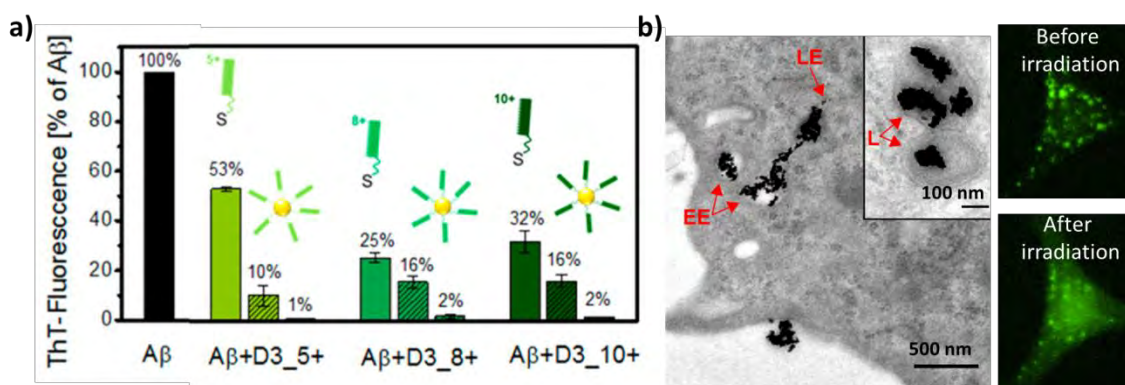


Figure 29 a) ThT fluorescence assay, indicating β -sheet aggregate content in A β , with free D3 peptide ligands as well as D3-gold-nanoconjugates. Ligands with different positive net charges (5+ - 8+) were tested. [3] b) TEM images of gold agglomerates localized within endosomes (EE=early endosomer, LE=late endosomes) as well as confocal images of cells prior to and after laser irradiation, indicating endosomal rupture and even distribution of a cargo dye in the cytoplasm.

[1] S. Petersen and S. Barcikowski, Phys. Chem. C., **113** (2009), 19830-19835.

[2] L. Gamrad, C. Rehbock, J. Krawinkel, B. Tumursukh, A. Heisterkamp and S. Barcikowski, Journal of Physical Chemistry C, **118** (2014), 118, 10302-10313.

[3] C. Streich, L. Akkari, C. Decker, J. Bormann, C. Rehbock, A. Muller-Schiffmann, F. C. Niemeyer, L. Nagel-Steger, D. Willbold, B. Sacca, C. Korth, T. Schrader and S. Barcikowski, Acs Nano, **10** (2016), 7582-7597.

[4] J. Krawinkel, U. Richter, M. L. Torres-Mapa, M. Westermann, L. Gamrad, C. Rehbock, S. Barcikowski and A. Heisterkamp, Journal of Nanobiotechnology, **14** (2016)

Synthesis routes of CeO₂ nanoparticles dedicated to organophosphorus degradation: a benchmark

I. Trenque^{1,3}, G. C. Magnano¹, F. Chaput³, M. Bugnet⁴, K. Masenelli-Varlot⁴, I. Pitault¹, S. Briançon¹, M. A. Bolzinger¹, D. Amans²

1- LAGEP, UCBL, CNRS UMR5007, F-69622, Villeurbanne, France

2- ILM, UCBL, CNRS UMR5306, F-69622, Villeurbanne, France

3- Ecole Normale Supérieure de Lyon, Laboratoire de Chimie, CNRS UMR5182, F-69634, Lyon, France

4- INSA-Lyon, UCBL, MATEIS, CNRS UMR5510, F-69621, Villeurbanne, France

isabelle.trenque@univ-lyon1.fr

Recent studies have shown the potential of cerium oxide nanoparticles for skin decontamination of chemical warfare agent (CWA)^{1,2}. Thanks to their surface properties, cerium oxide nanoparticles (CeO₂ NPs) act as reactive sorbents for the degradation of organophosphate compounds such as VX agent or sarin. In order to evaluate the influence of the size, the morphology and the surface state of the nanoparticles on skin decontamination efficiency, CeO₂ NPs with different shapes were elaborated by both chemical methods (hydrothermal synthesis) and physical methods (Pulse Laser Ablation in Liquids, or grinding). Single crystalline nano-octahedra, nanocubes, nanorods or small agglomerates of sub-10 nm nanoparticles were selectively obtained by hydrothermal method under different conditions (temperatures, concentrations and precursors)³. Pulsed Laser Ablation in Liquids (PLAL)⁴ was used to prepare 3-5 nm nanoparticles with promising surface state.

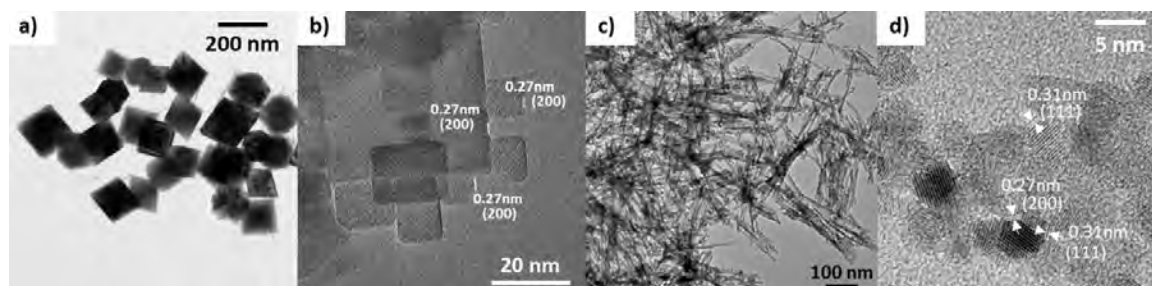


Figure 30 - Examples of morphologies obtained by hydrothermal (a, b, c) and by PLAL (d) processes.

Because the aim was to correlate the physicochemical properties of the nanostructures to the efficiency of the degradation of the toxic, a careful attention was given to the characterization of these particles. The composition, structure, morphology of the nanoparticles and their surface chemistry were studied using various techniques such as X-Ray diffraction (XRD), transmission electron microscopy (TEM), specific surface area analysis, Infrared and Raman spectroscopy. The efficiency of decontamination was evaluated *in vitro* measuring the degradation kinetics of Paraoxon organophosphate in presence of CeO₂ NPs. Results show an influence of both specific surface area and crystallographic facets of the nanoparticles.

[1] A. Salerno and *al.*, In vitro skin decontamination of the organophosphorus pesticide Paraoxon with nanometric cerium oxide CeO₂, *Chemico-Biological Interactions*, 267, 57-66, 2017.

[2] P. Janos and *al.*, Cerium dioxide as a new reactive sorbent for fast degradation of parathion methyl and some other organophosphates, *Journal of Rare Earths*, 32 (4), 360-370, 2014.

[3] H. X. Mai and *al.*, Shape-Selective Synthesis and Oxygen Storage Behavior of Ceria Nanopolyhedra, Nanorods, and Nanocubes, *J. Phys. Chem. B*, 109(51), 24380-24385, 2005.

[4] Z. Yan and D. B. Chrisey., Pulsed laser ablation in liquid for micro-/nanostucture generation, *Journal of Photochemistry and Photobiology C: Photochemistry Reviews*, 13, 204-223, 2012

Continuous laser fragmentation of colloidal particles: improving the process control and efficiency

F. Waag^{1,6}, A. R. Ziefuß^{1,6}, S. Siebeneicher^{1,6}, B. Gökce^{1,6}, C. Kalapu^{2,6}, G. Bendt^{2,6}, S. Salamon^{3,6}, J. Landers^{3,6}, U. Hagemann^{5,6}, M. Heidelmann^{5,6}, S. Schulz^{2,6}, H. Wende^{3,6}, N. Hartmann^{5,6}, M. Behrens^{2,6}, S. Barcikowski^{1,6}

1- Institute of Technical Chemistry I, University of Duisburg-Essen, Universitaetsstr. 7, 45141 Essen, Germany

2- Institute of Inorganic Chemistry, University of Duisburg-Essen, Universitaetsstr. 7, 45141 Essen, Germany

3- Faculty of Physics, University of Duisburg-Essen, Lotharstr. 1, 47057 Duisburg, Germany

4- Institute of Physical Chemistry, University of Duisburg-Essen, Universitaetsstr. 5, 45117 Essen, Germany

5- Interdisciplinary Center for Analytics on the Nanoscale, University of Duisburg-Essen, Carl-Benz-Str. 199, 47057 Duisburg, Germany

6- Center for Nanointegration Duisburg-Essen, University of Duisburg-Essen, Carl-Benz-Str. 199, 47057 Duisburg, Germany

friedrich.waag@uni-due.de

The suitability of nanocolloids produced by laser ablation in liquid (LAL) or processed by laser fragmentation in liquid (LFL) has been evaluated positively for various applications in different fields of research and technology [1]. The bare particle surfaces due to the absence of ligands and precursor residues makes laser-synthesized particles advantageous, in particular for the heterogeneous catalysis [2]. Furthermore, today's research in fields of the heterogeneous catalysis of the oxygen evolution reaction (OER) in the electrolysis of alkaline water focuses on transition metals like nickel, cobalt and iron as catalyst base elements [3].

In our recent study, we found a positive effect of LFL (free, liquid jet) on the catalytic properties of a CoFe_2O_4 OER nanocatalyst [4]. A highly increased activity, adjustable by the number of process cycles of LFL, could be observed. To clarify the reasons behind the improved properties, a detailed structural investigation of the products of LFL was applied and complex changes were discovered. Beside the formation of ultra-small particles (figure 1a), a lattice alteration was driven by LFL (figure 1b). Both effects partly correlate to electrochemical properties of the catalyst (figure 1c). However, also other effects like changes in the catalyst surface chemistry, a loss of crystallinity and the formation of byproducts occurred. Further understanding only seemed to be accessible by investigating the LFL process itself. Since all tracked properties significantly changed at least up to the tenth process cycle, a low process efficiency was assumed. It was found that the liquid jet was illuminated inhomogeneously at the applied experimental parameters by using a ray tracing simulation. The main reason is the circular bended surface of the liquid jet. To optimize the illumination, we developed a new setup with an elliptical bended jet. First experiments exhibit promising results towards higher efficiencies.

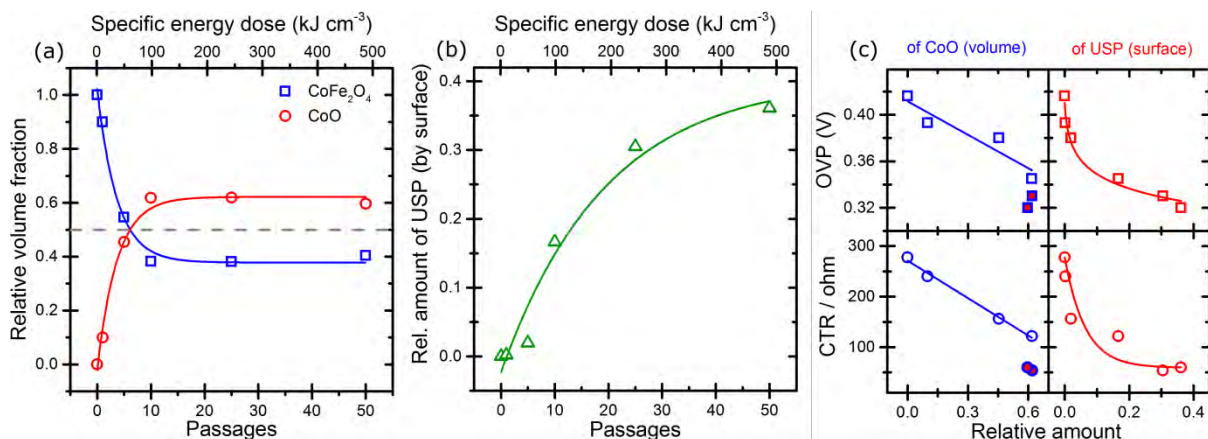


Figure 1. (a) Change of crystalline volume fractions and (b) the surface weighted relative amount of ultra-small particles (USP) depending on the process cycles (passages) of PLFL as well as (c) the correlation between electrochemical properties (CTR: charge transfer resistance, OVP: overpotential) and the amount of crystalline CoO and USP [4].

- [1] D. Zhang, B. Gökce, S. Barcikowski, Laser Synthesis and Processing of Colloids: Fundamentals and Applications, Chemical Reviews, 117, pp. 3990-4103, (2017).
 [2] J. Zhang, M. Chaker, D. Ma, Pulsed laser ablation based synthesis of colloidal metal nanoparticles for catalytic applications. Journal of Colloid and Interface Science, 489, pp. 138-149, (2017).
 [3] C. C. McCrory, S. Jung, J. C. Peters, T. F. Jaramillo, Benchmarking heterogeneous electrocatalysts for the oxygen evolution reaction. Journal of the American Chemical Society, 135, pp. 16977-16987, (2013).
 [4] F. Waag, B. Gökce, C. Kalapu, G. Bendt, S. Salamon, J. Landers, U. Hagemann, M. Heidelmann, S. Schulz, H. Wende, N. Hartmann, M. Behrens, S. Barcikowski, Adjusting the catalytic properties of cobalt ferrite nanoparticles by pulsed laser fragmentation in water with defined energy dose. Scientific Reports, 7, 13161, (2017).

Wavelength dependent electron temperature distribution in plasma produced by laser ablation in the water

Minsun Chen¹, Hao Liu¹, Xin Peng¹, Guomin Zhao¹

College of Advanced Interdisciplinary Studies, National University of Defence Technology, Changsha 410073, P. R. China

Main author email address: minsunchen12@163.com

We present a two-dimensional (2-D) Eulerian radiative hydrodynamic theoretical simulation results of electron temperature distribution in plasma produced by 532 nm and 1064 nm laser ablation in the water. The calculation simulates the interaction of laser radiation with a solid target and the subsequent expansion of the plasma in the ambient liquid. The three first-order quasi-linear partial differential equations of hydrodynamic flow are solved in the simulation. Both laser-target (leading to melting and vaporisation) and laser-plasma (leading to plasma heating via inverse bremsstrahlung) interactions are included. The calculations assume cylindrical symmetry, with the target and the region above the surface represented by a two-dimensional (z, r) mesh, where z and r define, respectively, the target surface normal and the radial coordinate orthogonal to z .

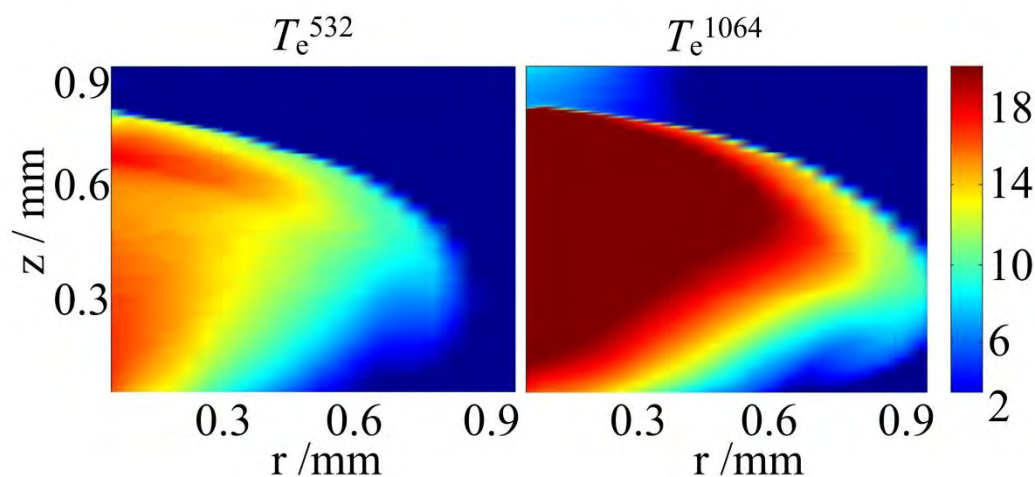


Figure 31 2-D spatial distributions of T_e in the plasma formed by laser ablation of a Si target in water at 532 nm (left column) and 1064 nm (right column) calculated at $\delta t = 100$ ns. The vertical and horizontal axes in each plot are z , the distance normal to the target surface (located at $z = 0$) and the radial distance r . The (linear) T_e scale shown using the false colour scheme inset within the top right panel is in eV, and common to all plots.

As shown in the Figure 1, plasma produced by 1064 nm laser is calculated to be much ‘hotter’ than that formed with the 532 nm pulse, and a much larger fraction of the plasma plume in water arising from 1064 nm ablation is calculated to have $T_e > 15$ eV. As a consequence, the 1064 nm plasma plume expands faster, which is agreed with previous works [1,2]. The reason is the decline of inverse bremsstrahlung absorption (IBA) of plasma from laser beam by the $\lambda^2 \sim 3$ factor [3], so the longer incident wavelength leads to a stronger IBA. The wavelength dependent results would be of importance to control the nanoparticle size in the laser ablation in liquid by alternative reaction dynamics.

[1] Kim, J., Reddy, D. A., Ma, R. & Kim, T. K. The influence of laser wavelength and fluence on palladium nanoparticles produced by pulsed laser ablation in deionized water. *Solid State Sciences* 37, 96-102 (2014).

[2] Hahn, A., Barcikowski, S. & Chichkov, B. N. Influences on Nanoparticle Production during Pulsed Laser Ablation. *Journal of Laser Micro* 3, 73-77 (2008).

[3] Zel dovich, I. A. B. Ra zer, I. U. P. *Physics of shock waves and high-temperature hydrodynamic phenomena.* (Dover Publications, 2002).

Exploring the origin of bimodal size distribution during picosecond laser ablation in liquids

**R. Streubel¹, A. Letzel¹, C-Y. Shih², J. Heberle³, M.V. Shugaev², C. Wu², M. Schmidt³,
L.V. Zhigilei², S. Barcikowski¹, B. Gökce¹**

*1- Technical Chemistry I and Center for Nanointegration Duisburg-Essen (CENIDE),
University of Duisburg-Essen, Universitaetsstr. 7, Essen 45141, Germany*

*2- Department of Materials Science and Engineering, University of Virginia,
395 McCormick Road, Charlottesville, Virginia 22904-4745, USA*

*3- Institute of Photonic Technologies, Friedrich-Alexander University Erlangen-Nürnberg,
Konrad-Zuse-Straße 3/5, Erlangen 91052, Germany*

rene.streubel@uni-due.de

The bimodal size distribution of colloidal suspensions produced by laser ablation in liquids (LAL) presents an obstacle for the direct use of colloids in a number of optics [1] and catalysis [2] applications, where a narrow monomodal nanoparticle size distribution is required. For Pt-group-metal catalyst, for instance, large nanoparticles may account for a major fraction of the total mass of the catalyst but make little contribution to the catalytic activity, which is controlled by the mass-specific surface area and is dominated by the small nanoparticles [2]. To understand the origin of bimodal size distributions occurring during LAL, we undertake a combined computational and experimental study. Based on the results of large-scale atomistic simulations we identify two distinct mechanisms of the nanoparticle formation. These mechanisms are: (1) the nucleation and growth of small nanoparticles in the metal-water mixing region and (2) the formation of larger nanoparticles through the breakup of the superheated molten metal layer generated at the plume-water interface [3].

In this contribution, we focus on the experimental data that supports these finding. A double pulse experimental study of picosecond LAL supported by high-speed shadowgraphy is utilized. It is shown that the cavitation bubble of the first picosecond pulse is surrounded by small satellite bubbles, which can be activated upon properly timed double pulse irradiation.

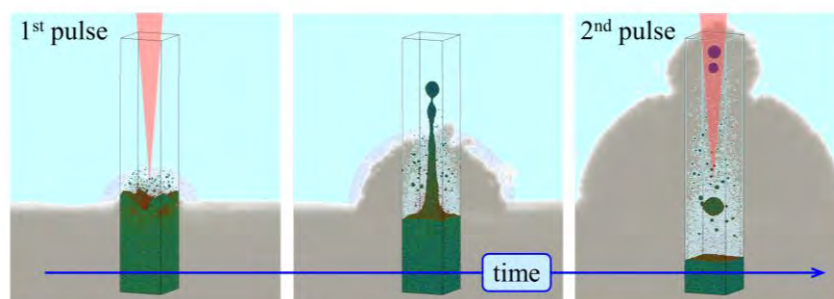


Figure 32. Scheme of the computationally predicted particle formation mechanism and results of the double pulse experiment (in the background) [3].

Figure 1 shows snapshots of a molecular dynamics simulation superimposed on images obtained in shadowgraphy experiments performed with double pulse irradiation. After interaction with the first laser pulse, both fractions of the predicted nanoparticles form, however only the larger nanoparticles penetrate the cavitation bubble boundary and enter the dense water environment (Fig. 1, center). The precisely timed second picosecond laser pulse interacts with these larger particles and induces a second cavitation bubble (Fig. 1, right).

- [1] J. C. Meier, C. Galeano, I. Katsounaros, J. Witte, H. J. Bongard, A. A. Topalov, C. Baldizzone, S. Mezzavilla, F. Schüth, and K. J. J. Mayrhofer, Design criteria for stable Pt/C fuel cell catalysts, *Beilstein J. Nanotechnol.*, 5, 44-67 (2014)
- [2] C. Ma, J. Yan, Y. Huang, and G. Yang, Directional Scattering in a Germanium Nanosphere in the Visible Light Region, *Adv. Opt. Mater.*, 5, 201700761 (2017)
- [3] C-Y. Shih, R. Streubel, J. Heberle, A. Letzel, M.V. Shugaev, C. Wu, M. Schmidt, B. Gökce, S. Barcikowski and L.V. Zhigilei, Two mechanisms of nanoparticle generation in picosecond laser ablation in liquids: The origin of the bimodal size distribution, under review

Pulsed laser ablation in supercritical CO₂ to synthesize Ti_xO_y nanoparticles

Amandeep Singh¹, Mari Honkanen¹, Jorma Vihinen², Turkka Salminen³, Juha-Pekka Nikkanen¹, Leo Hyvärinen¹, Erkki Levänen¹

1 - Laboratory of Materials Science, Tampere University of Technology, Tampere, FINLAND

2 - Laboratory of Mechanical Engineering and Industrial Systems, Tampere University of Technology, Tampere, FINLAND

3 - Laboratory of Photonics, Tampere University of Technology, Tampere, FINLAND

E-mail: amandeep.singh@tut.fi

Pulsed laser ablation in liquids (PLAL) is a promising technique to synthesize ligand free nanoparticles that are well suited for further functionalization. The liquid used in PLA is of utmost importance in order to obtain the desired phase from the same target material and has been well-reviewed in the past [1]. Most PLAL studies have been done in liquids at atmospheric pressure. Kuwahara et al, reported higher ablation efficiency of copper in pressurized CO₂ at elevated pressures [2]. The next revolutionary step in this field could be ablation in supercritical fluids. Above certain pressure and temperature, called critical point, all liquids transform to supercritical fluids in which they exhibit superior properties compared to normal liquids. Supercritical CO₂ (scCO₂) is the most commonly used supercritical fluid due to its relatively low critical point of 31.1 °C and a pressure of 7.4 MPa. scCO₂ is neither gas nor liquid but shows properties of both states, such as gas-like diffusivity, zero surface tension and liquid-like density [3]. Moreover, through simple manipulations in pressure and temperature, physical and thermal properties of scCO₂ can be changed from gas-like to liquid-like or vice-versa [4].

In this study, a 1064 nm, 250 ns fiber laser at 101 kHz was used to cause ablation of titanium target in scCO₂ at 10 MPa, 50 °C. In theory, enough energy from plasma should be there to cause CO₂ to decompose into its constituent elements/molecules and oxidize titanium clusters from plasma. Based on TEM, Raman and XRD results, we report formation of perfectly round nanoparticles that were multiphase oxides of titanium. We observed neither titanium-carbon-core-shell structure nor any carbides in the nanoparticles.

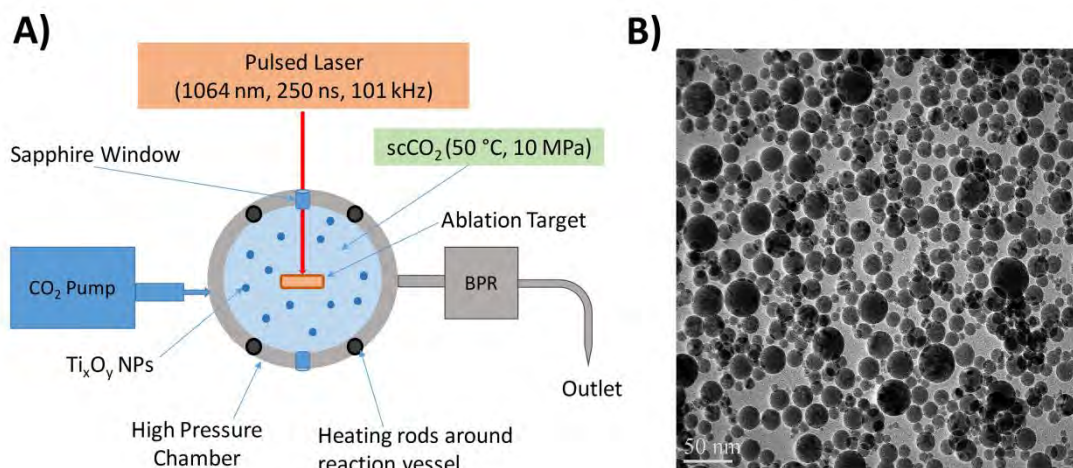


Figure 33 A) The experimental set-up for PLA in scCO₂ of titanium along with the laser parameters 1064 nm, 250 ns, 101 kHz and scCO₂ parameters 50 °C, 10 MPa. B) TEM micrograph of the obtained almost perfectly round nanoparticles using the aforementioned parameters.

[1] V. Amendola and M. Meneghetti, "What controls the composition and the structure of nanomaterials generated by laser ablation in liquid solution?," *Phys. Chem. Chem. Phys.*, vol. 15, no. 9, pp. 3027–3046, 2013.

[2] Y. Kuwahara, T. Saito, M. Haba, T. Iwanaga, M. Sasaki, and M. Goto, "Nanosecond Pulsed Laser Ablation of Copper in Supercritical Carbon Dioxide," *Jpn. J. Appl. Phys.*, vol. 48, no. 4, p. 40207, Apr. 2009.

[3] W. Leitner, "Designed to dissolve," *Nature*, vol. 405, no. 6783, pp. 129–130, May 2000.

[4] N. Takada and S. Machmudah, "Characteristics of optical emission intensities and bubblelike phenomena induced by laser ablation in supercritical fluids," *Jpn. J. Appl. Phys.*, vol. 10213, 2014.

Effect of Irradiation Time on Crystalline Structure of Silver Submicron Spherical Particles by Pulsed Laser Melting in Liquid

T. Nakamura¹, H. Magara¹, S. Sakaki², N. Koshizaki²

1- Institute of Multidisciplinary Research for Advanced Materials, Tohoku University

2- Graduate School of Engineering, Hokkaido University

Main author email address: nakamu@tagen.tohoku.ac.jp

Submicron spherical particles (SSPs) of metals, alloys, oxides and semiconductors have been successfully fabricated by pulsed laser melting of aggregates of source nanoparticles in liquid (pulsed laser melting in liquid, PLML) [1]. The fabricated SSPs generally have unique features of spherical shape, uniform size distribution and crystalline structure [2]. We had established a method for evaluation of inner crystalline structure of SPPs by electron backscatter diffraction (EBSD) using a bulk metallic glass substrate which has non crystallinity and good thermal and electron conductivity. In this study, effect of irradiation time on crystalline structure of silver SSPs was investigated by mean of EBSD, and growth mechanism of SSPs during laser irradiation was also discussed. Raw particles of silver with the diameter of smaller than 100 nm were dispersed into ultrapure water with the concentration of 200 ppm. The third harmonics of a Nd:YAG pulsed laser (wavelength: 355 nm, repetition rate: 10 Hz, pulse width: 7 ns, beam diameter: 8 mm) was used as a laser source for PLML without focusing, and vertically introduced to the surface of the colloidal suspension kept in a polypropylene reservoir. Laser fluence condition on the surface of the colloidal suspension was set at 50 mJ/cm². A magnetic stirrer was used to prevent gravitational settling of the suspension. Irradiation time was set from 100 sec to 180 min. Fabricated SSPs particles were collected by centrifugation with 1,500 rpm for 30 min. For EBSD analysis, Ag SSPs were fixed on a copper-based bulk metallic glass plate ($\phi=12$ mm, Cu₃₆Zr₄₈Ag₈Al, BMG Inc.) as a substrate to keep conductivity and suppress EBSD from it for microscopic analysis. Focused Ga⁺ ion beam (FIB) was used to obtain cross-sectional surface of the Ag SSPs. SEM images of the prepared samples revealed that hemispherical Ag SSPs were formed by FIB without any depositions and contaminations. EBSD mappings of Ag SSPs fabricated by PLML with different irradiation time of 100 sec and 180 min are shown in Fig. 1. Inner crystalline structure of Ag SSPs were mixture of multi- and single-domains colored in EBSD mappings. Mean domain size of Ag SSPs became large with the increase of irradiation time, and constant after certain time of irradiation. According to the result, crystalline Ag SSPs were formed through a repetitive multi-step process of melting and solidification suggested by A. Pyatenko et al. [3]. Crystal growth of Ag SSPs was not promoted by PLML of relatively large particles.

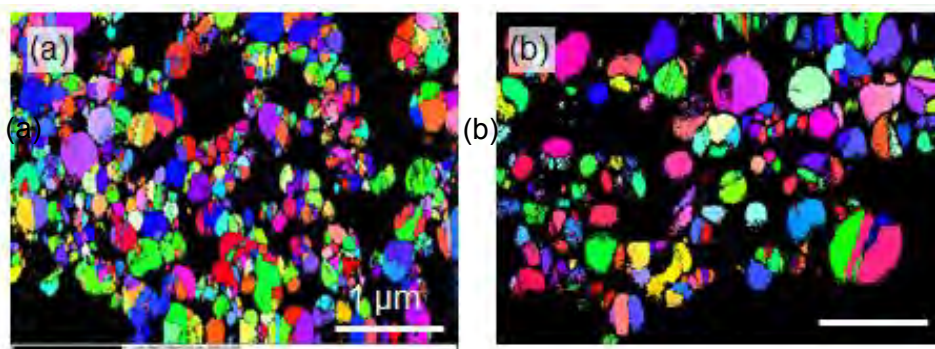


Figure 34 Inverse pole figure Z EBSD mappings of Ag SSPs fabricated by PLML with different irradiation time of (a) 100 sec and (b) 180 min.

[1] H. Wang, A. Pyatenko, K. Kawaguchi, X. Li, Z. Swiatkowska-Warkocka, N. Koshizaki, Selective pulsed heating for the synthesis of semiconductor and metal submicrometer spheres, *Angew. Chem. Int. Ed.*, **49**, 6361-6364, (2010).

[2] Y. Ishikawa, N. Koshizaki, A. Pyatenko, N. Saitoh, N. Yoshizawa, Y. Shimizu, Nano- and submicrometer-sized spherical particle fabrication using a submicroscopic droplet formed using selective laser heating, *J. Phys. Chem. C.*, **120**, 2439-2446, (2016).

[3] A. Pyatenko, H. Wang, N. Koshizaki, Growth mechanism of monodisperse spherical particles under nanosecond pulsed laser irradiation, *J. Phys. Chem. C.*, **118**, 4495-4500, (2014).

Milligram per second femtosecond laser generation of functional Se nanoparticles

I. Saraeva¹, A. Ivanova¹, A. Nastulyavichus¹, N. Smirnov¹, S. Kudryashov^{1,2}, A. Rudenko¹, R. Khmel'nitski¹, D. Kirilenko^{2,3}, P. Brunkov^{2,3}, A. Shakhmin⁴, Yu. Klevkov¹, N. Mel'nik¹, A. Baranov⁵, D. Zayarny¹, A. Ionin¹

1 - Lebedev Physical Institute, 119991, Moscow, Russia

2 - ITMO University, 197101, St. Petersburg, Russia

3 - Ioffe Institute, 194021, St.-Petersburg, Russia

4 - Peter the Great St. Petersburg Politechnic University, 195251, St.-Petersburg, Russia

5 - M.V. Lomonosov Moscow State University, 119899, Moscow, Russia

Main author email address: insar@lebedev.ru

The use of high-index dielectric materials provides a way of getting strong magnetic response in nanoscale. Strong Mie-resonances are induced in high-index NPs at spectral position, defined by the condition $\lambda/d \approx n$, where n is refractive index and d is the NP diameter [1,2]. In most published papers on dielectric nanophotonics Si nanoobjects are used, although there exists a number of materials, demonstrating similar properties. For example, Se is also a high-index material and, unlike silicon, has low melting and boiling temperatures, which favours the effective NPs yield during the laser-ablative processing. It is also biocompatible, which allows its use in the complex theragnostics procedures, and is a necessary element for human organism (recommended daily intake $\sim 55 \mu\text{g}$ [3]).

In our work, we report milligram-per-second production of Se NPs in water sols, which was realized through 7-W, 2 MHz-rate femtosecond laser ablation of a crystalline trigonal selenium pellet. The resulting NPs formation mechanism and their mass-removal yield were studied by optical profilometry and scanning electron microscopy characterization of the corresponding crater depths and topographies. Se NPs were studied as dry deposits by SEM, TEM and Raman spectroscopy, and were characterized by optical transmission, and dynamic light scattering spectroscopy in form of colloidal solutions. Se coatings on thin silica-supported silver films and bare silica glass slides, as well as on CaF_2 substrates, were characterized by SEM, energy-dispersive x-ray spectroscopy, and broadband (vis-mid IR) transmission spectroscopy, exhibiting crystalline Se NPs with high refractive index as promising all-dielectric sensing nanoblocks.

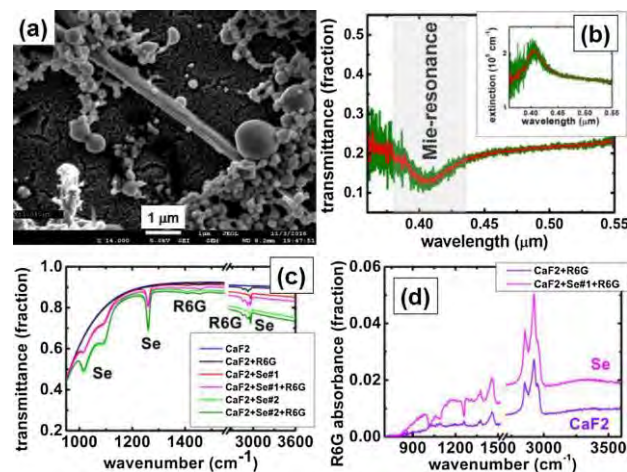


Figure 35 (a) SEM image of a SeNP dried deposit on a supported silver film. (b) UV-vis transmittance and extinction coefficient (inset) spectra of Se nanocoating on a CaF_2 substrate. (c) FT-IR transmittance spectra of bare CaF_2 substrates and Se nanocoatings on the CaF_2 substrates, both with and without 10^{-4} R6G monolayer. (d) FT-IR absorbance spectra of 10^{-4} R6G monolayer.

[1] A. Krasnok, A. Miroshnichenko, P. Belov, Yu. Kivshar, All-dielectric optical nanoantennas, *Optics Express*, vol. 20, pp. 20599–20604, (2012).

[2] A. Miroshnichenko, Yu. Kivshar, Fano Resonances in All-Dielectric Oligomers, *Nano Letters*, vol. 12, pp. 6459–6463, (2012).

[3] S. Skalickova, V. Milosavljevic, K. Cihalova, P. Horky, L. Richtera, V. Adam, Selenium nanoparticles as a nutritional supplement, *Nutrition*, vol. 33, pp. 83–90, (2017).

Surface Modification of Metal and Alloy Nanoparticles Fabricated by Laser-Induced Nucleation in Liquid

R. Kuroda¹, T. Nakamura², M. Nakagawa²

1- Graduated School of Engineering, Tohoku University

2- Institute of Multidisciplinary Research for Advanced Materials, Tohoku University

nakagawa@tagen.tohoku.ac.jp

Metal or alloy nanoparticles (NPs) have attracted much attention in research and industrial fields due to its interesting properties. For example, these are applied to conductive ink for printed-electronics^[1], catalysts with high catalytic activity^[2], and biochemical sensors with biocompatibility^[3]. However, metal or alloy NPs easily aggregate each other and make precipitations because of their high surface energy. One of the promising methods for stabilization of dispersion state of NPs is surface modification. We had demonstrated metal or alloy NPs formation by laser-induced nucleation in aqueous solution. All-proportional solid-solution alloy NPs with controllable compositions can be easily fabricated by the method^[4]. In this study, we demonstrated surface modification of metal or alloy NPs fabricated by laser-induced nucleation through phase transfer^[5]. Aqueous solutions of gold (Au) or platinum (Pt) ions were prepared by dissolving hydrogen tetrachloroaurate(III) trihydrate (HAuCl₄·3H₂O) or hydrogen hexachloroplatinate(IV) hexahydrate (H₂PtCl₆·6H₂O) in ultra-pure water. The concentration of metallic ion was set at 2.5×10^{-5} mol dm⁻³. Then, mixed solutions were prepared by mixing these solutions at a ratio of 1:1. All solutions were colourless and transparent. Femtosecond laser pulses ($\lambda=800$ nm, pulse width=100 fs, energy=5 mJ) were exposed to the aqueous solutions by an aspheric lens ($f=8$ mm, NA=0.5). The irradiation time was set to 30 minutes. The color of the Au ion solution became pale-red after laser irradiation indicating the formation of Au NPs which exhibit an absorption peak of surface plasmon resonance (SPR) around 520 nm, while the color of the Pt or mixed ion solutions became pale brown because Pt NPs show no SPR peaks in visible wavelength range. Aqueous suspensions of NPs after laser irradiation were vigorously stirred with toluene solution containing 1.0×10^{-5} mol dm⁻³ 1-hexanethiol for 10 min. After stirring, solutions separated into two toluene and aqueous phases. The toluene phase became pale-red in the suspension of Au NPs and pale brown in that of the alloy NPs, while the aqueous phase became transparent and colorless (Fig. 1 (b) and (c)). In the suspension of Pt NPs, however, color change in both phases was hardly observed before and after stirring (Fig. 1 (d)). Transmission electron microscope observation of the samples in toluene phase revealed that Au and alloy NPs were transferred into toluene phase after phase transfer (Fig. 2), however, no NPs were confirmed in toluene phase of Pt NPs suspension. Colloidal suspensions of Au and alloy NPs were stable for months due to the surface modification of Au and alloy NPs by 1-hexane thiol molecules. It was suggested that strong interatomic bonding force between Au and sulfur in a 1-hexanethiol molecule is one of the important factors for phase transfer of NPs from aqueous to organic phase.

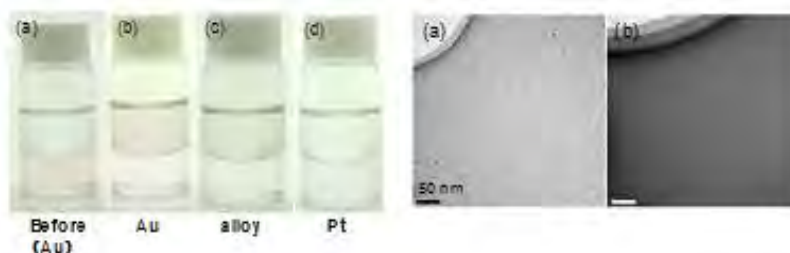


Fig. 1. Photographs of Au NPs suspensions (a) before phase transfer, and those of (b) Au, (c) alloy and (d) Pt NPs suspension after phase transfer.

Fig. 2. TEM images of (a) Au and (b) alloy NPs in toluene phase after phase transfer.

- [1] K. Fukuda, T. Sekine, Y. Kobayashi, D. Kumaki, M. Itoh, M. Nagaoka, T. Toda, S. Saito, M. Kurihara, M. Sakamoto, S. Tokito, Stable Organic Thin-film Transistors using Full Solution-processing and Low-temperature Sintering Silver Nanoparticle Inks, *Organic Electronics*, 13, 1660–1664, (2012).
- [2] M. M. Maye, J. Luo, L. Han, N. Kariuki, Z. Rab, N. Khan, H. R. Naslund, C. J. Zhong, Gold and Alloy Nanoparticle Catalysts in Full Cell Reactions, *Prepr. Pap.-Am. Chem. Soc., Div. Fuel Chem.*, 49, 938-939, (2004).
- [3] A. E. Ansary and L. M. Faddah, Nanoparticles as Biochemical Sensors, *Nanotechnology, Science and Applications*, 3, 66-76, (2010).
- [4] T. Nakamura, Y. Herhani, S. Sato, Fabrication of Solid-solution Gold–platinum Nanoparticles with Controllable Compositions by High-intensity Laser Irradiation of Solution, *J. Nanopart. Res.* 14, 785-793, (2012).
- [5] J. M. McMahon and S. R. Emory, Phase Transfer of Large Gold Nanoparticles to Organic Solvents with Increased Stability, *Langmuir*, 23, 1414-1418, (2007).

Automated focus adjustment for a high particle productivity rate by PLAL

M. Labusch^{1,2}, S. Wirtz³, G. Marzun¹, E. Cleve², D. Söffker³, S. Barcikowski¹

1- Center for Nanointegration Duisburg-Essen (CENIDE), Nano Energy Technic Center (NETZ), Technical Chemistry I, University of Duisburg-Essen, Universitätsstrasse 7, 45141 Essen, Germany

2- Institut für Lacke und Oberflächenchemie (ILOC), Hochschule Niederrhein, Adlerstraße 32, 47798 Krefeld, Germany

3- Chair of Dynamics and Control (SRS), University of Duisburg-Essen, Lotharstrasse 1, 47057 Duisburg, Germany

Marc.Labusch@uni-due.de

Pulsed laser ablation in liquids (PLAL) has been established as a simple and scale-able method to synthesize ligand-free nanoparticles [1]. To achieve a high throughput of laser generated colloids, a flow set-up is superior to a batch set-up. For high particle productivity rates it is required that PLAL's focal plane is continuously kept at a fixed distance close to the geometric focal plane initially set by the distance from the lens to the target surface. However, with longer ablation time the removal of material is leading to a shift of the working position. Thus, for a stable process over a long time period with a high particle productivity rate, the working distance (WD) needs to be adjusted [2]. Lu et al. showed that the ablation rate of Si in water correlates with the amplitude of the audible acoustic wave measured by a wide-band microphone at a frequency of 10 kHz [3]. In contrast, the aim of this work is to establish the measurement of the structure-borne acoustic emission (AE) of the PLAL as a real time monitoring method, which can be used to detect material changes [4], and using this signal as input for a control loop to automatically adjust the optimal WD.

For this purpose, a flow chamber with an integrated piezoelectric sensor was constructed to measure the AE related to the PLAL. As reference, the particle productivity rate was measured by online UV/VIS spectroscopy (Figure 1 A). The particle productivity rate and the AE energy were compared at different WD's (Figure 1 B).

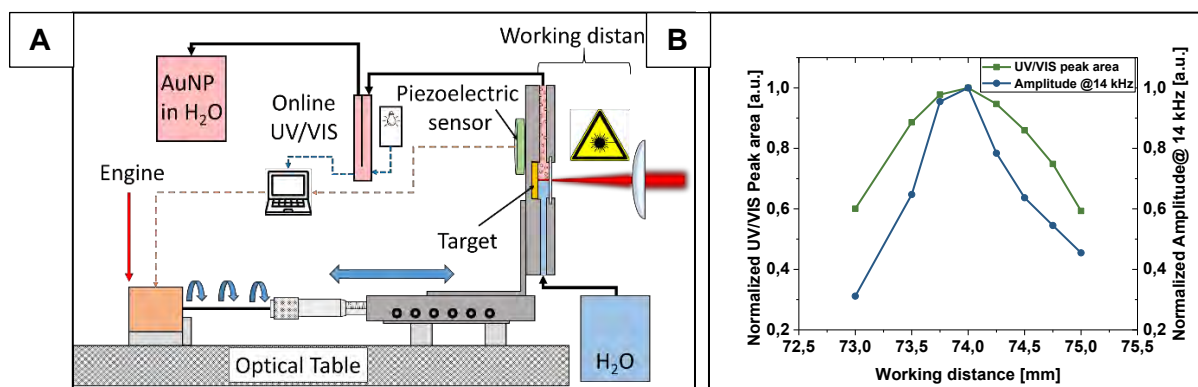


Figure 36 (A) Constructed flow chamber with integrated piezoelectric sensor and online UV/VIS spectroscopy. (B) UV/VIS peak area (450 nm – 600 nm) and amplitude of the acoustic emission at a frequency of 14 kHz at different working distances.

The measured energy of the AE at a frequency of 14 kHz shows a maximum at a WD of 74 mm. This result is in accordance with the UV/VIS spectroscopy, which indicates a maximum colloid concentration at the same WD and therefore the highest particle productivity rate. Assuming the convex behavior of the relations (Figure 1 B) a simple control algorithm can be realized to adjust the optimal positioning in real time allowing the maximum particle productivity rate.

[1] D. Zhang, B. Gökce, S. Barcikowski, Laser Synthesis and Processing of Colloids: Fundamentals and Applications, Chemical Reviews, Vol. 117 (5), pp. 3990-4103, (2017).

[2] S. Reich, P. Schönfeld, A. Letzel, S. Kolsakowski, M. Olbinado, B. Gökce, S. Barcikowski, A. Plech, Fluence Threshold Behaviour on Ablation and Bubble Formation in Pulsed Laser Ablation in Liquids, ChemPhysChem, Vol. 18, pp. 1084-1090, (2017).

[3] S. Zhu, Y. F. Lu, M. H. Hong, Laser ablation of solid substrates in a water-confined environment, Applied Physics Letters, Vol. 79 (9), pp. 1396-1398, (2001).

[4] D. Baccar, D. Söffker, Wear Detection by Means of Wavelet-based Acoustic Emission Analysis, Mechanical Systems and Signal Processing, Vol. 60-61, pp. 198-207, (2015).

A continuous and contamination-free process chain produces monodisperse, laser-synthesized heterogeneous co-catalysts

S. Kohsakowski^{1,2}, F. Seiser³, S. Barcikowski^{1,2}, T. Vinnay³, G. Marzun^{1,2}

1- University of Duisburg-Essen, Technical Chemistry I and Center of Nanointegration Duisburg-Essen (CENIDE), Universitätsstraße 7, 45141 Essen.

2- NanoEnergieTechnikZentrum (NETZ), Carl-Benz-Straße 199, 47057 Duisburg

3- Carl-Padberg Zentrifugenbau GmbH, Geroldsecker Vorstadt 60, 77933 Lahr.

Sebastian.Kohsakowski@uni-due.de

Pulsed laser ablation in liquids enables the synthesis of highly pure nanoparticles in a large scale [1]. However, the broad particle size distribution is an issue and has to be optimized especially for catalysis applications, where high surface-to-volume ratio is important. There are several approaches to narrow size distributions (adding a salt [2], re-irradiation [3], centrifugation [4]), but until now the techniques are limited to only some materials, show a low productivity and are discontinuous, that makes upscaling challenging. The main challenge is to up-scale the synthesis and size optimization by ensuring the purity of the catalyst. Thus, we have investigated a continuous nanoparticle size optimization step by centrifugation in a tubular bowl centrifuge. Polydisperse colloid productivities of 1-2.3 g/h for gold, silver and platinum could be realized using a ns-laser for a continuous particle production. By the subsequent investigation of centrifugation parameters for the separation of laser-generated Pt-NPs, the influence of the flow rate and rotation speed is observed.

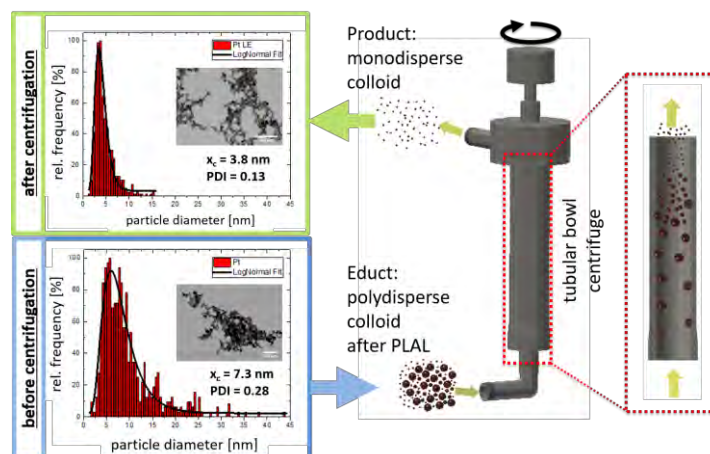


Figure 37: Schematically scheme of the continuous size selection process and TEM-images with associated size distributions for laser-generated Pt-NPs before and after centrifugation in the tubular bowl centrifuge.

An effective size optimization with a cut-off diameter of 10 nm is realized for rotation speeds higher than 36.000 rpm and flow rates around 50 ml/min. A Pt-NP productivity of monodisperse NPs < 10 nm of 0.32 g/h is obtained (in comparison to 0.005 g/h in a discontinuous standard ultracentrifuge). Finally, the experimental centrifugation results show an excellent agreement of the theoretically calculated cut-off diameter. A continuous nanoparticle production in a flow-chamber with a size separation by a tubular bowl centrifuge could be realized. The subsequent electrostatic [5] particle adsorption of these monodisperse NPs in a static mixer allows the establishment of a continuous process chain of ready-to-use heterogeneous catalysts.

[1] R. Streubel, S. Barcikowski, B. Gökce, Continuous multigram nanoparticle synthesis by high-power, high-repetition-rate ultrafast laser ablation in liquids, *Opt. Lett.*, 41, 1486-1489, (2016)

[2] V. Merk, C. Rehbock, F. Becker, U. Hagemann, H. Nienhaus, S. Barcikowski, In Situ Non-DLVO Stabilization of Surfactant-Free, Plasmonic Gold Nanoparticles: Effect of Hofmeister's Anions, *Langmuir*, 30, 4213-4222, (2014).

[3] M. Lau, I. Haxhijaj, P. Wagener, R. Intartaglia, F. Brandi, J. Nakamura, S. Barcikowski, Ligand-free gold atom clusters adsorbed on graphene nano sheets generated by oxidative laser fragmentation in water, *Chemical Physics Letters*, 610, 256 – 260, (2014).

[4] W. Dong, S. Reichenberger, S. Chu, P. Weide, H. Ruland, S. Barcikowski, P. Wagener, M. Muhler, The effect of the Au loading on the liquid-phase aerobic oxidation of ethanol over Au/TiO₂ catalysts prepared by pulsed laser ablation, *Journal of Catalysis*, 330, 497 – 506, (2015).

[5] G. Marzun, C. Streich, S. Jendrzey, S. Barcikowski, P. Wagener, Adsorption of Colloidal Platinum Nanoparticles to Supports: Charge Transfer and Effects of Electrostatic and Steric Interactions, *Langmuir*, 30, 11928-11939, (2014).

Influence of persistent microbubbles on nanoparticle productivity in laser synthesis of colloids

M.R. Kalus^{1,2}, R. Streubel¹, S. Barcikowski³, B. Gökce¹

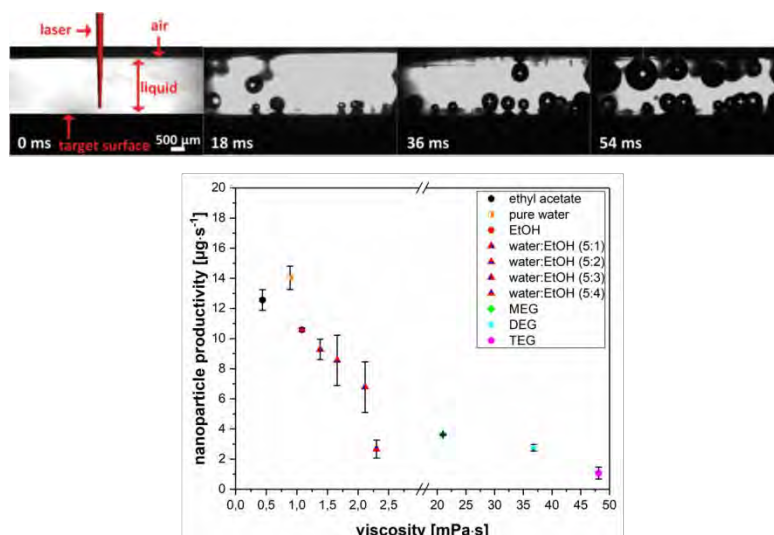
1- Technical Chemistry I, University of Duisburg-Essen and Center for NanoIntegration Duisburg-Essen CENIDE, Germany;

2- Particular GmbH, Germany

mark-robot.kalus@uni-due.de

Pulsed laser ablation in liquids is an innovative method, which enables the access to an almost unlimited array of colloidal nanoparticles characterized by an outstanding purity and representing promising candidates in many scientific fields [1]. However, the drawback of this method is its limited productivity compared to conventional chemical synthesis. Productivities of $>0,5\text{g/h}$ are necessary to make laser ablation synthesis more economical than wet chemical synthesis [2]. The productivity of the laser-based nanoparticle production method is limited by different entities such as laser-induced cavitation bubbles [3]. Strategies like increasing the applied laser power or using fast polygonal laser scanners are commonly used to enhance the nanoparticle output, but are linked to high investment costs [3].

Figure 38 (a): Illustration of the temporal development of persistent microbubbles generated during pulsed laser ablation in liquid.



(b) Dependence of nanoparticle productivity on the viscosity of different liquids.

Here, we present a more cost-effective way to increase the yield at a given power by optimizing laser power independent parameters. In this context, a second type of bubbles is introduced, which are often neglected, but also severely affect the productivity of the process [4]. With lifetimes from milliseconds to seconds, these so-called persistent microbubbles are systematically studied in this work by quantifying their composition, amount, size and dwell time in liquids with different viscosities and by relating the results to the nanoparticle productivities [4]. It is found that during synthesis liquid decomposition such as water splitting takes place. Depending on the liquid, these persistent microbubbles shield up to 65% of the incoming laser beam and require attention by means of reducing their dwell time in the ablation zone and enhancing the nanoparticle output by liquid flow. The highest productivities are achieved in liquids with the lowest viscosities.

[1] D. Zhang, B. Gökce and S. Barcikowski, Laser Synthesis and Processing of Colloids – Fundamentals and Applications”, Chemical Reviews, 117, pp. 3990-4103, (2017).

[2] S. Jendrzey, B. Gökce, M. Epple and S. Barcikowski, How Size Determines the Value of Gold - Economic Aspects of Wet Chemical and Laser-Based Metal Colloid Synthesis, Chemical Physics and Physical Chemistry, 18(9), pp. 1012-1019, (2017).

[3] R. Streubel, S. Barcikowski and B. Gökce, Continuous Multigram Nanoparticle Synthesis by High-Power, High-Repetition-Rate Ultrafast Laser Ablation in Liquid”, Optics Letters, 41, pp. 1486-1489, (2016).

[4] M.-R. Kalus, N. Baersch, R. Streubel, E. Goekce, S. Barcikowski and B. Goekce, How persistent microbubbles shield nanoparticle productivity in laser synthesis of colloids – quantification of their volume, dwell dynamics, and gas composition, Physical Chemistry Chemical Physics, 19(10), pp. 7112-7123, (2017).

Single-stage formation of Ag nanoparticles on α -Ag₂WO₄ network by femtosecond laser irradiation

Torres-Mendieta Rafael¹, de Assis Marcelo², Cordoncillo Eloisa³, Beltrán-Mir Héctor³, Mínguez-Vega Gladys⁴, de Oliveira Regiane C.², Leite Edson R.², Foggi Camila C.⁵, Vergani Carlos E.⁵, Longo Elson², and Andrés Juan⁶

¹Institute for Nanomaterials, Advanced Technologies and Innovation Technical University of Liberec, Studentská 1402/2, 461 17 Liberec, Czech Republic.

²CDMF-UFSCar, Universidade Federal de São Carlos, P.O. Box 676, CEP, 13565-905 São Carlos-SP, Brazil.

³Department of Inorganic and Organic Chemistry, University Jaume I (UJI), Castelló 12071, Spain.

⁴GROC-UJI, Institut de Noves Tecnologies de la Imatge (INIT, University Jaume I (UJI), Castelló 12071, Spain.

⁵FOAr-UNESP, Universidade Estadual Paulista, P.O. Box 1680, 14801903 Araraquara, SP Brazil.

⁶Department of Analytical and Physical Chemistry, University Jaume I (UJI), Castelló 12071, Spain.

Main author email address: Rafael.Torres@tul.cz

Silver tungstate (α -Ag₂WO₄), which is considered part of the ternary tungsten oxides family, has recently emerged as a multifunctional alternative over conventional wide band-gap semiconductors, owing to its potential in applications such as photocatalysis, photoswitching, among others [1]. Recent studies have also demonstrated that crystals of α -Ag₂WO₄ showed a metal nanoparticle (MNPs) growth attached to the semiconductor framework while analyzing the semiconductor by Transmission Electron Microscope (TEM), the phenomenon may lead to outstanding applications due to Ag segregation, such as ozone sensing and bacteriocidicity. Up to now, the MNPs growth has been limited to TEM processing, thus hampering its exploitation as a competitive bactericidal product among others [2]. In this communication, a different perspective is studied to scale-up the segregation of Ag nanoparticles (NPs) in the framework of the semiconductor. Femtosecond laser radiation (Ti:sapphire laser, 30 fs pulses, 1kHz, 800nm central wavelength) is used to irradiate large areas of α -Ag₂WO₄ in air, in order to promote an instantaneous nucleation and growth of Ag NPs. Afterwards, the material is tested as bactericidal agent against Methicillin-Resistant Staphylococcus Aureus ATCC 33591. Two different protocols are studied to consider the influence of the energy in the segregated species; a low energy regime leading to the synthesis of Ag nanoparticles anchored onto the surface of the semiconductor (Fig 1a), and a high energy regime leading to high material removal where the formation of Ag nanoparticles is accompanied by the synthesis of a new type of nanoalloy Ag_xW_yO_z (Fig 1b), and the biggest bactericidal activity is achieved.

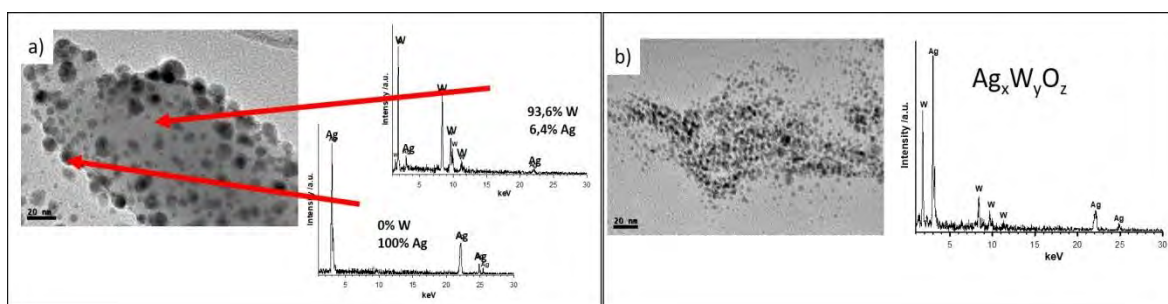


Figure 39 a) α -Ag₂WO₄ after being irradiated by fs radiation, b) Ag_xW_yO_z NPs formed when α -Ag₂WO₄ is irradiated at a high energy.

The results are compared with the segregation of Ag nanoparticles on α -Ag₂WO₄ using the accelerated electron beam from an electronic microscope under a high vacuum.

The samples irradiated by femtosecond radiation at a high fluence regime show the best antibacterial performance found in the literature up to now, a 32-fold improvement over non-irradiated α -Ag₂WO₄ [3]. We believe that the results found in current communication constitute an improvement over conventional multifunctional semiconductor synthesis approaches, which may inspire future developments.

[1] T. McGlone, C. Streb, D.-L. Long and L. Cronin, Assembly of pure silver-tungsten-oxide frameworks from nanostructured solution processable clusters and their evolution into materials with a metallic component. *Adv. Mater.* 22, 4275–4279 (2010).

[2] J. Andrés, et al. Structural and electronic analysis of the atomic scale nucleation of Ag on α -Ag₂WO₄ induced by electron irradiation. *Sci. Reports* 4, 5391 (2014).

[3] M. Assis, et al. Towards the scale-up of the formation of nanoparticles on α -Ag₂WO₄ with bactericidal properties by femtosecond laser irradiation. *Sci. Reports* 8, 1884 (2018).

Laser-assisted generation of elongated Au nanoparticles and subsequent dynamics of their morphology under pulsed irradiation in water

M.I.Zhilnikova^{1,2}, E.V. Barmina², G.A. Shafeev^{2,3}

1 - Theoretical Department of the Institute of Laser Physics, Siberian Federal University, 79/1700000, Krasnoyarsk, 660042, Russia

2 - Wave Research Center of A.M. Prokhorov General Physics Institute of the Russian Academy of Sciences, 38, Vavilov street, 119991 Moscow, Russian Federation

3 - National Research Nuclear University MEPhI (Moscow Engineering Physics Institute), 31, Kashirskoye highway, 115409, Moscow, Russian Federation

MZhilnikova@gmail.com

Laser generation of Au elongated nanoparticles (NPs) and their successive fragmentation and agglomeration are experimentally studied for the first time. Previously it was shown that laser-generation of elongated Au NPs was observed by ablation of Au colloidal solutions either with beta-active components or applied external field [1, 2]. In the present work first, laser-assisted formation of Au elongated nanoparticles by ablation of a solid Au (99, 99%) target in water was done using a Nd: YAG laser sources with pulse duration of 200 ns and pulse energy of 1mJ. Extinction spectrum correlating with TEM images of the mentioned above nanoparticles show the appearance of absorption signal in red region and near IR-spectrum that corresponds to longitudinal plasmon resonance of electrons in elongated nanoparticles [3, 4]. Second, generated elongated Au nanoparticles were exposed to pulsed laser beam with different pulse energy and ablation time. It was found that at early stages of irradiation (1-15 minute) NPs agglomerate as the NPs chains with size of order of 1 μm long. Further laser exposure results in fragmentation of these chains. Evolution of NPs size distribution was measured by disc-measuring centrifuge. Laser-induced process of agglomeration and fragmentation of Au elongated NPs are discussed.

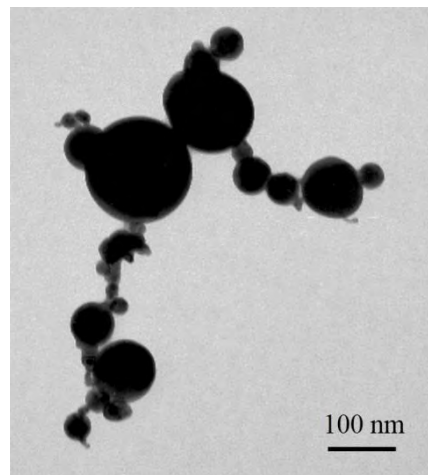


Fig.1. TEM view of nanoparticles obtained by nanosecond Nd:YAG laser radiation of elongated Au NPs in water

References:

- [1] Serkov A. A. et al., Self-assembly of nanoparticles into nanowires under laser exposure in liquids, *Chemical Physics Letters*, vol. 623, 93-97, (2015)
- [2] Y. Lu et al., Enzyme-functionalized gold nanowires for the fabrication of biosensors, *Bioelectrochemistry*, vol. 71, 211-216, (2007)
- [3] M.B. Mohamed et al., *Chemical Physics Letters*, vol. 317, 517-523, (2000)
- [4] Chang, Ser-Sing, et al., The shape transition of gold nanorods, *Langmuir* 15(3), 701-709, (1999)

MoS₂ quantum dots synthesized by pulsed laser ablation in a binary liquid

A. Jingmin Tang¹, B. Masanori Sakamoto¹, C. Ken-ichi Saitow^{1,2}

2- $c \quad c \quad -G \quad f \quad ch \quad c \quad f \quad c \quad c \quad H \quad h \quad , \quad (-AD) \quad H \quad h$
 $E : \quad w@h \quad h \quad . \quad c.jp.$

In the past few years, two-dimensional transition metal dichalcogenides (2D TMDs), such as molybdenum disulfide (MoS₂), have been extensively investigated as a typical layered material of semiconductors because of their excellent optoelectronic properties. Thus, many different synthesis methods have been recently developed to obtain low dimensional nanostructured MoS₂. There have been several reports on the exfoliation of MoS₂ by pulsed laser ablation in a liquid (PLAL). For instance, the nanoparticles MoS₂ had been produced by PLA in the water^{1,2} and 2D and 3D nanostructure MoS₂ were synthesized in the organic solvent³.

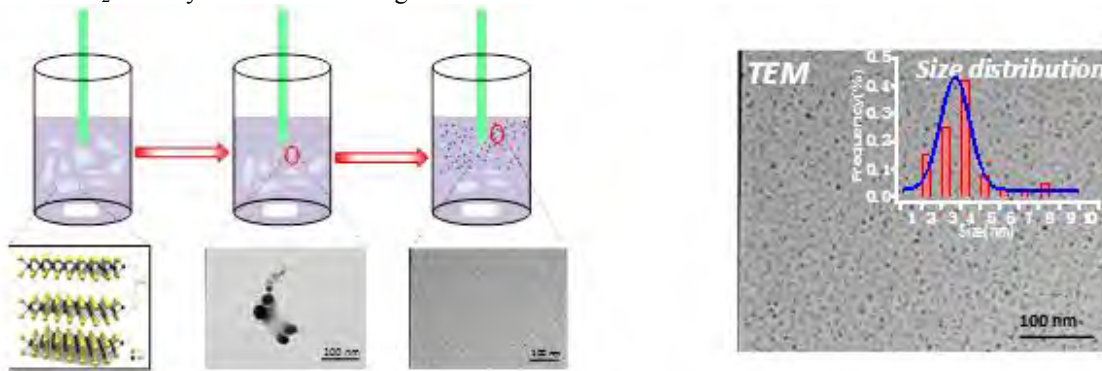


Figure. 1. Schematic diagram of the PLA procedure, they mainly include 3 steps. Firstly, bulk layered MoS₂ is dissolved in water and ethanol. Secondly, the layered MoS₂ is reduced to small particles with the size of 20-50 nm, and finally to nanosized particles ranging from 2-9 nm.

Here, we show the synthesis of MoS₂ quantum dots (QDs) with homogeneous size distribution using PLA in a binary liquid. Namely, MoS₂ powders dispersed in the liquid of water and ethanol were irradiated with a Q-switched Nd:YAG laser at an excitation wavelength of 532 nm, as illustrated in Fig. 1. The MoS₂ of layered material was effectively exfoliated and MoS₂ QDs with the size at around 4 nm were synthesized. In addition, we optimized the mixture ratio of the binary liquid for giving the excellent dispersion of MoS₂ QDs. Generation mechanism of the layered MoS₂ and QDs by PLA in the binary liquid are considered as a balance of deformation of layered MoS₂ in the binary liquid, whose amount is changed by the mixture ratio during PLA. As another important point, our method showed that MoS₂ QDs give a good performance for hydrogen evolution reaction (HER).

[1] H. Wu, R. Yang, B. Song, et al, *J. ACS nano*, 2011, 5(2): 1276-1281.
 [2] S. Alkis, T. Öztas, L.E. Aygün, et al, *J. Optics express*, 2012, 20(19): 21815-21820.
 [3] Oztas T, Sen H.S, Durgun E, et al, *J. physical chemistry C*, 2014, 118(51): 30120-20126.

Effects of ablation energy and time on SnS₂ nanoparticles by pulsed laser ablation in liquid

J. Johnny¹, S. Shaji^{1,2,#}, S. Sepulveda-Guzman^{1,2}, D.A. Avellaneda¹ and B. Krishnan^{1,2}

¹ Universidad Autónoma de Nuevo León, Facultad de Ingeniería Mecánica y Eléctrica, San Nicolás de los Garza, Nuevo León, México, 66455.

² Universidad Autónoma de Nuevo León - Centro de Innovación, Investigación y Desarrollo de Ingeniería y Tecnología (CIIDIT), Apodaca, Nuevo León, México, 66600

E-mail: sshajis@yahoo.com, sadasivan.shaji@uanl.edu.mx

As a green and novel technique for synthesizing nanoparticles, pulsed laser ablation in liquid (PLAL) receives wide attention from the researchers [1, 2]. Tin disulfide (SnS₂) is an n-type semiconductor with layered hexagonal structure which finds applications in photovoltaics and charge storage devices [3, 4]. In a previous work we reported rapid synthesis of SnS₂ NPs by PLAL in various liquid media [5]. Herein, we report the effects of laser fluence and ablation time on the morphology of SnS₂ nanoparticles (NPs) synthesized by PLAL. SnS₂ NPs were synthesized using laser wavelengths of 532 and 1064 nm in different liquid media. The as prepared particles were characterized by different techniques such as Transmission electron microscopy (TEM), X-ray photoelectron spectroscopy (XPS), Raman spectroscopy, UV-Visible absorption spectroscopy and Photoluminescence spectroscopy. Morphology, size and size distribution of the SnS₂ particles found to depend on both the laser fluence and ablation time. The crystalline structure of SnS₂ NPs is analyzed by HRTEM, SAED and Raman spectra. Elemental composition and chemical state of the nanoparticles are confirmed by the XPS analysis. Optical absorption, bandgaps and luminescence emission of these nanocolloids are also studied.

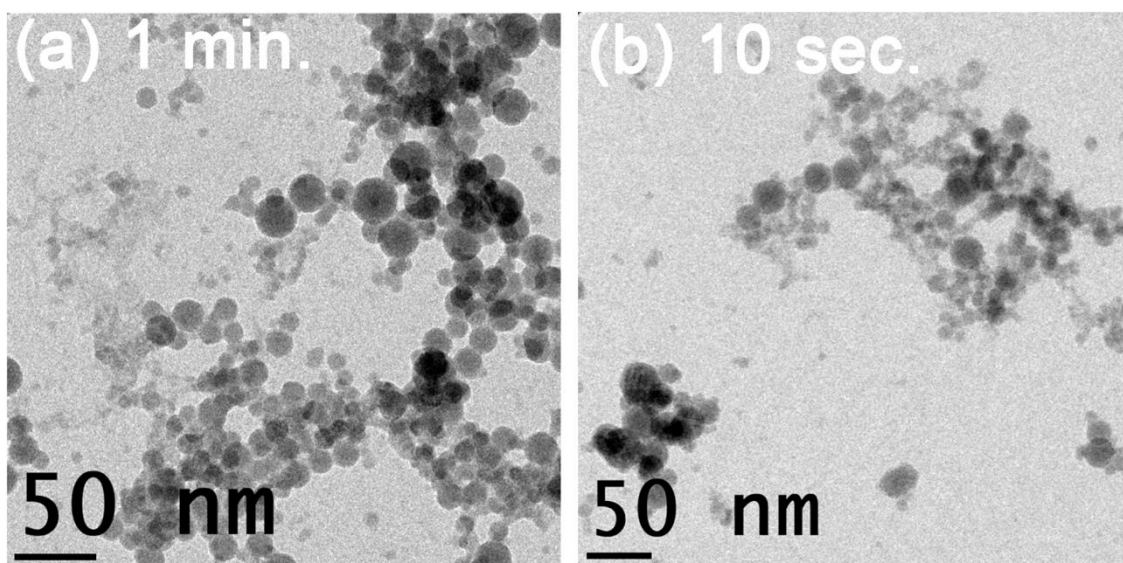


Fig.1 TEM micrographs of SnS₂ NPs synthesized by 1064 nm laser output for ablation times (a) 1 min. and (b) 10 sec. at constant fluence of 0.44 J/cm²

1. Amendola, V. and M. Meneghetti, *Laser ablation synthesis in solution and size manipulation of noble metal nanoparticles*. Physical Chemistry Chemical Physics, 2009. **11**(20): p. 3805-3821.
2. Zeng, H., et al., *Nanomaterials via Laser Ablation/Irradiation in Liquid: A Review*. Advanced Functional Materials, 2012. **22**(7): p. 1333-1353.
3. Seo, J.-w., et al., *Two-Dimensional SnS₂ Nanoplates with Extraordinary High Discharge Capacity for Lithium Ion Batteries*. Advanced Materials, 2008. **20**(22): p. 4269-4273.
4. Lucena, R., F. Fresno, and J.C. Conesa, *Hydrothermally synthesized nanocrystalline tin disulphide as visible light-active photocatalyst: Spectral response and stability*. Applied Catalysis A: General, 2012. **415-416**: p. 111-117.
5. Johnny, J., et al., *Facile and fast synthesis of SnS₂ nanoparticles by pulsed laser ablation in liquid*. Applied Surface Science, 2018. **435**: p. 1285-1295.

Surface Chemistry Of Colloidal Ligand-Free Gold Nanoparticles Generated By Laser Ablation

G. Laurens⁴, M. Patanen¹, J. Gaudin², I. Papagiannouli², V. Blanchet², R. Grisenti³, D. Amans⁴, C. Nicolas⁵, A. R. Milosavljević⁵, E. Robert⁵, J. D. Bozek⁵, M. De Anda Villa⁶, S. Macé⁶, S. Steydli⁶, C. Prigent⁶, E. Lamour⁶, D. Vernhet⁶, M. Trassinelli⁶, A. Lévy⁶

1- Nano and molecular systems research unit, Faculty of Science, P.O. Box 3000, 90014 University of Oulu, Finland
 2- Univ. Bordeaux, CNRS, CEA, CELIA (Centre Lasers Intenses et Applications), UMR5107, 33405 Talence, France
 3- Institut für Kernphysik, J. W. Goethe Universität Max-von-Laue-Str. 1, 60438 Frankfurt (M), Germany
 4- Institut Lumière matière, UMR5306 - UCBL - CNRS, 10 rue Ada Byron, 69622 Villeurbanne CEDEX, France
 5- Synchrotron O E O A b P 48 9 92 G f-sur-Yvette Cedex, France
 6- Sorbonne Université, CNRS UMR 7588, Institut des Nanosciences de Paris (INSP), 75252 Paris Cedex 05, France

Main author email address: gaetan.laurens@univ-lyon1.fr

Ligand free gold nanoparticles (AuNPs) have been synthesized by Pulsed Laser Ablation in Liquids. Their colloidal stability is commonly attributed to the negative Surface Charge of the first layer surrounding the NP. The surface charge can be induced by anions adsorption or pH [1-2]. The surface chemistry occurring on these surfactant-free AuNPs is then of primary importance. We will present here recent results of the surface characterization using a very surface sensitive characterization technique, namely synchrotron radiation excited photoelectron spectroscopy [3]. We have studied the surface composition/oxidation of gold NPs produced in aqueous solutions different salinities and pH. The colloidal suspension prepared using PLAL is aerosolized and a free-standing AuNP beam is studied, avoiding the influence of substrate or solvent. We have found signatures of halide-ions and possible gold oxidized atoms on the surface of the AuNPs. The demonstrated technique provides a promising new way to study bare gold surfaces and a complementary insight to colloidal stability.

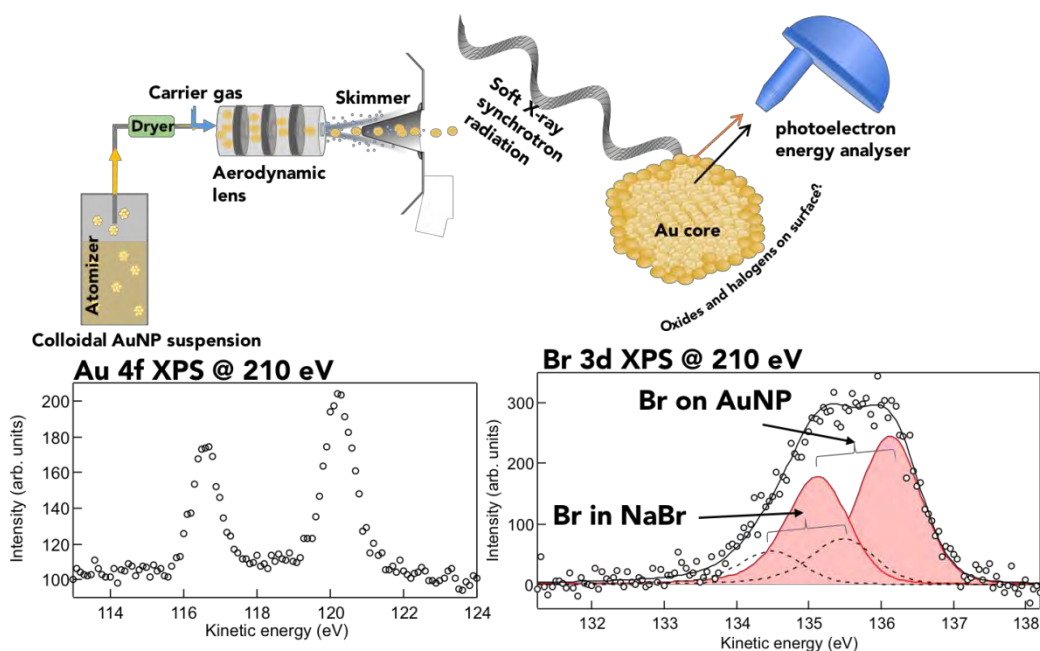


Figure 40 An aerosol of AuNPs is created using an atomizer. An aerodynamic lens focuses the AuNP beam to the interaction region with soft X-rays of PLEIADES beamline (Synchrotron SOLEIL). The Au 4f and Br 3d photolines are recorded with a hemispherical electron analyzer to learn from the bonding between AuNPs and the ionic species believed to be responsible for the colloidal stability

[1] V. Merk, C. Rehbock, F. Becker, U. Hagemann, H. Nienhaus, and S. Barcikowski, In Situ Non-DLVO Stabilization of Surfactant-Free, Plasmonic Gold Nanoparticles: Effect of Hofmeister's Anions, *Langmuir* **30**, 4213–4222 (2014)

[2] C. Rehbock, V. Merk, L. Gamrad, R. Streubel and S. Barcikowski, Size control of laser-fabricated surfactant-free gold nanoparticles with highly diluted electrolytes and their subsequent bioconjugation, *Phys. Chem. Chem. Phys.* **15**, 3057-3067 (2013)

[3] O. Sublemontier, C. Nicolas, D. Aureau, M. Patanen, H. Kintz, X.-J. Liu, M.-A. Gaveau, J.-L. Legarrec, E. Robert, F.-A. Barreda, A. Etcheberry, C. Reynaud, J. Mitchell, C. Miron, *X-ray Photoelectron Spectroscopy of Isolated Nanoparticles*, *J. Phys. Chem. Lett.* **5**, 3399–3403 (2014)

Doping inclusion in nanoparticles using pulsed laser ablation in liquid

Arsène Chemin¹, Julien Lam¹, Gaetan Laurens¹, Florian Trichard¹, Vincent Motto-Ros¹, Gilles Ledoux¹, Vitezslav Jary², Martin Nikl², Christophe Dujardin¹, David Amans¹

1- Univ Lyon, Université Claude Bernard Lyon 1, CNRS, Institut Lumière Matière, F-69622, VILLEURBANNE, France

2- Institute of Physics, Academy of Sciences of The Czech Republic, Cukrovarnicka 10, 16200 Prague 6, Czech Republic

arsene.chemin@ens-lyon.fr

Pulsed laser ablation in liquids (PLAL) is a versatile technological approach to produce nanoparticle colloids. Nowadays, PLAL is increasingly employed because the production rate is scalable, and the method ensures clean and ligand-free surfaces. Doping nanocrystals allows modifying their optical or electrical properties. In the case of PLAL, the standard route is to prepare doped material as a pellet using solid state reaction. But the issue of impurities (when unwanted) or doping ions (when wanted) coming from the surrounding liquid has never been raised. If the transfer of the species dissolved in a liquid into laser ablation plasma has been demonstrated [1], the penetration of the species within the nanoparticles has to be evaluated. In this contribution, we use salts in the solvent to dope the nanoparticles during the condensation of the plasma obtained by the ablation of undoped materials. It demonstrates the deep interaction between the plasma and the solvent. For this purpose, we prepared $\text{Gd}_2\text{O}_3:\text{Eu}^{3+}$ nanoparticles, a well-known red luminescent sesquioxides [2] containing gadolinium which is also known as a contrast agent for nuclear magnetic resonance imaging. We also prepared nano-ruby, i.e. $\alpha\text{-Al}_2\text{O}_3:\text{Cr}^{3+}$ nanoparticles, known as a pressure probe. In addition, Eu^{3+} and Cr^{3+} are well known structural probes, since their optical response depends strongly on the crystal field symmetry at the point defect. It thus brings information about the crystallinity, the crystallographic phase, and the defects of which the as-produced particles generally suffer. The ablation of undoped targets is performed in aqueous solution containing respectively Eu^{3+} ions for Gd_2O_3 target, and Cr^{3+} ions for Al_2O_3 target. The efficiency of the doping was quantitatively determined by the combination of light induced breakdown spectroscopy (LIBS), and luminescence spectroscopy.

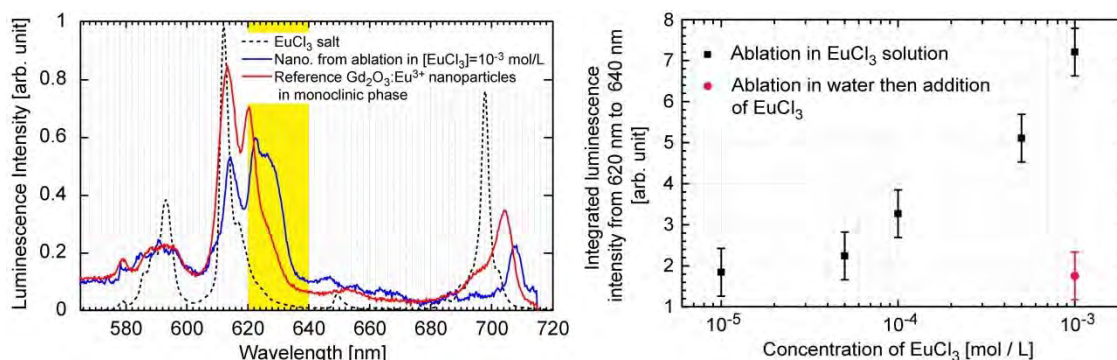


Figure 41: (left) Luminescence spectra of EuCl_3 salt (dashed line), nanoparticles obtained from pure Gd_2O_3 ablated in a solution of EuCl_3 at a concentration of $10^{-3} \text{ mol.L}^{-1}$ (solid blue line) and reference $\text{Gd}_2\text{O}_3:\text{Eu}^{3+}$ nanoparticles in a monoclinic phase. The blue curve shows features between 618 and 640 nm typical of monoclinic and hexagonal $\text{Gd}_2\text{O}_3:\text{Eu}^{3+}$ nanoparticles. (right) Integrated luminescence intensity from 620 nm to 640 nm for nanoparticles ablated in solution of different concentration of EuCl_3 . The higher the concentration, the stronger the luminescence.

[1] A.Matsumoto J. Phys. Chem. C, 119, 26506 (2015) / J.Lam, Appl. Phys. Lett., 108,074104 (2016)

[2] D.Nicolas et al., JCP 125, 171104 (2006) / B.Mercier et al., JCP 126, 044507 (2007)

Graphene Quantum Dots, Microstructures Fabricated using Femtosecond Laser Ablation in liquids

B. Chandu, M.S.S Bharati, S. Hamad, S. Venugopal Rao^{1, a}

¹Advanced Centre for Research in High Energy Materials (ACRHEM),

University of Hyderabad, Prof. C. R. Rao Road, Hyderabad 500046, Telangana, India

^aCorresponding author: soma_venu@uohyd.ac.in

Graphene quantum dots (GQDs) and few layers of Graphene with nanoparticles are promising materials due to their exceptional properties resulting in different applications such as bio-imaging, solar cells, light emitting diodes, filtration, optoelectronic devices, electronic displays, etc. In the last decade, several methods have been implemented to achieve Graphene patterns/GQDs such as chemical vapour deposition, wet-chemical etching, e-beam lithography etc. However, these methods are time consuming and needs multiple stages for fabrication. Unlike prior mentioned techniques, ultrafast laser ablation in liquid media technique is a promising approach to fabricate Graphene patterns/GQDs in single step.²⁻⁴ In the present study, well defined GQDs and few layers of Graphene and graphite (NSs) were fabricated through the single step process using femtosecond (fs) ablation of graphite target in (a) different liquid media (acetone, water, chloroform and CCl₄) and (b) with different pulse energies (25, 50, 100, 150 and 200 μ J) in acetone using \sim 50 fs pulses at 800 nm wavelength. The effect of liquid media during the ablation of graphite was explored by figuring out the surface morphology and elemental analysis studies. The fabricated nano-Graphene particles in liquid media were characterized by Transmission electron microscopy (TEM), selective area electron diffraction (SAED), HRTEM, Raman spectroscopy, UV –Visible and photoluminescence measurements. The estimated average sizes of nano-Graphene particles were in the range of 2–50 nm. SAED, HRTEM and Raman spectroscopy confirmed that different Graphene nano-composites were formed in different liquid media. As in the case of pulse energy dependent study, the mean sizes of particles are estimated to be 2–10 nm range. From the photoluminescence studies of Graphene quantum dots with different sizes, we observed the tuneable PL peak with in the spectra region of 350-450 nm. Moreover, we have performed ablation studies in air for the comparative studies. All fabricated NSs were characterized by field emission scanning electron microscope (FESEM) and Raman spectroscopy. In case of air media, periodicity in NSs was observed at lower laser energies while increasing the laser energy irregularity in periodicity with pillar kind of morphology was observed. Where as in case of liquid media, flower like morphology with graphene flakes on NSs were observed. The outcomes advance the fabrication of Graphene quantum dots and Graphene layers in different liquid media could be peculiar interest for diverse applications.

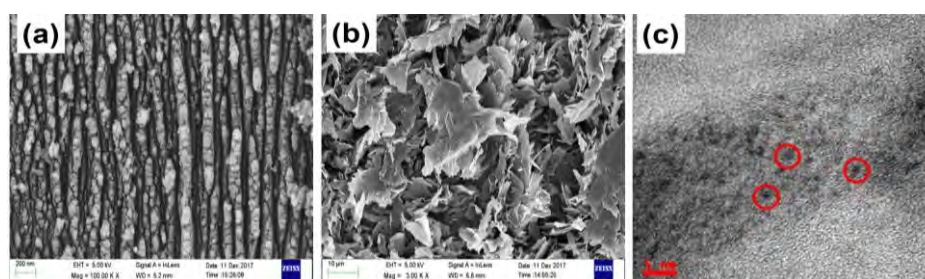


Figure 42 FESEM images of laser ablated regions on graphite target placed in (a) air (b) acetone and (c) HRTEM image of GQDs obtained at a pulse energy of 50 μ J.

- [1] K. S. Novoselov, Z. Jiang, Y. Zhang, S. Morozov, H. L. Stormer, U. Zeitler, J. Maan, G. Boebinger, P. Kim, and A. K. Geim, "Room-temperature quantum Hall effect in graphene", *Science* **315** (5817), 1379 (2007).
- [2] P. Russo, R. Liang, E. Jabari, E. Marzbanrad, E. Toyserkani, and Y. N. Zhou, "Single-step synthesis of graphene quantum dots by femtosecond laser ablation of graphene oxide dispersions", *Nanoscale* **8** (16), 8863-887 (2016).
- [3] X. Shi, X. Li, L. Jiang, L. Qu, Y. Zhao, P. Ran, Q. Wang, Q. Cao, T. Ma, and Y. Lu, "Femtosecond laser rapid fabrication of large-area rose-like micropatterns on freestanding flexible graphene films", *Sci. Rep.* **5**, 17557 (2015).
- [4] R. Kumar, R. K. Singh, D. P. Singh, E. Joanni, R. M. Yadav, and S. A. Moshkalev, "Laser-assisted synthesis, reduction and micro-patterning of graphene: recent progress and applications", *Coordination Chemistry Reviews* **342**, 34-79 (2017).
- [5] G. K. Podagatlapalli, S. Hamad and S. V. Rao, Trace-Level Detection of Secondary Explosives Using Hybrid Silver–Gold Nanoparticles and Nanostructures Achieved with Femtosecond Laser Ablation," *J. Phys. Chem. C* **119**, 16972-16983 (2015).

Hydrogen generation by laser irradiation of organic liquids

I.V. Baymler¹, E.V. Barmina², A.V. Simakin², G.A. Shafeev^{2,3}

*1*Moscow Institute of Physics and Technology (State University), 9 Institutskiy per., Dolgoprudny, Moscow Region, 141701, Russian Federation

*2*Wave Research Center at Prokhorov General Physics Institute, Russian Academy of Sciences, Vavilov Str., 38, Moscow, 119991, Russian Federation.

*3*National Research Nuclear University MEPhI (Moscow Engineering Physics Institute), Kashirskoe Highway 31, Moscow, 115409, Russian Federation.

ilyabaymler@yandex.ru

Laser ablation is a method of generation of chemically pure metal nanoparticles [1]. It was shown that generation of molecular hydrogen is possible by pulsed laser irradiation of water and colloids of iron and beryllium [2,3]. Laser irradiation leads to plasma formation of laser breakdown of liquid and following emission of hydrogen gas. Production rate of hydrogen strongly depends on concentration of metal nanoparticles in water solution.

In the present work the process of hydrogen generation is experimentally studied under exposure of organic liquids (ethanol, isopropanol, isobutanol, diethyl ether) to pulsed radiation of a Nd:YAG laser with the intensity of 10^{10} W/cm². Production rates of molecular hydrogen and its partial pressure depend on exposure time and number of carbon-hydrogen bonds of molecules. The results shown in fig. 1 are interpreted as dissociation of organic molecules by direct electron impact from breakdown plasma.

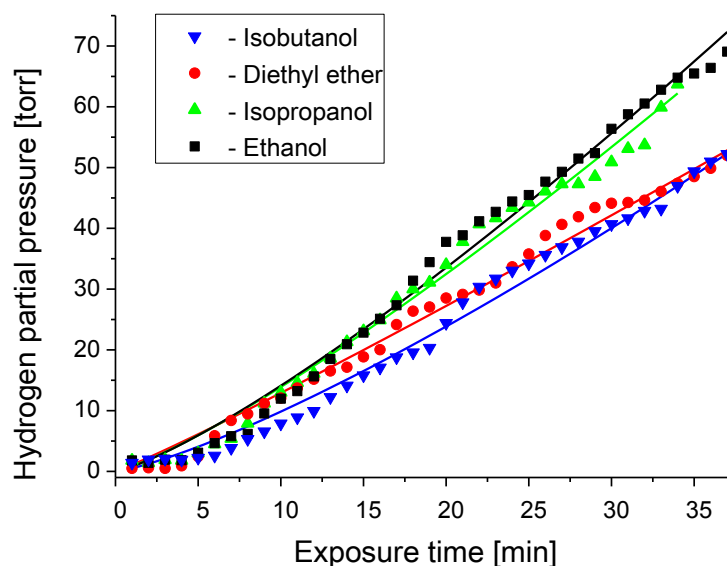


Figure 43. Time dependence of hydrogen partial pressure under laser exposure of different organic samples

[1] J. Nedderson, G. Chumanov, T. M. Cotton // Appl. Spectrosc. 1993, 47, 1959

[2] E.V. Barmina, A.V. Simakin, G.A. Shafeev, Hydrogen emission under laser exposure of colloidal solutions of nanoparticles // Chemical Physics Letters, v. 655–656, 2016, 35–38.

[3] I.A. Sukhov, G.A. Shafeev, E.V. Barmina, A.V. Simakin, O.V. Uvarov, V.V. Voronov, Hydrogen generation by laser irradiation of colloids of iron and beryllium in water // Quantum Electronic (2017), 47 (6):533

Fabrication of metal nanoparticles and nanoalloys by laser ablation in liquids

S. Oztulum and S. Aksoy

Department of Physics Engineering, Istanbul Technical University, 34469, Istanbul, Turkey

eaksoy@itu.edu.tr

Nanoparticles have a widespread use in medicine, photonics and energy applications [1]. Laser ablation has been used to prepared nanoparticles from a metal target surface in liquid [2]. The temperature and the pressure of the plume induced by laser irradiation are very high so crystalline nanoparticles can be obtained easily. Magnetic nanoparticles could be used in applications such as high-density storage media, magnetic ink, magnetic resonance contrast media, and more [3]. Rare earth material Gd and Ni-Mn-based Heusler alloys are a good candidate for room temperature solid-state refrigerators (SSR). In this talk, we give an overview of our recent research on laser-based synthesis of magnetic nanoparticles using femto/nanosecond laser [4]. The average grain size distribution and shape of nanoparticles are characterized by using SEM and TEM. The magnetization measurements are performed using a superconducting quantum interference device magnetometer. Superparamagnetic behaviour is observed at room temperature at some nanoalloys. In aqueous media, negatively charged nanoparticles are coated with polymers and the colloidal properties such as zeta potential values are defined for coated particles.

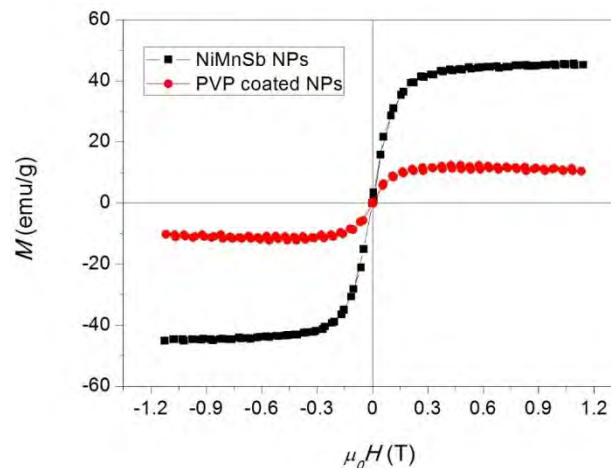


Figure 44 Magnetization measurement of laser ablated NiMnSb Heusler nanoparticles at room temperature. Red and black symbols represent PVP coated and uncoated particles.

- [1] W. J. Stark, P.R. Stoessel, W. Wohlleben and A. Hafner, Industrial applications of nanoparticles, Chemical Society Reviews, 44, pp. 5793-5805 (2015)
- [2] T. Yamamoto, Y. Shimotsuma, M. Sakakura, M. Nishi, K. Miura and K. Hirao, Intermetallic magnetic nanoparticle precipitation by femtosecond laser fragmentation in liquid, Langmuir, 27, pp. 8359-8364 (2011).
- [3] L. Mohammed, H. G. Gomaa, D. Ragab and J. Zhu, Magnetic nanoparticles for environmental and biomedical applications: A review, Particuology, 30, pp. 1-14 (2017)
- [4] S. Aksoy, Synthesis and characterization of NiMnIn nanoparticles, Journal of Magnetism and Magnetic Materials, 373, pp. 236-239, (2015).

Gas Sensing by Laser-Ablated Nanomaterials

P. Shankar¹, S.A. Kulinich¹

1- Tokai University, Institute of Innovative Science and Technology, Hiratsuka, Kanagawa 259-1292, Japan

Main author email address: skulinich@tokai-u.jp

Nanomaterials prepared via laser ablation in liquid (LAL) are known to be applied in several fields, including such as electronics, catalysis and photocatalysis, biomedicine, optics and optoelectronics, energy related technologies and so on [1]. As LAL products are often semiconductor metal oxides (or metal sulfides) with unique morphology and surface defects, such materials may also be attractive as components for chemiresistive gas sensors. Nevertheless, to date, only a few attempts were made to exploit LAL-generated nanomaterials as gas sensors [2,3]. Niu and co-workers showed sensing of ethanol and acetone by hollow ZnS nanoparticles [2]. Later, Xiao et al used LAL-produced WO₃ nanoflakes to make a device that sensed ethanol at 150 °C [3]. No devices working at room temperature were reported.

In this work, we fabricated gas sensors based on ZnO and SnO_x nanomaterials prepared by means of ns- and ms- pulsed lasers in water. We show that such nanomaterials can demonstrate selective and sensitive gas sensing at room temperature [4,5]. Figure 1 presents ZnO nanoparticles prepared by ns-pulsed laser in water (a) and their dynamic response curve towards ethanol (b) recorded at room temperature.

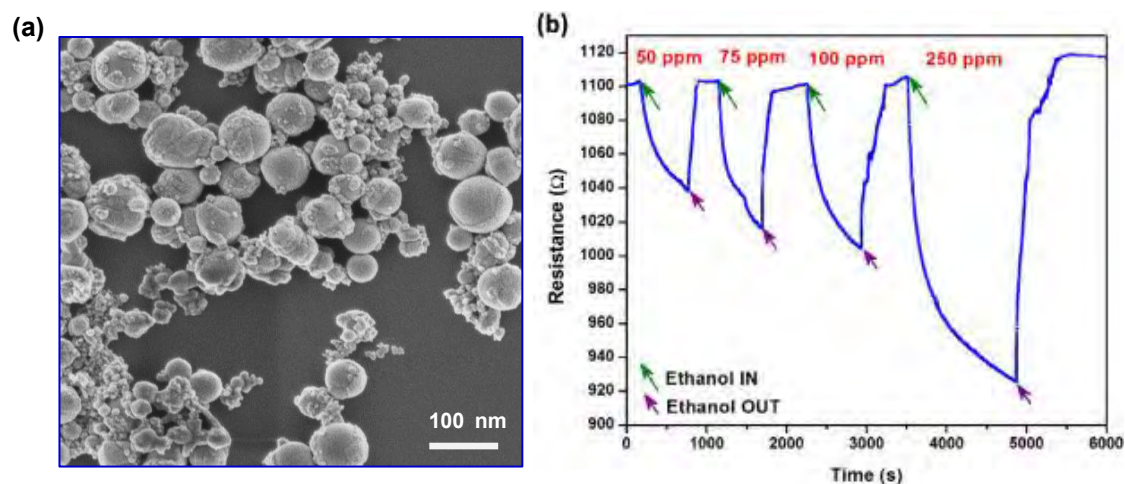


Figure 45. (a) SEM image of ZnO nanoparticles produced by ns-laser in water medium and (b) dynamic response curve of sensor device based on such nanoparticles towards ethanol at room temperature [4].

- [1] H.B. Zeng, X.W. Du, S.C. Singh, S. A. Kulinich, S.K. Yang, J.P. He, W.P. Cai, Nanomaterials via laser ablation/irradiation in liquid: A review, *Adv. Funct. Mater.*, vol.22, pp.1333-1353, (2012).
- [2] K. Y. Niu, J. Yang, S. A. Kulinich, J. Sun, X. W. Du, Hollow nanoparticles of metal oxides and sulfides: Fast preparation via laser ablation in liquid, *Langmuir*, vol.26, pp.16652-16657, (2010).
- [3] J. Xiao, P. Liu, Y. Liang, H. B. Li, G. W. Yang, Porous tungsten oxide nanoflakes for highly alcohol sensitive performance, *Nanoscale*, vol.4, pp.7078- 7083, (2012).
- [4] T. Kondo, Y. Sato, P. Shankar, M. Kinoshita, P. Shankar, N.N. Mintcheva, M. Honda, S. Iwamori, S.A. Kulinich, Room temperature ethanol sensor based on ZnO prepared via laser ablation in water, *Jpn. J. Appl. Phys.*, vol.56, 080304, (2017).
- [5] M. Honda, T. Kondo, T. Owashi, P. Shankar, S. Iwamori, Y. Ichikawa, S.A. Kulinich, Nanostructures prepared via laser ablation of tin in water, *New J. Chem.*, vol.41, pp. 11308-11316, (2017).

Interaction of AgNPs produced by PLAL with human proteins and protein corona assessment

M. Dell'Aglio¹, M. Nardella², V. Mangini², A. De Giacomo^{2,1}, F. Arnesano^{2,1}

1. Institute of Nanotechnology, CNR-NANOTEC, c/o Department of Chemistry, University of Bari, Via Orabona 4, 70126 Bari-Italy

2. Department of Chemistry, University of Bari, Via Orabona 4, 70126 Bari-Italy

marcella.dellaglio@cnr.it

Since the use of silver nanoparticles (AgNPs) in everyday products and biomedical devices is increasing, also toxicity, efficiency, transportation, and processing of AgNPs in a biological system is becoming important. The formation of protein corona upon interaction of nanoparticles with proteins is a key issue in the study of AgNPs internalization in human cells. The native conformation of proteins interacting with AgNPs can be altered, sometimes resulting in the exposure of protein epitopes normally hidden within the protein core, thus causing unexpected biological responses [1,2]. Here, two case studies are presented, describing the interaction of AgNPs produced by pulsed laser ablation in liquid (PLAL) with intracellular copper transport proteins and with human ubiquitin (Ub).

Cells use different pathways to ensure uptake, storage and export of copper. In humans, the Cu chaperone Atox1 provides Cu(I) to the metal-binding domains (MBDs) of two P_{1B}-type ATPases: the Menkes (Atp7a) and Wilson (Atp7b) disease proteins. Both Atox1 and the first MBD of Menkes (Mnk1), which are partners *in vivo*, can bind a Cu(I) ion through two cysteine residues of a conserved CXXC motif [3]. The main objective of this work was to obtain direct evidence of the interaction of Atox1 and Mnk1 with AgNPs. Although the two proteins share a similar structure, their behavior with AgNPs is found to be substantially different. Moreover, since Ag(I) and Cu(I) have similar coordination properties, proteins involved in copper homeostasis are the main candidates for binding Ag(I) ions released by AgNPs in cells, thus an impact of AgNPs on copper metabolism is expected.

AgNPs also interact with ubiquitin; the resulting system was incubated with human serum albumin (HSA) or whole human serum (HS), in order to investigate the stability of protein corona. Since the hardening of protein corona depends on the presence of free thiol groups, a lysine in position 48 of Ub has been replaced with a cysteine. The interaction of wild-type Ub and K48C mutant with AgNPs was assessed in terms of dynamic exchange with HSA and other binders contained in human serum, which led to some considerations on the evolution of protein corona when AgNPs are incubated in a biological fluid.

Finally, the behavior of AgNPs produced by PLAL was compared with that of AgNPs produced by chemical synthesis, thus revealing some important differences in interaction with proteins. The entire characterization was performed by monitoring the SPR band of AgNPs using UV-visible spectroscopy and protein signals using NMR-based approaches.

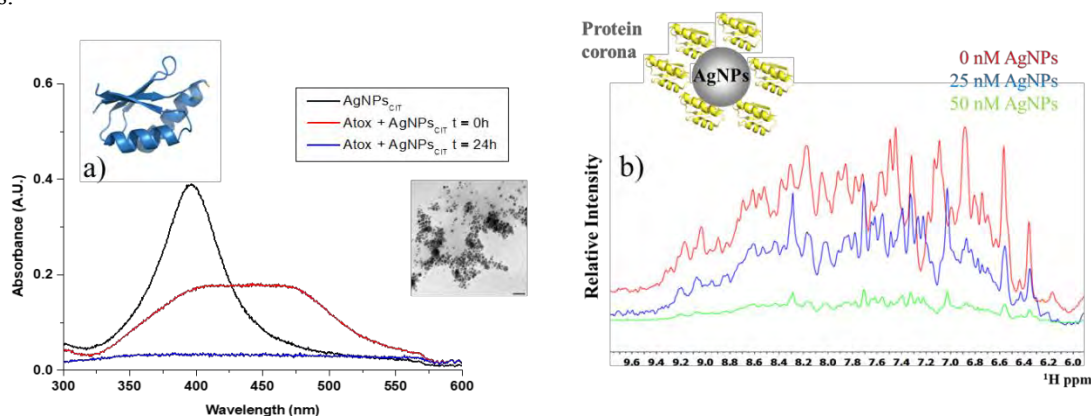


Fig.1: a) UV-vis spectra and TEM image of AgNPs incubated with Atox1, b) Amide proton region of ¹H NMR spectra of Mnk1 (4 μM) in the presence of various concentration of AgNPs.

- [1] Dell'Aglio, M., Mangini, V., Valenza, G., De Pascale, O., De Stradis, A., Natile, G., Arnesano, F., De Giacomo, A. "Silver and gold nanoparticles produced by pulsed laser ablation in liquid to investigate their interaction with Ubiquitin"(2016) Applied Surface Science, pp. 297–304
 [2] V. Mangini, M. Dell'Aglio, De Stradis A., De Giacomo A., De Pascale O., G. Natile, and F. Arnesano *Chemistry* **20**, 10745-10751 (2014)
 [3] F. Arnesano, L. Banci, I. Bertini, S. Ciofi-Baffoni, E. Molteni, D. L. Huffman, and T. V. O'Halloran *Genome Res.* **12**, 255-271 (2002).

Hydrogen production by ultrasound assisted liquid laser ablation of an Al-Mg alloy in water

L. Escobar Alarcón¹, J.L. Iturbe-García², F. González-Zavala^{1,4}, D.A. Solís-Casados³,

E. Haro-Poniatowski⁴

1- Departamento de Física, Instituto Nacional de Investigaciones Nucleares, Apdo. Postal 18-1027, CDMX 11801, México.

2- Departamento de Química, Instituto Nacional de Investigaciones Nucleares, Apdo. Postal 18-1027, CDMX 11801, México.

3- Universidad Autónoma del Estado de México, Facultad de Química, CP 50120, Toluca, Estado de México, México.

4- Departamento de Física, Universidad Autónoma Metropolitana Iztapalapa, Apdo. Postal 55-534, CDMX, México.

luis.escobar@inin.gob.mx

The laser ablation of solids in liquid medium has been actively used in the last two decades for the synthesis and processing of nanoparticles. An important effect of the plasma formation as a result of the laser-solid interaction is that some of the plasma surrounding liquid is vaporized producing a cavitation bubble. This bubble expands to its maximum size and then collapses, this process occurs at temperatures of thousands of Kelvin degrees and pressures of several GPa [1]. Under these extreme conditions if the liquid is water, splitting in hydrogen and oxygen occur, so that it can be considered as a way to produce hydrogen. In fact, the generation of hydrogen by laser irradiation of powder carbon in water has been reported as a method of its production [2]. The combination of laser ablation in liquid with an ultrasound field has been investigated for producing nanosheets in colloidal suspensions with interesting results, in particular increase the production rate [3]. Figure 1a shows the experimental configuration used to produce hydrogen. A ns pulsed Nd: YAG laser was used to ablate an Al-Mg alloy immersed in 20 mL of demineralized water for 5 minutes. The laser beam was directed perpendicular to the surface of the metal target contained inside of a sealed glass flask. The flask was connected through a flexible hose to a glass beaker with water, in which an inverted graduated cylinder was placed; the volume of the produced gas (hydrogen) was determined directly by measuring the displacement of the liquid. Experiments varying the laser fluence from 27 to 77 J/cm², with and without the presence of an ultrasonic field, were performed.

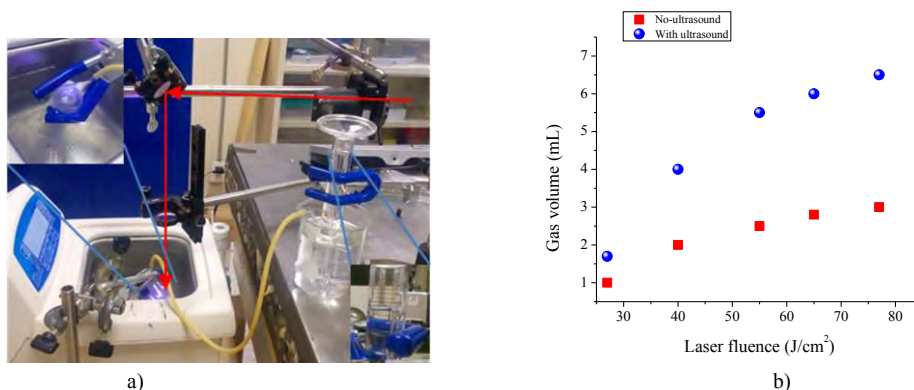


Figure 46. (a) Experimental setup for hydrogen production, (b) produced gas volume as a function of the laser fluence used to ablate the Al-Mg target with and without ultrasound.

The obtained results are shown in figure 1b. Without ultrasound the produced gas volume increases from 1 to 3.0 ml increasing the laser fluence from 27 to 77 J/cm². When experiments were performed in presence of the ultrasonic field a significant enhancement of the produced gas was observed; the volume increases from 1.7 to 6.5 mL at the same fluences. No gas production with ultrasound only was observed. Therefore, hydrogen production is more efficient under ultrasound assisted laser ablation. Additionally, the nanostructures formed in each case were also characterized.

[1] T. Tsuji, Y. Tsuboi, N. Kitamura, M. Tsuji, *Appl. Surf. Sci.*, 229, 365 (2004).

[2] I. Akimoto, K. Maeda, N. Ozaki, *J. Phys. Chem. C*, 117, 18281 (2013).

[3] L. Escobar-Alarcón, E. Velarde Granados, D.A. Solís-Casados, O., Olea-Mejía, M. Espinosa-Pesqueira, E. Haro-Poniatowski, *Appl. Phys. A* 122, 433 (2016).

Stable colloidal suspension of TiO₂ nanoparticles in aqueous solution prepared by nanosecond laser pulses and their photocatalytic performances

Y. K. Kim¹ and H. Kang²

1- Department of Energy Systems Research, Ajou University Suwon, 16499 South Korea

2- Department of Chemistry, Ajou University, Suwon, 16499 South Korea

Main author email address: yukwonkim@ajou.ac.kr

Laser ablation techniques have been frequently used to prepare TiO₂ nanoparticles [1,2] for applications such as photocatalysts and solar cells. Here, the detailed experimental conditions of laser ablation were found to be critical in determining their photocatalytic properties. Laser power and wavelength were reported to determine the final chemical composition and the detailed morphology of the TiO₂ nanostructures. In this study, a simple laser ablation technique employing nanosecond infrared laser pulses was used for the preparation of a stable colloidal TiO₂ suspension in pure water. In this method, a transparent TiO₂ aqueous solution can be obtained within a few minutes. SEM analysis in Fig. 1 revealed that the average size of the nanoparticles was about 20 – 40 nm. The variation in size, however, had little influence in the resulting photodegradation rate of organic dye under the given condition. Instead, the photodegradation rate was related to the number of colloidal TiO₂ particles in the aqueous solution which increased in proportion to the ablation time as shown in Fig. 1. As the TiO₂ particle density increased further, however, the photoactivity was measured to be gradually reduced due to the formation of TiO₂ aggregates. Our results confirmed that well-dispersed small TiO₂ nanoparticles of about a few tens nm can be readily formed by laser ablation within only a few minutes and can be used as highly efficient photocatalysts for photocatalytic remediation of water [3].

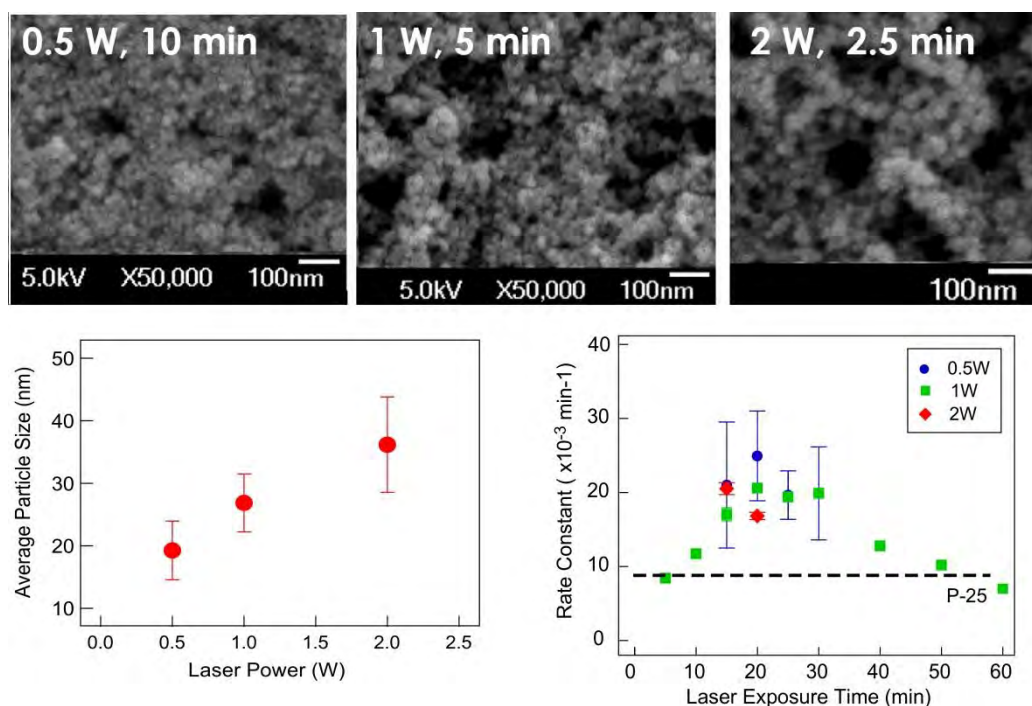


Figure 47 SEM images of TiO₂ nanoparticles prepared at different laser powers and the average size plotted against the laser power. Also shown in graph is the comparison of their photocatalytic activities prepared at different laser time and powers.

[1] A. Nath, S. S. Laha and A. Khare, Appl. Surf. Sci., 257, 3118 (2011).

[2] M. Zimbone, M.A. Buccheri, G. Cacciato, R. Sanz, G. Rappazzo, S. Boninelli, R. Reitano, L. Romano, V. Privitera and M.G. Grimaldi, Appl. Catal., B, 165, 487 (2015).

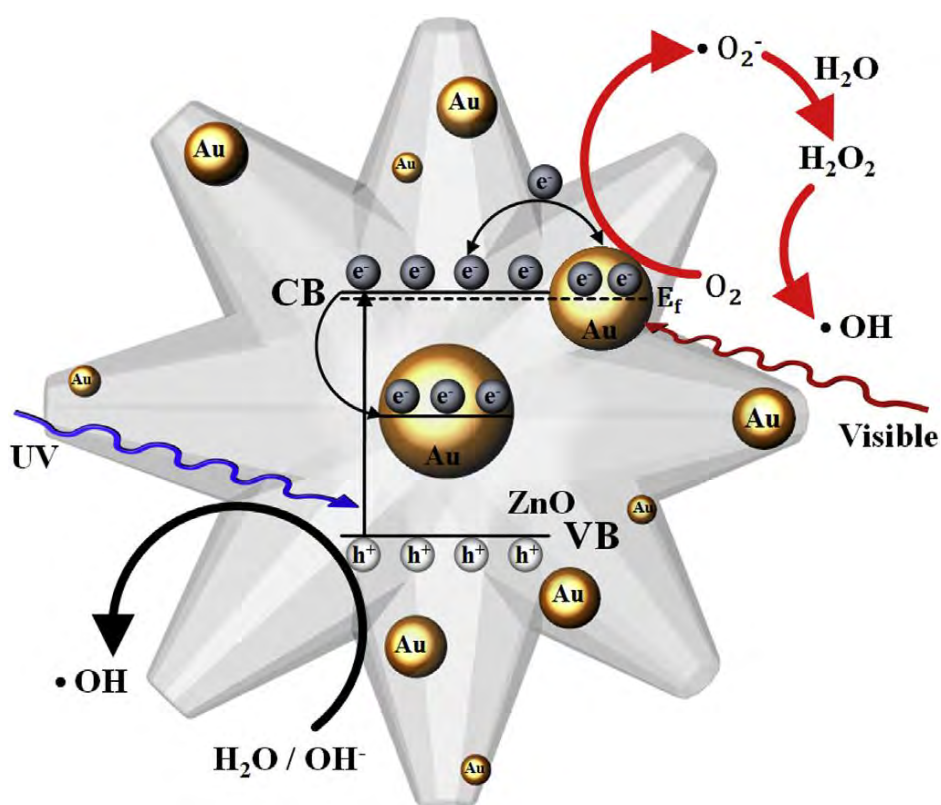
Improved photocatalytic activity of Au-doped Au@ZnO core-shell flower shaped nanocomposites

Seung Heon Lee^a, Hyeon Jin Jung^a, Ravindranadh Koutavarapu^a, Seulki Lee^a, Myong Yong Choi^{a,*}

^a Department of Chemistry (BK21+) and Research Institute of Natural Science, Gyeongsang National University, Jinju, 52828, Republic of Korea

*E-mail mychoi@gnu.ac.kr

We introduce a simple and low-cost three-step hydrothermal and pulsed laser ablation technique for the fabrication of flower-like pure ZnO nanostructures, Au@ZnO core-shell nanocomposites, and Au@ZnO/Au core-shell nanocomposites doped with various concentrations (5, 10, and 15 wt%) of Au nanoparticles without using surfactants or catalysts to enhance the catalytic performance of ZnO under UV-visible irradiation. The decoration of Au nanoparticles on the surface of ZnO promoted the absorption of visible light due to the surface plasmon resonance of Au. Further, we evaluated the photocatalytic performance of the nanocomposites in the degradation of methylene blue (MB). Our findings revealed that the Au@ZnO/Au core-shell nanocomposites with 5 wt% of doped Au NPs demonstrated the highest photocatalytic activity. In addition, radical-scavenging experiments were conducted to determine the main reactive species formed in the reaction mixture, and accordingly, a plausible photocatalytic reaction mechanism for the enhanced photodegradation of MB is presented.



Scheme 1. Proposed reaction mechanism for enhanced photocatalytic activity of the Au@ZnO/Au nanocomposites.

- [1] S.G. Kumar, K.S.R.K. Rao, Comparison of modification strategies towards enhanced charge carrier separation and photocatalytic degradation activity of metal oxide semiconductors (TiO₂, WO₃ and ZnO), *Appl. Surf. Sci.* 391, 124-148, (2017).
- [2] V. Ramasamy, C. Anandan, G. Murugadoss, Synthesis and characterization of ZnS/ZnO/CdS nanocomposites, *Mater. Sci. Semicond. Process.* 16, 1759-1764, (2013).
- [3] Y. Tan, Y. Zhang, L. Kong, L. Kang, F. Ran, Nano-Au@PANI core-shell nanoparticles via in-situ polymerization as electrode for supercapacitor, *J. Alloy. Compd.* 722, 1-7, (2017).

Synthesis and characterization of black TiO₂ nanoparticles by pulsed laser ablation in liquid for photocatalysis

V.A.Zuñiga-Ibarra¹, S. Shaji^{1,2, #}, B. Krishnan^{1,2}, S. Sepulveda-Guzman^{1,2} and D.A.Avellaneda¹

1- Universidad Autónoma de Nuevo León, Facultad de Ingeniería Mecánica y Eléctrica, San Nicolás de los Garza, Nuevo León, México, 66455.

2- Universidad Autónoma de Nuevo León - Centro de Innovación, Investigación y Desarrollo de Ingeniería y Tecnología (CIIDIT), Apodaca, Nuevo León, México, 66600

E-mail: sshajis@yahoo.com, sadasivan.shaji@uanl.edu.mx

Black titanium dioxide (TiO₂) is the titanium oxide nanomaterial with engineered crystalline disorder / defects with presence of sub-oxides of titanium. Black TiO₂ nanoparticles produced by different methods showed enhanced photocatalytic activity under visible light than ordinary TiO₂ nanoparticles (NPs) [1, 2]. Pulsed laser ablation in liquid (PLAL) is a promising technique for synthesizing nanostructures due to its simplicity, less usage of toxic reagents and absence of costly vacuum systems [3]. In the present study, photocatalytic activity of black TiO₂ NPs synthesized by PLAL is examined. Nanoparticles of black TiO₂ were prepared by pulsed laser ablation in liquid technique by ablating TiO₂ (black) target in liquid environment using an Nd:YAG laser (532 and 1064nm, 10 ns, 10 Hz) in different solvents. Morphology of the as synthesized particles was characterized by transmission electron microscopy (TEM) and scanning electron microscopy (SEM) where the crystalline structure of the particles was determined by selected area electron diffraction (SAED). Raman analysis and X-ray photoelectron spectroscopy (XPS) were employed to identify structure and chemical states of the NPs respectively. Photocatalytic activity of these NPs was evaluated by degradation of methylene blue under visible light irradiation. Results of the morphology, structure, optical and photo catalytic properties of black TiO₂ nanomaterials are reported in this study.

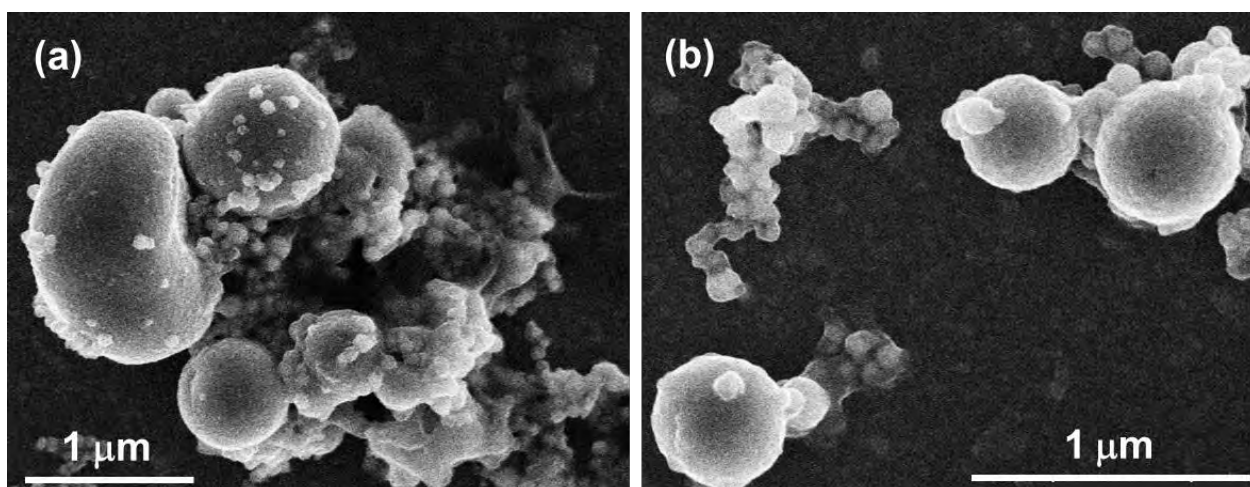


Figure 48. SEM Micrographs of black TiO₂ NPs synthesized by PLAL in Isopropyl alcohol.

References

- [1] Mengkun Tian, Masoud Mahjouri-Samani, Gyula Eres, Structure and Formation Mechanism of Black TiO₂ Nanoparticles, *ACS Nano*, vol. 9, pp. 10482-10488, (2015).
- [2] Xing Chen, Dongxu Zhao, Kewei Liu, Laser-Modified Black Titanium Oxide Nanospheres and their photocatalytic activities under Visible light, *ACS Appl. Mater. Interfaces*, vol. 7, pp 16070–16077, (2015)
- [3] G.W. Yang, Laser ablation in liquids, *Progress in Materials Science*, vol. 52, pp. 648-698, (2007).

Laser Ablation in Liquids Induced Ni/rGO Catalysts with Ultrahigh Electrocatalytic Activity and Stability in Methanol Oxidation

Hongmei Sun,^{1,2} Yixing Ye,¹ Jun Liu,^{*1} Zhenfei Tian,¹ Yunyu Cai,¹ Pengfei Li¹, Changhai Liang^{* 1,2}

1-Key Laboratory of Materials Physics and Anhui Key Laboratory of Nanomaterials and Nanotechnology, Institute of Solid State Physics, Hefei Institutes of Physical Science, Chinese Academy of Sciences, Shushanhu Road 350, Hefei 230031, China.

*2-Department of Materials Science and Engineering, University of Science and Technology of China, Jinzhai Road 96, Hefei, 230026, China
Jun Liu: jliu@issp.ac.cn*

Achieved of highly-active and durable nickel (Ni)-based catalysts for methanol oxidation reaction (MOR) to replace commercial platinum/carbon (Pt/C) is always full of challenge [1-3]. To find an efficient strategy to obtain ultrafine Ni nanoparticles (NPs) with the mostly exposed active sites and keep a high stability against severe aggregation is significant to acquire optimal Ni-based catalysts for MOR. By combination of laser ablation in liquids (LAL) and in situ reducing process, pure Ni nanoparticles with ultrafine size (1.5-3.6 nm) embedded in reduced graphene oxides (rGO) were synthesized. Such kind of Ni/rGO composite catalysts present ultrahigh catalytic activity (1600 mA/mg) and excellent stability (1020 mA/mg retained after 1000 cycles), which is better than that of previously reported Ni-based non-platinum catalysts and commercial Pt/C catalysts. These excellent electrochemical performance should be ascribed to the fine particle size and uniform dispersion of Ni NPs, as well as the efficient charge transfer and strong interfacial contact between rGO and Ni NPs.

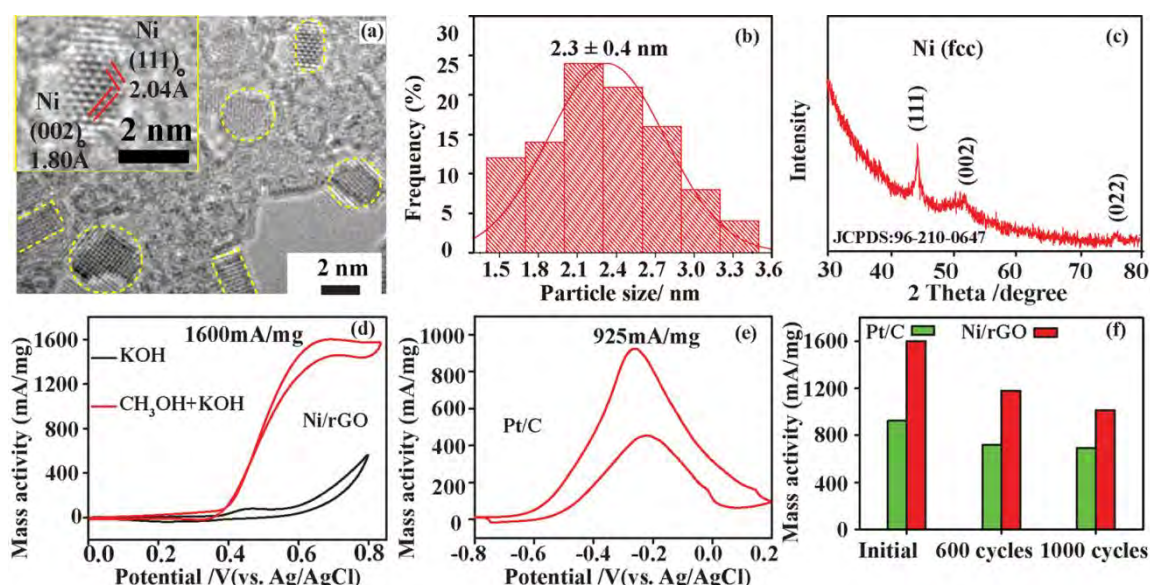


Figure 1 (a-c) HRTEM image, size distribution histogram and XRD pattern of Ni/rGO catalysts, respectively. (d) CV curves of the Ni/rGO catalysts commercial Pt/C catalysts in 1 M KOH with/without 1 M CH₃OH at a scan rate of 50 mV/s; (e) CV curves of the in 1 M KOH with 1 M CH₃OH at a scan rate of 50 mV/s; (f) Catalytic mass activity of Ni/rGO catalysts and commercial Pt/C catalysts at different cycles.

- [1] L. Y. Wang, G. G. Zhang, Y. Liu, W. F. Li, W. Lu, H. T. Huang, Facile synthesis of a mechanically robust and highly porous NiO film with excellent electrocatalytic activity towards methanol oxidation, *Nanoscale*, 8, 11256-11263, (2016).
 [2] A. A. Shaha, N. Yasmeena, G. Rahmana, S. Bilal, High Electrocatalytic Behaviour of Ni Impregnated Conducting Polymer Coated Platinum and Graphite Electrodes for Electrooxidation of Methanol, *Electrochimica Acta*, 224, 468-474, (2017).
 [3] H. Zhu, J. T. Wang, X. L. Liu, X. M. Zhu, Three-dimensional porous graphene supported Ni nanoparticles with enhanced catalytic performance for Methanol electrooxidation, *International Journal of Hydrogen Energy*, 42, 11206-11214, (2017).

Plasmon sensing properties of laser prepared noble metal colloids

Marcello Condorelli¹, Giuseppe Compagnini¹, Luisa D'Urso¹, Orazio Puglisi¹, Enza Fazio²

1- Dipartimento di Scienze Chimiche, Università di Catania – Viale A.Doria 6 – Catania 95125 (Italy)

2- Dip.to di Scienze Matematiche e Informatiche, Scienze Fisiche e Scienze della Terra Università di Messina - Messina, Italy

Main author email address: marselo88ct@gmail.com

In advanced sensing applications, plasmon resonances induced by metal nanostructures serve as sensitive probes to detect local variations in the surrounding environment at the molecular level. A typical example is given by the variation of the plasmon resonance position as a function of the refractive index, surrounding a nanoparticle and induced by molecular adsorption. For this reason nanoplasmonic sensing is emerging as a simple and extremely sensitive strategy for real-time detection of several chemical interactions[1].

In this frame, laser produced or modified metal nanoparticle colloids (Laser Ablation in Liquids, LAL or Laser Modification in liquids LML) can be considered an interesting starting point for developing new plasmonic materials, taking advantages from their peculiarities such as purity, electroaffinity and versatility[2,3].

In this contribution we intend to discuss about the plasmon sensing features of as prepared LAL silver and gold colloids. Plasmon sensing has been tested by evaluating the plasmon resonance shift in liquids with different refractive indices as shown in the figure.

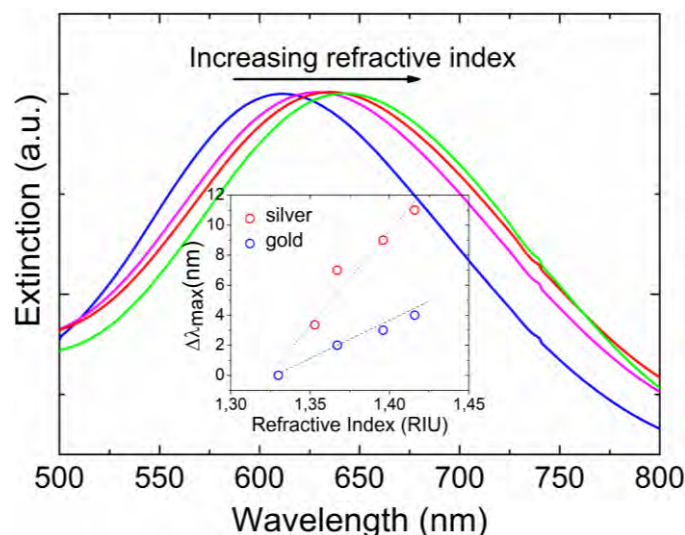


Figure 49 Extinction spectra of noble metal nanoparticles in different solution of sucrose with varying refractive index.

As the intrinsic refractive index (n) of the dispersion increases, the dipole plasmon resonance position redshifts with different efficiencies, depending on the overall colloidal properties. The same figure reports this shift ($\Delta\lambda_{\max}$) as a function of n for LAL produced silver and gold colloids and evidences their relative sensitivity. We have extended this study to different nanostructures composed by pure noble metals and their alloys as well as to differently shaped particles, thus opening applications in the field of low cost chemical-biological refractive index sensors[4].

- [1] L.Guo, J.A.Jackman, H.H.Yang, P.Chen, N. J Cho, D.H.Kim, Strategies for enhancing the sensitivity of plasmonic nanosensors, *Nano Today*, vol. 10, pp. 213–239 (2015)
- [2] S.Barcikowski, G.Compagnini, Advanced nanoparticle generation and excitation by lasers in liquids, *Phys.Chem. Chem. Phys.* vol.15, pp.3022–3026 (2013)
- [3] D.Zhang, B.Gökce, S.Barcikowski, Laser Synthesis and Processing of Colloids: Fundamentals and Applications, *Chem.Rev.*, vol.117, pp.3990–4103 (2017)
- [4] D. E. Charles, D. Aherne, M. Gara, D. M. Ledwith, Y. K. Gun'ko, J. M. Kelly, W. J. Blau, M. E. Brennan-Fournet, Versatile solution phase triangular silver nanoplates for highly sensitive plasmon resonance sensing, *ACS Nano*, vol. 4, pp. 55–64, (2010).

Laser fabrication and temperature dependent upconversion properties of $\text{Gd}_2\text{O}_3:\text{Yb}^{3+}, \text{Ho}^{3+}$ nanoparticles

Dihu Chen¹, Zhen Liu¹, Huawei Deng¹, Aixiang Wei²

1- School of Electronics and Information Technology, Sun Yat-sen University, Guangzhou 50275 P.R. China

2- School of Materials and Energy, Guangdong University of Technology, Guangzhou 510275 P.R. China

Main author email address: stscdh@mail.sysu.edu.cn

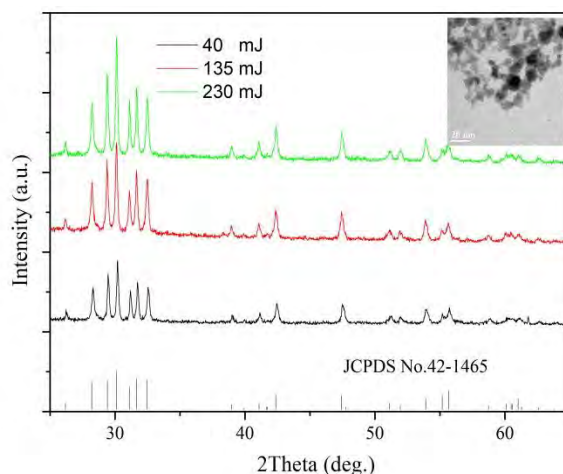


Figure 50 XRD patterns of $\text{Gd}_2\text{O}_3:\text{Yb}^{3+}, \text{Ho}^{3+}$ nanoparticles with different laser ablated power. Inset is the TEM images of $\text{Gd}_2\text{O}_3:\text{Yb}^{3+}, \text{Ho}^{3+}$ ablated at 135 mJ laser power.

Rare-earth doped materials have long played an important role in the development of color display, light-emitting displays, bio-imaging, temperature sensor applications [1]. In previous literatures, rare-earth doped nanocrystals have been proved can be efficiently synthesized via pulsed laser ablation in water, which has advantages of ligand-free and environmental friendly [2,3]. Here, we report the structural and morphological properties of $\text{Yb}^{3+}, \text{Ho}^{3+}$ co-doped Gd_2O_3 nanoparticles prepared by pulsed laser ablation in water at different irradiated laser energy varied from 40 mJ to 230 mJ. The structural properties were characterized by X-Ray diffraction, and the results confirm that the as-synthesized samples are all crystallized with monoclinic structure. Moreover, the morphologies of these samples revealed by transmission electron microscope suggest that high pulsed laser power result in the emergence of bigger nanoparticles with size over 20 nm. Additionally, the upconversion properties of synthesized $\text{Yb}^{3+}, \text{Ho}^{3+}$ codoped Gd_2O_3 nanoparticles excited by 980 nm laser was also investigated. The possible mechanism of upconversion was discussed through energy level diagram and the pumping power dependent upconversion emission intensity. The temperature dependence of upconversion properties of $\text{Yb}^{3+}, \text{Ho}^{3+}$ co-doped Gd_2O_3 nanoparticles ablated at 135 mJ laser power were also investigated in the temperature range from 130 K to 290 K. These results show that pulsed laser ablation in liquid is a facile method for fabrication of monoclinic $\text{Yb}^{3+}, \text{Ho}^{3+}$ co-doped Gd_2O_3 nanoparticles and the synthesized $\text{Yb}^{3+}, \text{Ho}^{3+}$ co-doped Gd_2O_3 nanoparticles via this method can be an excellent candidate for non-contact temperature sensing material.

[1] Liu Z, Jiang G, Wang R, Temperature and concentration effects on upconversion photoluminescence properties of Ho^{3+} , and Yb^{3+} codoped $0.67\text{Pb}(\text{Mg}_{1/3}\text{Nb}_{2/3})\text{O}_3-0.33\text{PbTiO}_3$, multifunctional ceramics, *Ceramics International*, 42(9), 11309-11313, (2016).

[2] Luo N, Tian X, Yang C, Ligand-free gadolinium oxide for in vivo T1-weighted magnetic resonance imaging, *Physical Chemistry Chemical Physics*, 15(29), 12235-12240, (2013)

[3] Luo N, Yang C, Tian X M, et al. A general top-down approach to synthesize rare earth doped- Gd_2O_3 nanocrystals as dual-modal contrast agents, *Journal of Materials Chemistry B*, 2(35):5891-5897, (2014)

Laser-induced Au Nanoparticles Encapsulated in Ultrathin Carbon Shells as Excellent Bifunctional Electrocatalysts

Chao Zhang^{1,2}, Jun Liu¹, Yixing Ye¹, Yunyu Cai¹, Changhao Liang^{1,2*}

1-Key Laboratory of Materials Physics and Anhui Key Laboratory of Nanomaterials and Nanotechnology, Institute of Solid State Physics, Hefei Institutes of Physical Science, Chinese Academy of Sciences, Hefei 230031, China

2-Department of Materials Science and Engineering, University of Science and Technology of China, Jinzhai Road 96, Hefei, 230026, China

Chao Zhang: zc1992@mail.ustc.edu.cn

Carbon encapsulation is a prevailing strategy to enhance the electrocatalytic activity and stability of metal nanoparticles [1-3]. Herein, we prepare Au nanoparticles (NPs) encapsulated in ultrafine carbon shells by laser ablation of Au target in acetone, without addition of any other chemical reagents or subsequent heat treatment. Importantly, the carbon shells not only enhance the electrocatalytic activity, but also prevent the degeneration of core Au NPs in the harsh electrolytes. Such Au@C NPs exhibited excellent catalytic activity toward oxygen reduction reaction (ORR) with an onset potential of 0.98 V and a half-wave potential of 0.87 V, which is even better than that of commercial Pt/C. Meanwhile, a remarkable hydrogen evolution reaction (HER) catalytic activity was also observed with a low onset potential of 100 mV and an overpotential of only 170 mV at a current density of 10 mA cm⁻² in acidic media. Moreover, Au@C catalysts present superior stability and high activity for 3000 CV cycles for ORR in 0.1 M KOH and at least 10 h for HER in 0.5 M H₂SO₄. This work demonstrated that Au@C NPs with special core-shell structure could be served as an ORR and HER electrocatalysts for fuel cells and water splitting.

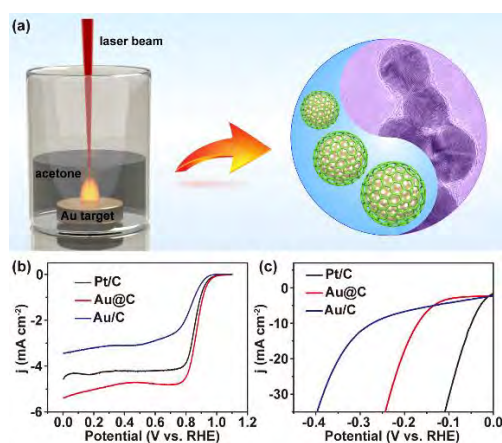


Figure 1. (a) Illustration of the LAL technique, schematic and TEM images of the final products. (b) LSV curves of Pt/C, Au@C, Au/C in O₂-saturated 0.1 M KOH at a scan rate of 5 mV s⁻¹ with a rotation speed of 1600 rpm. (c) Polarization curves of Pt/C, Au@C and Au/C in 0.5 M H₂SO₄.

[1] H. M. Zhang, C. H. Liang, J. Liu, Z. F. Tian, G. S. Shao, The formation of onion-like carbon-encapsulated cobalt carbide core/shell nanoparticles by the laser ablation of metallic cobalt in acetone, *Carbon*, 55, 108-115 (2013).

[2] H. M. Zhang, J. Liu, Z. F. Tian, Y. Y. Ye, Y. Y. Cai, C. H. Liang, K. Terabe, A general strategy toward transition metal carbide/carbon core/shell nanospheres and their application for supercapacitor electrode, *Carbon*, 100, 590-599 (2016).

[3] D. H. Deng, L. Yu, X. Q. Chen, G. X. Wang, L. Jin, X. L. Pan, J. Deng, G. Q. Sun, X. H. Bao, Iron Encapsulated within Pod-like Carbon Nanotubes for Oxygen Reduction Reaction, *Angew. Chem. Int. Ed.*, 52, 371-375, (2013).

Possible mechanisms of bimetallic nanoparticle formation by laser co-ablation of liquid colloids

T. E. Itina¹, Z. Swiatkowska-Warkocka², S. Mottin¹, G.I. Tselikov³, A.A. Popov³, A.V. Kabashin³, and M. Wolny-Marszalek²

1- Laboratoire Hubert. Curien, UMR CNRS 5516, UJM/ Univ. Lyon, 18 rue B. Lauras, 42000 Saint-Etienne, France

2- Institute of Nuclear Physics Polish Academy of Sciences, PL-31342 Krakow, ul. Radzikowskiego 152, Poland

3- Laboratoire LP3, Université de la Méditerranée, Parc Scientifique et Technologique de Luminy, 13288, Marseille, France

tatiana.itina@univ-st-etienne.fr

Recently, bimetallic magneto-plasmonic nanoparticles (NPs) have found numerous applications, in particular as promising contrast agents suitable for bio-imaging and for cancer theranostics. To obtain these NPs with a desired size and morphology, we use laser ablation in liquids as one of the promising synthesis methods that are able not only to satisfy green photonics criteria but also provide ultra-pure and very small nanoparticles particularly suitable for the above cited biomedical applications.

Herein, NPs were produced from a mixture of colloidal solutions containing gold and either cobalt or iron nanoparticles in different proportions, which were then irradiated by a femtosecond laser (Figure 1a). As a result, different nanocomposites are obtained ranging from dumbbells to core-shells and alloys.

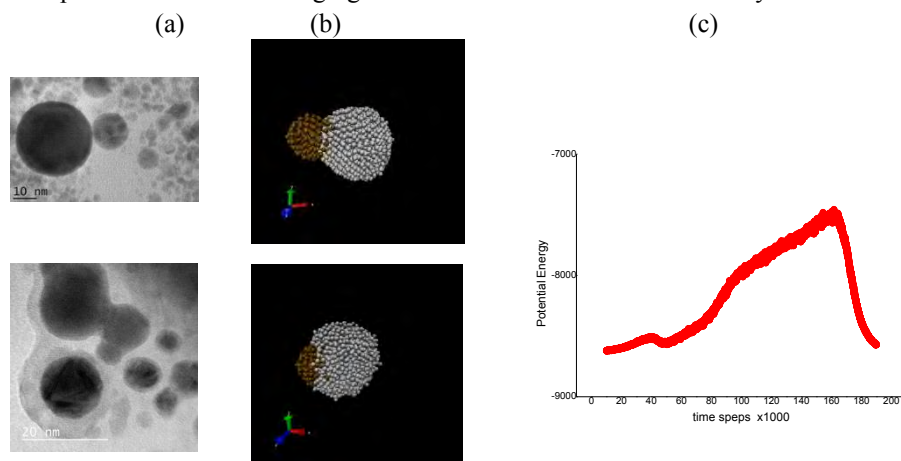


Figure 1 (a) Typical TEM images and related size distributions of laser-synthesized Au@Co (above) and Au@Fe₂O₃ core-shell (below) composites obtained by femtosecond pulsed laser irradiation in water. Here, laser repetition rate is 10kHz, $\lambda=1030$ nm, beam diameter 2.5mm, pulse energy 100 μ J, (b)–snapshots from MD simulations; (c) –calculated total potential energy time evolution, eV.

To analyse the possible formation mechanisms of different nanocomposites obtained by laser heating of the colloidal NP mixtures, we performed a series of molecular dynamics (MD) simulations (Figure 1b). In particular, for each nanomaterial, we varied such parameters as initial nanoparticle sizes and final NP temperature. Then, aggregation/coalescence kinetics was visualized and analysed from the energetic and topological points of view. As a result, several cases were revealed. On one hand, when the initial sizes and final temperatures of the participating nanoparticles were comparable, mostly dumbbells or alloys were formed (the latter were evidently found at higher temperatures). On the other hand, when one type of NPs were much more absorbing and larger than the other ones, core-shell formation was observed in the MD simulations. The corresponding energy time-evolution was monitored clearly demonstrating the possibility of four distinct stages in the core-shell formation process (Figure 1c): first, nanoparticles stick together forming an interface; the heating leads to the melting of one of the colliding particles and its atoms start covering the colder one. Finally, the hotter and larger NP completely “swallows” the colder and smaller one. We note that during this process the final surface area is considerably decreased, so that the potential energy is minimized. The obtained MD simulation results are used to analyse recent experimental findings and to predict the optimum experimental conditions required for either core-shells or alloys formation.

Solvent as a Carbon and Nitrogen Source for Graphitic Carbon and Nitrogen-doped Graphitic Carbon Shells on Nickel Nanoparticles

Seung Jun Lee, Hyeon Jin Jung, Seung Heon Lee, Myong Yong Choi*

*Department of Chemistry (BK21+) and Research Institute of Natural Science,
Gyeongsang National University, Jinju 52828, Republic of Korea*

*venus272@gnu.ac.kr, mychoi@gnu.ac.kr**

Graphitic carbon (GC) and nitrogen-doped graphitic carbon (NdGC) shells have been synthesized on Ni nanoparticles (NPs) from solvents used in pulsed-laser ablation in liquid (PLAL). The facile one-pot synthesis was achieved at room temperature and atmospheric pressure by ablating the pulsed laser onto a Ni plate submerged in a solvent, which acted as the carbon and nitrogen source for the GC and NdGC shells. The formation of GC and NdGC shell-encapsulated Ni (Ni@GC and Ni@NdGC) NPs was simply and selectively achieved by selecting a specific solvent (hexane and acetonitrile), respectively. Meanwhile, Ni and Ni@NiO NPs were fabricated by pulsed-laser ablation in methanol and deionized water, respectively.

The Ni NPs were characterized by X-ray diffraction, X-ray photoelectron spectroscopy, field-emission scanning electron microscopy, high-resolution transmission electron microscopy, fast Fourier transform analysis, selected area electron diffraction, and Fourier transform Raman spectroscopy. The Raman spectroscopic analysis revealed the graphitic shells were composed of well-organized graphitic structures. Furthermore, the potential applications of the NPs as chemical shields in acidic conditions and to supercapacitor devices were tested in strong acidic solutions and using cyclic voltammetry measurements, respectively. The plausible growth mechanisms of various kinds of Ni NPs prepared by PLAL in different solvents are discussed.

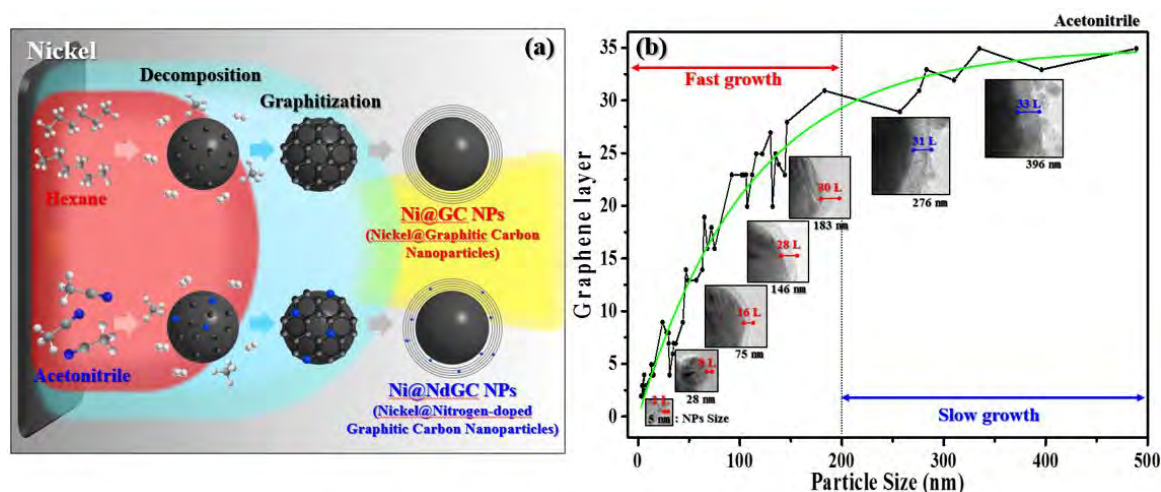


Figure 51 (a) Schematic view of the formation mechanism of the Ni@GC and Ni@NdGC NPs.
(b) Number of NdGC layers grown plotted as a function of the Ni NPs size.

- [1] C. Rehbock, V. Merk, L. Gamrad, R. Streubel, S. Barcikowski, Size control of laser-fabricated surfactant-free gold nanoparticles with highly diluted electrolytes and their subsequent bioconjugation, *Phys. Chem. Chem. Phys.*, 15, 3057-3067, (2013)
- [2] A. De Giacomo, M. Dell'Aglio, A. Santagata, R. Gaudiuso, O. De Pascale, P. Wagener, G. C. Messina, G. Compagnini, S. Barcikowski, Cavitation dynamics of laser ablation of bulk and wire-shaped metals in water during nanoparticles production, *Phys. Chem. Chem. Phys.*, 15, 3083-3092, (2013)

Laser-ablative fabrication of hybrid Se@Au, Si@Au/Ag nanoparticles via heterogeneous condensation

A. A. Ionin,¹ A. A. Rudenko,¹ I. N. Saraeva,¹ R. A. Khmelnskiy,¹
D. A. Zayarny,¹ N. V. Luong,¹ D. H. Tung,² P. V. Duong,² P. H. Minh,² S. I. Kudryashov^{1,3}

¹- Lebedev Physical Institute, Leninskiy prospect 53, 119991 Moscow, Russia

²- Institute of Physics, Vietnam Academy of Science and Technology, 18 Hoang Quoc Viet, Cau Giay, Hanoi, Vietnam

³- ITMO University, Kronverkskiy prospect 49, 197101 St. Petersburg, Russia

Main author email address: sikudr@lebedev.ru, sikudryashov@corp.ifmo.ru

Among different types of NPs, hybrid metal-dielectric/semiconductor structures are of a particular interest, as they combine the unique properties of both plasmonically-resonant metal particles and the polaritonically-resonant high-index dielectric or semiconductor nano- and (sub)microparticles, demonstrating both electrical and magnetic multipolar resonances, suitable for diverse advanced applications as basic elements for precise sensing devices, ultrafast light switches and non-linear optical elements with high tunability and sensitivity, etc. [20 – 24]. In our work we report the facile synthesis of colloidal Se@Au (Fig. 1), Si@Au, Si@Ag (Fig. 2) NPs via nanosecond IR ($\lambda = 1040$ nm, pulsewidth FWHM $\tau = 120$ ns, average pulse energy up to 1 mJ, repetition rate up to 80 kHz) through either laser plasma-mediated photoreduction of 0.03 mM aqueous solutions of chloroauric acid (HAuCl_4) and silver nitrate (AgNO_3) above the surface of the immersed silicon wafer, or direct ablation of bulk targets. The resulting NPs, prepared at different laser intensities were analysed in terms of their extinction coefficients in the form of hydrosols by UV-vis spectroscopy and as deposits by scanning electron microscopy and energy-dispersive X-ray spectroscopy.

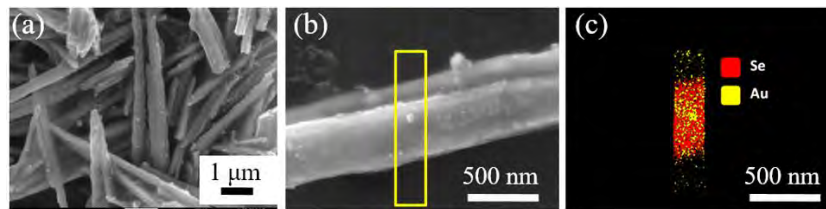


Figure 52 SEM-images of Au-decorated Se nanorods (a, b); the corresponding elemental composition by EDX spectroscopy (c).

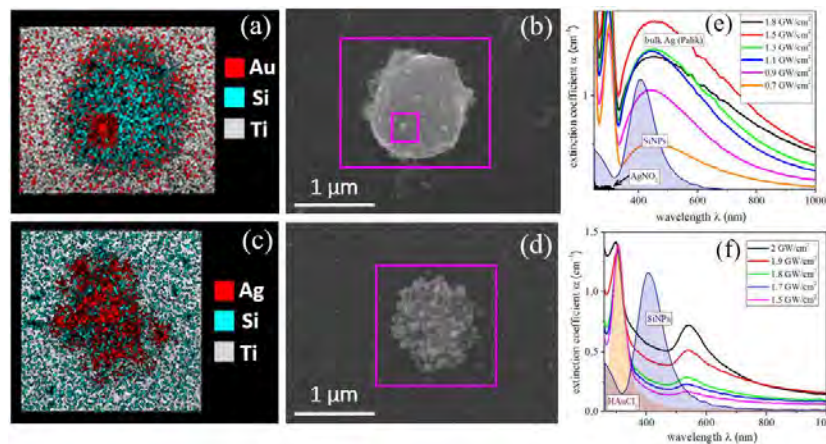


Figure 2 Dry deposits of Si@Au (a, b) and Si@Ag (c, d) NPs: SEM images (b, d) and the corresponding elemental analysis by EDX spectroscopy (a, c).

[1] R. Noskov, A. Krasnok, Y. Kivshar, Nonlinear metal–dielectric nanoantennas for light switching and routing, *New Journal of Physics*, vol. 14, 093005, (2012).

[2] D. Zuev, S. Makarov, I. Mukhin, V. Milichko, S. Starikov, I. Morozov, I. Shishkin, A. Krasnok, P. Belov, Fabrication of Hybrid Nanostructures via Nanoscale Laser-Induced Reshaping for Advanced Light Manipulation, *Advanced Materials*, vol. 28, pp. 3087–3093, (2016).

[3] C. R. Phipps, Jr., T. P. Turner, R. F. Harrison, G. W. York, W. Z. Osborne, G. K. Anderson, X. F. Corlis, L. C. Haynes, H. S. Steele, K. C. Spicochi, Impulse coupling to targets in vacuum by KrF, HF and CO₂ single-pulse lasers, *Journal of Applied Physics*, vol. 64, pp. 1083 – 1093, (1988).

Laser Fabrication of Organic Nanoparticle Colloids Having Strong Near-Infrared Absorption

T. Asahi, T. Himeda, R. Kihara

Graduate School of Science and Engineering, Ehime University, 3 Bunkyo, Matsuyama, Ehime, Japan

Main author email address: asahi.tsuyoshi.mh@ehime-u.ac.jp

Recently, nanoparticle colloids having strong absorption in a near infrared region have attracted considerable interest in the research fields of bio-imaging and phototherapy. In the present work, we demonstrate fabrication of biocompatible aqueous colloids of phthalocyanine and naphthalocyanine by nanosecond laser fragmentation in water [1], and discuss their potential applications to photothermal imaging of biological tissue and phototherapy.

The suspension of 5,9,14,18,23,27,32,36-Octabutoxy-2,3-naphthalocyanine (ONc: Fig. 1B) and Aluminum phthalocyanine chloride (AIClPc: Fig. 1C) microcrystalline powders (25 mwt%) in Pluronic[®] F127 aqueous solution (0.25 wt%) were exposed to ns Nd³⁺:YAG laser pulses (532 nm wavelength, 6 ns FWHM, 10 Hz repetition rate). Figure 2 shows the absorption spectra of the prepared nanoparticle colloids prepared at the laser fluence of 140 mJ/cm² for 20 min irradiation. The NP colloids exhibited an absorption peak at 880 nm for ONc and at 620 nm for AIClPc. The particle size obtained from DLS measurement was about 100 nm and the nanoparticle colloids were stably dispersed for longer than 1 week not only in pure water but also in phosphate buffered saline (PBS) solution. On the other hand, the colloids prepared by laser irradiation in pure water were not dispersed stably in PBS solution. The details of the effects of laser irradiation conditions and the concentration of Pluronic[®] F127 will be presented and the optimal preparation condition of the nanoparticle colloids will be discussed.

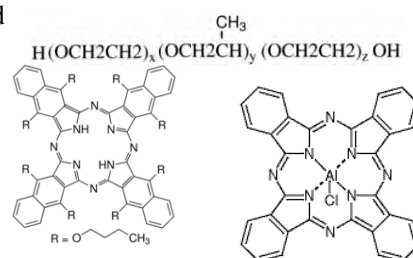


Fig. 1 Molecular structure of Pluronic[®] F127, ONc, and AIClPc

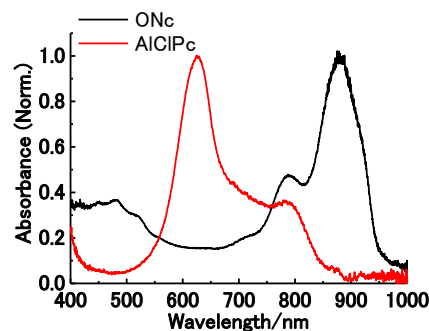


Fig. 2 Absorption spectra of prepared ONc and AIClPc NP colloid

[1] T. Asahi, T. Sugiyama, and H. Masuhara, Laser Fabrication and Spectroscopy of Organic Nanoparticles, *Acc. Chem. Res.*, 41, 1790-1798, (2008).

Optimizing the catalytic activity of Pulsed Laser Ablation Surface-Mediated Excitation and Reduction (PLASMER) synthesized metal-silica nanocomposites

Mallory G. John, Katharine Moore Tibbetts

Department of Chemistry, Virginia Commonwealth University, Richmond, VA 23284, USA

Main author email address: johnmg@vcu.edu

Preparation of metal, semiconductor, and oxide nanoparticles (NPs) via laser ablation has the advantages of a simple experimental setup and the generation of stable colloidal NPs without added surfactants [1-3]. Another laser-assisted approach to fabricate metal NPs involves photochemical reduction of metal ions by reactive species (e_{aq}^- , hydrogen and hydroxyl radicals) generated upon multiphoton absorption of solvent molecules [4-6]. This work combines these two approaches into one step where femtosecond laser pulses ablate a solid target immersed in an aqueous metal salt solution, which we call Pulsed Laser Ablation Surface-Mediated Excitation and Reduction (PLASMER). This talk presents the synthesis, characterization, and investigation of the catalytic activity of silica-Au NPs prepared via the PLASMER approach. We are able to generate silica-Au NPs by ablating a silicon wafer immersed in an aqueous $KAuCl_4$ solution, where Au(III) ions are reduced to Au clusters from the energetic species produced in the laser-Si wafer interaction. Figure 1 shows the HRTEM image (a) and HAADF-EDX spectrum (b) of a representative silica-Au NP sample synthesized via the PLASMER technique. To test the catalytic activity of the silica-Au NPs, we employ the common model reaction of 4-nitrophenol reduction to 4-aminophenol by $NABH_4$ [7,8]. The catalytic activity toward 4-nitrophenol reduction of the silica-Au NPs was improved by adjusting the precursor solution pH from 4.4 ($k_1 = 0.017 \text{ L m}^{-2} \text{ s}^{-1}$) to pH 7.7 ($k_1 = 0.030 \text{ L m}^{-2} \text{ s}^{-1}$) with added KOH. A similar trend was observed when Pd^{2+} was introduced into the precursor solution to generate silica-Pd/Au NPs; an increase in the catalytic rate constant accompanied an increase in precursor solution pH. The relationship between the bonding environment of the silica-metal NPs and their catalytic activity will be discussed. The PLASMER technique can be generalized to any metal precursor or target material to produce a wide range of metal inorganic oxide nanocomposites.

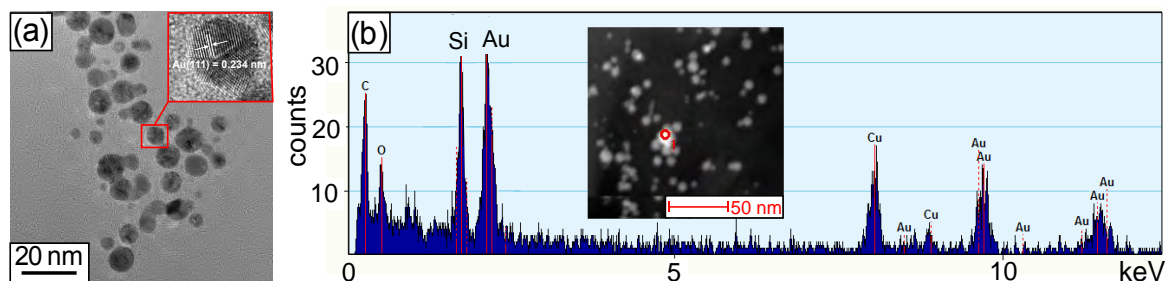


Figure 53: (a) HRTEM image of silica-Au NP sample; mean diameter $6.5 \pm 2.3 \text{ nm}$. Line spacing characteristic of Au(111) plane. (b) HAADF-EDX spectrum of representative silica-Au NP sample.

- [1] Zeng, H.; Du, X.-W.; Singh, S. C.; Kulinich, S. A.; Yang, S.; He, J.; Cai, W. Nanomaterials via Laser Ablation/Irradiation in Liquid: A Review. *Advanced Functional Materials* **2012**, *22*, 1333–1353.
- [2] Ermakov, V. A.; Jimenez-Villar, E.; Silva Filho, J. M. C. d.; Yassitepe, E.; Mogili, N. V. V.; Iikawa, F.; de Sá, G. F.; Cesar, C. L.; Marques, F. C. Size Control of Silver-Core/Silica-Shell Nanoparticles Fabricated by Laser-Ablation-Assisted Chemical Reduction. *Langmuir* **2017**, *33*, 2257–2262, PMID: 28186767.
- [3] Jiménez, E.; Abderrafi, K.; Abargues, R.; Valdés, J. L.; Martínez-Pastor, J. P. Laser-Ablation- Induced Synthesis of SiO_2 -Capped Noble Metal Nanoparticles in a Single Step. *Langmuir* **2010**, *26*, 7458–7463.
- [4] V. K. Meader, M. G. John, C. J. Rodrigues, and K. M. Tibbetts, “Roles of Free Electrons and H_2O_2 in the Optical Breakdown-Induced Photochemical Reduction of Aqueous $[AuCl_4]^-$ ” *J. Phys. Chem. A* **121**(36) 6742-6754 (2017)
- [5] K. M. Tibbetts, B. Tangeysh, J. H. Odhner, and R. J. Levis, “Elucidating Strong Field Photochemical Reduction Mechanisms of Aqueous $[AuCl_4]^-$: Kinetics of Multiphoton Photolysis and Radical-Mediated Reduction” *J. Phys. Chem. A* **120**(20) 3562-3569 (2016) [6] Odhner, J. H.; Tibbetts, K. M.; Tangeysh, B.; Wayland, B. B.; Levis, R. J. Mechanism of Improved Au Nanoparticle Size Distributions Using Simultaneous Spatial and Temporal Focus- ing for Femtosecond Laser Irradiation of Aqueous $KAuCl_4$. *The Journal of Physical Chemistry C* **2014**, *118*, 23986–23995.
- [7] Zhao, P.; Feng, X.; Huang, D.; Yang, G.; Astruc, D. Basic concepts and recent advances in nitrophenol reduction by gold- and other transition metal nanoparticles. *Coordination Chemistry Reviews* **2015**, *287*, 114 – 136.
- [8] Herves, P.; Perez-Lorenzo, M.; Liz-Marzan, L. M.; Dzubiella, J.; Lu, Y.; Ballau, M. Catalysis by metallic nanoparticles in aqueous solution: model reactions. *Chem. Soc. Rev.* **2012**, *41*, 5577–5587.

A Study on the Origin of Oxygen in Particles Synthesized by Laser Ablation in Liquids

S. Siebeneicher¹, G. Marzun¹, H. Bönnemann², C. Lehmann², B. Spliethoff², C. Weidenthaler² and S. Barcikowski¹

¹ Technical Chemistry I and Center for Nanointegration Duisburg-Essen (CENIDE),
University of Duisburg-Essen, Universitaetsstr. 7, 45141 Essen (Germany)

² Max-Planck-Institut für Kohlenforschung, Kaiser-Wilhelm-Platz 1, 45470 Mülheim an der Ruhr (Germany)

stephan.barcikowski@uni-due.de

Laser Synthesis of Colloids is a versatile route for nanoparticle generation. However, control over particle properties, like elemental composition, of less noble metals is difficult due to their sensitivity to oxidation under standard and especially under pulsed laser ablation conditions [1]. Several indications were found that oxygen from the decomposition of water might influence the formation of alloy nanoparticles due to oxidation [2]. To be able to tune the particle composition, a detailed understanding of the oxidation pathway is needed, as recent literature did not consider the fact of dissolved O₂ in solvents when analysing the oxidation of NPs [3]. Therefore, in this study the origin of oxygen is elucidated by differentiating between dissolved oxygen and molecular oxygen intrinsically available, e.g. in H₂O [4]. For this purpose, copper and PtCu alloy targets were processed in air-saturated (H₂O_{air}) and oxygen-free (H₂O_{Ar}) water as well as in air-saturated acetone using a Schlenk ablation chamber followed by characterizing the colloids under exclusion of ambient O₂ with XRD and EDX to show their elemental composition. The measurement

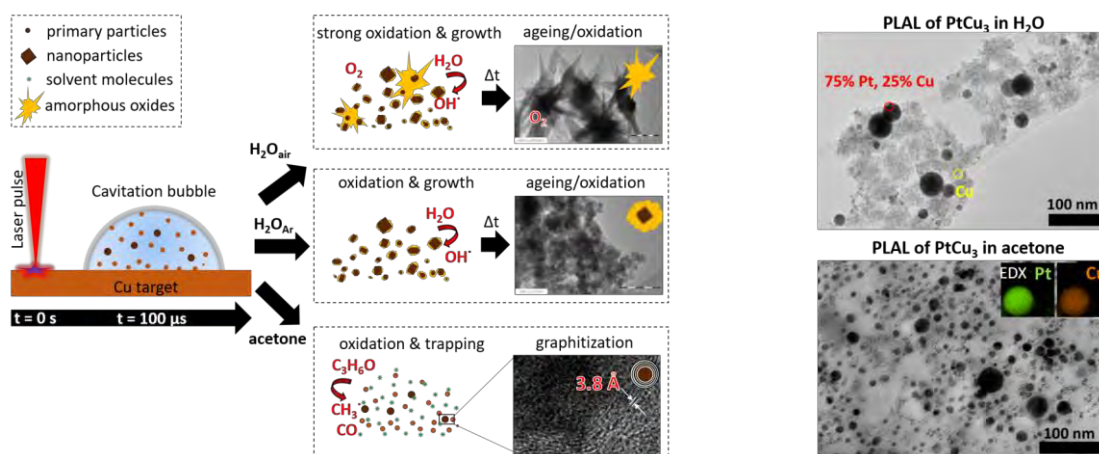


Figure 54 Scheme of the synthesis of Cu_xO_y and PtCu₃ nanoparticles in air-saturated (H₂O_{air}), oxygen-free (H₂O_{Ar}) water and acetone

data revealed that removing all dissolved O₂ from water is not able to inhibit oxidation of Cu, confirming water decomposition and thus the importance of bound oxygen in the reaction pathway. Similarly, using acetone will hinder oxidation more strongly even though the solubility of O₂ in it is higher than in water. Oxidation of Cu as a sensible compound in PtCu₃ also governs the nanoalloy formation which is why ablation of a PtCu₃ target only leads to a homogeneous nanoalloy if acetone is used. This behaviour can be explained by the formation of a graphitic shell that also stabilizes the NPs against oxidative aging. Our analyses illustrate that the decomposition of solvent during laser ablation in liquids is of major concern when it comes to predicting nanoparticle generation. This knowledge becomes essential when synthesizing mixed metal catalysts especially when alloying of noble and less noble metals is desired.

- [1] D. Zhang, B. Gökce, S. Barcikowski, Laser Synthesis and Processing of Colloids: Fundamentals and Applications, Chem. Rev., 117, 3990-4103, (2017).
 [2] G. Marzun, A. Levish, V. Mackert et al. Laser synthesis, structure and chemical properties of colloidal nickel-molybdenum nanoparticles for the substitution of noble metals in heterogeneous catalysis, J. Colloid Interface Sci., 489, 57-67, (2017).
 [3] K. Amikura, T. Kimura, M. Hamada et al., Copper oxide particles produced by laser ablation in water, Appl. Surf. Sci., 254, 6976- 6982, (2008).
 [4] G. Marzun, H. Bönnemann, C. Lehmann et al., Role of Dissolved and Molecular Oxygen on Cu and PtCu alloy Particle Structure during Laser Ablation Synthesis in Liquids, ChemPhysChem, 18, 1175-1184, (2017).

An Approach for High-Yield Submicrometer Spherical Particles by Pulsed Laser Melting in Liquid

Y. Ishikawa¹, H. Yoshihara², N. Koshizaki²

1- Nanomaterial Research Institute, National Institute of Advanced Industrial Science and Technology (AIST),
Central 5, 1-1-1 Higashi, Tsukuba, Ibaraki 305-8565, Japan

2- Graduate School of Engineering, Hokkaido University, Kita 13 Nishi 8, Kita-ku, Sapporo, Hokkaido 060-8628, Japan

ishikawa.yoshie@aist.go.jp

Mass production is an extremely important issue for material process engineering using a laser. Laser irradiation to a flowing suspension is one of the effective approach to solve this problem [1-2]. In contrast, we reported an automated batch system for pulsed laser melting in liquid (PLML) [3]. Batch system easily achieves high yield of submicrometer spherical particles by irradiation time extension. Batch system also has an advantage in spherical particle formation utilizing chemical reaction between particle and suspension media, such as carbide formation reaction of B particles by organic solvent and metal oxide particle reduction in organic solvent, because multi-pulse laser irradiation to respective particles is necessary to completely progress the chemical reaction. Therefore, we have attempted to study parameter effects on sphere formation efficiency in batch system.

Figure 1 (a) shows SEM images of Ag particles dispersed in deionized water irradiated by a Nd:YAG laser (pulse width: 5 ns, wavelength: 355 nm, and beam diameter: 6.5 mm) at $67 \text{ mJ cm}^{-2} \text{ pulse}^{-1}$ and 600 pulses in a cylindrical batch cell (basal plane diameter: 1.5 cm) agitated using a magnetic stirrer at 1 and 20 Hz. Obviously larger spherical particles were observed in 1 Hz irradiation than that in 20 Hz. Residual raw nanoparticles were frequently observed in particles obtained at 20 Hz. Cumulative frequency size distributions of spherical particle volume obtained at these two laser frequencies are depicted in Fig. 1 (b). Fraction of large particles in the obtained particles at 1 Hz is larger than that at 20 Hz.

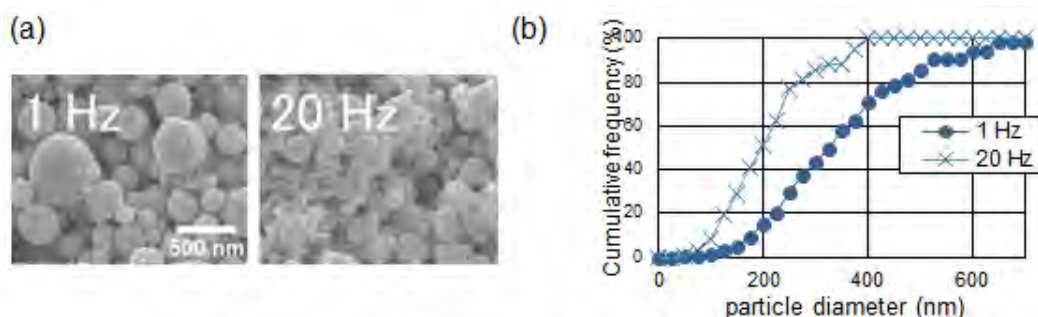


Figure 1 (a) SEM images of Ag particles obtained by 600-pulse laser irradiation, and (b) cumulative frequency size distributions of spherical particle volume obtained at 1 and 20 Hz

Long time interval between laser pulses at low pulse frequency brings long moving distance of particles by suspension stir, resulting in sufficient particle exchange in an irradiation space in suspension. In contrast, most particles in the irradiation space are continuously exposed by next pulses at high frequency, due to a short time interval between pulses. Thus, low pulse frequency irradiation is more efficient for high yield of spherical particles than that at high frequency with the same number of pulses. These results suggest stirring conditions of suspension affect spherical particle formation efficiency in batch irradiation system. Based on these results, we will propose and discuss a new approach on irradiation system at presentation.

[1] D.S. Zhang, M. Lau, S.W. Lu, S. Barcikowski, B. Gokce, Germanium Sub-Microspheres Synthesized by Picosecond Pulsed Laser Melting in Liquids: Educt Size Effects, *Sci. Rep.*, vol. 7, 40355, (2017).

[2] W. Philipp, S. Barcikowski, Laser fragmentation of organic microparticles into colloidal nanoparticles in a free liquid jet, *Appl. Phys. A*, vol. 101, pp. 432-439, (2010).

Influence of Picosecond Laser Irradiation on Synthesis of Spherical Particles by Pulsed Laser Melting in Liquid

S. Sakaki¹, K. Saitow^{2,3}, M. Sakamoto², H. Wada⁴, Z. Swiatkowska-Warkocka⁵,
Y. Ishikawa⁶, N. Koshizaki¹

1- Graduate School of Engineering, Hokkaido University, Sapporo, 060-8628, Japan

2- Department of Chemistry, Graduate School of Science, Hiroshima University, Higashi-hiroshima, 739-8526, Japan

3- Natural Science Center for Basic Research and Development (N-BARD), Hiroshima University, Higashi-hiroshima, 739-8526, Japan

4- School of Materials and Chemical Technology, Tokyo Institute of Technology, Yokohama, 226-8502, Japan

5- Institute of Nuclear Physics, Polish Academy of Sciences, PL-31342, Kraków, Poland

6- Nanomaterials Research Institute, National Institute of Advanced Industrial Science and Technology (AIST), Tsukuba, 305-8565, Japan

sakaki.shota@frontier.hokudai.ac.jp

Recently, submicrometer spherical particle formation by pulsed laser melting in liquid (PLML) has been reported [1]. In PLML, nanosecond laser is usually used for synthesis of submicrometer spherical particles. However, recent study indicated that the particles dissipate heat energy by cooling effect of surrounding liquid even during several tens of nanoseconds heating [2]. Therefore, picosecond laser irradiation would be effective in fabricating submicrometer spherical particles [3]. Here, submicrometer spherical particles were fabricated via both picosecond and nanosecond laser irradiation under similar conditions to study the effect of picosecond laser irradiation on the synthesis of the submicrometer spherical particles.

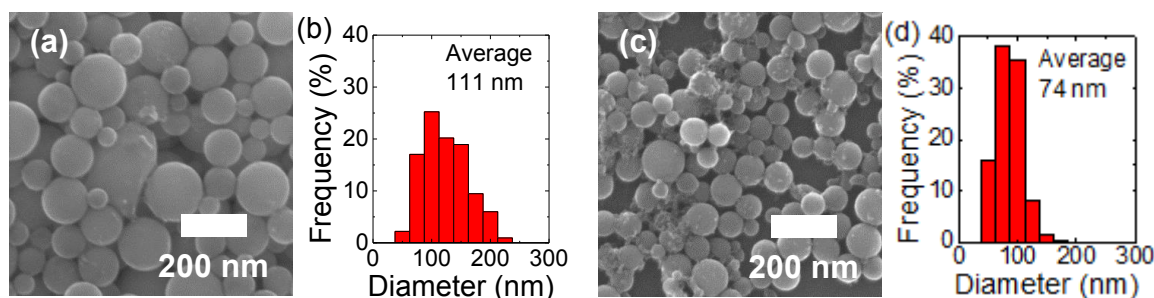


Figure 55 TiN particles irradiated (a) with a nanosecond laser and (c) with a picosecond laser at the laser fluence of $67 \text{ mJ pulse}^{-1} \text{ cm}^{-2}$ and the corresponding size distributions of TiN particles irradiated (b) with a nanosecond laser and (d) with a picosecond laser.

TiN raw particles ($< 50 \text{ nm}$) were dispersed in deionized water at a concentration of 0.2 g/L . A nanosecond laser (Continuum Powerlite Precision 8000, 532 nm wavelength, 7 ns pulse width) and a picosecond laser (Continuum PY61C-10, 532 nm wavelength, 40 ps pulse width) were used for laser irradiation with agitation. Figs. 1(a) and 1(c) shows SEM images of particles irradiated with a pulsed laser with different pulse widths at a laser fluence of $67 \text{ mJ pulse}^{-1} \text{ cm}^{-2}$. Based on these SEM images, the size distributions of the spherical particles irradiated with a pulsed laser were graphed by measuring the sizes [Figs. 1(b) and 1(d)]. The average diameter of the particles irradiated with the nanosecond laser was 111 nm and that of the particles irradiated with the picosecond laser was 74 nm . This size decrease which depends on pulse width would be derived from the thermal diffusion length during pulsed laser heating. The thermal diffusion length during nanosecond laser heating (233 nm) is larger than the particles obtained by nanosecond laser irradiation. Therefore, thermal energy diffuses from the surface to the entire particle during pulsed laser heating, resulting in homogeneous heating and melting of the particles. In contrast, the thermal diffusion length during picosecond laser heating (17.6 nm) is smaller than the particles obtained by picosecond laser irradiation. Therefore, particles are partially heated at the incident light side of the particle surface. The size of the obtained particles decreases with decreasing thermal diffusion length.

[1] Y. Ishikawa, Y. Shimizu, T. Sasaki, and N. Koshizaki, Boron Carbide Spherical Particles Encapsulated in Graphite Prepared by Pulsed Laser Irradiation of Boron in Liquid Medium, *Appl. Phys. Lett.* **91**, 161110, (2007).

[2] S. Sakaki, H. Ikenoue, T. Tsuji, Y. Ishikawa, and N. Koshizaki, Pulse-Width Dependence of the Cooling Effect on Sub-Micrometer ZnO Spherical Particle Formation by Pulsed-Laser Melting in a Liquid, *ChemPhysChem* **18**, 1101-1107, (2017).

[3] D. Zhang, M. Lau, S. Lu, S. Barcikowski, and B. Gökçe, Germanium Sub-Microspheres Synthesized by Picosecond Pulsed Laser Melting in Liquids: Educt Size Effects, *Sci. Rep.* **7**, 40355 (2017).

Influence of external magnetic field on the morphology of Au nanoparticles obtained by laser ablation in water

**G. A. Shafeev^{1,2}, I. I. Rakov¹, K. O. Ayyyzy³, G. N. Mikhailova⁴, A. V. Troitskii⁴,
L. K. Antonova⁴**

¹Wave Research Center of A.M. Prokhorov General Physics Institute of the Russian Academy of Sciences, 38, Vavilov street, 119991, Moscow Russian Federation

²National Research Nuclear University MEPhI (Moscow Engineering Physics Institute), 31, Kashirskoye highway, 115409, Moscow, Russian Federation

³Th E c fH gh P f E c “ c w fPh c T ch g ()” 9
Institutsky lane, 141700, Dolgoprudny, Moscow region, Russian Federation

⁴A.M. Prokhorov General Physics Institute of the Russian Academy of Sciences, 38, Vavilov street, 119991, Moscow, Russian Federation
ignat.rakov@gmail.com

Previously it was shown how the process of laser fragmentation of Au NPs was influenced by external magnetic field [1]. The fragmentation proceeds faster due to interaction of plasma of laser breakdown with magnetic field. In this communication the influence of permanent magnetic field up to 7 Tesla on optical properties and morphology of colloidal solutions of Au nanoparticles generated by laser ablation in liquid is experimentally studied in absence of laser radiation. It is established that external magnetic field affects the behavior of diamagnetic Au NPs in water, which leads to their agglomeration and formation of nanowires. This is confirmed by extinction spectra of the solution since the formation of nanowires is accompanied by appearance of longitudinal plasmon resonance located in the red and infrared domains of spectrum. TEM images analysis (Fig. 1) also confirms the presence of nanowires, since the aspect ratio varies with the initial colloid and the colloid that has been in the magnetic field. After the end of magnetic field action, Au NPs partially decompose into individual elongated nanoparticles. This process is associated with ferromagnetic properties presence of small size Au NPs. It should be noted ferromagnetic properties of Au NPs were reported earlier [2]. Second, special experimental parameters were found under which the highest concentration of elongated Au NPs in colloidal solution is achieved. In previous works such nanoparticles were generated with the use of beta-active substances or in external fields [3].

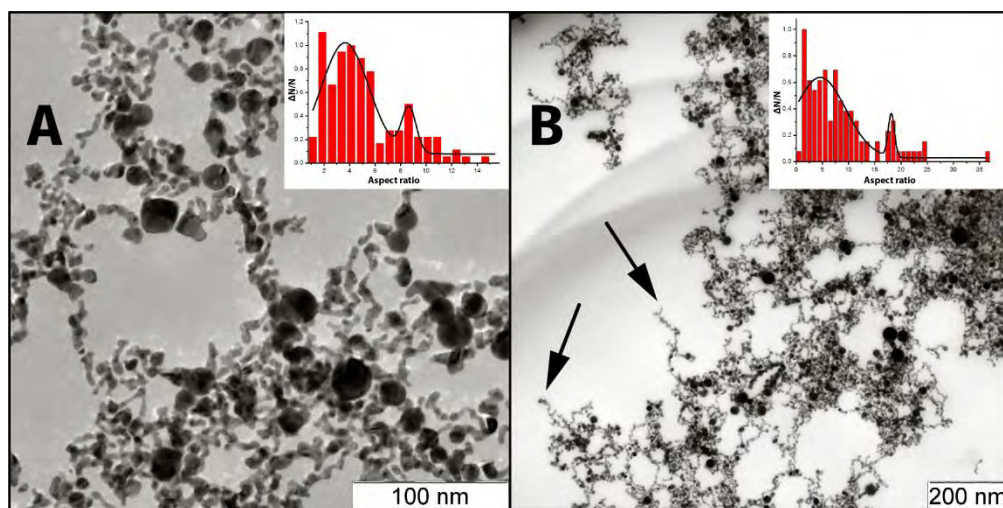


Fig. 1. TEM images of initial (A) Au NPs and Au NPs after being in 7 T external magnetic field (B). In the insets: aspect ratio of elongated Au NPs before (left) and after exposure to magnetic field.

Formation of Au nanowires is attributed to the interaction of the magnetic field with electrons that participate in the longitudinal plasmon resonance of elongated Au NPs, since the size distribution of spherical Au NPs is not affected by magnetic field.

[1] A. A. Serkov, I. I. Rakov, G. A. Shafeev et al., Influence of external magnetic field on laser-induced gold nanoparticles fragmentation, Applied Physics Letters, vol. 109, 053107, (2016)

[2] V. Tuboltsev, A. Savin, A. Pirojenko, J. Raisanen. Magnetism in Nanocrystalline Gold, ACS Nano, 7(8), pp 6691-6699, (2013)

[3] Serkov A. A. et al., Self-assembly of nanoparticles into nanowires under laser exposure in liquids, Chemical Physics Letters, vol. 623, 93-97, (2015).

Laser Assisted Formation of Immiscible Alloy Nanoparticles in Liquids

**N. Tarasenka¹, A. Nevar¹, V. Kiris¹, N. Tarasenko¹,
A. Nominé², H. Kabbara², J. Ghanbaja², M. Trad², T. Belmonte²**

1- B. I. Stepanov Institute of Physics, National Academy of Sciences of Belarus, Nezalezhnasti Ave. 68, 220072 Minsk, Belarus
2- Institut Jean Lamour – UMR 7198 CNRS – Université de Lorraine – Parc de Saurupt – F 54011 Nancy, France

natalie.tarasenka@dragon.bas-net.by

Alloying of normally immiscible metals (and elements in general) has gained a considerable interest in last decades due to valuable properties and potential applications of such alloys. Despite many experimental and theoretical researches carried out aiming to produce alloys of immiscible metals, the synthesis of immiscible alloys with the desirable homogeneous microstructure is still a challenge using conventional methods. Traditional methods for the production of alloys consist in mixing of liquid metals or sintering of metallic particles. Recently laser assisted technique based on the laser irradiation of colloidal nanoparticles (NPs) has been demonstrated as promising synthesis route for alloying of immiscible metals (AuFe, AuCo, and AuNi) [1] and fabrication of nanocomposites [2]. In this paper in order to create immiscible alloy system of homogeneous microstructure, a two step plasma-laser-assisted strategy is proposed. The technique is based on electrical discharge treatment of micropowders in liquids combined with post-discharge laser induced modification. The Ag–Cu, Si–Sn and Ge–Sn systems were selected to demonstrate the capabilities of the proposed technique. The experimental results showed that the developed technique is capable for preparation of immiscible alloys. The formation of alloyed nanocrystals was proved by the results of UV-Vis and Raman spectroscopy, EDX and HRTEM measurements (Figure 1).

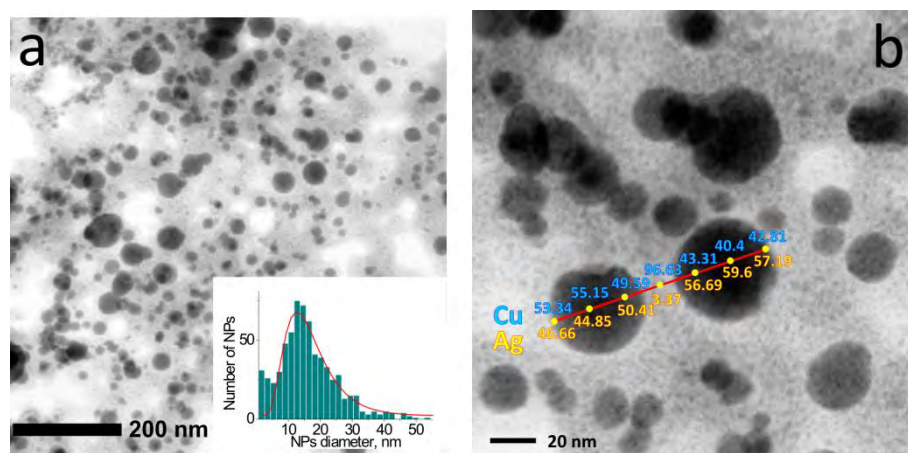


Figure 56 Results of analysis of the synthesized particles of Ag-Cu alloy: a – TEM image, b – The EDS scanning of 532 nm laser irradiated NPs along the selected direction (Ag L α , Cu K α) proving the composition homogeneity of the prepared particles.

It has been shown that alloyed particles are partially formed at the first plasma treatment stage. However, the particles have broad size distribution and non-uniform inner structure. Laser-induced processes resulted in narrowing of the particle size distribution with the average diameter of around 15 nm. The EDX mapping showed the uniform distribution of the elements in the particles indicative of alloyed NPs formation. We suggest that the formation of the metastable phase alloys occurs through the agglomeration of NPs, very fast heating, and fast cooling/solidification processes.

[1] Z. Swiatkowska-Warkocka, A. Pyatenko, F. Krok, et al. Synthesis of new metastable nanoalloys of immiscible metals with a pulse laser technique. *Sci Rep*, vol. 5, pp. 9849 - . (2015).

[2] A. Butsen, N. Tarasenko, N. Tarasenka, V. Pankov Preparation of Composite Nanoparticles by Laser Processing of the Mixture of Colloidal Solutions. *Physics, Chemistry and Applications of Nanostructures, Proceedings of International Conference Nanomeeting-2015*, World Scientific Publishing, Singapore, 287-290 (2015).

Comparison of Magnetite Nanoparticles Obtained by Pulsed Laser Ablation in Water and Air

A. Shabalina, I. Lapin, D. Goncharova, V. Svetlichnyi

Tomsk State University, Russia, Tomsk, Lenin av., 36, 634050

v_svetlichnyi@bk.ru

Among iron oxide phases, magnetite (Fe_3O_4) exhibit specific magnetic and other properties allowing its use in biomedical applications [1]. A crucial factor for these applications is the particles surface state. It is strongly affected by the synthetic pre-history of the material. Chemical methods of magnetite synthesis may lead to the contamination of the particles surface with the precursors or by-products of the chemical reaction. Among physical techniques of nanoparticles preparation, pulsed laser ablation (PLA) of metallic targets, may be distinguished by such advantages as low cost, simplicity, rapidity, and the possibility of obtaining stable nanoparticles colloids and powders without addition of surfactants and stabilizing agents [2]. In the present work nanoparticles of magnetite were obtained via PLA in water and in air and their structure and composition were investigated and compared.

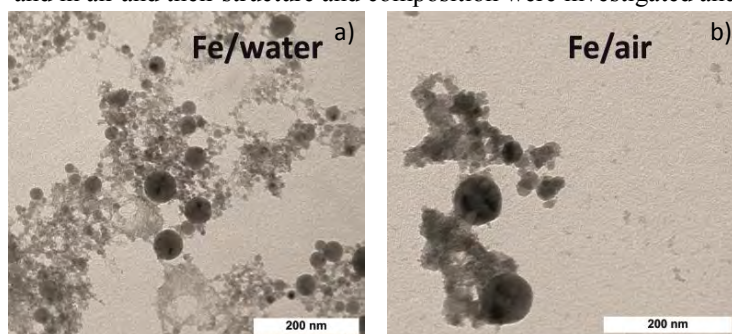


Figure 1 TEM-images of the Fe/water (a) and Fe/air (b) samples.

TEM images of the samples obtained are presented in Fig. 1. The majority of particles has the size below 10 nm, but there are larger particles fraction (around 100 nm). Particles from Fe/water sample form less dense agglomerates than those of Fe/air sample. Some XRD peaks of magnetite, maghemite and hematite overlap (Fig. 2a). It can be seen that Fe/water sample contains metallic iron (~0.5%).

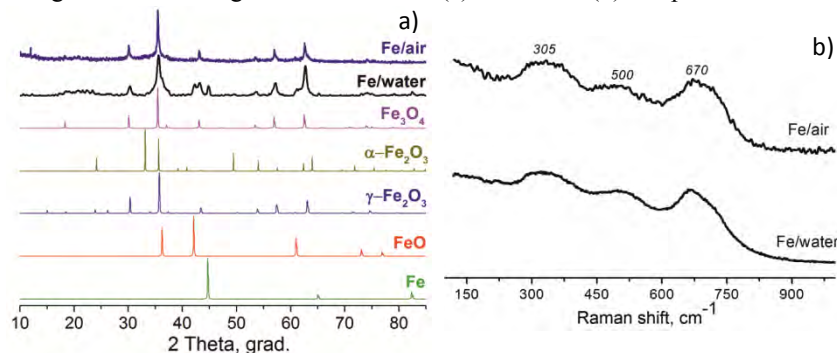


Figure 2 XRD patterns (a) and Raman spectra (b) of the Fe/water and Fe/air samples.

Raman spectroscopy is known to allow one to determine the phase composition of iron oxide sample. All the signals from Raman spectra for both Fe/air and Fe/water samples (Fig. 2b) belong to magnetite [3].

Pulsed laser ablation of metallic iron both in air and in water allows obtaining magnetite nanoparticles of 10 and around 100 nm. The samples from air and water slightly differ in composition and the tendency of particles to agglomeration. The

particles obtained do not contain additional molecules (stabilizers, surfactants) on their surface that is important for their application in biomedicine.

[1] W. Wu, C.Z. Jiang, V.A.L. Roy, Designed synthesis and surface engineering strategies of magnetic iron oxide nanoparticles for biomedical applications, *Nanoscale*, vol.8, pp. 19421-19474, (2016).

[2] D. Yang, Applications of Laser Ablation–Thin Film Deposition, *Nanomaterial Synthesis and Surface Modification (InTech)*, Chapter 11, (2016).

[3] O.N. Shebanova and P. Lazor, Raman spectroscopic study of magnetite (Fe_3O_4): a new assignment for the vibrational spectrum, *Journal of Solid State Chemistry*, vol. 174, pp. 424-430, (2003).

Structure of nanoparticles from colloids obtained by pulsed laser ablation of copper in a liquid

D. Goncharova, V. Svetlichnyi, I. Lapin

Tomsk State University, Russia, Tomsk, Lenin av., 36, 634050

dg_va@list.ru

From the time of the first synthesis of nanoparticles by pulsed laser ablation in liquids (PLAL), the technologies of “laser colloids” obtaining were optimized significantly. A huge number of nanostructures with different compositions and shapes were obtained [1]. However, to obtain stable colloids with specified characteristics, it is necessary to study the mechanism of PLAL, to investigate complex chemical reactions that occur between the target and the solvent during the laser excitation [2], and to take a look inside the subsequent process of the colloidal solution aging.

In this study, pulsed laser ablation of a metallic target of copper in various liquid media was carried out (Nd:YAG laser, 1064 nm, 20 Hz, 7 ns) similar to [3]. Water and ethanol were chosen as model solvents. Peroxidic (H_2O_2), alkaline (NaOH) and acidic (HNO_3) mediums were used to clarify the mechanism of synthesis. The copper system was chosen as the most complicated, since the oxidation of copper nanoparticles (NPs) may form both oxides of Cu^{+1} and Cu^{+2} . Moreover, one of the copper oxides can easily turn into another, which makes the study more difficult. Often there is no reproducibility under similar synthesis conditions.

Morphology, optical and electrokinetic characteristics of the obtained colloidal solutions were studied. Solutions were dried in order to investigate the particles obtained by the methods of SEM, XRD, and Raman spectroscopy. After that, obtained powders were again dispersed in water. In order to determine the influence of drying on the dispersions, optical and electrokinetic characteristics were determined again.

As an example, Figure 1 shows the absorption spectra of colloidal solutions, and TEM images of NPs prepared by copper PLA in various liquid media. Mechanisms of the formation of copper oxide NPs were established, the influence of drying and aging of the prepared nanoparticles were investigated.

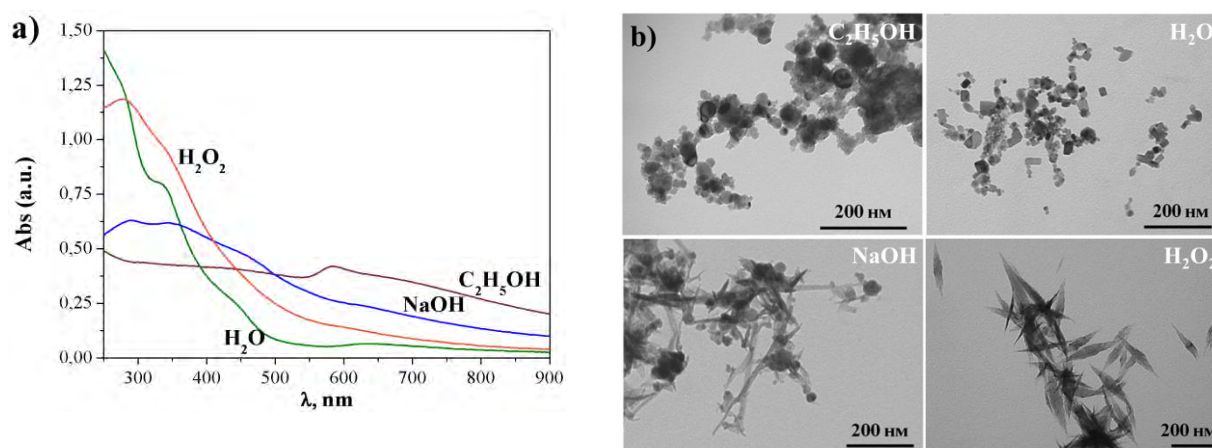


Figure 57 UV-vis absorption spectra (a), TEM images (b), NPs obtained by copper PLA in ethyl alcohol, water, NaOH and H_2O_2 .

The results obtained are important for understanding the chemical reactions of copper-based NPs occurring in a liquid, as well as for application of copper-containing PLAL dispersions in general.

- [1] V. Amendola and S. Barcikowski, Quarter-century of nanoparticle generation by lasers in liquids: Where are we now, and what's next?, *Journal of Colloid and Interface Science*, 489, 1-2, (2017).
 [2] H. Zeng, X.-W. Du, S. C. Singh, S. A. Kulinich, S. Yang, J. He and W. Cai, *Nanomaterials via Laser Ablation/Irradiation in Liquid: A Review*. *Advanced Functional Materials*, 22, 1333-1353, (2012).
 [3] D. A. Goncharova, I. N. Lapin and E. S. Savelyev, V. A. Svetlichnyi, Structure and properties of nanoparticles fabricated by laser ablation of bulk metal copper targets in water and ethanol, *Russian Physics Journal*, 60, 7, 1197-1205, (2017).

Scaling relationships for film-to-nanoparticles conversion during nanosecond laser ablation of silver films of variable thickness

A. Nastulyavichus¹, S. Kudryashov^{1,2}, N. Smirnov¹, A. Rudenko¹, D. Zayarny¹, A. Ionin¹

1- Lebedev Physical Institute, Leninskiy prospect 53, 119991 Moscow, Russia

2- ITMO University, Kronverkskiy prospect 49, 197101 St. Petersburg, Russia

email: ganuary_moon@mail.ru

Due to their unique properties, nanoparticles are used in various fields of science and technology, including such as nanophotonics and nanoplasmonics [1-3]. To date, one of the most simplest and high-performance methods for obtaining nanoparticles is the laser ablation [4]. The method is non-toxic and allows to obtain nanoparticles with given characteristics.

There are many studies on obtaining nanoparticles from bulk targets by the laser method in liquids. In the same work, laser ablation of thin silver films with various thicknesses in water was carried out in order to obtain colloids of nanoparticles with a given concentration. Silver thin films were produced by magnetron sputtering in an argon atmosphere on SiO₂ substrates. Laser ablation was performed with the use of an Yb³⁺-doped fiber laser HTFMark, Bulat (central wavelength $\lambda = 1064$ nm, pulsewidth FWHM $\tau = 120$ ns). Laser pulses with different pulse energies $E=0.2-0.4$ mJ, coming at $f = 20$ kHz, were focused by the objective of the galvanoscanner into a 32- μm wide ($1/e$ -diameter $\sigma_{1/e}$) spot on a wet sample surface and scanned across 10x20 mm² area with 33-lines/mm filling at the scan velocity $V = 40-250$ mm/s.

As a result, colloids of silver nanoparticles were obtained, whose average size is 18-30 nm. The colloidal solutions were investigated using a spectrophotometer in the UV-visible range. Deposited Ag particles were inspected by scanning electron microscopy (Figure 1). The transmittance spectra of the films of various thickness were used to determine the spectral position of the plasmon resonance, and the optical density in the resonance peak together with the mean size of nanoparticles.

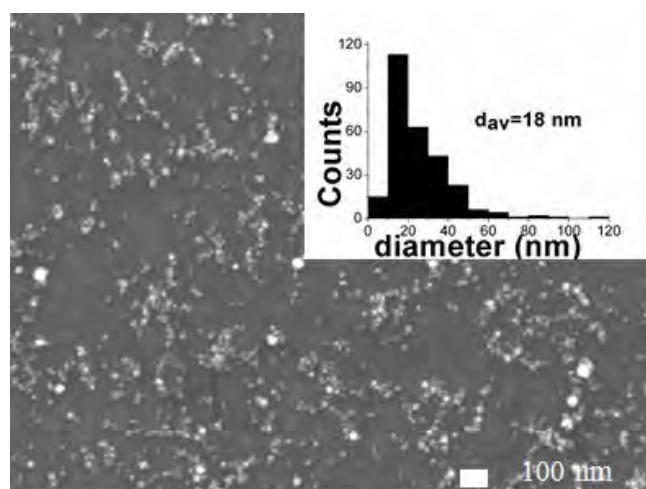


Figure 58 SEM-image of Ag nanoparticles on silicon substrate+ particle size distribution

- [1] X. Kong, Y. Ding, R. Yang, Z. Wang, Single-crystal nanorings formed by epitaxial self-coiling of polar nanobelts, *Science*, vol. 303, pp. 1348–1351, (2004).
- [2] R. Taylor, S. Coulombe, T. Otonari, P. Phelan, A. Gunawan, Small particles, big impacts: a review of the diverse applications of nanofluids, *Journal of Applied Physics*, vol. 113, 011301, (2013).
- [3] Y. Yin, R. Rioux, C. Erdonmez, S. Hughes, G. Somorjai, A. Alivisatos, Formation of hollow nanocrystals through the nanoscale Kirkendall effect, *Science*, vol. 304, pp. 711–714, (2004).
- [4] A. Ionin, A. Ivanova, R. Khmel'nitskii, Y. Klevkov, S. Kudryashov, N. Mel'nik, A. Nastulyavichus, A. Rudenko, I. Saraeva, N. Smirnov, D. Zayarny, A. Baranov, D. Kirilenko, P. Brunkov, A. Shakhmin, Milligram-per-second femtosecond laser production of Se nanoparticle inks and ink-jet printing of nanophotonic 2D-patterns, *Applied Surface Science*, vol. 436, pp. 662-669, (2018).

Photo-catalytic activity of ZnO nanostructures obtained by micromachining a high purity Zn target with a picosecond pulsed laser

**Luisa D'Urso¹, Salvatore Spadaro², Martina Bonsignore²,
Orazio Puglisi¹, Giuseppe Compagnini¹, Fortunato Neri², and Enza Fazio²**

¹ *Dip. di Scienze Chimiche, Università di Catania, Catania, Italy*

² *Dip. di Scienze Matematiche e Informatiche, Scienze Fisiche e Scienze della Terra (MIFT), Università di Messina, Messina, Italy*

ldurso@unict.it

Photocatalytic degradation of organic dyes was carried out using ZnO nanorods under UV light irradiation. In this work, zinc oxide (ZnO) and zinc oxide/metal (ZnO/Me=Au, Ag) nanocolloids were prepared by picosecond pulsed laser ablation (ps-PLA), using a Zn, Au and Ag metallic targets in water media at 80°C. [1] ZnO and metal nanocolloids were produced by separate ablation processes. The ablation of Zn and metal targets was made, at a typical laser power density of 2.0 W/cm², by a galvanometric scanner which enables step-and-scan target surface micromachining at 10 mm/sec scanning speed. This green and versatile tool allows the processing of the target with high precision and reliability, ensuring the formation of contaminant-free nanostructures and the absence of by-products. Metal decorated ZnO nanostructures were obtained by mixing zinc oxide and metal colloidal solutions, immediately after their production. For comparison, ZnO/Me nanostructures were grown at room temperature using both a picosecond and nanosecond pulsed laser source. An improvement of the photo-catalytic efficiency was observed in the presence of metal nanoparticles,[2] specially when ZnO sample was characterized by well defined nanorod structures.[3]

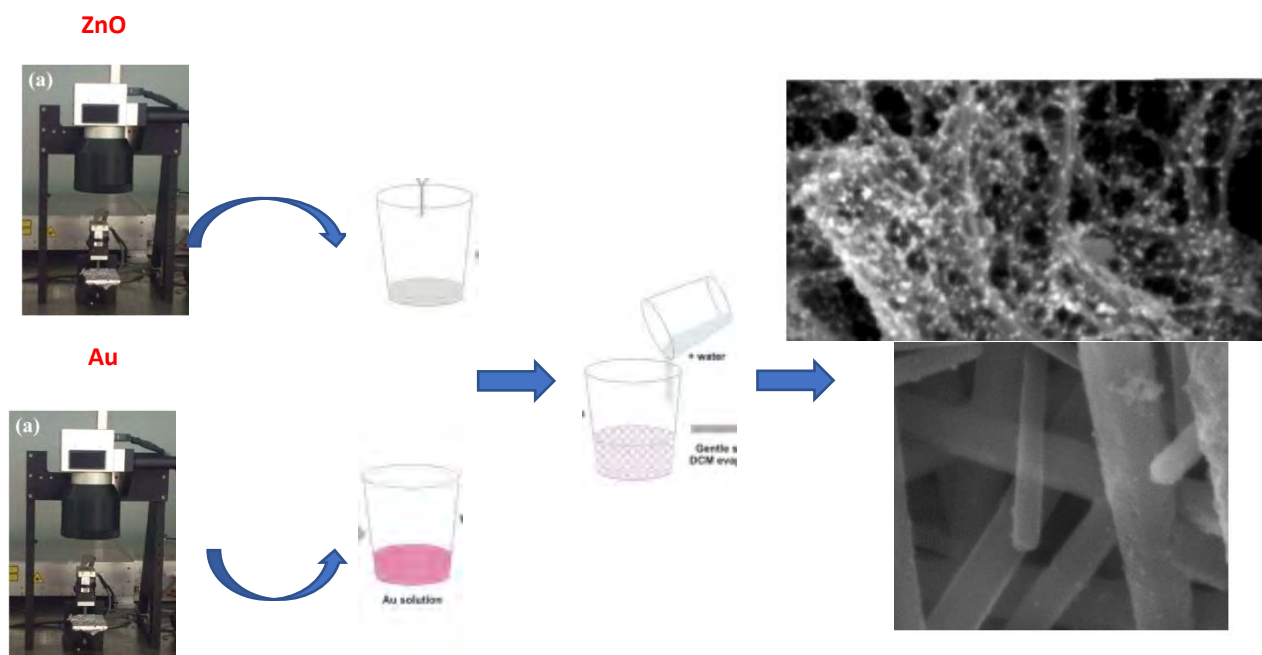


Figure 1: Schematic illustration of the synthesis of the Au decorated ZnO nanorods.

[1] L. D'Urso¹, S. Spadaro, M. Bonsignore, S. Santangelo, G. Compagnini, F. Neri, and E. Fazio, Zinc oxide nanocolloids prepared by picosecond pulsed laser ablation in water at different temperatures EPJ Web of Conferences 167, 04008 (2018)

[2] J. Manna, T.P. Vinod, K. Flomin, R. Jelinek, Photocatalytic hybrid Au/ZnO nanoparticles assembled through a one-pot method., J. Colloid and Interface Sci. **460**, 113-118 (2015)

[3] X. Zhang, J. Qin, Y. Xue, P. Yu, B. Zhang, L. Wang, R. Liu, Effect of aspect ratio and surface defects on the photocatalytic activity of ZnO nanorods Scientific Reports **4**, Article number: 4596 (2014)

Femto/picosecond pulsewidth-dependent yield of metal and Si nanoparticles

I. N. Saraeva¹, S. I. Kudryashov^{1,2}, A. A. Rudenko¹, A. A. Ionin¹

1- Lebedev Physical Institute, Leninskiy prospect 53, 119991 Moscow, Russia

2- ITMO University, Kronverkskiy prospect 49, 197101 St. Petersburg, Russia

Main author email address: insar@lebedev.ru

The dependence of silver, gold and silicon NPs yield on laser pulsewidth $\tau = 0.3 - 10$ ps, gradually tuned during IR ($\lambda = 1030$ nm) multi-shot laser ablation of solid targets in deionized water or isopropyl alcohol, was studied by measuring optical transmission of their hydrosols in the UV – near IR range. The derived extinction coefficient spectra exhibited non-monotonous dynamics versus τ in case of water medium use and were correlated to SEM-acquired topologies of corresponding ablated surface spots and resulting NP size distributions, as well as with the single-shot ablation threshold values and $1/e$ -radii of ablated spots w_{abl} , measured for a silver and silicon target in air.

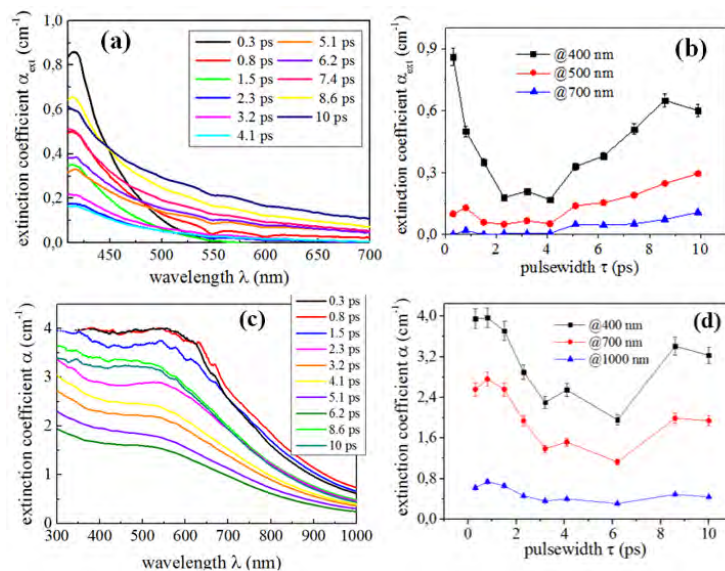


Figure 59 Experimental extinction coefficient spectra of Ag (a) and Si (c) colloids, fabricated at different pulsewidths in water; the corresponding extinction coefficient α_{ext} as a function of τ (b, d).

The observed phenomenon may be explained by (1) the diminished yield of NPs and surface ablation rate at the intermediate pulsewidths of 2-4 ps may be related to the increase of wet ablation thresholds for the growing τ values; (2) laser filamentation in the 2-mm thick top immersing medium layer can enhance inhomogeneous focusing inside the resulting filaments and to provide the initial local ablative damage to the surface [1, 2]; (3) ultrafast boiling of intact water layer near the target surface [3] at rather low (≥ 647 K) near-critical temperatures for water on ps timescale. Different subsequent – nucleate and surface film boiling – temporal stages can differently perturb laser energy deposition into the target, with longer (> 4 ps) ps laser pulses providing energy deposition slow enough to yield in film boiling stage, more favourable for laser beam delivery to the ablation spot. However, laser pulses with intermediate τ , providing heating of the surface till the critical temperature of water during their duration, can exert significant optical perturbation – e.g., strong scattering – during the nucleate boiling stage.

[1] A. Ionin, S. Kudryashov, S. Makarov, L. Seleznev, D. Simitsyn, JETP Letters, vol. 90, pp. 423–427, (2009).

[2] W. Liu, O. Kosareva, I.S. Golubtsov, A. Iwasaki, A. Becker, V.P. Kandidov, S.L. Chin, Femtosecond laser pulse filamentation versus optical breakdown in H₂O, Applied Physics B, Vol. 76, pp. 215–229 (2003).

[3] V. Kotaidis, C. Dahmen, G. von Plessen, F. Springer, A. Plech, Journal of Chemical Physics, vol. 124, 184702, (2006).

Plasmonic and Magnetic Nanocomposites

R.K. Soni, M.P. Navas

Department of Physics, Indian Institute of Technology Delhi, New Delhi 110016, India

ravisoni@physics.iitd.ac.in

Palladium nanoparticles and bimetallic nanocomposites are extensively used in catalytic reactions, SERS and sensing [1, 2]. Bimetallic palladium nanocomposites with silver, gold and iron are prepared by different laser ablation methods to fabricate core-shell and alloy nanostructures. Sequential ablation method is used for synthesis of core-shell nanoparticles, whereas metal junction ablation is used for synthesis of alloy nanoparticles. Presence of gold or silver in nanocomposite alters plasmonic response and iron in nanocomposite modifies magnetic response, as shown in figure 1. Moreover, the localised plasmon resonance wavelength is tuneable in core-shell nanoparticles with shell thickness in accordance with core and shell plasmon hybridization and in alloy nanoparticles with composition.

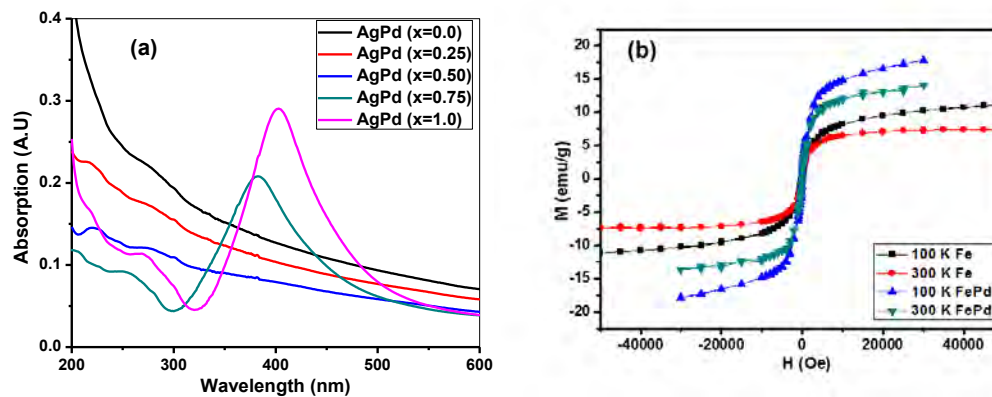


Figure 60 (a) Absorption spectra of Ag–Pd nanoparticles prepared by laser ablation in water and (b) Hysteresis curve (M vs H) of Fe and Fe.Pd nanoparticles measured at 300 and 100 K.

Magnetic $\text{Fe}_{70}\text{Pd}_{30}$ alloy nanoparticles of average size 9 nm prepared by ablation of FePd alloy target display extended absorption in UV region and super-paramagnetic behaviour [3]. Further, in ZFC curve a broad peak associated with the blocking temperature is observed at 240 K and 180 K for Fe and $\text{Fe}_{70}\text{Pd}_{30}$ nanoparticles, respectively. The calculated effective anisotropy constant from blocking temperature is $2 \times 10^5 \text{ J/m}^3$ and $1 \times 10^5 \text{ J/m}^3$ for Fe and $\text{Fe}_{70}\text{Pd}_{30}$ respectively. Hysteresis curve (M vs H curve) of the fabricated Fe and $\text{Fe}_{70}\text{Pd}_{30}$ magnetic nanoparticles is shown in figure 1(b). The M vs H measurements are done above and below the blocking temperature at 300 and 100 K. Saturation of magnetizations for bulk $\text{Fe}_{70}\text{Pd}_{30}$ alloy is 160 emu/g at 300 K but significantly reduced in nanoparticles due to broken bonds and frustration of exchange interactions in nanoparticles leading to surface spin canting and disorder. These effects become significant with decreasing particle size. The observed coercivity of $\text{Fe}_{70}\text{Pd}_{30}$ nanoparticles is 103 and 31 Oe at 100 and 300 K, respectively. The non-zero value of coercivity at 300 K, temperature above blocking temperature in both samples is attributed to large particle size distribution of laser ablated nanoparticles.

- [1] P. Verma, Y. Kuwahara, K. Mori, H. Yamashita, Pd/Ag and Pd/Au bimetallic nanocatalysts on mesoporous silica for plasmon-mediated enhanced catalytic activity under visible light irradiation, *J. Mater. Chem. A* 4, 10142-10150 (2016).
- [2] J. Chen, B. Wiley, J. McLellan, Y. Xiong, Z-Y. Li, Y. Xia, Optical Properties of Pd–Ag and Pt–Ag Nanoboxes Synthesized via Galvanic Replacement Reactions, *Nano Lett.* 5, 2058-2062 (2005).
- [3] Y. Ito, A. Miyazaki, S. Valiyaveetil, T. Enoki, Magnetic Properties of Fe–Pd Alloy Nanoparticles, *J. Phys. Chem. C*, 114, 11699–11702 (2010).

The Luminescence of Silicon-based Nanoparticles Produced by Laser Ablation in Liquid

D. M. Popovic¹, A. Kushima², A. A. Zekic¹, B. Kasalica¹, M. Trtica³, J. Ciganovic³, M. Z. Sarvan¹, and M.M. Bogdanovic¹

1- University of Belgrade, Faculty of Physics, Studentski trg 12, 11001 Belgrade, Serbia

2- Advanced Materials Processing and Analysis Center, Department of Materials Science and Engineering, University of Central Florida, Orlando, Florida 32816, USA

3- Vinca Institute of Nuclear Science, University of Belgrade, P.O. Box 522, 11001 Belgrade, Serbia

Main author email address: drdmpopovic@gmail.com

Silicon-based nanoparticles (SiNPs) are attracting attention for applications in various fields, from energy storage to bio-imaging [1,2]. The pulsed laser ablation of solid target in liquid media (LAL) is the quality technique of nanoparticles fabrication, because it is simple, fast, reduces the contamination risk [3,4], etc. Here, SiNPs are synthesized by ps- laser (150 ps, 1064 nm, 7 mJ/pulse) ablation in liquid of silicon single-crystal plates. The additional continuous wave (CW) green laser (532nm) was employed during the process and the energies were in the range of 200-1000 mJ. The obtained SiNPs exhibit good blue photoluminescence (PL) properties, strongly impacted by introducing the CW laser in the ablation process. The impact depends both on the energy of the CW laser and the PL excitation wavelength. The obtained results indicate that for the excitation below 310nm (4eV), the increase in CW laser power leads to an increase in the photoluminescence, and such trend changes if the energy of the excitation photons is below 4eV. This is in good accordance with our previously published results [5], which showed that introduction of the CW laser in the ablation process affects the PL properties of the silicon-based nanoparticles, which may be useful for applications.

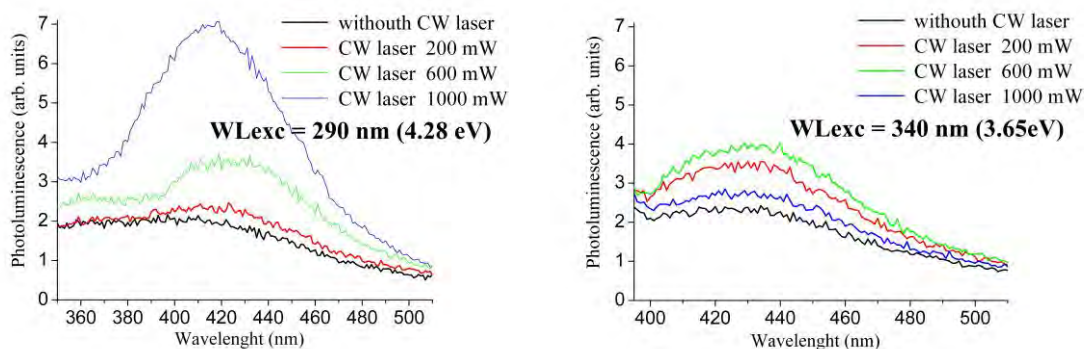


Figure 1 The photoluminescence spectra (excitation 290 nm and 340 nm) of SiNPs produced by pulsed laser ablation with and without applying the CW laser (200mW, 600mW and 1000mW, respectively).

[1] A. Verma and F. Stellacci, Effect of surface properties on nanoparticle–cell interactions, *Small* 6(1), 12–21 (2010).

[2] C. Caltagirone, A. Bettoschi, A. Garau, and R. Montis, Silica-based nanoparticles: A versatile tool for the development of efficient imaging agents, *Chem. Soc. Rev.* 44(14), 4645–4671 (2015).

[3] W. T. Nichols, T. Sasaki, and N. Koshizaki, Laser ablation of a platinum target in water. I. ablation mechanisms, *Journal of applied physics* 100(11), 114911–114916 (2006).

[4] S. Petersen and S. Barcikowski, In situ bioconjugation: Single step approach to tailored nanoparticle-bioconjugates by ultrashort pulsed laser ablation, *Adv. Funct. Mater.* 19(8), 1167–1172 (2009).

[5] D. M. Popovic, A. Kushima, M. I. Bogdanovic, J. S. Chai, B. Kasalica, M. Trtica, J. Stasic, A. A. Zekic, Continuous wave laser for tailoring the photoluminescence of silicon nanoparticles produced by laser ablation in liquid. *Journal of Applied Physics*, 122(11), 113107 (2017).